1614

NAS-NS
3107

APPLICATIONS OF COMPUTERS TO NUCLEAR AND RADIOCHEMISTRY

NATIONAL ACADEMY OF SCIENCES
NATIONAL RESEARCH COUNCIL

NUCLEAR SCIENCE SERIES

RADIOCHEMICAL TECHNIQUES

U. S.
ATOMIC
ENERGY
COMMISSION

COMMITTEE ON NUCLEAR SCIENCE

S. K. Allison, *Chairman*
University of Chicago

R. D. Evans, *Vice Chairman*
Mass. Institute of Technology

Lewis Slack, *Secretary*
National Research Council

E. C. Anderson
Los Alamos Sci. Laboratory

N. E. Ballou
U.S. Naval Radiological Defense Laboratory

C. J. Borkowski
Oak Ridge Natl. Laboratory

Robert G. Cochran
A & M College of Texas

Ugo Fano
National Bureau of Standards

Herbert Goldstein
Columbia University

Bernd Kahn
Taft Sanitary Engineering Center

J. J. Nickson
Memorial Hospital (New York)

R. L. Platzman
Argonne National Laboratory

D. M. Van Patter
Bartol Research Foundation

George W. Wetherill
University of California (Los Angeles)

LIAISON MEMBERS

Paul C. Aebersold
Atomic Energy Commission

Joseph E. Duval
Air Force Office of Scientific Research

Jerome Fregeau
Office of Naval Research

J. Howard McMillen
National Science Foundation

SUBCOMMITTEE ON RADIOCHEMISTRY

N. E. Ballou, *Chairman*
U. S. Naval Radiological Defense Laboratory

G. R. Choppin
Florida State University

H. M. Clark
Rensselaer Polytechnic Institute

R. M. Diamond
Lawrence Radiation Laboratory

A. W. Fairhall
University of Washington

Jerome Hudis
Brookhaven National Laboratory

J. D. Knight
Los Alamos Scientific Laboratory

J. M. Nielsen
General Electric Company (Richland)

G. D. O'Kelley
Oak Ridge National Laboratory

R. P. Schuman
Atomic Energy Division
Phillips Petroleum Company (Idaho Falls)

E. P. Steinberg
Argonne National Laboratory

P. C. Stevenson
Lawrence Radiation Laboratory

D. N. Sunderman
Battelle Memorial Institute

CONSULTANT

J. W. Winchester
Massachusetts Institute of Technology

NAS-NS
3107
CHEMISTRY

APPLICATIONS OF COMPUTERS TO NUCLEAR AND RADIOCHEMISTRY

Proceedings of a Symposium
Gatlinburg, Tennessee
October 17-19, 1962

Edited by G. D. O'Kelley
Oak Ridge National Laboratory, Oak Ridge, Tennessee

Printed in USA. Price $2.50. Available from the Office of Technical Services, Department of Commerce, Washington 25, D. C.

Foreword

The Subcommittee on Radiochemistry is one of a number of subcommittees working under the Committee on Nuclear Science within the National Academy of Sciences – National Research Council. Its members represent government, industrial, and university laboratories in the areas of nuclear and radiochemistry.

The Subcommittee has concerned itself with the preparation of publications, nuclear education, special problems, and sponsorship of symposia on selected current topics in nuclear and radiochemistry. A series of monographs on the radiochemistry of essentially all the elements and on radiochemical techniques is being published. Initiation and encouragement of publication of articles on nuclear education in the areas of chemistry have occurred, and development and improvement of certain educational activities (e.g., laboratory and demonstration experiments with radioactivity) have been encouraged and assisted. Radioactive contamination of reagents and materials has been investigated and specific recommendations made.

This series of monographs has resulted from the need for comprehensive compilations of nuclear and radiochemical information. Each monograph collects in one volume the pertinent information required for radiochemical work with an individual element or with a specialized technique. The U.S. Atomic Energy Commission has sponsored the printing of the series.

Comments and suggestions for further publications and activities of value to persons working with radioactivity are welcomed by the Subcommittee.

N. E. Ballou, Chairman
Subcommittee on Radiochemistry

Preface

This volume contains all the papers and a panel discussion presented at the symposium on "Applications of Computers to Nuclear and Radiochemistry," which was held in Gatlinburg, Tennessee, October 17–19, 1962. The symposium was sponsored by the Subcommittee on Radiochemistry of the NAS-NRC Committee on Nuclear Science and by the U.S. Atomic Energy Commission; the Chemistry Division of the Oak Ridge National Laboratory acted as host.

The Organizing Committee for the symposium was composed of D. G. Gardner, R. L. Heath, G. D. O'Kelley (Chairman), and D. N. Sunderman. The Committee was greatly assisted in its work by D. D. Cowen of the Oak Ridge National Laboratory, who made the local arrangements, and by Lewis Slack of the Division of Physical Sciences, National Academy of Sciences – National Research Council.

The composition and makeup for this volume were performed by the Technical Publications Department, Technical Information Division, Oak Ridge National Laboratory. Without the contributions from this experienced and competent group, it would have been impossible to meet the publication schedule for these *Proceedings*.

The editor wishes to thank the authors, who supplied manuscripts for all papers included in this volume. It will be noted that the tone and the length of the papers vary a great deal; however, because of the short time permitted for publication, editorial changes were held to a minimum. It also would have been desirable to make the notation uniform. Such extensive revisions not only would have involved considerable time, but also would have greatly increased the probability of introducing errors in the mathematical material; with minor exceptions, the authors' notations were therefore left unchanged. In general, each author has defined any unusual symbols or notation, and each paper has been checked for self-consistency. It is hoped that the varied notation will not present difficulties to the initiated reader.

Many of the papers included computer programs to accompany the mathematical description of the various methods. For reasons of space, it was not possible to include these programs; rather, it was felt that copies of particular programs, together with information about their use, could best be circulated on an individual basis by the authors.

The panel discussion in (5-2) was prepared from a stenotypist's record. In several instances, the transcript was either incomplete or garbled; here, attempts were made to reconstruct the discussion to reflect the content of what was said. Time did not permit a review of the manuscript by the panelists. In this case, as well as for the rest of the volume, the speakers deserve the credit for whatever is good in the *Proceedings*, and the editor is prepared to accept the blame for the errors.

G. D. O'Kelley

Oak Ridge, Tennessee
March 1963

Contents

SESSION 3
Chairman: *J. E. Monahan*

SESSION 4
Chairman: *R. L. Heath*

SESSION 5
Chairman: *G. D. O'Kelley*

SESSION 6
Chairman: *D. N. Sunderman*

* * * * *

Session 1

Chairman: D. G. Gardner

Department of Chemistry,
Illinois Institute of Technology,
Chicago 16, Illinois

(1-1) GENERALIZED LEAST SQUARES AND THE INVERSION OF SYMMETRIC POSITIVE DEFINITE MATRICES

M. H. Lietzke
Chemistry Division, Oak Ridge National Laboratory [1]
Oak Ridge, Tennessee

In curve fitting and in the quantitative treatment of experimental data the method of least squares, invented independently by Legendre and Gauss, is widely used. At the present time attempts are being made, for example in the fitting of spectral data, to determine ever larger numbers of parameters. In many cases the underlying mathematical models are highly nonlinear, and convergence difficulties may be encountered. In any least-squares fit involving the determination of a large number of parameters, however, the accumulation of roundoff error during the course of the computation, resulting in a loss of significance, is one of the most serious restrictions. In this paper the method of least squares as carried out on a high speed computer is described; and since the inversion of a symmetric positive definite matrix must be performed, a comparison of several methods of carrying out the inversion of such matrices is given.

LINEAR REGRESSION – THE METHOD OF LEAST SQUARES [1]

Suppose that a quantity y has been observed as a function of another quantity x, the resulting values being $y_1, y_2, \ldots, y_n$ for $x_1, x_2, \ldots, x_n$. Assume that a functional relationship

$$y = f(x, \alpha_1, \ldots, \alpha_m), \qquad m < n \tag{1}$$

exists, where the $\alpha_1, \ldots, \alpha_m$ represent m unknown parameters. According to the method of least squares those values are chosen as estimates of the parameters which minimize the weighted sum of squares

$$\Sigma w_i r_i^2 = \sum_{i=1}^{n} \{y_i - f(x_i, \alpha_1, \ldots, \alpha_m)\}^2 w_i \tag{2}$$

[1] Operated by Union Carbide Corporation for the U.S. Atomic Energy Commission.

of the deviations of the sample values y_i from the values computed with Eq. (1) and the estimates of the parameters. The w_i in Eq. (2) represents the weight associated with each data point. If the y_i are normally and independently distributed with constant variance and Eq. (1) is linear with respect to the parameters $\alpha_1, \ldots, \alpha_m$, then the least-squares estimates of $\alpha_1, \ldots, \alpha_m$ are both maximum likelihood and minimum variance unbiased estimates. If, however, linear regression is applied to a nonlinear model the foregoing statement does not hold. About all that can be said in the nonlinear case is that if the observation vector consists of elements which are independent and have constant variance, then the variance-covariance matrix approaches asymptotically the variance-covariance matrix in the linear case as the number of samples becomes large. However, the underlying mathematical techniques are the same in either the linear or nonlinear case.

In carrying out a least-squares fit to an equation

$$y = f(x_1, \ldots, x_l, \alpha_1, \ldots, \alpha_m) , \tag{3}$$

where the $x_1, \ldots, x_l$ are the l independent variables and the $\alpha_1, \ldots, \alpha_m$ are the m unknown parameters, estimates are first made of the values of the parameters. Using these approximate values of the parameters an observation matrix X is set up consisting of column vectors of the partial derivatives of the dependent variable with respect to each of the parameters evaluated at each data point. Thus

$$X = \begin{pmatrix} \left(\frac{\partial y}{\partial \alpha_1}\right)_1 & \left(\frac{\partial y}{\partial \alpha_2}\right)_1 & \cdots & \left(\frac{\partial y}{\partial \alpha_m}\right)_1 \\ \left(\frac{\partial y}{\partial \alpha_1}\right)_2 & \left(\frac{\partial y}{\partial \alpha_2}\right)_2 & \cdots & \left(\frac{\partial y}{\partial \alpha_m}\right)_2 \\ \vdots & \vdots & & \vdots \\ \left(\frac{\partial y}{\partial \alpha_1}\right)_n & \left(\frac{\partial y}{\partial \alpha_2}\right)_n & \cdots & \left(\frac{\partial y}{\partial \alpha_m}\right)_n \end{pmatrix}$$

where the subscripts on the partial derivatives indicate evaluation at the respective data points. The partial derivatives may be evaluated either numerically or analytically. The matrix X is then transposed and the $X^T X$ product is formed. If weights other than unity are assigned to the data points the $X^T W X$ product is formed where W is a matrix containing the weight associated with each data point on the principal diagonal and zeros in all the off-diagonal positions. Next a column vector Y is formed whose elements are the differences between the measured values of the dependent variable and values calculated using Eq. (3) with the current estimates of the parameters. Then the vector solution of the matrix equation

$$X^T W X \, C = X^T W Y$$

or

$$C = (X^T W X)^{-1} X^T W Y \tag{4}$$

gives a vector C whose elements are correction factors to be applied to the initial estimates of the parameters. The iteration process is repeated with corrected estimates of the parameters until the conditions for an arbitrary stopping criterion have been met. (It should be mentioned that in linear cases, such as in polynomial fitting, it is more efficient to use specific routines which avoid iteration.)

In order to calculate the variances and covariances for the parameters, the inverse of the X^TWX matrix is used. The product $[\Sigma w_i r_i^2/(n-m)]\,(X^TWX)^{-1}$, after convergence to the "correct" solution, gives an estimate of the variance-covariance matrix which contains the variances of the parameters on the principal diagonal and the covariances in the off-diagonal positions.

One of the limitations of the least-squares method has already been mentioned: accumulation of roundoff error may destroy all significance, especially if a large number of parameters is being determined. In the application of linear regression to nonlinear models, additional limitations should be noted: (1) the estimates of the precision of the parameters are not exact, (2) the calculation may not converge to a solution, and (3) in case of convergence there is no guarantee that the method will converge to the desired answer. In carrying out the calculation a sum of squares surface is searched for a minimum. However, this surface may contain many local minima, and hence it may be important in some cases to have good estimates of the parameters to ensure convergence to the correct minimum.

INVERSION OF THE X^TWX MATRIX

When a least-squares fit involves the determination of a large number of parameters it becomes important to choose a matrix inversion scheme which will result in a minimum loss of significance. Other considerations, such as the memory capacity of the computer, may also influence the choice. Some inversion schemes, such as the Choleski [2] and congruent transformation [3] methods, take advantage of the fact that the X^TWX matrix is symmetric and positive definite and, operating only on the upper or the lower triangle of the matrix, require much less memory capacity.

In order to assess the utility of several standard methods for inverting large symmetric positive definite matrices the Gauss-Jordan [4], Choleski, congruent transformation, and rank annihilation [5] methods were tried. To give a fair comparison of the methods each was programmed in FORTRAN using only single precision arithmetic. The error indicators were then computed using double precision arithmetic so that the latter calculation was not a limiting factor. All the methods used are well known and need not be described here.

The matrix chosen for testing the inversion routines was A where the elements a_{ij} of A are given by

$$a_{ij} = \begin{cases} 2 & (i = j) \\ -1 & (|i-j| = 1) \\ 0 & (|i-j| > 1) \end{cases}.$$

The inverse of A is given by $C/(n+1)$ where the elements c_{ij} of C are given by

$$c_{ij} = \begin{cases} i(n-i+1) & (i=j) \\ c_{i,j-1} - i & (j>i) \\ c_{ji} = c_{ij} & (j<i) \end{cases}$$

and n is the order of the matrix. A is a symmetric positive definite matrix; it has a P-condition number of approximately $4n^2/\pi^2$. In respect to both form and condition the matrix A is analogous to a least-squares matrix derived from a well designed experiment. In addition to A the matrices A^2 and A^3 were also inverted. The inverse of A^2 is given by $C^2/(n+1)^2$, while the inverse of A^3 is given by $C^3/(n+1)^3$. The latter two matrices have P-condition numbers of $16n^4/\pi^4$ and $64n^6/\pi^6$, respectively, and are hence progressively more ill conditioned. In this respect they correspond to least-squares matrices from increasingly more poorly designed experiments.

In carrying out the comparison of the various inversion methods the matrix A, A^2, or A^3 was generated and inverted by each method to give $(M)^{-1}_{\text{approx}}$. Then the exact inverse was generated (using the above formulas and double precision arithmetic) and as a measure of error the quantity Q defined as

$$Q = \frac{1}{n^2} \sum_{ij} \left| (M)^{-1}_{\text{exact}} - (M)^{-1}_{\text{approx}} \right|_{ij} \tag{5}$$

was computed for each method, where M represents A, A^2, or A^3. The computations were performed with matrices of order 10, 15, 20, 25, and 30. In addition to Q two other quantities, recommended as error measures by Newman and Todd [6],

$$a = \frac{1}{n^2} \sum_{ij} |r_{ij}| \tag{6}$$

and

$$f = \frac{1}{n} \left\{ \sum_{ij} r_{ij}^2 \right\}^{1/2} \tag{7}$$

were calculated, where $R = (r_{ij})$ is the error matrix taken as

$$(M)^{-1}_{\text{approx}} (M) - I = R \ , \tag{8}$$

where I is the identity matrix.

THE A MATRIX

All the methods tried gave an approximate inverse that was very close to the exact inverse of the A matrix for all orders from 10 to 30. Hence, any one of the methods would be suitable for a well-conditioned least-squares matrix in this range. The inverse matrix produced by the congruent transformation method was good to one in the eighth significant figure even for order 30. The Gauss-Jordan method and the Choleski method were close behind in that order. Not only did the congruent transformation method produce an inverse closest to the exact inverse of the A matrix, but the values

of a and f [as defined by Eqs. (6 and 7)] computed from the approximate inverse were lower than the corresponding values derived from the Gauss-Jordan and Choleski inversion routines (see Table 1). All of the methods produced inverse matrices, all elements of which were lower than the exact inverse for all orders from 10 to 30.

THE A^2 MATRIX

In the inversion of the A^2 matrix the effect of the condition of the matrix starts to become apparent. This matrix is not as well conditioned as the A matrix; in fact, its condition number is the square of the condition number for the A matrix and hence is proportional to the fourth power of the order.

In the inversion of the A^2 matrix for all orders from 10 to 30 the Gauss-Jordan method produced an inverse matrix closest to the exact inverse. The congruent transformation, the Choleski, and the rank annihilation methods gave very similar results and were somewhat inferior to the Gauss-Jordan method. The inverse matrices produced by the latter method were good to one part in 600,000 for order 10 to one part in 20,000 for order 30. The corresponding figures for the other methods were one part in about 150,000 for $n = 10$ to one part in about 3000 for $n = 30$. The values of Q, a, and f for the A^2 matrix are shown in Table 1.

THE A^3 MATRIX

An examination of the values of Q for the A^3 matrix (Table 1) indicates that the two Gauss-Jordan routines [7, 8] produce inverses that are the closest to the exact inverse, except that at order 15 the Choleski method is closer than Gauss-Jordan II. (The two Gauss-Jordan routines both perform all floating point arithmetic in single precision; however, the second differs from the first in that proper rounding is used.) The first Gauss-Jordan routine is good to one part in 80,000 for $n = 10$, to one part in 1100 for $n = 20$, and to one part in 400 for $n = 30$; while the corresponding figures for the other are one part in 50,000, one part in 10,000, and one part in 130. Close behind the Gauss-Jordan routines for $n = 10$ is the congruent transformation method; however, for $n = 15$ to 30 the Choleski method produces a more nearly exact inverse. At $n = 30$ the rank annihilation method appears slightly better than the congruent transformation method, producing an inverse each element of which is good to one part in 16.

In addition to the above observations concerning the closeness of the approximate inverse to the exact inverse it should be noted that the Gauss-Jordan I and congruent transformation routines produced inverse matrices whose elements were in all cases smaller than those of the exact inverse; while the inverse matrices produced by the rank annihilation method were for all orders greater than the exact inverse. The elements of the inverse matrices of orders 10, 15, and 20 produced by the Gauss-Jordan II routine were greater than those of the exact inverse, while for orders 25 and 30 they were smaller. The Choleski routine produced an inverse matrix at orders 10 and 15 with elements smaller than those of the exact inverse, while at orders 20, 25, and 30 the inverse matrix elements were greater than those of the exact inverse. The low value of Q at $n = 20$ for the Gauss-Jordan II routine reflects the fact that the elements of the approximate inverse are passing through a transition from all

Table 1. A Comparison of the a, f, and Q Values as a Function of Matrix Order and Inversion Method

n	Matrix	Gauss-Jordan I[a]			Gauss-Jordan II[b]		
		A	A^2	A^3	A	A^2	A^3
10	a	1.3×10^{-8}	9.6×10^{-6}	6.7×10^{-4}	1.4×10^{-8}	5.6×10^{-7}	3.3×10^{-5}
	f	1.9×10^{-8}	1.4×10^{-5}	1.1×10^{-3}	2.2×10^{-8}	7.8×10^{-7}	4.4×10^{-5}
	Q	4.8×10^{-8}	2.7×10^{-5}	2.1×10^{-3}	6.7×10^{-8}	3.2×10^{-5}	2.8×10^{-3}
15	a	2.3×10^{-8}	3.6×10^{-5}	3.0×10^{-2}	2.3×10^{-8}	2.6×10^{-6}	2.0×10^{-4}
	f	3.6×10^{-8}	7.1×10^{-5}	4.7×10^{-2}	3.7×10^{-8}	3.8×10^{-6}	2.9×10^{-4}
	Q	7.8×10^{-8}	8.3×10^{-5}	2.6×10^{-2}	1.8×10^{-7}	2.3×10^{-4}	2.2×10^{-1}
20	a	3.7×10^{-8}	1.1×10^{-4}	5.0×10^{-1}	3.7×10^{-8}	6.8×10^{-6}	1.5×10^{-3}
	f	6.1×10^{-8}	1.6×10^{-4}	8.1×10^{-1}	6.0×10^{-8}	9.9×10^{-6}	2.0×10^{-3}
	Q	1.2×10^{-7}	1.1×10^{-3}	3.4	3.7×10^{-7}	1.0×10^{-3}	3.8×10^{-1}
25	a	4.3×10^{-8}	4.3×10^{-4}	3.4	4.8×10^{-8}	1.1×10^{-5}	5.7×10^{-3}
	f	7.1×10^{-8}	7.2×10^{-4}	5.8	8.0×10^{-8}	1.6×10^{-5}	7.9×10^{-3}
	Q	2.0×10^{-7}	5.2×10^{-3}	27.	6.6×10^{-7}	3.7×10^{-3}	44.
30	a	5.1×10^{-8}	1.3×10^{-3}	13.	5.6×10^{-8}	2.0×10^{-5}	1.7×10^{-2}
	f	8.2×10^{-8}	2.0×10^{-3}	23.7	9.4×10^{-8}	2.9×10^{-5}	2.5×10^{-2}
	Q	3.9×10^{-7}	1.9×10^{-2}	69.	1.1×10^{-6}	1.3×10^{-2}	258.

Table 1 (continued)

n	Matrix	Choleski			Congruent Transformation			Rank Annihilation	
		A	A^2	A^3	A	A^2	A^3	A^2	A^3
10	a	2.0×10^{-8}	1.6×10^{-6}	8.7×10^{-5}	1.0×10^{-8}	1.2×10^{-6}	5.6×10^{-5}	2.2×10^{-5}	1.5×10^{-3}
	f	3.1×10^{-8}	2.2×10^{-6}	1.1×10^{-4}	1.5×10^{-8}	1.4×10^{-6}	7.2×10^{-5}	2.6×10^{-5}	2.0×10^{-3}
	Q	1.3×10^{-7}	1.1×10^{-4}	2.1×10^{-2}	5.9×10^{-9}	1.0×10^{-4}	1.3×10^{-2}	8.8×10^{-5}	2.6×10^{-1}
15	a	4.0×10^{-8}	8.9×10^{-6}	1.6×10^{-3}	0.0	4.3×10^{-6}	5.2×10^{-4}	4.2×10^{-5}	6.4×10^{-3}
	f	5.8×10^{-8}	1.4×10^{-5}	2.2×10^{-3}	0.0	5.6×10^{-6}	7.1×10^{-4}	5.9×10^{-5}	1.1×10^{-2}
	Q	2.4×10^{-7}	1.7×10^{-3}	1.3×10^{-1}	0.0	1.2×10^{-3}	1.3	1.5×10^{-3}	9.1
20	a	5.7×10^{-8}	1.8×10^{-5}	1.4×10^{-2}	1.6×10^{-8}	9.1×10^{-6}	2.3×10^{-3}	7.5×10^{-5}	5.2×10^{-2}
	f	8.8×10^{-8}	2.7×10^{-5}	1.9×10^{-2}	2.6×10^{-8}	1.2×10^{-5}	3.2×10^{-3}	1.0×10^{-4}	9.4×10^{-2}
	Q	2.4×10^{-7}	1.1×10^{-2}	8.3	1.0×10^{-8}	7.4×10^{-3}	29.	1.2×10^{-2}	97.
25	a	7.4×10^{-8}	4.0×10^{-5}	6.4×10^{-2}	1.8×10^{-8}	1.5×10^{-5}	5.7×10^{-3}	1.9×10^{-4}	2.6×10^{-1}
	f	1.2×10^{-7}	5.5×10^{-5}	9.6×10^{-2}	3.1×10^{-8}	2.0×10^{-5}	7.5×10^{-3}	2.7×10^{-4}	4.7×10^{-1}
	Q	3.7×10^{-7}	4.5×10^{-2}	130.	6.2×10^{-8}	2.7×10^{-2}	229.	3.9×10^{-2}	440.
30	a	8.9×10^{-8}	1.2×10^{-4}	2.2×10^{-1}	1.9×10^{-8}	2.9×10^{-5}	1.5×10^{-2}	4.0×10^{-4}	9.1×10^{-1}
	f	1.4×10^{-7}	1.7×10^{-4}	3.7×10^{-1}	3.2×10^{-8}	4.0×10^{-5}	2.3×10^{-2}	6.4×10^{-4}	1.4
	Q	6.4×10^{-7}	1.4×10^{-1}	751.	2.2×10^{-8}	1.1×10^{-1}	1885.	9.0×10^{-2}	1386.

[a] D. Cohen, ref [7].
[b] R. Burrus and D. Bogert, ref [8].

being too large to all being too small. The same is true for the low value of Q at $n = 15$ for the Choleski method, except that the transition is in the opposite direction.

It is evident that if the a and f values alone were used to compare the approximate inverses of the A^3 matrix produced by the various inversion methods, then the congruent transformation method would appear to be as good as the Gauss-Jordan method. However, the Gauss-Jordan I routine produced an inverse for $n = 30$ good to one part in 400, while the inverse produced by the congruent transformation method was good only to one part in 15. Thus, the Q values reflect the observed bias between the exact and approximate inverses, while the a and f values may not. A possible explanation in the latter case may be in the fact that the A^3 matrix contains elements of alternating sign while all the elements of the inverse matrix are positive. Hence there may be some cancellation of errors in forming the $(M)^{-1}_{approx} M$ product in Eq. (8), this effect becoming more pronounced as the matrix becomes more ill conditioned. Also the A^3 matrix contains many zeros (in fact, a higher proportion the larger the order), and hence the errors in some of the inverse matrix elements do not show up in the a and f values.

From the foregoing calculations it appears that any one of the matrix inversion methods tried will invert a well-conditioned least-squares matrix of order 10 to 30. When the matrix becomes ill conditioned then the Gauss-Jordan method appears to be clearly superior (at least for the matrices studied). However, if memory capacity must be considered and only a triangular array can be tolerated, then the Choleski method appears to be superior to the congruent transformation method for large n. From a study involving the inversion of several well-conditioned least-squares matrices of orders to $n = 29$ all the methods tried gave a and f values about two to three orders of magnitude smaller than those obtained with the A^3 matrix and consistent with those obtained with the A matrix.

ACKNOWLEDGMENT

The author wishes to express his appreciation to Dr. R. W. Stoughton, Dr. H. A. Levy, and Mrs. Marjorie P. Lietzke for interesting and helpful discussions on the methods and to R. J. White for programming several of the inversion routines.

REFERENCES

[1] Marjorie P. Lietzke, *Polfit II, an IBM 7090 Program for Polynomial Least Squares Fitting*, ORNL-3132 (April 1961).

[2] "Contributions to the Solution of Systems of Linear Equations and the Determination of Eigenvalues," *Natl. Bur. Std. (U.S.), Appl. Math. Ser.* No. 39, p 31 (1954).

[3] W. R. Busing and H. A. Levy, "A Procedure for Inverting Large Symmetric Matrices," *Comm. ACM* **5**, 445 (1962).

[4] Anthony Ralston and H. S. Wilf, *Mathematical Methods for Digital Computers*, p 39, Wiley, New York, 1960.

[5] *Ibid.*, p 73.

[6] Morris Newman and John Todd, "The Evaluation of Matrix Inversion Programs," *J. Soc. Ind. Appl. Math.* **6**, 466 (1958).

[7] Donald Cohen, "Algorithm 58 (corrected)," *Comm. ACM* **4**(5) (1961).

[8] R. Burrus and D. Bogert (after J. B. Rabin per Apex-635, Flight Propulsion Laboratory Department, General Electric, p 103 (July 12, 1961).

(1-2) BRUNHILDE – A CODE FOR ANALYZING MULTICOMPONENT RADIOACTIVE DECAY CURVES

Walter E. Nervik
Lawrence Radiation Laboratory, University of California
Livermore, California

During the past years the Radiochemistry Section of the Chemistry Division at the Lawrence Radiation Laboratory has developed a number of computer codes for analyzing multicomponent radioactive decay curves. As may be expected, the earlier codes had rather limited capabilities, while the later modifications became increasingly complex and more sophisticated. In addition, the earlier codes were written for the IBM 650 computer and were severely restricted by its small memory and low calculating speed, while the latest code is written for the much faster and more versatile IBM 7090.

The program in current use is called "Brunhilde." In addition to doing everything that its predecessors did, this code includes many other kinds of calculations because of the larger memory and higher calculating speed of the IBM 7090 computer. The Brunhilde code is intended to be run by the "Monitor" system, and so it is imperative that the code be written in such a way that the computer does not stop when something goes wrong. Ideally, the machine should determine what is wrong, correct it, and go on with the calculation; or, if corrective action is not possible, it should go on to the next problem. Brunhilde has been written in this way, and there is almost nothing that will make the machine stop and dump its memory. All reasonable errors, and many unreasonable ones, will cause a suitable comment to be printed by the machine before it takes appropriate action.

Data are presented to the computer on a series of punched cards of various types. A "Control Card" bears information relevant to the problem as a whole, such as zero time, chemical yield, or aliquot factor, as well as the identity of the sample. Each measurement on a counter gives rise to a single data card giving the identity of the sample and all information pertinent to that individual count. Each background measurement also gives rise to a card of similar format. Instructions to the computer are inserted by the use of subsidiary cards.

Operations of the Brunhilde code may be broken down into four general categories: (1) acceptance and storage of input data; (2) calculation and resolution of the decay curve; (3) printout of data for individual samples; and (4) printout of data for replicate samples.

ACCEPTANCE AND STORAGE OF INPUT DATA

Since there are many different kinds of input cards, each with a unique arrangement of information, the machine first checks to see what kind of card it is reading, then takes appropriate action, converting numbers as they are presented on the input cards to numbers that are suitable for calculation, and storing everything in its proper location. Numbers which are converted include:

1. Time: All times are converted first to days and thousandths of days from 1 January 1952, then to days and thousandths of days from time zero. The time of a count is taken as the midpoint of the count.

2. Counting rate: The gross counting rate is obtained by adding 0.5 scalers to the number of scalers on the data card and converting to counts per minute. (When the scale factor is 1, no half scaler is added.)

3. Weighting factor: The weighting factor ("Variance") of each gross count is obtained in the following manner:

$$\text{VARIANCE} = \frac{(\text{Gross count}) + \dfrac{(\text{Scale factor} - 1)^2}{(12.0)\,(\text{Duration of count})}}{(\text{Duration of count})} .$$

All of the input cards for a given sample are read into the computer, one card at a time, until an "end" card is reached, at which point the machine begins its calculations. While being read, the cards are continually being checked for compatibility. If a card is not compatible with the sample being considered it is rejected and the machine prints a suitable comment before going on to the next card. Examples of incompatibility include: (1) wrong counter, (2) wrong control word, (3) extra "end" card, (4) data card being read when no control card information is available, and (5) background card in excess of 300 for a single sample.

In addition to rejecting individual cards the computer will reject an entire sample if a computation is not possible. Conditions under which this will occur include:

1. no data cards (or not enough data cards available to resolve the desired number of components),
2. no control cards,
3. no components listed on the control card,
4. a component is listed on the control card for which no data are stored in the memory.

When all input data are in, the computer first converts the time of each count to days and thousandths of days from the time of the first count, then obtains background data for each count. Normally the machine will pick out the closest background count before and after each data count. Since it is possible for either or both of these background counts to be missing, the background count which is actually used for a given data count is obtained in the following manner:

1. No background data available: An average background for the counter on which the sample was counted is used. The "1/Sigma" value for these data points is then

$$\left[\frac{1}{(\text{Variance of gross count})}\right]^{1/2}.$$

2. No previous background count: The closest subsequent background count is used.
3. No subsequent background count: The closest previous background count is used.
4. Both background counts available: A linear interpolation is made between the two background counts to the time of the data count. The average background variance is also a linear interpolation between the variances of the two background counts.

In cases 2, 3, and 4 the "1/Sigma" value for the data point is:

$$\left[\frac{1}{(\text{Variance of gross count}) + (\text{Variance of background count})}\right]^{1/2}.$$

As a check on the effect of high background counts on the final solution, a data point is labeled "suspect" if either its previous or subsequent background is greater than twice the average background for the counter and if the background is greater than three times the "Sigma" value for the count. The implication of a "suspect" classification will be explained in a later section.

After the data counts have been corrected for background the computer obtains the shelf ratios and self-scattering correction values for each component. When the correction factors are not available a value of 1.0 is used.

CALCULATION AND RESOLUTION OF THE DECAY CURVE

1. Details of the Calculation

After all counts have been corrected for background, 100% yield, and aliquot factor, it is desired that a best fit be obtained to a curve of the form:

$$A_t = \sum_j x_j e^{-\lambda_j t},$$

where A_t is the net counting rate, t is the time after the zero time, x_j is the counting rate at zero time of each species present, and λ_j is the decay constant for each species.

The least-squares fitting operation is done by a matrix algebra technique which has been described elsewhere [1] in some detail. Briefly, the technique is as follows:

The data are considered to be given by a set of equations,

$$A_i = \sum_j x_j e^{-\lambda_j t_i}. \qquad (1)$$

These are then weighted according to the standard deviation σ_i of A_i (*not* the variance!)

$$y_i = \frac{A_i}{\sigma_i} = \sum_j x_j \frac{e^{-\lambda_j t_i}}{\sigma_i} . \tag{2}$$

These equations may be represented in matrix form as $(y) = [A]\ (x)$, where brackets indicate matrices and parentheses indicate vectors. The elements A_{ij} of the matrix $[A]$ are

$$A_{ij} = \frac{e^{-\lambda_j t_i}}{\sigma_i} ,$$

where $1 \leqq j \leqq N$, the number of components and $1 \leqq i \leqq M$, the number of data points.

In matrix notation, the "normal equations" whose solutions give the best values for x_j are obtained as follows:

$$[A^t]\ (y) = [A^t]\ [A]\ (x) , \tag{3}$$

where $[A^t]$ is the transpose of $[A]$; then,

$$(x) = \left[[A^t]\ [A] \right]^{-1} \left([A^t]\ (y) \right) . \tag{4}$$

The inversion of the matrix $[A^t]\ [A]$ inevitably involves some figure loss. Instead, we proceed as follows: consider the matrix $[A]$, which is in general not square, that is, there are more rows than columns. To each column after the first we add an appropriate multiple of the first column, the multiplying factor for each column being so chosen that each modified column is orthogonal to the first column, that is, the sum of the cross products of terms is zero. When all columns have been modified, the process is repeated to make all columns subsequent to the modified second column orthogonal to it; then all columns subsequent to the (twice modified) third column orthogonal to it; and so on until all columns of the matrix $[A]$ have been modified to give a matrix $[B]$, all of whose columns are mutually orthogonal. This operation is equivalent to multiplying $[A]$ from the right by a square, $N \times N$ upper triangular matrix $[U]$ (all terms below the principal diagonal are zeros) to give $[B]$, thus: $[A]\ [U] = [B]$.

The matrix $[U]$ may be obtained by treating an $N \times N$ unit matrix in the same fashion as the $[A]$ matrix, that is, multiplying the corresponding columns by the same factors and adding to the appropriate columns as in the $[A]$ matrix.

Since the columns of $[B]$ are all mutually orthogonal, the product $[B^t]\ [B]$ is a diagonal matrix, since the off-diagonal terms (which involve sums of cross products) are all zero. Let $[B^t]\ [B] = [D]$; note that $[B^t] = [U^t]\ [A^t]$ by the rules of matrix algebra. Returning to the normal equations, $[A^t]\ [A](x) = [A^t](y)$. We multiply by $[U^t]$ and insert the factor 1, represented by $[U]\ [U]^{-1}$, to give

$$[U^t]\ [A^t]\ [A]\ [U]\ [U]^{-1}(x) = [U^t]\ [A^t](y) , \tag{5}$$

or

$$[B^t]\,[B]\,[U]^{-1}(x) = [U^t]\,[A^t](y)\ ,$$

or

$$[D]\,[U]^{-1}(x) = [B^t](y) = [U^t]\,[A^t](y)\ .$$

Hence,

$$(x) = [U]\,[D]^{-1}\,[B^t](y) = [U]\,[D]^{-1}\,[U^t]\,[A^t](y)\ , \tag{6}$$

which gives us our values for the components x_j of (x). The inversion of a diagonal matrix is accomplished simply by replacing each element with its reciprocal, and involves no figure loss.

Comparing with Eq. (4) we see also that

$$[U]\,[D]^{-1}\,[U^t] = [A^t]\,[A]^{-1}\ , \tag{7}$$

the inverse matrix of the normal equations, which is the so-called "error matrix." This matrix is also less subject to errors due to figure loss than the matrix obtained by direct matrix inversion.

The deviations r_i from the calculated curve are simply obtained by substituting the calculated values of x_j into Eq. (1) and subtracting the calculated from the observed values. A more elegant method exists: in the orthogonalization procedure described above, the vector (y) is duplicated; one vector is retained unchanged for computation according to Eq. (5), while the other is treated as if it were an additional column of the matrix $[A]$, that is, it is modified to be orthogonal to each column of the matrix $[A]$ in turn. When the procedure is completed, the modified vector components will be found to be the deviations of the corresponding points from the curve, with signs reversed and each deviation weighted by $1/\sigma_i$. We then have the intriguing result that we have computed the deviations from the calculated curve before we have computed the curve itself.

In summary, data needed to begin the least-squares fitting calculation include the time and counting rate of each count and the decay constant for each component. Data obtained from the calculation include the activity of each component at the time of the first count; the deviation of each point from the calculated curve, weighted by "1/Sigma" for that point (i.e., r_i/σ_i); and the "error matrix."

2. Elimination of Bad Points and Criteria for Recalculation

In any method of analysis of decay data, criteria are needed for rejecting "bad points," or points which fall so far off a smooth curve that they may be considered of no value. The Brunhilde code handles bad data by assigning each data point to one of three categories: "OK," "suspect," or "reject." All points are assumed "OK" until they meet requirements for joining one of the other categories. A point may become "suspect" because of a high background count or, as more often happens, it may become "suspect" if its residual (r_i/σ_i) is greater than 3.0 and greater than 5% of (A_i/σ_i). These limits are set rather arbitrarily but seem to be a reasonably valid cause for suspicion to be aroused. If, in addition to meeting

the requirements for a "suspect" point, a residual (r_i/σ_i) has a sign which is different than both of its adjacent points, that point is rejected. (Here it is assumed that if we have two adjacent "good points" a calculated curve will pass reasonably close to each of them and their residuals may, or may not, have the same sign. If a sufficiently bad "bad point" is placed between the two "good points" however, the calculated curve will be displaced toward the "bad point" to such an extent that the signs of the residuals of both "good points" will be opposite to that of the "bad point.")

When the computer has completed a least-squares fitting of the data it examines all of the data points. If any points meet the requirements for rejection, they are discarded and the least-squares calculation repeated. If no points are to be rejected the computer analyzes the overall calculation to see that it is satisfactory.

In the output of the least-squares calculation, the sum of the squares of the weighted residuals (r_i/σ_i) is equivalent to χ^2. The "expected" value of χ^2 is $(N - j)$ [(where N is the number of data points and j is the number of components, with a variance of $2(N - j)$]. The Brunhilde code computes

$$V = \chi^2/(N - j) \, . \tag{8}$$

If $V \leqq 1.00$ we consider the fit to the data to be as good as can be expected.

If $V \geqq 1.00$ the code computes $Q = [2/(N - j)]^{1/2}$, the expected standard deviation of V. Rather arbitrarily again, we assume that if $(V - 1)/Q \geqq 5.0$, the entire calculation is suspect and should be repeated. When this "chi-squared test" is met the computer rejects all points which were suspect and recalculates. If no points are suspect the answers are printed out with a suitable comment. If the computer is obliged to reject suspicious points and recalculate more than three times, it rejects the entire sample, prints out the answers to the third calculation plus appropriate remarks, and goes on to the next sample. The computer will also reject an entire sample if it has to throw out so many points that it cannot perform a least-squares calculation on those remaining.

3. Precision of Results

The results x_j are regarded as "best estimates" based on the data, and not as absolute answers. An estimate of the reliability of the x_j can be obtained from the error matrix obtained in Eq. (7). The procedure is as follows: If V [Eq. (8)] is less than or equal to 1.00, ignore it; if V is greater than 1.00, multiply the diagonal elements of the error matrix by V. These elements are then the variances of the corresponding x_j. Multiplication by V accounts (approximately) for any random errors in measurements not included in the calculation of the σ_i. It is usually convenient for ease of interpretation to express the standard deviation of the x_j as a fraction of x_j, that is, $(VE_{jj})^{1/2}/x_j$.

PRINTOUT OF DATA FOR INDIVIDUAL SAMPLES

In deciding on the kind and arrangement of information that was to be printed out for individual samples the line of reasoning was as follows:

1. If the sample is a good one, that is, no bad points, the only items of interest are the answers and their precision, plus such data as half-life, shelf correction, SSA correction, counting geometry, sample weight, zero time, etc.
2. If there are "suspect" or "reject" points then detailed information on all points is needed.
3. All printed data should be labeled.

An example of the output information for a single sample is shown in Figs. 1 and 2. The labels for the data should be self-explanatory, but a clarification of the numbers is in order.

The first page of data for a single sample (Fig. 1) contains the answers to the least-squares fitting calculation plus the data pertinent to the sample itself. The date of the calculation is printed on the first line, followed by a "category" heading. Curves are often resolved more than once, and it has proven useful to have headings such as "First Wild Guess," "Preliminary Numbers," and "Final Numbers" to identify the calculation. The next line prints the name of the experiment, after which data from the control card are printed, that is, the experiment number, sample identification number, element identification number, zero time, sample weight, 100% weight, "Sr^{90}" weight, and the aliquot factor. Next, the control card is reproduced exactly as it was submitted. In the "Comments on Input Data" section an explanation is given for any input card that has been rejected and for any data point whose background is high. The time of the data point as it is punched on the data card is also printed so that the card can be more easily identified. The next section contains half-life, correction factors, and counting geometry data for all components. The results of the calculation are next presented, with information as to the number of data points, "suspect" points and "rejected" points. The first column gives the total counts per minute of each component at zero time, with all correction factors except shelf ratio and self-scattering corrections applied. The second column gives the combined shelf ratio and SSA correction, while the third column gives the product of the first two columns. Column four gives the "percent standard deviation" of the value in column three, obtained from the equation $\%\ \text{STND DEV} = 100(VE_{jj})^{1/2}/x_j$.

If a recalculation is necessary because of a high "chi-squared test" value and the presence of "suspect" points, the computer explains what it is doing before printing the answers to the second calculation.

Once the calculation is completed and the answers printed out, the computer skips to a new page for printout of detailed information on the sample. On this second page (Fig. 2) the first two lines of the first page are repeated, that is, experiment number, sample identification, etc. Next comes a table containing detailed information on each count. The data in each column, according to column

heading, are as follows:

1. TIME: The time of the count as it is printed on the data card. These will always be time ordered, whether the data cards were time ordered or not.
2. TMINUSTO: The time of the midpoint of the count minus the zero time.
3. NETCPM: Is the counting rate corrected for background only.
4. TOTCPM: Is the NETCPM value corrected for chemical yield and the aliquot factor, that is,

$$\text{TOTCPM} = (\text{NETCPM}) \left[\frac{(\text{Aliquot factor})\ (100\%\ \text{yield})}{(\text{Sample weight})\ (\text{Sr}^{90}\ \text{weight})} \right] .$$

5. WT FACTOR: The "weighting factor" of each point, calculated from the equation

$$(\text{Wt factor})_i = \frac{\sigma_i^{1/2}}{\sum_{l=1}^{N} (1/\sigma_l^2)} ,$$

where N is the total number of data points.

6. DTPREVBKGD: Consists of two columns. The first is the difference in time (in days and hundredths) between the time of the data point and the closest previous background, while the second is the closest previous background.
7. DTSUBSBKGD: Consists of two columns. The first is the difference in time between the time of the data point and the closest subsequent background, while the second is the closest subsequent background count.
8. BKGD: The background count that was actually used to correct that data point.
9. PCTDEV: Is the percent deviation of each point from the calculated curve, obtained from

$$(\text{PCTDEV})_i = \left[\frac{(\text{TOTCPM})_i - \sum_{l=1}^{j} x_l\, e^{-\lambda_l t_i}}{\sum_{l=1}^{j} x_l\, e^{-\lambda_l t_i}} \right] (100.0) .$$

10. NOSIGUDEV: The number of sigma units that each point deviates from the calculated curve, obtained from

$$(\text{NOSIGUDEV})_i = \frac{(\text{TOTCPM})_i - \sum_{l=1}^{j} x_l\, e^{-\lambda_l t_i}}{\sigma_i} .$$

11. RLBLTY: Is a measure of the "reliability" of a point, expressing the net counting rate of each data point as a multiple of its own standard deviation, that is,

$$(\text{RLBLTY})_i = \frac{(\text{NETCPM})_i}{\sigma_i} .$$

If $(\text{NETCPM})_i$ is zero or negative $(\text{RLBLTY})_i$ is assigned a value of 999999.9.

```
DATE OF THIS CALCULATION IS  12.280  C 7/21

 F I N A L N U M B E R S F I N A L N U M B E R S F I N A L N U M B E R S F I N A L N U M B E R S
 F I N A L N U M B E R S F I N A L N U M B E R S F I N A L N U M B E R S F I N A L N U M B E R S
 F I N A L N U M B E R S F I N A L N U M B E R S F I N A L N U M B E R S F I N A L N U M B E R S


CODE NAME       SCRAMBLED CARDS

EXPT SAMPLE IDENT ELEMENT IDENT ZERO TIME   SAMPLE WT WT100  SR90 WT ALIQUOT FACTOR
  22       011            42         60  321405   23.31   38.29    1.00   2.5000000E 01

CONTROL CARD
    62242501116032140523.31 38.29 1.00.2500000E 024209943099   -0   -0   -0
COMMENTS ON INPUT DATA
DATA CARD AT TIME 325905 REJECTED   WRONG COUNTER
CONTROL CARD AT 321405 NOT USED    CONTROL CARD DATA ALREADY ON FILE
DATA  CARD  AT  325905  NOT  USED    WRONG  CONTROL  WORD
DATA POINT AT TIME   325436  SUSPECT BECAUSE OF HIGH BACKGROUND
DATA POINT AT TIME   325898  SUSPECT BECAUSE OF HIGH BACKGROUND

HALFLIFE AND CORRECTION FACTORS USED
COMPONENT   HALFLIFE      STND CTR   STND SHELF  ACTUAL CTR ACTUAL SHELF  SSA CORR    SHELF CORR
    MO 99      2.75170E 00      6           5           6           5        1.0000E 00  1.0000E 00
    TC 99      2.52000E-01      0           0           6           5        1.0000E 00  1.0000E 00

RESULTS OF CALCULATION INVOLVING   22 DATA POINTS    OF WHICH    2 ARE SUSPECT AND    0 WERE REJECTED

COMPONENT   TOTCPM AT TO  SSA AND SHELF   TOTCPM AT TO    PERCENT
            UNCORRECTED   CORR FACTOR     CORRECTED       STND DEV
    MO 99   6.658640E 06   1.000000E 00   6.658640E 06     0.2329
    TC 99  -1.249525E 08   1.000000E 00  -1.249525E 08    -8.0872

CHI2 TEST ON PREVIOUS CALCULATION WAS AN UNSATISFACTORY        3.9734E 01
I AM REJECTING      2 SUSPICIOUS  POINTS AND RECALCULATING


RESULTS OF CALCULATION INVOLVING   22 DATA POINTS    OF WHICH    0 ARE SUSPECT AND    2 WERE REJECTED

COMPONENT   TOTCPM AT TO  SSA AND SHELF   TOTCPM AT TO    PERCENT
            UNCORRECTED   CORR FACTOR     CORRECTED       STND DEV
    MO 99   6.662359E 06   1.000000E 00   6.662359E 06     0.2791
    TC 99  -1.261532E 08   1.000000E 00  -1.261532E 08    -8.5523
```

Fig. 1. First Page of Output for a Decay-Curve Analysis of Data from a Single Sample by Use of the Brunhilde Code.

DATE OF THIS CALCULATION IS 12.280 C 7/21

F I N A L N U M B E R S F I N A L N U M B E R S F I N A L N U M B E R S F I N A L N U M B E R S
F I N A L N U M B E R S F I N A L N U M B E R S F I N A L N U M B E R S F I N A L N U M B E R S
F I N A L N U M B E R S F I N A L N U M B E R S F I N A L N U M B E R S

CODE NAME SCRAMBLED CARDS

EXPT	SAMPLE IDENT	ELEMENT IDENT	ZERO TIME	SAMPLE WT	WT100	SR90 WT ALIQUOT FACTOR	CHANNEL
22	011	42	60 321405	23.31	38.29	1.00 2.5000000E 01	0

TIME TMINUSTO	NETCPM	TOTCPM	WT FACTOR	DTPREVBKGD		DTSUBSBKGD		BKGD	PCTDEV	NOSIGUDEV	RLBLTY	STATUS
323516 2.110E 00	8.614E 04	3.5376E 06	5.9475E-03	0.02	105.4	0.59	108.2	105.5	0.071	0.242	340.6	OK
323732 2.325E 00	8.499E 04	3.4903E 06	1.8688E-02	0.23	105.4	0.38	108.2	106.5	-0.233	-1.392	595.7	OK
324142 2.735E 00	8.039E 04	3.3014E 06	1.9574E-02	0.03	108.2	0.39	102.7	107.8	0.745	4.265	576.7	OK
324562 3.155E 00	7.215E 04	2.9628E 06	2.6495E-02	0.03	102.7	0.40	106.0	103.0	-0.848	-5.151	602.1	OK
324992 3.585E 00	6.654E 04	2.7324E 06	3.3897E-02	0.03	106.0	0.41	107.1	106.1	1.413	8.749	628.1	OK
325436 4.029E 00	5.890E 04	2.4188E 06	3.7510E-02	0.03	107.1	0.43	984.1	172.1	0.230	0.	0.	REJECT
325898 4.490E 00	5.201E 04	2.1359E 06	4.7973E-02	0.03	984.1	0.43	199.0	925.4	-0.631	-0.	0.	REJECT
326351 4.943E 00	4.654E 04	1.9113E 06	6.1119E-02	0.02	199.0	0.09	105.4	181.1	-0.362	-2.141	589.9	OK
326545 5.137E 00	4.384E 04	1.8004E 06	7.2719E-02	0.03	108.8	1.01	106.0	108.7	-1.453	-8.936	606.2	OK
327389 5.983E 00	3.639E 04	1.4945E 06	1.7753E-02	0.88	108.8	0.16	106.0	106.5	1.241	3.047	248.6	OK
328160 6.755E 00	3.004E 04	1.2338E 06	1.2277E-02	0.03	106.0	0.56	106.0	106.0	1.508	2.536	170.7	OK
328751 7.346E 00	2.564E 04	1.0531E 06	1.4309E-02	0.03	106.0	0.56	106.0	106.0	0.549	0.859	157.3	OK
329342 7.937E 00	2.194E 04	9.0115E 05	1.6623E-02	0.03	106.0	0.56	106.0	106.0	-0.147	-0.214	145.1	OK
329936 8.531E 00	1.914E 04	7.8616E 05	1.8940E-02	0.03	106.0	0.56	109.3	106.2	1.169	1.561	135.1	OK
330531 9.126E 00	1.634E 04	6.7105E 05	2.2008E-02	0.03	109.3	0.57	108.2	109.3	0.318	0.394	124.3	OK
331129 9.724E 00	1.404E 04	5.7664E 05	2.5387E-02	0.03	108.2	1.20	107.1	108.2	0.219	0.250	114.7	OK
332359 1.095E 01	1.054E 04	4.3296E 05	3.3123E-02	0.03	107.1	0.58	104.9	107.0	2.574	2.469	98.4	OK
332967 1.156E 01	9.020E 03	3.7042E 05	7.9714E-02	0.03	104.9	0.48	105.3	105.0	2.272	2.900	130.6	OK
333844 1.244E 01	7.220E 03	2.9648E 05	9.8205E-02	0.01	105.4	0.23	106.4	105.5	2.093	2.378	116.0	OK
334 87 1.268E 01	6.618E 03	2.7179E 05	1.0645E-01	0.01	106.4	0.23	107.8	106.5	-0.500	-0.557	110.7	OK
334336 1.293E 01	6.417E 03	2.6353E 05	1.0951E-01	0.01	107.8	0.46	110.7	107.9	2.718	2.881	108.9	OK
334727 1.332E 01	5.715E 03	2.3468E 05	1.2178E-01	0.41	107.8	0.07	110.7	110.3	0.942	0.954	102.2	OK

DXODLM MATRIX SENSITIVITY OF COUNTS TO HALFLIFE

NUCLIDE	MO 99	TC 99	000000 0	000000 0	000000 0
MO 99	-1.19744E 00	-1.02884E-02	0.	0.	0.
TC 99	-1.00141E 01	-6.37667E 00	0.	0.	0.

CHI2 TEST VALUE IS 3.98E 01 CHI2 VALUE IS 2.57E 02
THE JIGGLE VALUE IS 1.0891E 00 PERCENT AFTER 13 ITERATIONS

SENSITIVITY OF CHI2 TO HALFLIFE
MO 99 4.74359E 02
TC 99 1.86282E 01

Fig. 2. Second Page of Output Data from the Brunhilde Code, Which Gives the Detailed Information on Which the Summary of Fig. 1 Was Based.

ERROR MATRIX

8.37990E 06	-1.37353E 07	0.	0.	0.
-1.37353E 07	7.42511E 07	0.	0.	0.

PERCENT OF EACH COMPONENT AT TIME OF EACH COUNT

NUCLIDE	MO 99	TC 99	000000 0	000000 0	000000 0
TMINUSTO					
2.110E 00	91.146	8.854	0.	0.	0.
2.325E 00	94.628	5.372	0.	0.	0.
2.735E 00	98.002	1.998	0.	0.	0.
3.155E 00	99.291	0.709	0.	0.	0.
3.585E 00	99.756	0.244	0.	0.	0.
4.029E 00	99.920	0.080	0.	0.	0.
4.490E 00	99.975	0.025	0.	0.	0.
4.943E 00	99.992	0.008	0.	0.	0.
5.137E 00	99.995	0.005	0.	0.	0.
5.983E 00	99.999	0.001	0.	0.	0.
6.755E 00	100.000	0.000	0.	0.	0.
7.346E 00	100.000	0.000	0.	0.	0.
7.937E 00	100.000	0.000	0.	0.	0.
8.531E 00	100.000	0.000	0.	0.	0.
9.126E 00	100.000	0.000	0.	0.	0.
9.724E 00	100.000	0.000	0.	0.	0.
1.095E 01	100.000	0.000	0.	0.	0.
1.156E 01	100.000	0.000	0.	0.	0.
1.244E 01	100.000	0.000	0.	0.	0.
1.268E 01	100.000	0.000	0.	0.	0.
1.293E 01	100.000	0.000	0.	0.	0.
1.332E 01	100.000	0.000	0.	0.	0.

CHI2 TEST ON PREVIOUS CALCULATION IS TOO HIGH 39.754 BUT NO POINTS ARE SUSPICIOUS

END OF PROBLEM

Fig. 2 (continued).

12. STATUS: Indicates the status of each point at the end of the final calculation.

The table in Fig. 2 titled "Percent of each component at time of each count" is presented as a convenience, so that the amount of each component present in the sample at any of the counting times can be seen at a glance. Column one lists the (time of count – zero time) in the same sequence as the main data table, while each of the following columns gives the abundance data pertinent to one of the nuclides being resolved. Each of the abundance values is calculated from the equation

$$(\text{PCTCNT})_i = \frac{|x_l\, e^{-\lambda_l t_i}|\ (100)}{\sum_{K=1}^{j} |X_K\, e^{-\lambda_K t_i}|}.$$

PRINTOUT OF DATA FOR REPLICATE SAMPLES

When the calculations on a sample and all of its replicates have been completed and all of their answers printed out, the computer skips to a new page and prints a summary sheet before going on to the next sample. This "Compiled Data Sheet" is intended to provide a concise summary of the more important data pertaining to the calculation of each of the replicate samples, plus average values, "*K* factors," and "*R* factors" for each of the components.

An example of a typical summary sheet is shown in Fig. 3. After the date, category, and experiment code name, the printout identifies the experiment, element, and sample numbers and then gives the zero time for the calculation. Next is presented a table of the results of the calculations on each of the replicate samples. This table first identifies the components and gives the half-lives that were used in resolving the curves; then, for each replicate sample, it gives the replicate number, the corrected total counts per minute at zero time, the percent standard deviation for each component, and, in the last column, the final "chi-squared test" value. The next line gives an arithmetical average of the "CPM" values of all of the replicate samples for each component plus a root-mean-square deviation of the replicate sample values from the arithmetical average, that is,

$$\text{AVCPM} = \frac{\sum_{\text{All Replicates}} (\text{TOTCPM CORR})_i}{\text{Number of Replicates}},$$

$$\text{PCTSTDEV} = \frac{\left\{\sum_{\text{All Replicates}} [(\text{TOTCPM CORR})_i - \text{AVCPM}]^2\right\}^{1/2}}{(\text{Number of Replicates}) - 1}.$$

The line labeled "Delta Fract Error" contains numbers pertaining to the calculation of the "WTDAVCPM" and "PCTERROR" columns of the next table. In this calculation it is assumed that there are two kinds of errors associated with the resolution of the decay curves of a set of replicate samples. The first is a purely statistical deviation of the actual counts from those that would have given a smooth curve, that is, the "Sigma" value from the least-squares resolution of the curves. The second is much more difficult to determine precisely, but it includes random

DATE OF THIS CALCULATION IS 12.255 C 7/21

PRELIMINARY NUMBERS PRELIMINARY NUMBERS PRELIMINARY NUMBERS PRELIMINARY NUMBERS
PRELIMINARY NUMBERS PRELIMINARY NUMBERS PRELIMINARY NUMBERS PRELIMINARY NUMBERS
PRELIMINARY NUMBERS PRELIMINARY NUMBERS PRELIMINARY NUMBERS PRELIMINARY NUMBERS

CODE NAME GNOME NOUGAT 3

COMPILED DATA FOR EXPT 3 ELEMENT 60 SAMPLE 6
TIME ZERO
61 344500

NUCLIDE	ND147	000000 0	000000 0	000000 0	000000 0
HALFLIFE	1.1040E 01	0.	0.	0.	0.

REPLICATE	CPM	PCTSTDEV	CPM	PCTSTDEV	CPM	PCTSTDEV	CPM	PCTSTDEV	CPM	PCTSTDEV	CHI2T
1	2.5348E 03	0.49	0.	0.	0.	0.	0.	0.	0.	0.	0.41
2	2.5117E 03	0.42	0.	0.	0.	0.	0.	0.	0.	0.	0.
	AV CPM		AV CPM		AV CPM		AV CPM		AV CPM		
	2.5232E 03	0.65	0.	0.	0.	0.	0.	0.	0.	0.	
DELTA FRACT ERROR		0.64		0.		0.		0.		0.	

COMPONENT	WTD AV CPM	PCT ERROR	CPM MO99	RATIO TO MO	PCT ERROR	K FACTOR	R FACTOR	PCT ERROR
ND147	2.5232E 03	4.5788E-01	1.2616E 05	1.9999E-02	5.0902E-01	1.3550E-02	1.4760E 00	1.0778E 00

REFERENCE GEOMETRY

COMPONENT	REF CTR 1 2 3 4 5	REF SHELF 1 2 3 4 5	STND CTR 1 2 3 4 5	STND SHELF 1 2 3 4 5	SAMPLE WTS	SR90 WTS	CH
REPLICATE							
1	5 0 0 0 0	9 0 0 0 0	5 0 0 0 0	9 0 0 0 0	5.33	1.00	0
2	5 0 0 0 0	9 0 0 0 0	5 0 0 0 0	9 0 0 0 0	4.64	1.00	0

CORRECTION FACTORS USED
SSA CORRECTION FACTORS

NUCLIDE	ND147	000000 0	000000 0	000000 0	000000 0
1	1.0000	0.	0.	0.	0.
2	1.0000	0.	0.	0.	0.

SHELF RATIO CORRECTION FACTORS

NUCLIDE	ND147	000000 0	000000 0	000000 0	000000 0
1	1.0000	0.	0.	0.	0.
2	1.0000	0.	0.	0.	0.

END OF PROBLEM

Fig. 3. A "Compiled Data Sheet" from a Calculation Using the Brunhilde Code.

errors not covered by the first category such as weighing errors, pipetting errors, etc. Thus each component in a series of replicate samples will have a series of answers plus a series of deviations, where each deviation may be considered as the sum of two terms, that is, $X_1 \pm \sigma_1 \pm \delta$, $X_2 \pm \sigma_2 \pm \delta$, $X_3 \pm \sigma_3 \pm \delta$, ... , $X_Q \pm \sigma_Q \pm \delta$. The "Delta" terms are assumed to be the same for each of the replicate samples. An arithmetical average of the answers is given by

$$\bar{X} = \frac{1}{Q} \sum_{Q} X_i ,$$

with a deviation of

$$\bar{\sigma} = \frac{1}{Q} \left(\sigma_1^2 + \sigma_2^2 + \sigma_3^2 + Q\delta^2 \right)^{1/2} = \frac{1}{Q} \left(\sum_{Q} \sigma_i^2 + Q\delta^2 \right)^{1/2} .$$

The mean square deviation of the replicate answers from the average answer is given by

$$\bar{\sigma}^2 = \frac{\sum_{Q} (X_i - \bar{X})^2}{Q(Q-1)} .$$

Substituting this value of $\bar{\sigma}^2$ in the previous equation and solving for δ^2 gives

$$\delta^2 = \frac{Q^2 \bar{\sigma}^2 - \sum_{Q} \sigma_i^2}{Q} .$$

Since the statistical counting errors are usually less than other random errors associated with replicate samples, the $(Q^2 \bar{\sigma}^2)$ term dominates, and δ^2 is positive.

With δ^2 determined, a "weighted average" of the replicate answers may be obtained using the combined deviation $(\sigma_i + \delta)$ for each sample, that is,

$$(\mathrm{WTDAV}) = \frac{\sum_{Q} \left(\frac{X_i}{\sigma_i^2 + \delta^2} \right)}{\sum_{Q} \left(\frac{1}{\sigma_i^2 + \delta^2} \right)} ,$$

and the overall error of the weighted average may be calculated from the combined deviations of all of the replicates:

$$\bar{\sigma}_{\mathrm{final}} = \frac{\left(\sum_{Q} \frac{1}{\sigma_i^2 + \delta^2} \right)^{1/2}}{\sum_{Q} \frac{1}{\sigma_i^2 + \delta^2}} = \frac{1}{\left(\sum_{Q} \frac{1}{\sigma_i^2 + \delta^2} \right)^{1/2}} .$$

In the Brunhilde code printout, all of the error data are printed as percent, that is, the "PCTSTDEV" values are obtained from $100\,\sigma_i/X_i$. Similarly, the "Delta Fract Error" terms are calculated from $100[\delta/(\text{WTDAV})]_i$, and the "PCT ERROR" of the weighted average is calculated from $100[\bar{\sigma}_{\text{final}}/(\text{WTDAV})]_i$.

The most important part of the "Compiled Data" sheet is the table giving the final answers for all of the replicate samples. Progressing by column headings, this table contains:

1. COMPONENT: The symbol and mass number for each component.
2. WTD AV CPM: The "weighted average count per minute" value, calculated as described in the previous section.
3. PCT ERROR: The "final" error value for the "WTD AV CPM" term, obtained as described in the previous section.
4. CPM MO99: If Mo^{99} data are available this column will contain the Mo^{99} value which is used to obtain the "Ratio to Mo" number in the next column.
5. RATIO TO MO: (WTD AV CPM)/ (CPM MO99).
6. PCT ERROR: The "percent error" of the "Ratio to Mo" number, obtained from:

$$(\text{PCT ERROR})_i = \left[\left(\bar{\sigma}^2_{\text{final}} \right)^2_{\text{Mo}} + \left(\bar{\sigma}_{\text{final}} \right)^2_i \right]^{1/2} .$$

7. K FACTOR: If "R" factors are to be calculated, this column contains the thermal neutron "Ratio to Mo" value for this nuclide.
8. R FACTOR: Contains the value for the term (RATIO TO MO)/(K FACTOR).
9. PCT ERROR: The "percent error" of the "R Factor" number, obtained from

$$(\text{PCT ERROR})_i = \left[\left(\bar{\sigma}_{\text{final}} \right)^2_i + \left(\bar{\sigma}_{\text{final}} \right)^2_{\text{Mo}} + \left(\bar{\sigma}_{\text{final}} \right)^2_{\text{K Factor}} \right]^{1/2} .$$

For Mo^{99} samples, this table of final answers is modified somewhat. Columns 1, 2, and 3 are the same as for other nuclides. The remaining columns are as follows:

4. K FACTOR: Contains a number representing the number of fissions of U^{235} with thermal neutrons that are required to give one Mo^{99} count in the "standard" Mo^{99} counting geometry.
5. FISSIONS: Contains the product $(\text{WTDAV})_i$ (K FACTOR).
6. PCT ERROR: The "percent error" of the "fissions" number, obtained from

$$(\text{PCT ERROR})_i = \left[\left(\bar{\sigma}_{\text{final}} \right)^2_i + \left(\bar{\sigma}_{\text{final}} \right)^2_{\text{K Factor}} \right]^{1/2} .$$

The remainder of the "Compiled Data" sheet for replicate samples is devoted to a summary of the kind of information which is not normally needed but which can be of value in explaining poor results. It also permits a rapid check to be made of all counting geometries and correction factors to ensure that all replicates are calculated in the same manner.

The first portion of this summary is the "Reference Geometry" table, which contains information on the "standard" counting geometry and the actual counting geometry

for each of the components and each of the replicates. One row of this table is used for each of the replicates. The columns are arranged as follows:

1. REPLICATE: Contains the replicate number.
2. REF CTR: Is actually made up of five columns, one for each component, numbered 1, 2, 3, 4, 5. Each column contains the number of the counter for which the "WTD AV CPM" value of that component was calculated in the previous table. If no shelf ratio corrections were made on that component, the number will be the actual counter number. If a shelf ratio correction was used, the number will be the counter to which the original count was corrected.
3. REF SHELF: Arranged in the same manner as the "Ref Ctr" column. The combined "Ref Ctr" and "Ref Shelf" numbers give the counter and shelf numbers for which the data in the "WTD AV CPM" column were calculated.
4. STND CTR: Arranged in the same manner as the previous two columns. Contains the "standard counter" number for each component of each replicate.
5. STND SHELF: Arranged in the same manner as the previous three columns. Contains the "standard shelf" number for each component of each replicate.
6. SAMPLE WTS: Contains the sample weight of each replicate sample.
7. SR90 WTS: Contains the Sr^{90} weight of each replicate sample.

The "CORRECTION FACTORS USED" table contains a summary of all the SSA and shelf ratio corrections used for each component of each replicate sample. One column, headed by the element symbol and mass number, is used for each component; one row is used for each replicate sample in each of the "SSA" and "shelf ratio" portions of the table. The replicate numbers are given in column one.

With these data it is possible to determine at a glance the status of any of the "WTD AV CPM" numbers. Thus, if all of the numbers in column 1 of the "Ref Ctr" column are the same as their corresponding numbers in column 1 of the "STND CTR" column, and if the numbers in column 1 of the "REF SHELF" column are the same as those in column 1 of the "STND SHELF" column, the "WTD AV CPM" value for the first component was calculated for that nuclide's standard geometry. If the shelf ratio corrections for that nuclide are all 1.00, the sample was counted in its "standard geometry" position.

In addition to summarizing the answers to replicate answers for a given nuclide and experiment, the Brunhilde code summarizes all answers for all nuclides in a given experiment on one sheet. This type of tabulation is very convenient when a concise tabulation is desired but the numbers are changed frequently; the computer is used to keep all records up to date instead of this having to be done by hand. The kind of information used in this tabulation and its arrangement in the printout are rather specialized features of the code that are better tailored to suit each user, so no example of the printout is given here.

In summary, the Brunhilde code has been found most satisfactory for resolving most of the radioactive decay curves obtained in our laboratory. The provisions under which the computer inspects the input data, applies any desired shelf, counter, or self-scattering corrections, evaluates the fit of the data points to the calculated curve, and estimates the precision of the entire calculation are such that, on the average, the machine resolution of these decay curves gives better results than those that can be obtained by hand. Not the least advantage to this type of operation is the speed of the calculation. On the IBM 7090 a typical calculation involving 30 data points and including data read-in and evaluation, resolution of three components, recalculation if

necessary, printout of answers, and tabulation of collected data will take about ten seconds of machine time.

REFERENCE

[1] R. Von Holdt, *Proceedings of the Western Computer Conference* (1959).

(1-3) CLSQ, THE BROOKHAVEN DECAY CURVE ANALYSIS PROGRAM[1]

J. B. Cumming
Chemistry Department, Brookhaven National Laboratory, Upton, L.I., New York

INTRODUCTION

A program for the analysis of multicomponent decay curves by a least-squares procedure has been coded for an IBM 7090 computer. The FORTRAN language has been used for the main calculation and FAP for some of the subroutines. Provision for determining half-lives of the nuclear species is provided by an iterative routine starting from a set of trial values. The general philosophy adopted in coding this problem has been to give the user considerable flexibility in data handling.

MATHEMATICAL METHOD

The data of a radioactive decay curve consist of n measurements of the counting rates, f_i, of the sample at times t_i. If m independent nuclear species are present, then the set of data satisfies n equations of the form

$$f_i = \sum_{j=1}^{m} x_j e^{-\lambda_j t_i} + v_i , \qquad (1)$$

where an individual term in the sum, $x_j e^{-\lambda_j t_i}$, represents the contribution of the jth component to the total activity at time t_i. The residual, v_i, at that point is due to statistical fluctuations and experimental errors. Since the m coefficients x_j enter

[1]Research performed under the auspices of the U.S. Atomic Energy Commission.

these equations linearly, a solution by the least-squares method is possible. The condition for such a solution is that

$$\sum_{i=1}^{n} p_i v_i^2 = \text{minimum} , \tag{2}$$

where p_i is the weight assigned to the square of each residual. In terms of the standard deviation, σ_i, of the ith counting rate

$$p_i = 1/\sigma_i^2 . \tag{3}$$

It is convenient to adopt the matrix notation of Hamilton and Schomaker [*1*] and used by Harmer [*2*]. In this notation, Eqs. (1) and (2) become

$$F_{n1} = A_{nm} X_{m1} + V_{n1} , \tag{4}$$

and

$$V'_{n1} P_{nn} V_{n1} = \text{minimum} . \tag{5}$$

In Eqs. (4) and (5) the subscripts indicate the dimensions (rows and columns respectively) of the matrices. The symbol V'_{n1} represents the transpose of matrix V_{n1}. The least-squares solution for the matrix of the unknown coefficients, X_{m1}, is given by

$$A'_{nm} P_{nn} F_{n1} = A'_{nm} P_{nn} A_{nm} X_{m1} . \tag{6}$$

To solve this equation for X_{m1}, we define

$$B_{mm} = A'_{nm} P_{nn} A_{nm} . \tag{7}$$

The B_{mm} matrix is inverted to obtain B_{mm}^{-1} and the solution for the unknown coefficient matrix is given by

$$X_{m1} = B_{mm}^{-1} A'_{nm} P_{nn} F_{n1} . \tag{8}$$

The variance of the ith coefficient is obtained from the corresponding diagonal element of B_{mm}^{-1},

$$\sigma_{x_i}^2 = (B_{mm}^{-1})_{ii} . \tag{9}$$

The decay constants, λ, do not enter linearly in Eq. (1); hence, a least-squares solution for their best values is not possible. However, if the terms are expanded in terms of small changes, δx_j and $\delta\lambda_j$, from a set of initial guesses x_j^0 and λ_j^0 as shown below,

$$(x_j^0 + \delta x_j)\, e^{-(\lambda_j^0 + \delta\lambda_j)t_i} \approx (x_j^0 + \delta x_j)\, e^{-\lambda_j^0 t_i} - x_j^0 \delta\lambda_j t_i\, e^{-\lambda_j^0 t_i} \tag{10}$$

a solution for the $\delta\lambda$ terms is now possible. An iterative procedure may then be used until any desired degree of convergence is attained. (A convergent solution will not necessarily be obtained in all cases.) In the matrix notation, one extra column of the

form $t_i e^{-\lambda_j t_i}$ is added to A_{nm} for each unknown half-life, and one extra row is added to X_{m1}.

THE CLSQ PROGRAM

The CLSQ decay curve analysis program has been coded for operation on an IBM 7090 under control of the FORTRAN Monitor System. It is designed to process sequentially an unlimited (subject to time limitations only) number of problems. Each problem has arbitrarily been limited to 200 data points and 10 components. The input

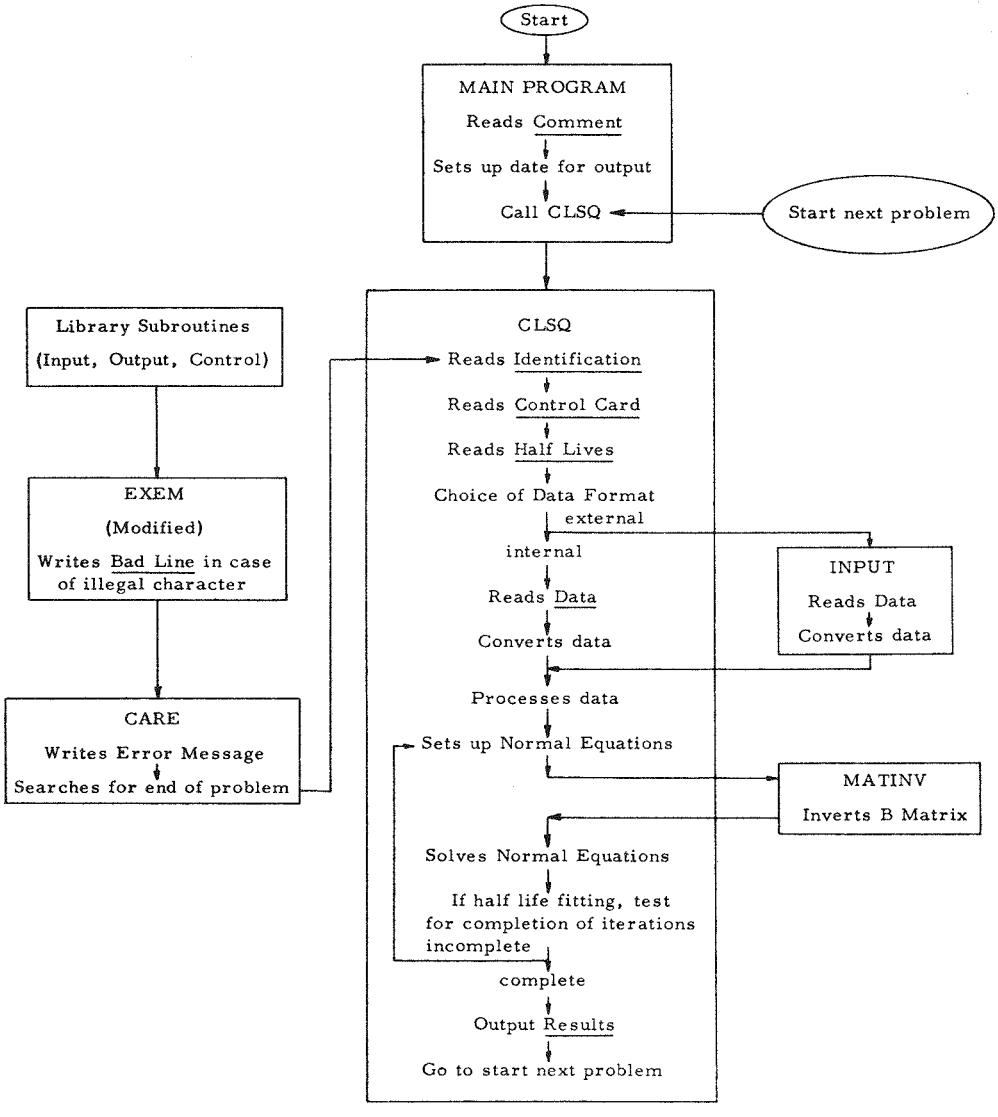

Figure 1.

data are initially punched on cards which are then transferred to magnetic tape by an IBM 1401 for input to the IBM 7090. An organizational diagram (not a true flow diagram) is shown in Fig. 1. The overall program has been coded as a main program and various subroutines and will now be discussed.

The *Main Program* (MNPRØ) is coded in FAP. It is entered at the start of each run and reads 42 alphanumeric characters (7 six-character words) from one card as a *Comment* (CØMNT) [3]. It then acquires the date from memory and sets it up for output with CØMNT as an output heading on each problem. Control is then transferred to CLSQ.

CLSQ (FORTRAN coded) is the major subroutine in the present program. On entry from MMPRØ it reads 72 alphanumeric characters to serve as *Identification* (NAME) of the particular problem (subheading on output). It then reads a *Control Card* which selects the various calculational and input options and supplies necessary parameters. Figure 2 shows the format of the Control Card. The number of

CLSQ DECAY CURVE ANALYSIS PROGRAM, INPUT DATA

	1	2	3	4	5	6	7	8	9	10	11	12	13	14	15	16	17	18	19	20	21	22	23	24	25	26	27	28	29	30	31	32	33	34	35	36	37	38	39	40	41	42
IDENTIFICATION	C	U	M	M	I	N	G		A	G	S	-	2	3		U	+	D		W	-	3																				
	NC		NV			CNV						BGD				SIGMA			BGD		IN		IT		BLOCK		SCOFF		RJT		KCS									
CONTROL		5			1			.	0	5	1	2	5	.				5	.			1					5		.	5												
	HALF LIFE					UNIT																																				
HALF LIVES	1	1	2	.		M																																				
		1	0	.		M																																				
		2	0	.	4	M																																				
		1	5	.		H																																				
			1	.		Y																																				

NOTES: 1. HALF LIFE UNITS ARE M,H,D OR Y.
2. BLOCK TO CONTAIN COUNTER DEADTIME IN μSEC.
3. SCOFF SETS % SIGMA CUT OFF ON RATES.
4. DECIMAL POINTS TO BE PLACED IN DOTTED COLUMNS WHERE SHOWN.
5. – IN COLUMN 12 OF CONTROL CARD CAUSES INDIVIDUAL BACKGROUND SUBTRACTION.
6. LAST DATA CARD MUST HAVE END IN COLUMNS 40, 41, & 42 AND EOB UNDER STARTING TIME.

Figure 2.

components, NC, is given in columns 2 and 3. In column 6 the number, NV, of unknown half-lives is specified. The program will treat the first NV of the NC components as variable. The limitation

$$NC + NV \leqq 10 \tag{11}$$

has been imposed arbitrarily. In columns 9, 10, and 11 a number CNV (.05 in the example) is supplied to govern how far the iterations will proceed. Iterations will be continued until the ratio of change in the decay constant to the standard deviation of the decay constant is less than CNV for all NV variable half-lives. If CNV is zero a maximum of nine iterations will be performed.

In columns 12 through 17 the counter background is entered for subtration from the data. A background standard deviation may be entered in columns 18 through 23 for root-mean-square addition to the standard deviation of each point. An option here (in conjunction with the external input only) allows subtraction of backgrounds which vary from point to point on the curve. To use this, a negative background is entered. This is ignored and background subtraction is performed by the INPUT subroutine.

Columns 24 and 25 (IN) specify the input data format. A zero or blank causes CLSQ to use its own input format while a positive integer transfers to the external subroutine INPUT as shown in Fig. 1.

Columns 26 and 27 (IT) are normally left blank. A number punched in this field causes output of intermediate matrices and a check of the inversion routine by multiplication

$$B^{-1}_{mm} B_{mm} = U_{mm} . \tag{12}$$

Columns 28, 29, and 30 (BLOCK) are the *counter dead time* in microseconds (5 μsec in the example of Fig. 2).

Columns 31, 32, and 33 (SCOFF) set a cutoff (in percent) on the smallest value at which the program will use the standard deviation from statistics alone. In the example the standard deviation of any point will never be less than 0.5% of the rate, regardless of how many counts may have been recorded.

Columns 34, 35, and 36 (RJT) if not blank or zero cause the program to examine its output and reject those points which fall further than RJT times the standard deviation from the curve. The fit is then repeated.

A number in column 38 (KCS) causes the program to enter a *known component subtraction* routine which treats the last KCS of the half-lives as having known intercepts. It reads these intercepts from cards after the data are input, and appropriately subtracts these components from the decay curve before fitting. KCS cannot exceed 5 and the sum NC + NV + KCS cannot exceed 10.

After reading the information on the control card, CLSQ then reads the list of NC half-lives (one per card). The first NV of these are considered first guesses. Half-life units may be minutes (M), hours (H), days (D), or years (Y). If no unit is given it is taken to be M. For internal use, decay constants in min^{-1} are calculated.

The data from the decay curve are now read in. The external subroutine INPUT (coded in FORTRAN and called by IN=1 on the control card) has been used most frequently. Its input format is shown in Fig. 3. For each point the subroutine calculates the counting rate, its variance, and the time (in minutes) at the midpoint of the count. Point by point background subtraction is also performed if called for by a negative background on the control card. Control is then returned to CLSQ. The internal input of CLSQ reads midpoint time, counting rate, and variance for each point in a 3E13.6 format. In either input, the last data card is either blank or contains a time which will be interpreted as the time of the end of bombardment.

After rates, variances, and midtimes are calculated, CLSQ converts times to times relative to the first count, corrects for deadtime, subtracts background, applies the SCOFF criterion to the variances, and performs the KCS option if called for. The intercepts of the known components and their standard deviations are obtained from cards which follow the end of bombardment card. The format is 2E13.5 with one intercept and its standard deviation on each card.

The program now proceeds to set up the necessary equations for the least-squares analysis as outlined above. Inversion of the B matrix is accomplished by the subroutine MATINV [4] and the normal equations are solved. If half-lives were to be determined, this first pass considered them fixed at the initial guesses. This pass then supplies the initial guesses for the intercepts which are used in the next iterative analysis. Results of the first pass are also output for comparison. A typical

CLSQ DECAY CURVE ANALYSIS PROGRAM, INPUT DATA

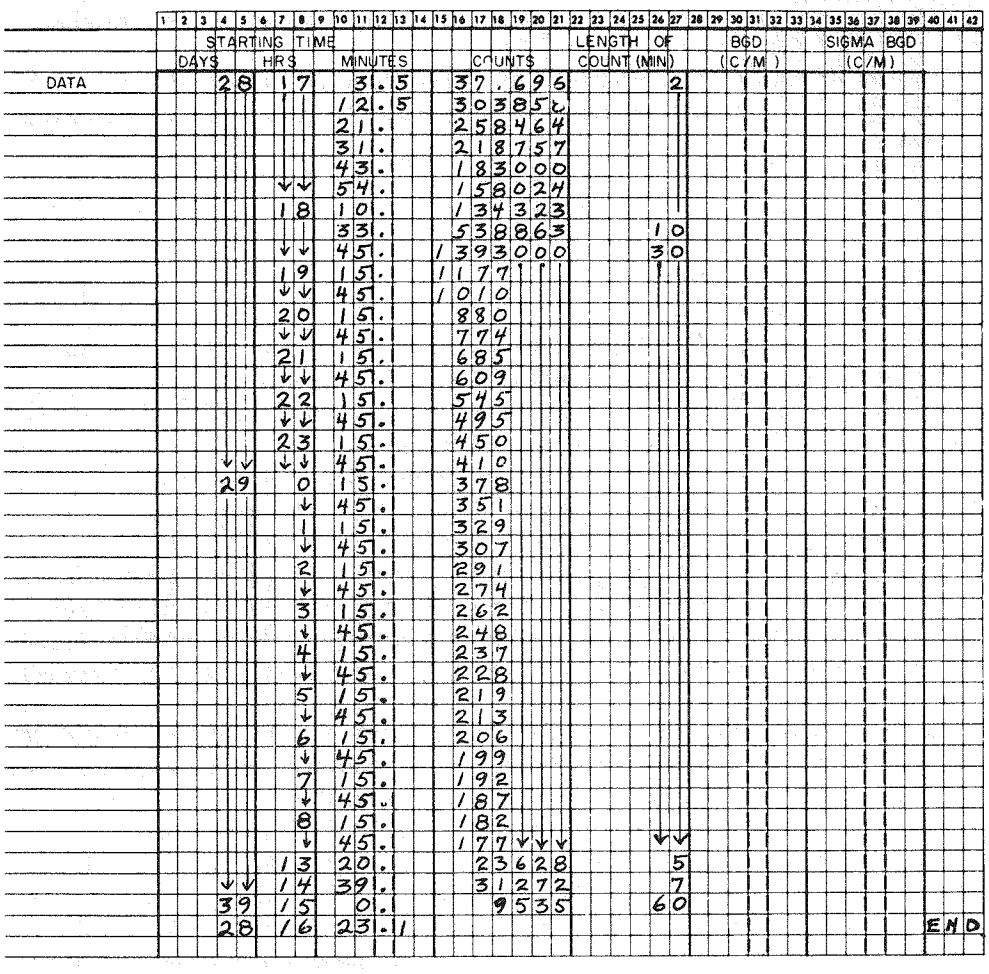

Figure 3.

output is shown in Fig. 4. The quantity FIT is given by

$$\text{FIT} = \sqrt{\frac{V'_{n1} P_{nn} V_{n1}}{n-m}} \,. \tag{13}$$

It should be pointed out that $V'_{n1} P_{nn} V_{n1}$ is essentially χ^2 for the number of degrees of freedom $(n-m)$. Its expectation value is $(n-m)$ and its variance is $2(n-m)$.

If half-lives are to be fitted, the program now proceeds to perform the necessary operations. The changes in a given decay constant at each iteration are damped so that they can never exceed one-half the value of the decay constant. Each change in a decay constant is also tested to ensure convergence. There is some evidence that the test for convergence in the present program is too strong and should be relaxed to allow a slightly larger change to follow a smaller one. When all changes in

```
CLSQ DECAY CURVE ANALYSIS PRØGRAM          10/03/62

CUMMING AGS-23 U+D W-3

NP= 4C NC= 5 NV=0 CNV=0.05 BGD=125.00 SBGD= 5.00 BLØCK= 5.0 SCØFF=0.5 RJT=-0.  KCS=0

          HALF LIFE  SIGMA H    CPM AT E0B      SIGMA     DECAY FACTØR
CØMP( 1)   112.000M   0.   M  0.88832E 05   0.25032E 03   0.12920E 01
CØMP( 2)    10.000M   0.   M  0.11027E 06   0.33324E 05   0.17631E 02
CØMP( 3)    20.400M   0.   M  0.41368E 06   0.59996E 04   0.40824E 01
CØMP( 4)    15.000H   0.   H  0.11904E 05   0.20326E 02   0.10324E 01
CØMP( 5)     1.000Y   0.   Y  0.36485E 02   0.53433E 01   0.10001E 01

FIT=  0.956

    T(I)          F(I)          FCALC(I)          V(I)          SIGMAF(I)      RATIØ(I)
 0.            0.18865E 06   0.18791E 06   0.74564E 03   0.94326E 03     0.79
 0.90000E C1   0.15376E 06   0.15450E 06  -0.74583E 03   0.76878E 03    -0.97
 0.17500E 02   0.13052E 06   0.13088E 06  -0.36405E 03   0.65258E 03    -0.56
 0.27500E C2   0.11026E 06   0.11005E 06   0.20730E 03   0.55131E 03     0.38
 0.39500E C2   0.92079E 05   0.91946E 05   0.13366E 03   0.46040E 03     0.29
 0.50500E C2   0.79412E 05   0.79835E 05  -0.42331E 03   0.39706E 03    -1.07
 0.66500E C2   0.67415E 05   0.67190E 05   0.22559E 03   0.33708E 03     0.67
 0.93500E C2   0.54005E 05   0.53549E 05   0.45598E 03   0.27002E 03     1.69
 0.11550E 03   0.46489E 05   0.46229E 05   0.25994E 03   0.23245E 03     1.12
 0.14550E 03   0.39237E 05   0.39007E 05   0.23054E 03   0.19619E 03     1.18
 0.17550E 03   0.33637E 05   0.33575E 05   0.61483E 02   0.16818E 03     0.37
 0.20550E 03   0.29280E 05   0.29246E 05   0.34048E 02   0.14640E 03     0.23
 0.23550E C3   0.25731E 05   0.25696E 05   0.35137E 02   0.12865E 03     0.27
 0.26550E 03   0.22752E 05   0.22742E 05   0.10188E 02   0.11376E 03     0.09
 0.29550E 03   0.20209E 05   0.20266E 05  -0.56991E 02   0.10105E 03    -0.56
 0.32550E 03   0.18069E 05   0.18183E 05  -0.11353E 03   0.90346E 02    -1.26
 0.35550E 03   0.16398E 05   0.16423E 05  -0.25018E 02   0.81989E 02    -0.31
 0.38550E 03   0.14894E 05   0.14931E 05  -0.37617E 02   0.74469E 02    -0.51
 0.41550E 03   0.13557E 05   0.13664E 05  -0.10631E 03   0.67786E 02    -1.57
 0.44550E C3   0.12488E 05   0.12582E 05  -0.93687E 02   0.62441E 02    -1.50
 0.47550E 03   0.11586E 05   0.11656E 05  -0.69148E 02   0.57932E 02    -1.19
 0.50550E 03   0.10852E 05   0.10859E 05  -0.70879E 01   0.54259E 02    -0.13
 0.53550E C3   0.10117E 05   0.10170E 05  -0.53183E 02   0.50585E 02    -1.05
 0.56550E 03   0.95829E 04   0.95722E 04   0.10619E 02   0.47914E 02     0.22
 0.59550E 03   0.90153E 04   0.90500E 04  -0.34689E 02   0.45077E 02    -0.77
 0.62550E 03   0.86147E 04   0.85913E 04   0.23448E 02   0.43074E 02     0.54
 0.65550E 03   0.81474E 04   0.81858E 04  -0.38472E 02   0.40737E 02    -0.94
 0.68550E 03   0.77802E 04   0.78253E 04  -0.45071E 02   0.38901E 02    -1.16
 0.71550E 03   0.74798E 04   0.75025E 04  -0.22689E 02   0.37399E 02    -0.61
 0.74550E C3   0.71795E 04   0.72117E 04  -0.32211E 02   0.35897E 02    -0.90
 0.77550E 03   0.69792E 04   0.69478E 04   0.31367E 02   0.34896E 02     0.90
 0.80550E 03   0.67456E 04   0.67070E 04   0.38621E 02   0.33728E 02     1.15
 0.83550E 03   0.65120E 04   0.64857E 04   0.26319E 02   0.32560E 02     0.81
 0.86550E 03   0.62784E 04   0.62811E 04  -0.27102E 01   0.31392E 02    -0.09
 0.89550E 03   0.61116E 04   0.60909E 04   0.20632E 02   0.30558E 02     0.68
 0.92550E 03   0.59447E 04   0.59132E 04   0.31577E 02   0.29724E 02     1.06
 0.95550E C3   0.57779E 04   0.57461E 04   0.31773E 02   0.28890E 02     1.10
 0.12180E 04   0.46025E 04   0.45858E 04   0.16670E 02   0.31147E 02     0.54
 0.12980E C4   0.43441E 04   0.43018E 04   0.42253E 02   0.25753E 02     1.64
 0.15745E C5   0.33919E 02   0.35796E 02  -0.18774E 01   0.52582E 01    -0.36
```

Figure 4.

decay constants satisfy the CNV requirement the program proceeds to output the results as shown in Fig. 5. By comparison with Fig. 4 it is seen that FIT is significantly improved by inclusion of the variable half-life and that 110 min is a better value than the first guessed 112-min value.

Since the present program runs under control of the FORTRAN Monitor, a change has been made in the library routine EXEM. Rather than skipping the entire days' run in case of an illegal character in the input, EXEM now writes out the bad line and transfers to subroutine CARE as shown in Fig. 1. CARE then searches for a

```
CLSQ DECAY CURVE ANALYSIS PRØGRAM          10/03/62

CUMMING AGS-23 U+D W-3


NP= 4C NC= 5 NV=1 CNV=0.05 BGD=125.00 SBGD= 5.00 BLØCK= 5.0 SCØFF=0.5 RJT=-0.  KCS=0


   ITERATIØNS PERFØRMED= 3  CØNVERGENT


            1ST CØMP       2ND CØMP       3RD CØMP       4TH CØMP       5TH CØMP
   D       0.630442E-02
DELTA( 2)  0.115122E-03
DELTA( 3)  0.48C803E-06
 SIGMA     0.265903E-04


         HALF LIFE  SIGMA H    CPM AT E0B      SIGMA      DECAY FACTØR
CØMP( 1)  109.946M   0.464M  0.91337E 05  0.54585E 03  0.12982E 01
CØMP( 2)   10.000M   0.    M  0.18830E 06  0.37895E 05  0.17631E 02
CØMP( 3)   20.4C0M   0.    M  0.39086E 06  0.79976E 04  0.40824E 01
CØMP( 4)   15.000H   0.    H  0.11993E 05  0.28498E 02  0.10324E 01
CØMP( 5)    1.000Y   0.    Y  0.34733E 02  0.53580E 01  0.10001E 01


FIT=  0.614

    T(I)          F(I)          FCALC(I)        V(I)          SIGMAF(I)      RATIØ(I)
 0.              0.18865E 06   0.18843E 06   0.22546E 03   0.94326E 03     0.24
 0.90000E C1     0.15376E 06   0.15429E 06  -0.52894E 03   0.76878E 03    -0.69
 0.17500E C2     0.13052E 06   0.13050E 06   0.11999E 02   0.65258E 03     0.02
 0.27500E C2     0.11026E 06   0.10976E 06   0.49989E 03   0.55131E 03     0.91
 0.39500E C2     0.92079E 05   0.91857E 05   0.22217E 03   0.46040E 03     0.48
 0.50500E C2     0.79412E 05   0.79918E 05  -0.50599E 03   0.39706E 03    -1.27
 0.66500E C2     0.67415E 05   0.67436E 05  -0.20541E 02   0.33708E 03    -0.06
 0.93500E 02     0.54005E 05   0.53876E 05   0.12840E 03   0.27002E 03     0.48
 0.11550E 03     0.46489E 05   0.46526E 05  -0.37102E 02   0.23245E 03    -0.16
 0.14550E 03     0.39237E 05   0.39218E 05   0.18995E 02   0.19619E 03     0.10
 0.17550E C3     0.33637E 05   0.33700E 05  -0.63301E 02   0.16818E 03    -0.38
 0.20550E 03     0.29280E 05   0.29301E 05  -0.20442E 02   0.14640E 03    -0.14
 0.23550E 03     0.25731E 05   0.25699E 05   0.32104E 02   0.12865E 03     0.25
 0.26550E 03     0.22752E 05   0.22710E 05   0.42190E 02   0.11376E 03     0.37
 0.29550E 03     0.20209E 05   0.20212E 05  -0.29536E 01   0.10105E 03    -0.03
 0.32550E 03     0.18069E 05   0.18117E 05  -0.47264E 02   0.90346E 02    -0.52
 0.35550E 03     0.16398E 05   0.16351E 05   0.46320E 02   0.81989E 02     0.56
 0.38550E C3     0.14894E 05   0.14860E 05   0.33724E 02   0.74469E 02     0.45
 0.41550E 03     0.13557E 05   0.13596E 05  -0.38431E 02   0.67786E 02    -0.57
 0.44550E 03     0.12488E 05   0.12520E 05  -0.31518E 02   0.62441E 02    -0.50
 0.47550E C3     0.11586E 05   0.11600E 05  -0.14042E 02   0.57932E 02    -0.24
 0.50550E 03     0.10852E 05   0.10811E 05   0.40266E 02   0.54259E 02     0.74
 0.53550E 03     0.10117E 05   0.10131E 05  -0.13802E 02   0.50585E 02    -0.27
 0.56550E 03     0.95829E 04   0.95407E 04   0.42141E 02   0.47914E 02     0.88
 0.59550E 03     0.90153E 04   0.90260E 04  -0.10689E 02   0.45077E 02    -0.24
 0.62550E 03     0.86147E 04   0.85743E 04   0.40403E 02   0.43074E 02     0.94
 0.65550E 03     0.81474E 04   0.81754E 04  -0.27998E 02   0.40737E 02    -0.69
 0.68550E 03     0.77802E 04   0.78207E 04  -0.40474E 02   0.38901E 02    -1.04
 0.71550E 03     0.74798E 04   0.75032E 04  -0.23356E 02   0.37399E 02    -0.62
 0.74550E 03     0.71795E 04   0.72170E 04  -0.37542E 02   0.35897E 02    -1.05
```

Figure 5.

card with the characters END in columns 40, 41, and 42; hence, this word should appear in this location on the last card of each problem. On finding an END it then transfers to CLSQ and starts the next problem.

Further details on the program may be obtained from the author.

CONCLUSIONS

Experience has shown that when such a program is available it will be used for analyses of most decay data with a considerable saving in time over graphical procedures. Furthermore its results are not subjective and its error estimates are considerably more meaningful than those guessed from the graphical analyses. Small

effects, such as presence of impurities or improper half-lives which would not have been seen in a graphical analysis, become apparent in the least-squares procedure.

The author is indebted to Mrs. R. Larsen and Mr. K. Fuchel for their assistance during the coding of this problem.

REFERENCES

[1] W. Hamilton and V. Schomaker (unpublished).

[2] D. S. Harmer, BNL 544(T-141) (1959) (unpublished). Note: The present paper has interchanged the notation for the X and A matrices from that used by Harmer.

[3] During current operation, CØMNT reads "CLSQ Decay Curve Analysis Program." However, CØMNT offers a convenient way to wish users of the program a "Merry Christmas," etc.

[4] This program, share distribution No. 664 AN F402, was coded by B. S. Garbow, Argonne National Laboratory (1959).

(1-4) ANALYSIS OF MULTICOMPONENT DECAY CURVES BY USE OF FOURIER TRANSFORMS

Donald G. Gardner
Department of Chemistry, Illinois Institute of Technology
Chicago 16, Illinois

and

Jeanne C. Gardner
Department of Chemistry, College of Pharmacy, University of Illinois
Chicago 12, Illinois

INTRODUCTION

Frequently it happens that experimental data may best be represented by a sum of exponentials of the form

$$f(t) = \sum_{i=1}^{n} N_i^0 \exp(-\lambda_i t) . \qquad (1)$$

The problem is not one of mere curve fitting because the parameters have physical significance. Therefore it is necessary that the true parameters be accurately estimated. This implies that the number of components n must also be determined, for if

n is not known, any "accurate" estimation of the parameters begins to lose its meaning.

The two essential difficulties that are inherent in the problem are that we must deal with data that only approximate $f(t)$ over a finite range in t, and that the exponential series possesses such strongly nonorthogonal properties that the parameters are extremely sensitive to minor fluctuations in the data. In certain fields of research, experimental techniques have reached such a level of automated excellence that the experimenter is overwhelmed by great amounts of very good data. In such fields the first difficulty may no longer exist. Since the data themselves are becoming more reliable, the method of analyzing the data assumes greater importance. High-speed computers now make it possible to investigate mathematical methods for treating data that were too laborious to use in the past. In spite of the increasing accuracy of the data, the nonorthogonal properties of the exponential series still poses a formidable problem.

The approach to the solution of this problem that will be described here has undergone a preliminary evaluation by L. Laush, W. Meinke, and the present authors, and the results were published [1] in 1959. At that time only the problem of separated and unrelated components was considered. Recently work on this problem was resumed, particularly with reference to the case of chain-type interactions wherein one component is produced as the result of the disappearance of another component.

The growth and decay problem may also be expressed as a sum of exponentials; however, the coefficients will in general no longer be positive. Consider for example, a situation where

$$\text{Species } 1 \longrightarrow \text{Species } 2 \longrightarrow \text{Species } 3.$$

This would be termed a two-component decay chain, and if only Species 1 were present at time zero, then

$$f(t) = N_1^0 \left(1 + \frac{\lambda_2}{\lambda_2 - \lambda_1}\right) e^{-\lambda_1 t} - \frac{\lambda_1}{\lambda_2 - \lambda_1} N_1^0 e^{-\lambda_2 t} . \tag{2}$$

Depending on the relative sizes of the λ_i values, the second coefficient could be negative.

SOLUTION BY FOURIER TRANSFORMS

In ref [1] mention is made of previous approaches to this problem, and this discussion will not be repeated here. The present approach is based on the fact that the exponential series may be represented by a Laplace integral equation:

$$f(t) = \sum_{i=1}^{n} N_i^0 \exp(-\lambda_i t) = \int_0^\infty g(\lambda) \exp(-\lambda t)\, d\lambda . \tag{3}$$

Here $g(\lambda)$ is a sum of delta functions, but due to the error inherent in the experimental estimate of $f(t)$ and in the numerical computations necessary to obtain $g(\lambda)$, a plot of $g(\lambda)$ vs λ will appear in the form of a frequency spectrum. The presence of a true peak in the spectrum indicates a component, the abscissa value at the center of a peak is the decay constant λ_i, and the height of the peak is proportional to the coefficient N_i^0.

The function $g(\lambda)$, actually $g(\lambda)/\lambda$, is obtained as follows. The variables λ and t are transformed to give $\lambda = e^{-y}$ and $t = e^{x}$. Then

$$f(e^{x}) = \int_{-\infty}^{\infty} \exp\left[-e^{(x-y)}\right] g(e^{-y})\, e^{-y}\, dy \ . \tag{4}$$

If we define $F(\mu)$ as the Fourier transform of $e^{x}f(e^{x})$, it can be shown [1] that

$$F(\mu) = (2\pi)^{1/2}\, G(\mu)K(\mu), \tag{5}$$

$$g(\mu) = [1/(2\pi)^{1/2}][F(\mu)/K(\mu)] \ . \tag{6}$$

Here $G(\mu)$ is the Fourier transform of $g(e^{-y})$, and $K(\mu)$ turns out to be the Euler integral for the complex Gamma function,

$$K(\mu) = [1/(2\pi)^{1/2}]\,\Gamma(1 + i\mu) \ . \tag{7}$$

To obtain $g(e^{-y})$ we take the inverse Fourier transform of $G(\mu)$,

$$g(e^{-y}) = \frac{1}{2\pi} \int_{-\infty}^{\infty} \frac{F(\mu)}{K(\mu)}\, e^{-iy\mu}\, d\mu \ . \tag{8}$$

Since $g(e^{-y})dy = [g(\lambda)/\lambda]d\lambda$, a plot of $g(e^{-y})$ vs y is equivalent to a plot of $g(\lambda)/\lambda$ vs λ.

COMMENTS ON THE NUMERICAL SOLUTION

Briefly, the method of solution involves essentially only two integrations. First, $F(\mu)$ is found. This is divided by the complex gamma function given in Eq. (7), and finally $g(e^{-y})$ is found using Eq. (8). The Gamma functions can be found most easily from tabulations [2].

It is clear that one cannot numerically integrate from $-\infty$ to ∞, as required in Eq. (8). A similar situation holds for $F(\mu)$. Here we must use the limits $\pm x_0$:

$$(2\pi)^{1/2}\, F(\mu) = \int_{-x_0}^{x_0} e^{x} f(e^{x}) \exp(i\mu x)dx + E(x_0, \mu) \ . \tag{9}$$

The value calculated for $(2\pi)^{1/2}\, F(\mu)$ will be in error by at least the amount $E(x_0,\mu)$. This cutoff in x produces error ripples that tend to obscure the true peaks in the spectrum. Hence it is often necessary to extrapolate the experimental data to larger values of t in order to reduce this effect.

The cutoff at $\pm\mu_0$ in Eq. (8) tends to affect the frequency of the error ripples and the breadth of the true peaks. The larger the value of μ_0 the better the resolution will be in the final results. However, the maximum usable value of μ_0 depends on how good the initial data are. If μ_0 is chosen too large, the error ripples will tend to increase and obscure the results. If μ_0 is chosen too small, there will be an unnecessary loss in resolution. What is usually done is to repeat the analysis for several progressively larger values of μ_0 until the error ripples begin to grow. This repeated analysis has further advantages that will be mentioned later.

The numerical integration scheme that is employed apparently is quite critical. This is because the exponential terms in the integrals must be represented by trigonometric functions that tend to oscillate rapidly for large values of the arguments. The Trapezoidal Rule yields much better results than Simpson's Rule, for example. It is now planned to investigate the Trapezoidal Rule with an end point correction as well as Filon's method [3].

RESULTS

The case of independent exponential decay curves will be considered first. The results for single-component curves for two values of μ_0 are shown in Fig. 1. It should be noted that whereas the error ripples shift position as a function of μ_0, the true peak does not. This provides one method for distinguishing true peaks from error ripples – merely repeat the analysis for several μ_0 values and note which peaks do not shift positions.

A two-component decay curve is analyzed in Fig. 2. In both curves the principal peaks are of the same height. This arises because we are plotting $g(\lambda)/\lambda$ vs λ, and both the coefficient and the λ value of the second component are a factor of 10 smaller than those of the first component. Furthermore, the breadth of the two peaks is the same, which means the resolution is constant over the entire range. This fact is useful in analyzing unknown curves. If, for example, two λ values are too close together to be resolved, the peak may be wider than that expected for a single component. This is illustrated in Fig. 3. Here the triangle shows the width expected for a single component.

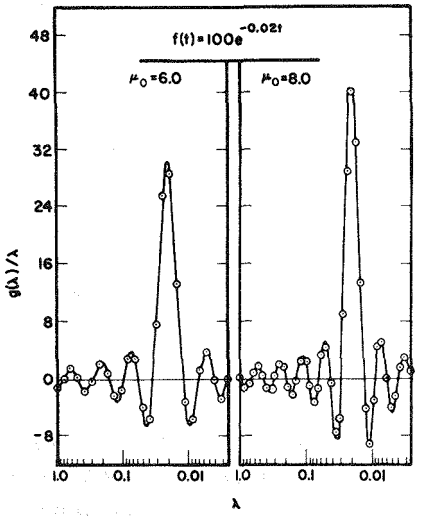

Fig. 1. Effect on the Resolution of Increasing μ_0 from 6.0 to 8.0.

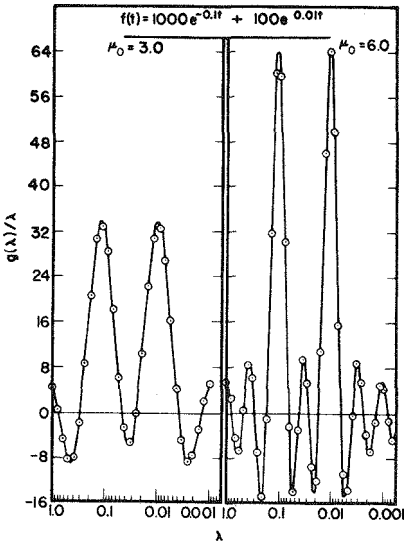

Fig. 2. Effect on the Resolution of Increasing μ_0 from 3.0 to 6.0.

Figure 4 shows the results obtained from a four-component decay curve. Here the relatively large error peak at a λ value of about 0.0035 can be distinguished from a true peak in a number of different ways. One of the best ways is to compare the width of the peak at its base (where the ordinate is zero) with the width of true peaks. Other checks include varying μ_0 to see if the peak shifts position, and also examining the original data to see if a component with such a decay constant is reasonable.

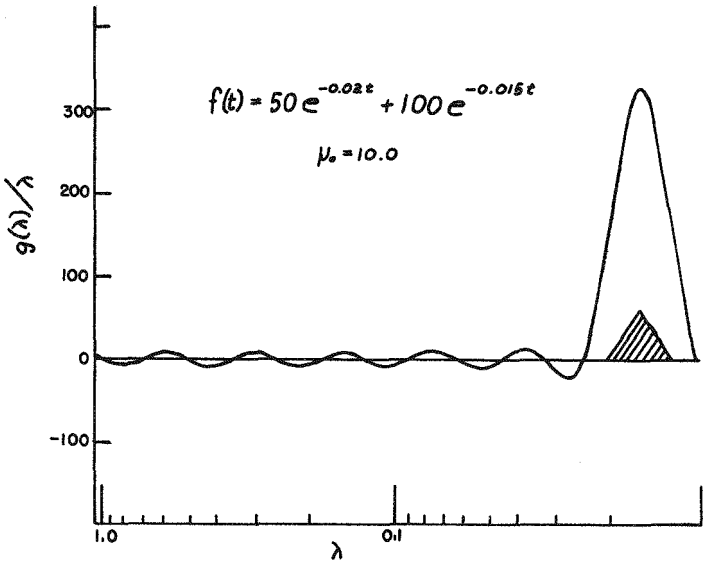

Fig. 3. Peak-Broadening Effect for Two Unresolved Components. Expected peak width for a single component is shown by the triangle.

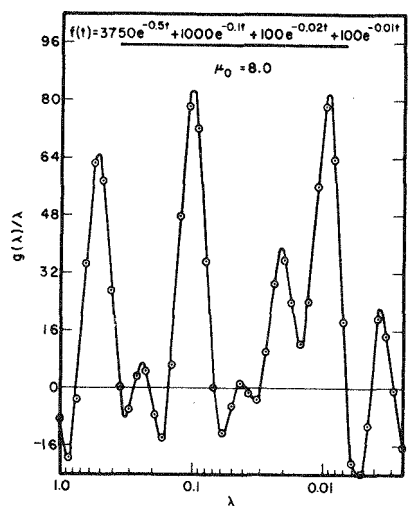

Fig. 4. Resolution of a Four-Component Decay Curve.

Only 27 data points were used in this four-component curve. By the use of a double-precision nonlinear least-squares program on an IBM 7070 machine, an attempt was made to analyze the same set of data. When a fit to a three-component curve was required, the program found the first two components rather well and averaged the last two components into a single component. When we tried to fit four- or five-component curves to the same set of data the program always failed. Either negative coefficients were obtained or parameters went to zero. With this particular program at least, it was impossible to fit the data properly using the nonlinear least-squares approach.

Figure 5 illustrates what happens when the original data do not span a large range in t (recall $t = e^{x}$). The previous curves have used data cutoff at $|x_0| = 7$. Here we cut off $|x_0|$ at 5.25. When the final integration is carried out to $\mu_0 = 6$, the error ripples completely obscure the true peak (shown as the dark triangle). However, even in this poor case relatively good results can be obtained if a somewhat poorer resolution is accepted. When μ_0 is restricted to 4, the error ripples are greatly reduced and the true peak appears at the proper λ value.

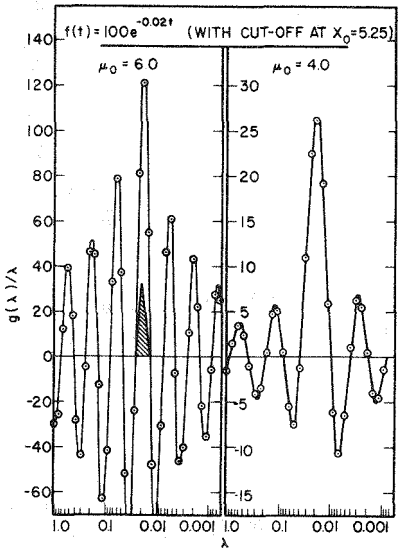

Fig. 5. Effect of the Cutoff in x_0 on the Analysis of a Single-Component Decay Curve.

Let us consider next the case of growth and decay. As an example, let us suppose that Species 1 decays to Species 2, which decays in turn to Species 3. Let $\lambda_1 = 0.02$ and $\lambda_2 = 0.1$, and assume that only Species 1 was present at time zero. Since these species are radioactive nuclei, then we will be interested in the disintegration rate rather than the number of atoms of each species. Under these conditions, and if $N_1^0 = 1000$, then

$$f(t) = 45e^{-0.02t} - 25e^{-0.1t} . \qquad (10)$$

Figure 6 gives a plot of $f(t)$ vs t, showing the typical maximum in the curve. A Fourier analysis of this data is illustrated in Fig. 7. The result of a negative coefficient is merely a negative peak in the spectrum. We expect that indeed a negative

peak is present at about that value, but the peak is too small compared to the ripple size to be determined accurately. This is not surprising since the coefficients indicate that the negative peak should be only $\frac{1}{9}$ the size of the positive peak. Fortunately it is not necessary to measure the height of the negative peak in this case.

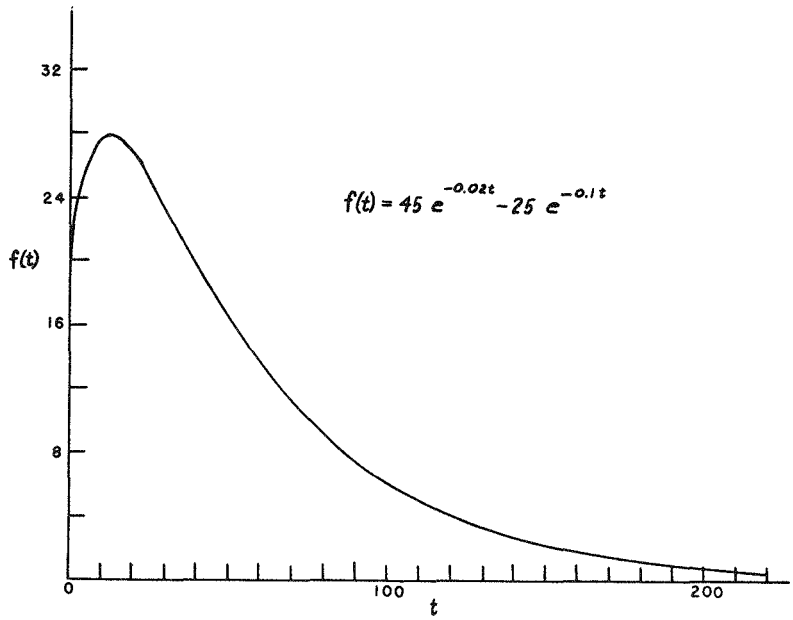

Fig. 6. Typical Shape of a Growth and Decay Curve. Here, $f(t)$ is the disintegration rate.

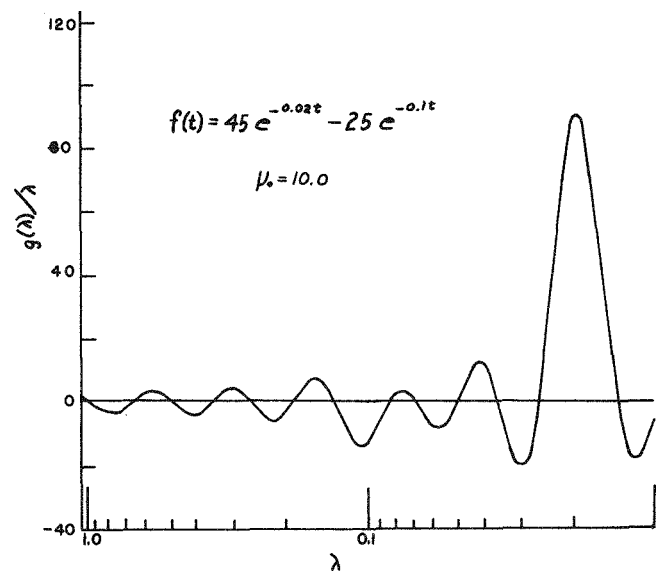

Fig. 7. Analysis of the Decay Curve Shown in Fig. 6.

The λ value for the positive peak is evident in the figure, as is the height of the peak. Since the height is directly proportional to the coefficient, it is merely necessary to run a standard decay curve with a known coefficient at the same value of μ_0 to determine what the proportionality factor is. In the present case, you would then know that one component was $45e^{-0.02t}$. If this function is subtracted from the initial data, the second component would be obtained immediately.

CONCLUSION

A method has been described for the analysis of multicomponent exponential decay curves that is applicable both to the decay of independent species and also to the case of growth and decay chains. One advantage of the method lies in the fact that it is not necessary to have initial estimates of the parameters before the analysis, as in curve-fitting procedures such as the nonlinear least-squares method. Furthermore, to these authors' knowledge, it is the only approach where the number of components automatically "falls out" of the analysis Full use is made of the accuracy that is inherent in the data since the data are treated as a whole, as opposed to some "subtraction-type" methods wherein all but the shortest-lived components are determined using fewer points than are actually available. Finally, the occurrence of λ values very close together does not endanger the entire solution as in other methods.

So far the Fourier transform method has only undergone a preliminary evaluation. The full power of the method has yet to be determined because so far only crude integration schemes have been employed in the numerical computations. Furthermore, no work has been done on attaching error bounds to the final results. Further work on these and other points is underway at this time.

ACKNOWLEDGMENT

The authors are indebted to Dr. L. Massey of Universal Oil Products Company for the use of his nonlinear least squares program and IBM 7070 computer.

REFERENCES

[1] D. G. Gardner, J. C. Gardner, G. Laush, and W. W. Meinke, *J. Chem. Phys.* **31**, 978 (1959).

[2] "Tables of Gamma Functions for Complex Arguments," *Natl. Bur. Std. (U.S.), Appl. Math. Ser.* No. 34 (1954).

[3] L. N. G. Filon, *Proc. Roy. Soc. Edinburgh* **49**, 38 (1928–29).

(1-5) ANALYSIS OF MULTICOMPONENT RADIOACTIVE DECAY CURVES[1]

Robert E. Shafer
Lawrence Radiation Laboratory, University of California
Livermore, California

GENERAL INTRODUCTION

I shall attempt to review the literature on analysis of multicomponent decay curves, including some recent work by Gardner *et al.* [2]. In their paper, Gardner *et al.* suggested the possibility of using a step function to characterize the decay rate of a sample. It is well known that a function characterizing a Fourier transform is uniquely determined; that is, for example if $g(\alpha)$ is a given function,

$$g(\alpha) = \int_0^\infty f(t) \cos \alpha t \, dt \, . \tag{1}$$

Then, there is but one function $f(t)$ satisfying this relationship. To characterize a step function $F(\alpha)$, let

$$F(\alpha) = \begin{cases} 1 & \text{if } 0 < \alpha < \beta \\ \frac{1}{2} & \text{if } \alpha = \beta \\ 0 & \text{if } \alpha > \beta \end{cases} \tag{2}$$

whose conditions are satisfied by the Fourier integral:

$$\frac{2}{\pi} \int_0^\infty \sin \beta u \cos \alpha u \frac{du}{u}. \tag{3}$$

The method of Gardner *et al.* utilizes the relation

$$\int_0^\infty e^{-bt} t^{iu} \, dt = \frac{\Gamma(1 + iu)}{b} \left[\cos(u \log b) - i \sin(u \log b)\right] , \tag{4}$$

which is a natural consequence of obtaining the gamma function. We may characterize $\sin(u \log b)$, using Eq. (4) so that we have

$$\sin(u \log b) = -\frac{b}{2i} \int_0^\infty e^{-bt} \left[\frac{t^{iu}}{\Gamma(1 + iu)} - \frac{t^{-iu}}{\Gamma(1 - iu)} \right] dt \, , \tag{5}$$

thus obtaining the double integral

$$F(\alpha) = -\frac{b}{\pi i} \int_0^\infty \frac{\cos \alpha u}{u} \int_0^\infty e^{-bt} \left[\frac{t^{iu}}{\Gamma(1 + iu)} - \frac{t^{-iu}}{\Gamma(1 - iu)} \right] dt \, du \, , \tag{6}$$

---

[1] A more complete treatment of the material presented here may be found in ref [1].

where

$$F(\alpha) = \begin{cases} 1 & 0 < \alpha < \log b \\ \frac{1}{2} & \alpha = \log b \\ 0 & \alpha > \log b \end{cases} .$$

If one has a decay curve of two independent components, then suppose this decay curve is $A e^{-b_1 t} + B e^{-b_2 t}$, and $0 < b_1 < b_2$. Then, if this function is substituted into Eq. (6) and numerical integration is applied, we would have

$$\begin{aligned} G(\alpha) &= \frac{A}{b_1} + \frac{B}{b_2} \qquad 0 < \alpha < \log b_1 , \\ &= \frac{B}{b_1} \qquad \log b_1 < \alpha < \log b_2 , \\ &= 0 \qquad \alpha > b_2 . \end{aligned} \tag{7}$$

Graphically, we would have

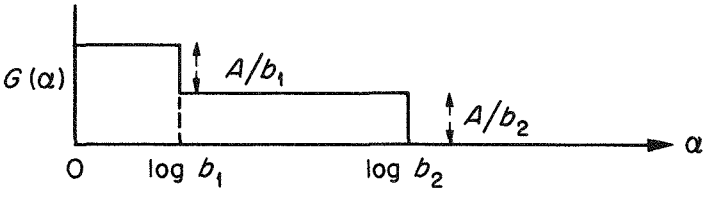

On the other hand, we may have one dependent radioactive isotope satisfying the condition

$$\begin{aligned} \frac{dy_1}{dt} &= -k_1 y_1 \\ \frac{dy_2}{dt} &= -k_2 y_2 + k_1 y_1 . \end{aligned} \tag{8}$$

Such a system of equations has the solution

$$\begin{aligned} y_1 &= A e^{-k_1 t} \\ y_2 &= k_1 \frac{A e^{-k_1 t}}{k_1 - k_2} + B_0 e^{-k_2 t} , \end{aligned} \tag{9}$$

and the rate of radioactive decay is

$$A k_1 e^{-k_1 t} + \frac{A k_1^2}{k_1 - k_2} e^{-k_1 t} + B_0 k_2 e^{-k_2 t} . \tag{10}$$

Now, if $y_2(t) = 0$ at $t = 0$ and $k_2 < k_1$, B_0 is negative. By the above analysis we may have, graphically,

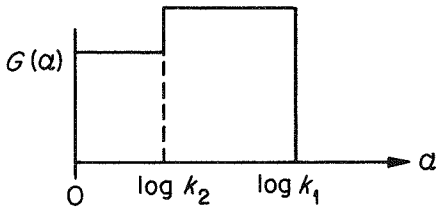

On the other hand, if $y_2(t) = 0$ at $t = 0$ and $k_2 > k_1$, graphically we have

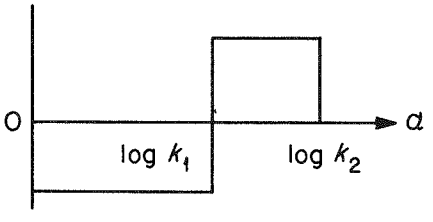

If we apply the analysis of Gardner *et al.* [2] to the problem, then we find $d/d\alpha\, G(\alpha)$ from an equation of the form of Eq. 6. Let us suppose that the integration step defined in Eq. (5) is exact. Suppose also that the limits of integration in Eq. (6) are finite; that is, for some large value M, we evaluate

$$\int_0^M \frac{\cos \alpha u}{u} \sin (u \log b)\, du \,. \tag{11}$$

We have

$$\int_0^M [\sin(\alpha u + u \log b) + \sin(-\alpha u + u \log b)] \frac{du}{2u}$$

$$= \frac{1}{2}[\mathrm{Si}(\alpha M + M \log b) + \mathrm{Si}(-\alpha M + M \log b)] \,, \tag{12}$$

which, multiplied by $2/\pi$, satisfies the conditions given in Eq. (2) as $M \to \infty$. Now if we differentiate this expression with respect to α, we have

$$\frac{1}{2}\left[\frac{\sin(\alpha M + M \log b)}{(\alpha + \log b)} + \frac{\sin(-\alpha M + M \log b)}{(\alpha - \log b)}\right] .$$

Clearly, the first expression is bounded. The second expression, however, is not and will have the characteristic appearance

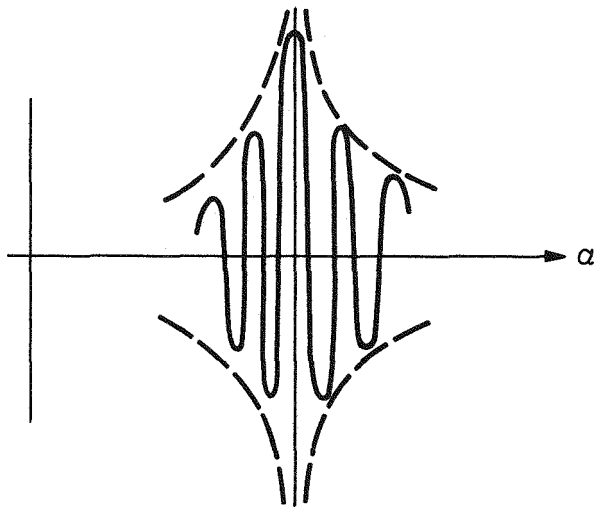

in which the envelope is closely related to a hyperbola. It may also be stated that the application of numerical analysis, particularly the unrestricted use of Simpson's rule, may be quite disadvantageous. For example, suppose that we evaluate

$$\int_{-\pi}^{\pi} \cos t\, f(t)dt ,$$

where $f(t)$ is assumed to be a fifth degree polynomial. Then

$$\int_{-\pi}^{\pi} \cos t\, f(t)dt = -\frac{\pi}{\pi^2 - 6}\left[f\left(\sqrt{2\pi^2 - 12}\right) + f\left(-\sqrt{2\pi^2 - 12}\right)\right] + \frac{2\pi}{\pi^2 - 6} f(0)$$

$$= 0.815\,[-f(-2.78) + 2f(0) - f(2.78)] .$$

Instead, by Simpson's rule, we have

$$\int_{-\pi}^{\pi} [\cos t\, f(t)]\, dt = \frac{\pi}{3}[-f(-3.14) + 4f(0) - f(3.14)] .$$

This example is not particularly badly chosen because we may be numerically evaluating a subinterval in Eq. (11) in which $f(u) = (\cos \alpha u)/u$; $\sin(u \log b)$ is chosen between $u = (n + 1/2)\,(\pi/\log b)$ and $(n + 5/2)\,(\pi/\log b)$; and b is unknown although possibly large.

Another objection to this procedure would be one of evaluating Eq. (5) numerically. We have the expression

$$\frac{1}{2i}\left[\frac{t^{iu}}{\Gamma(1 + iu)} - \frac{t^{-iu}}{\Gamma(1 - iu)}\right] = \frac{\sin(u \log t)}{\operatorname{Re} \Gamma(1 + iu)} + \cos(u \log t)\, \operatorname{Im} \frac{1}{\Gamma(1 + iu)} . \quad (13)$$

However,

$$\frac{1}{|\Gamma(1+iu)|} = \sqrt{\frac{\sinh \pi u}{\pi u}}.$$

We may only presume that the first (t) integration for a fixed value of u will be zero, since $(u\pi/\sinh \pi u)^{1/2}$ becomes quite small for large values of u.

Another possibility of finding the possible half-lives of a sample would be to find the value of α which corresponds to a value of $\beta = 1/b$ in Eq. (2). Physically speaking, $1/b$ is proportional to the half-life itself so that by choosing $\alpha = 1/b$ we have found the half-life. It is known that

$$\frac{1}{b}\sin\frac{u}{b} = \int_0^\infty e^{-bt}\, bei(2\sqrt{ut})\, dt\,. \tag{14}$$

Then this expression satisfying Eq. (2) and $\beta = 1/b$ is satisfied by the double integral

$$\frac{2}{\pi} b \int_0^\infty \frac{\cos \alpha u}{u} \int_0^\infty e^{-bt}\, bei(2\sqrt{ut})\, dt\, du\,, \tag{15}$$

where $bei(x)$ is one of Kelvin's functions. For large values of $bei\,(2\sqrt{ut})$

$$bei(2\sqrt{ut}) \sim \frac{\exp[(4ut)^{1/4}]}{\sqrt{4\pi\sqrt{ut}}} \times [\text{periodic function}]\,,$$

so that although $bei(x)$ becomes indefinitely large, for any positive value of b, $e^{-bt}\, bei(2\sqrt{ut})$ will always converge to zero as $t \to \infty$.

Fourier analysis is not a unique method of analysis of data. Indeed a more general theorem is

$$\int_0^\infty J_{\nu+1}(ax)\, J_\nu(xy)\, dx = \begin{cases} a^{-1-\nu}\, y^\nu & 0 < y < a \\ 0 & a < y < \infty \end{cases} \tag{16}$$

of which Fourier analysis only involves $\nu = -\frac{1}{2}$.

Generally,

$$\frac{1}{p} J_{\nu+1}\left(\frac{a}{p}\right) = \int_0^\infty e^{-pt}\, J_{\nu+1}(\sqrt{2at})\, I_{\nu+1}(\sqrt{2at})\, dt \tag{17}$$

so that we have

$$\int_0^\infty J_\nu(xy) \int_0^\infty e^{-pt}\, J_{\nu+1}(\sqrt{2tx})\, I_{\nu+1}(\sqrt{2tx}) \frac{dt\, dx}{(py)^\nu} = \begin{cases} 1 & 0 < y < 1/p \\ 0 & 1/p < y \end{cases}. \tag{18}$$

This method allows us to select a particular segment of data which may be more important for analysis. If $-1 < \nu < -\frac{1}{2}$, the initial data is more heavily weighted. Otherwise, if $\nu > -\frac{1}{2}$ the middle portion of our data is more heavily selected for analysis.

An elementary procedure to follow would be to evaluate

$$F\frac{\alpha}{\beta} = \begin{cases} 0 & 0 < \alpha/\beta < 1 \\ \frac{1}{2} & \alpha/\beta = 1 \\ 1 & 1 < \alpha/\beta < 2 \end{cases} \tag{19}$$

in which $F(\alpha/\beta)$ is a polynomial of arbitrarily high degree. Considering a typical component of the sample $A\,e^{-pt}$ we have

$$\begin{aligned} t &= 0 \quad Ae^{-0} = A \\ t &= u \quad A\,e^{-u} \\ t &= 2u \quad A\,e^{-2u} \\ t &= 3u \quad A\,e^{-3u} \\ &\text{etc.,} \end{aligned} \tag{20}$$

which form terms of a polynomial. Now if we compute

$$F(be^{-u}) = A(x_0 + x_1\,e^{-u}b + x_2\,e^{-2u}b^2 + x_3e^{-3u}b^3 \ldots + x_ne^{-nu}b^n)\,, \tag{21}$$

then when $b = e^u$, the polynomial increases stepwise; b is an arbitrary parameter.

If we were to characterize

$$F(x) = \begin{cases} 0 & 0 < x < 1 \\ \frac{1}{2} & x = 1 \\ 1 & 1 < x < 2 \end{cases}$$

as a series of Legendre polynomials, an examination shows that the slope does not rise quickly at $x = 1$, so that between $0.8 < x < 1.2$ we have a nearly constant slope. If we characterize a set of polynomials $S(x)$ in which

$$\int_{-1}^{1} \log(x)\, S_m(x)\, S_n(x)\, dx = \begin{cases} 0 & m \neq n \\ 1 & m = n \end{cases},$$

then the fifth order polynomial will have a greater slope at $x = 1$ than the Legendre polynomial. It appears that if our accuracy of experiment is 1%, then the fifth order polynomial is about the best hope we have of obtaining the half-life. If e^{-p_1}, e^{-p_2} were within 50% of each other, these numbers would be indistinguishable by inspection of $F(be^{-u})$.

A PROPOSED METHOD OF ANALYSIS

During an experiment, it is standard practice to find the "average" count over a given interval of time. In this way, statistical errors which are present will be minimized and it is assumed that the counting rate during this time interval is constant.

For each component, we have

$$\int_{t_1}^{t_2} A e^{-pt}\, dt = A\left(\frac{e^{-pt_1} - e^{-pt_2}}{p}\right)$$

$$= \frac{A}{p} e^{-p(t_1+t_2/2)} \left[e^{-(t_1-t_2/2)p} - e^{+(t_1-t_2/2)p} \right]$$

$$= \frac{A}{p} e^{-p(t_1+t_2/2)} \left[p(t_1 - t_2) + \frac{1}{24} p^3 (t_1 - t_2)^3 + \dots \right] .$$

Therefore, the "average" is nearly equal to $A \exp[-p(t_1 + t_2/2)]$.

A derivation of the expected error associated with such a procedure is in the Appendix.

A method of analysis will now be proposed in which the total cumulative count is given. It is hoped that an electronic analog computer may be used during the counting procedure itself and that the derived results will be immediately available to the experimenter.

Let

$$f(\tau) = \int_0^{\tau} A e^{-pt}\, dt$$

where Ae^{-pt} is the counting rate. Then $f(\tau) = A/p(1 - e^{-p\tau})$ and as $\tau \to \infty$, $f(\tau) \to A/p$.

I shall use the suggestion of Gardner *et al.* [2] to characterize each p_i. It seems that if we compare, say $A/p(1 - e^{-.01t})$ and $2A/p(1 - e^{-.005t})$ for $0 < t < 10$, that these functions are nearly indistinguishable:

$$\frac{A}{p}(1 - e^{-pt}) \approx \frac{A}{p} \log (1 + pt) ,$$

if pt is a small number. Therefore, for each component, we shall consider the computation of $A/p \log^n (1 + p)$; $n = 1, 2, 3, \dots$. It can be shown [2] that

$$\int_0^{\infty} \left[\frac{1 - e^{p\tau}}{p\tau}\right] e^{-\tau} \frac{\tau^{\sigma}}{\Gamma(1+\sigma)}\, d\tau = \int_0^1 \frac{du}{(1 + pu)^{1+\sigma}} = \frac{1}{\sigma p}\left[1 - (1 + p)^{-\sigma}\right] . \quad (22)$$

If we expand the first integrand as a function of σ, $|\sigma| < 1$, we obtain

$$\frac{1}{p}\left\{ \log (1 + p) - \frac{\sigma}{2!} \log^2 (1 + p) + \frac{\sigma^2}{3!} \log^3 (1 + p) - \frac{\sigma^3}{4!} \log^4 (1 + p) \dots \right\} . \quad (23)$$

The function $\tau^{\sigma}/\Gamma(1 + \sigma)$ may be expanded as a Taylor series of σ into the following form:

$$e^{\sigma \log \tau} \exp\left(\sigma\gamma - \frac{\sigma^2}{2}\zeta(2) + \frac{\sigma^3}{3}\zeta(3) - \frac{\sigma^4}{4}\zeta(4) + \frac{\sigma^5}{5}\zeta(5) \dots\right) . \quad (24)$$

We thereby obtain a set of integrals of the form

$$I_n = \frac{1}{p}\log^n(1+p)$$

$$= (-1)^{n+1}\, n \int_0^\infty \left(\frac{1-e^{-p\tau}}{p\tau}\right) e^{-\tau}\left[\sum_{k=0}^{n-1} A_{n-1-k}\binom{n-1}{k}\log^k \tau\right] d\tau\,. \qquad (25)$$

With this set of integrals, we may evaluate $\log(1+p_i)$ for five components. The five components will be $A_1 e^{-p_1 t} + A_2 e^{-p_2 t} \ldots + A_5 e^{-p_5 t}$. The system of equations which relates the five components to the integrals may be solved [*1*] by using the method suggested by Sylvester; $\lambda_i = \log(1+p_i)$ by this method. The determinant in λ is a fifth degree polynomial and is satisfied for some a_i by

$$1 + a_1\lambda + a_2\lambda^2 + a_3\lambda^3 + a_4\lambda^4 + a_5\lambda^5 = 0\,,$$

which is factored into the form

$$\left(1-\frac{\lambda}{\lambda_1}\right)\left(1-\frac{\lambda}{\lambda_2}\right)\left(1-\frac{\lambda}{\lambda_3}\right)\left(1-\frac{\lambda}{\lambda_4}\right)\left(1-\frac{\lambda}{\lambda_5}\right) = 0\,.$$

If the leading term $a_5 \to 0$, note that one of $1/\lambda_i \to 0$, that is, the leading coefficient of λ^5 vanishes and therefore there is at most one *less* component than was assumed.

APPENDIX

Estimation of Probable Error of an Experiment

If we have N particles in a sample emitting radiation, then let $p(t)$ represent the probability that any particular particle emits radiation. The distribution function describing this event will be

$$\sum_{m=0}^{N} p^m (1-p)^{N-m}\binom{N}{m}x^m$$

in which the coefficient of x^m is the probability that m particles have been emitted. The most likely event will be $n = pN$, especially if this number is large.

Now applying Stirling's approximation, we have

$$p^m(1-p)^{N-m}\binom{N}{m} \cong \frac{1}{\sqrt{2\pi}}\sqrt{\frac{1}{pN}+\frac{1}{N-pN}}\left(\frac{pN}{m}\right)^m\left(\frac{N-Np}{N-m}\right)^{N-m}$$

$$\cong \frac{1}{\sqrt{2\pi}}\sqrt{\frac{1}{pN}+\frac{1}{N-pN}}\exp\left[-\frac{(pN-m)^2}{2}\left(\frac{1}{pN}+\frac{1}{N-pN}\right)\right],$$

which is a Gaussian distribution.

If we sum m between $pN \pm 2[(1/pN)+(1/N-pN)]^{1/2}$ we find that the probability is about 96% of obtaining a value of m between these two bounds. If $N \to \infty$,

it can be shown that for any $\mathcal{E} > 0$

$$P\{pN - pN\mathcal{E} \leq m \leq pN + pN\mathcal{E}\} \to 1 ,$$

so that p is a true probability, for any value of p, $0 < p < 1$.

REFERENCES

[1] R. E. Shafer, *Analysis of Multicomponent Radioactive Decay Curves,* UCRL-7084-T (1962).

[2] D. G. Gardner, J. C. Gardner, G. Laush, and W. W. Meinke, *J. Chem. Phys.* **31**, 978 (1959); see also D. G. Gardner and J. C. Gardner, paper 1-4, these *Proceedings.*

Session 2

Chairman: J. B. Cumming

Brookhaven National Laboratory, Upton, Long Island, N.Y.

(2-1) A COMPUTER PROGRAM FOR ANALYSIS OF COMPLEX CONTINUOUS BETA-RAY SPECTRA[1]

S. B. Burson, R. G. Helmer,[2] and T. Gedayloo
Argonne National Laboratory
Argonne, Illinois

INTRODUCTION

In collaboration with W. J. Cody and J. A. Gregory of the Argonne Applied Mathematics Division, a two-stage computer program (for the IBM 704) has been developed for the analysis of complex beta-ray spectra. Only the second stage will be described. The first stage accomplishes standard data reduction.

A spectrum comprising as many as 13 components can be analyzed. Each component is presumed to consist of a linear combination of allowed and unique-first-forbidden transitions and is represented by three parameters: the slope m of its Fermi plot (related to relative intensity), the end-point energy ϵ_0, and the "shape-partition factor" α. Before the calculation, initial estimates must be made for all parameters of the components assumed to be present.

The free, or unfixed, parameters are varied simultaneously in order to minimize the function

$$\chi^2 = \sum_i w_i [N_i - \bar{N}_i(p_j)]^2 ,$$

where N_i and $\bar{N}_i(p_j)$ are the experimental and calculated counting rates, and w_i is the weight factor.

There are 17 options that must be exercised by the user before any calculation is made. Four of these are expressed by means of sense switches; the remaining 13 are indicated through the choice of control constants punched on the control card that represents the calculation. The program will process up to 400 data points. The computer for which the program was designed has a storage capacity of 32,000 words and

[1]Work performed under the auspices of the U.S. Atomic Energy Commission.

[2]Present address: Phillips Petroleum Company, Idaho Falls, Idaho.

the running time has averaged 5–10 min. The program was compiled by use of FORTRAN and is on punched cards. The input and output data are on magnetic tape except in the case of optional on-line printing by means of sense switch 3.

ANALYSIS

In this program, the method of iterated least-squares fitting is applied to an experimentally measured beta-ray spectrum. The approach has the distinct advantage that it is possible to quantitatively separate beta components whose end points are quite close together. This circumstance often renders the conventional "peeling" procedure extremely difficult if not entirely impossible. However, the options of the program are such that all of the flexibility that accompanies manual analysis is retained.

The substance of the least-squares procedure is to assume some analytic function that is believed to represent the experimental observations and then adjust the parameters of this function until the best fit is obtained. The words "best fit" are used in a statistical sense.

A simplifying assumption is made in this program, which (although false in detail) makes it possible to write an analytic expression that can represent a very large class of beta-ray spectra. The assumption is that any single component has either an allowed shape or a unique-first-forbidden shape, or (more generally) that it can be represented by a linear combination of these two shapes.

The expression used to represent the allowed shape is

$$N(\eta) = m^2 f(Z,\eta)(\epsilon_0 - \epsilon)^2 L_0(\eta)\,, \qquad \text{(allowed)} \tag{1}$$

where $\epsilon^2 = \eta^2 + 1$, $m^2 = (\text{const})\ g^2 M^2$, $f(Z,\ \eta) = \eta^2 F(Z,\ \eta)_{\text{screened}}$, and $L_0(\eta)$ is the shape factor. The expression holds to a very close approximation for transitions of either allowed or ordinary-first-forbidden character. The Fermi plots of these spectra are linear to within a few percent. In Eq. (1), the counting rate $N(\eta)$ is expressed as a function of the energy ϵ. The parameter m combines the intensity scale factor, related to instrumental transmission and source strength, with the nuclear matrix element. This is one of the parameters that must be adjusted in order to make the expression match the data.

The Fermi factor f is the product of the square of the momentum and the true Fermi function. The Fermi functions are not interpolated, but are computed directly by means of a subroutine based on the screened Fermi function

$$F = \frac{2}{\pi^3}(2R)^{2S}\left[\frac{1}{\Gamma(3+2S)}\right]^2\left[\frac{\epsilon_\nu \eta_\nu}{\epsilon\eta}\right]\eta_\nu^{2S}\,[\Gamma(1+S+i\delta_\nu)]^2\, e^{\pm\pi\delta_\nu}\,, \tag{2}$$

where

R = the nuclear radius,
$S = (1-\alpha^2 Z^2)^{1/2} - 1$,
$\delta_\nu = \alpha Z \epsilon_\nu/\eta_\nu$,
$\epsilon_\nu = \epsilon \mp V_0$,
$V_0 = (30.9/5.11\times 10^5) Z^{4/3}$.

The shape-correction factor L_0 is derived by interpolation from a table that must be read into the computer at the beginning of the analysis.

For a single component of allowed shape, it is sufficient to determine the best values of the two parameters, m and the end-point energy ϵ_0.

The expression used to represent a component having unique-first-forbidden shape (that is, $\Delta I = 2$ with a change of parity) is

$$N(\eta) = m^2 f(Z,\eta)(\epsilon_0 - \epsilon)^2 \frac{1}{12}[(\epsilon_0 - \epsilon)^2 L_0 + 9L_1] , \quad \text{(unique)} \quad (3)$$

where $m^2 = (\text{const})\ g^2 M^2$. The terms in the expression have the same meanings as before and again there are only two adjustable parameters.

If one now assumes that a single component comprises contributions from two transitions, one with allowed shape and one with unique shape, the distribution can be represented by

$$\bar{N}_j = m_j^2 f(\epsilon_{0j} - \epsilon)^2 \left\{(1 - \alpha_j)L_0 + \frac{\alpha}{12} j [(\epsilon_{0j} - \epsilon)^2 L_0 + 9L_1]\right\} . \quad (4)$$

The end-point energy is still a well-defined parameter. However, the slope m may take on a somewhat obscure meaning. It would not, of course, be physically meaningful to factor out two different matrix elements and combine them into a single coefficient. A means of treating this problem will be described later. It is necessary to introduce a new variable parameter α that expresses the relative partition of the spectrum into the two different shapes. A single component is thus described by these three parameters.

In general, the beta spectrum will comprise a number of components with various end-point energies. If the presence of J such components is assumed, the distribution is

$$\bar{N} = \sum_{j=1}^{j=J} \bar{N}_j(m_j^2, \epsilon_{0j}, \alpha_j) . \quad (5)$$

To describe any complex spectrum comprising J components, there are $3J$ parameters to be adjusted. This is the equation that is used in the program to calculate the theoretical counting rate to be compared with the data. The best values of these $3J$ parameters are to be determined by a least-squares procedure.

The calculation to determine the best values of the parameters that define the experimental spectrum minimizes the function

$$\chi^2 = \sum_i w_i [N_i - \bar{N}_i(p_j)]^2 , \quad (6)$$

where N_i is the experimental and $\bar{N}_i(p_j)$ the calculated count, by setting

$$\frac{\partial \chi^2}{\partial p_j} = 0 \quad (7)$$

simultaneously for all values of j. This calculation cannot be done explicitly unless the analytic function used to fit the data is linear in the variables, so the expression for

$\overline{N}$ is expanded in a Taylor series. This approximation then requires that original estimates be provided for all of the variable parameters. These original estimates correspond to the point about which the expansion is being made. The results of the first calculation are then fed back into the equation as input estimates and the calculation is repeated. This iterative procedure constitutes a series of successive approximations which, it is hoped, will converge upon the desired best values of the parameters. In addition to providing original estimates for all of the variable parameters, it is necessary to specify some criterion of convergence in order to know when to stop the calculation. This condition is specified by the expression

$$\left|\frac{\Delta p_j}{p_j}\right| < \delta \ . \tag{8}$$

The calculation is terminated when the condition is simultaneously satisfied for all of the parameters, that is, when the relative change becomes less than some specified number.

OPTIONS

Seventeen options must be exercised in order to specify the details of each calculation. These are referred to as INPUT OPTIONS. Thirteen of the decisions are indicated by numbers punched on a control card; the remaining four are indicated by the positions of four sense switches on the computer. Many of the constants are purely of a procedural nature and will be mentioned only briefly. Table 1 lists the control constants.

Table 1. Options Available for the Control Constants

Input	Options
1. Data $[\eta, N(\eta), Z, \rho]$	$(\leqq 400)$, 0, −1
2. Shape $[\eta, L_0(\eta), L_1(\eta)]$	1, 0, −1
3. Weight factors	1, 0
4. Bypasses	$(\leqq 19)$, 0, −1
5. Presubtraction	$\pm(\leqq 13)$, 0
6. Components	$(\leqq 13)$, 0, −1
7. Fixed parameters	$(\leqq 36)$, 0, −1
8. End-point systems	$(\leqq 6)$, 0, −1
9. Chi-squared	$(\leqq 10)$, 0, −1
10. Number of iterations, test	$(\leqq 100)$, −1
11. Errors	2, 1, 0
12. Postsubtraction	1, 0
13. Output data	2, 1, 0

1. The first constant indicates where the experimental data are to be found and the form in which they are tabulated. Original input data are always on magnetic tape, but this tape can be from either of two sources. On the one hand the tape can be in decimal form, made from a deck of punched cards. These cards will contain the data properly corrected and reduced, most likely manually. In this case, the control constant is a positive integer equal to the number of data points. On the other hand, if the data reduction was accomplished by means of Stage I of this program, the output tape of that calculation will be in binary from and will be compatible with the input requirements of this analysis program. Zero is then used as the control constant. The third choice, −1, indicates that the experimental data have already been stored in the memory of the computer.

2. The tables of shape factors, which are always needed, are taken from the compilation by Rose *et al.* [*1*]. If the calculation is the first in a series, or is the only one, the cards must always be present, and the choice of shape option 1 indicates to the machine that the cards are to be read. Immediately after reading the cards, the values of L_0 corresponding to the data points are obtained by interpolating in the table of shape factors. The other two choices for the constant specify whether the machine should use the interpolated values again (option −1), or whether it should reinterpolate (option 0).

3. The user has the option of using the statistical weights (option 1) or not (option 0). This control constant indicates that decision. There are some applications of the program in which weight factors are not meaningful, and machine time is conserved by not using them.

4. The program will accommodate up to 400 data points. The least-squares fit can be made to any desired region of the spectrum. As many as 19 groups of adjacent points can be bypassed and excluded from the calculation. This only excludes them from the least-squares calculation, however, and in all other respects the spectrum remains intact. This option makes it possible to cull the data or to eliminate obviously bad points (points beyond the highest end-point energy, groups of points on internal conversion lines, etc.). It also allows the program to be used in a more limited sense in which components are fitted and peeled off one at a time as in the classical method. This flexibility has proved to be extremely valuable. The other two choices, 0 and −1, correspond to using no bypasses or to using the same ones that were specified for the previous fit.

5. If the data have already been partly analyzed and one or more of the components have already been determined with certainty, these components can be subtracted from the data before proceeding to the least-squares fit. Up to 13 such components can be subtracted.

6. The iterated least-squares procedure requires one to have some knowledge of the composition of the spectrum, or at least to be able to make an educated guess. This control constant indicates the number of components that are expected to be present in the region of the spectrum that is being fitted. The estimates of the three parameters that define each of the components are punched on cards and included in the accompanying data deck. If the choice −1 is used, the final values of the parameters that were calculated in the previous fit will be used as input estimates. This freedom makes it possible to invoke a wide variety of analytical approaches to the same data.

7. Any of the parameters can be held fixed at their input values and then released during successive fits after the computer has improved the values of those that are allowed to vary. This has been particularly valuable in conjunction with the shape-partition parameters.

8. In many cases the difference in energy between two end points will be known exactly from scintillation experiments, measurements on internal-conversion electrons, or Coulomb excitation. This knowledge can be incorporated into the calculation in the form of a "related end point" system. Both end points will be allowed to vary simultaneously; but the difference in energy will remain fixed. Up to six such systems of related end points can be included in the calculation with as many as eleven end points being combined into a single system.

9. The value of χ^2, which is used as a measure of the goodness of the fit, is computed only for the data points that were not bypassed. It is also possible to partition the spectrum into groups of data points and compute the partial χ^2 for each group. This device can sometimes give a clue as to why and where the fit is not good.

10. The tenth control constant limits the number of times (≤ 100) the computer will try to make the fit. The upper limit on the number of iterations is specified and if the calculation does not converge in that many iterations, the machine will stop and await further instructions. If the series of calculations does converge, the results are printed out automatically and the next control card is read without interruption.

In conjunction with this constant, a card must be punched and placed in the data deck. This card provides the criterion for convergence [Eq. (8)].

11. There are two ways of propagating errors through a subtraction. One of these utilizes the off-diagonal elements of the inverse matrix that is calculated during the least-squares fit. These off-diagonal terms relate to the correlation between the parameters. The simpler formula uses only the diagonal elements which can be computed without the matrix. Either formula can be invoked if the subtraction is to be carried out after a fit has been made, since the matrix is still present in the machine. However, in the case of presubtraction, there is no choice; only the diagonal elements can be used.

12. This constant specifies whether or not the components that were calculated should be subtracted before the next fit is commenced. If the subtraction is carried out, the errors are propagated according to the formula that was selected by the previous control constant, and the residual spectrum is written into the memory unit in place of the original data.

13. The last control constant indicates how much of the information that was calculated should be printed on the output tape that is used on the off-line printer. This decision is dictated by the needs of the particular problem.

SENSE SWITCHES

The sense-switch options are listed in Table 2.

1. Sense switch 1 is used to frustrate the iterative procedure. It accomplishes this by automatically setting all of the computed parameter changes to zero. This facility has a number of applications that will be discussed later.

2. Sense switch 2 is used when the machine fails to converge. If the number of iterations reaches the limit and the machine stops, a second attempt to reach convergence on the same set of input information can be instituted by pressing the start button. If it is decided to abandon that particular calculation, sense switch 2 is put down and the start switch is then pressed. This causes the computer to advance to the next control card and continue in the series of programmed calculations.

3. Sense switch 3 permits on-line printing of a very limited amount of information. With sense switch 3 down, the interim values of the parameters are printed on-line after each iteration. Examination of these numbers for a few iterations often enables the operator to decide whether or not to continue trying the fit.

4. Sense switch 4 provides a limited control over the mechanism of the least-squares fit itself. Each iteration results in a calculated group of correction terms that are added to each of the variable parameters before the next matrix is set up. If the amount by which each of the parameters is allowed to step is reduced, the rate at which the series converges is reduced. However, this reduction also has the effect of damping oscillations that may result when any of the corrections are too large.

Table 2. Sense-Switch Options

	Up	Down
1.		Force convg.
2.		Next fit
3.	Off-line	On-line
4.	$0.875\,\Delta$	$0.437\,\Delta$

PRINTED OUTPUT

The information that can be included in the printed output is (*a*) all input data, (*b*) η, ϵ, L_0, L_1, and the Fermi functions, (*c*) N, σN, $\bar{N}$, N', $\sigma N'$, areas, and χ^2, (*d*) the Fermi plots (σ), and (*e*) m_j, σm_j, ϵ_{0j}, $\sigma\epsilon_{0j}$, α_j, and $\sigma\alpha_j$. The various ways in which this information can be grouped will not be discussed. All input information (the instrument settings and the associated counting rates and errors) is included in the output. The conversions of instrument field settings to momenta and energies, the interpolated values of the shape factors, and the Fermi functions are included.

In addition to the original counting rates, the theoretical counting rate, calculated from the best values of the parameters, is also printed. The difference between the data and the theoretical counting rate is always calculated and printed out. In order to determine relative intensities of the various components, the area under the theoretical momentum spectrum of each component is calculated. The values of χ^2 and/or the partial χ^2 values are printed.

The Fermi plot of the entire computed spectrum is printed and, if required, the separate Fermi plots of the individual components can be calculated.

Finally, it prints the last values of all the variable parameters that were computed by the iteration that converged.

APPLICATIONS OF THE PROGRAM

The most valuable facility of the program is the least-squares analysis. There is a wide variety of ways in which the analysis can be carried out. By way of illustration, some of the work that has been done on the beta-ray spectrum of W^{188} will be described. Tungsten-188 has a half-life of 65 days and decays by β^- emission to Re^{188}. In turn, the ground state of Re^{188} decays to levels in Os^{188}, but with the much shorter half-life of 18 hr.

Almost the entire decay of the rhenium daughter is to the ground state and first excited state of osmium at 155 kev; both components have end-point energies close to 2 Mev. On the other hand, the total decay energy of the W^{188} parent (whose spectrum is the one under study) is less than 0.4 Mev.

The first calculation was a fit to a small group of data points immediately above the end point of the tungsten portion of the spectrum. The rhenium spectrum was assumed to consist of but a single component of allowed shape, so the least-squares fit was carried out with fixed end point and shape-partition factor. This is shown in Fig. 1. It was assumed that the extrapolation under the tungsten spectrum would contribute little error.

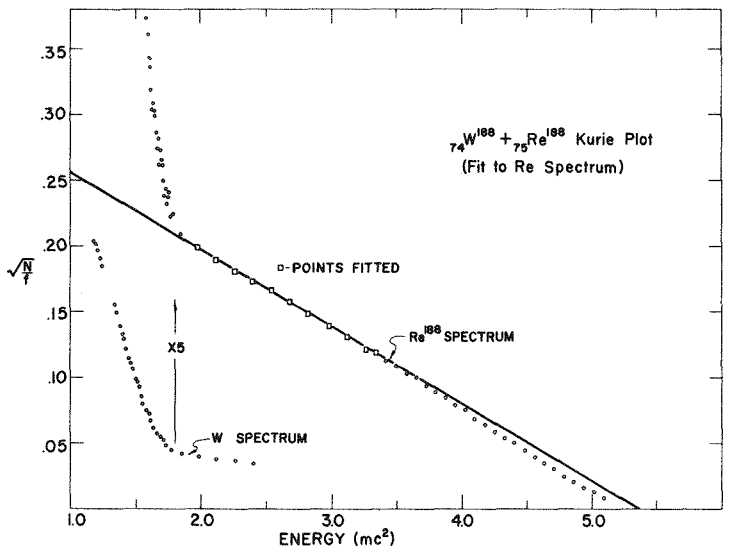

Fig. 1. Beta-Ray Spectrum of W^{188} in Equilibrium with Its Daughter Re^{188}. A single component of allowed shape is fitted to the rhenium portion of the spectrum immediately beyond the tungsten end point for the purpose of extrapolation.

From the results of this fit, a new table of input data was compiled and the computer was reentered with only the tungsten spectrum. This reentry was necessary because the difference in atomic number necessitates the use of a different table of shape factors.

Visual examination of the Fermi plot of the difference spectrum revealed the presence of two components. The fit made to these data is shown in Fig. 2. The higher energy

component is due to the presence of a contaminant, W^{185}, while the lower energy component represents decay from the ground state of W^{188} to the ground state of Re^{188}. Attempts to fit the rhenium portion of the spectrum are still in progress and will not be described.

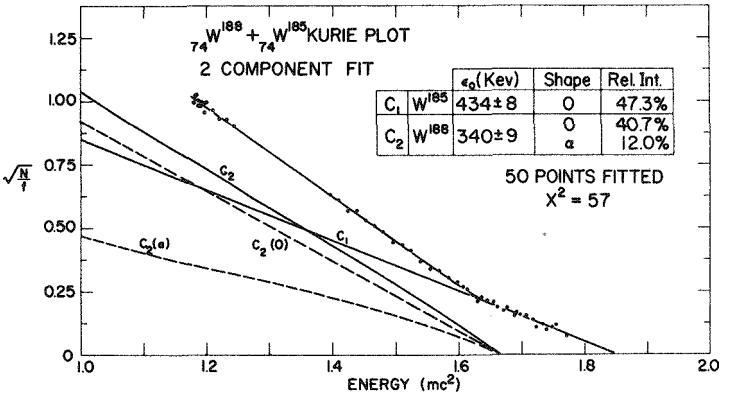

Fig. 2. Two-Component Fit to the Beta-Ray Spectrum of W^{188}. The component of higher energy is due to the W^{185} contaminant.

In addition to this main facility, provision is made for several subordinate calculations. These do not depend primarily upon the least-squares fitting facility. Within a few minutes of machine time, any desired set of Fermi functions can be calculated. The shape-correction factors L_0 and L_1 can be interpolated for an arbitrary table of momenta. After a satisfactory fit has been made, the log ft values of various components in the spectrum can be quickly calculated.

Sense switch 1, which causes the computer to converge after one iteration, has a number of applications. The Fermi plot for a typical beta-ray distribution with any end-point energy can be constructed. Figure 3 shows a typical calculation of this kind. The shape of a pure allowed Fermi plot for a component with an energy of 2 Mev is compared with a pure unique-first-forbidden component with the same end-point energy. This sense switch also permits the subtraction of previously determined components in such a way that the off-diagonal terms may be included in the propagation of errors.

It was mentioned earlier that the meaning of the slope m becomes ambiguous when the shape partition factor for any component is neither 0 nor 1. A method of resolving this ambiguity is inherent in a combination of the two facilities for fixing parameters and relating end points. If one assumes that a single component whose shape factor is neither zero nor unity comprises two independent components with equal end points, introducing two components instead of one makes it possible to determine the relative intensities of the fractions. Two components are assumed; their end points are set equal but they are entered as a related-end-point system. The shape-partition factor of one is set equal to zero and that of the other to unity and both are held fixed. The least-squares fit is then accomplished by varying the three remaining parameters, namely, the common end point and the two independent slopes. The two values of the

areas then represent the intensities of the allowed and unique fractions of the component. These illustrations represent but a few of the combinations of the available options that we have tried. It is believed that there are many more that have not yet been attempted or explored.

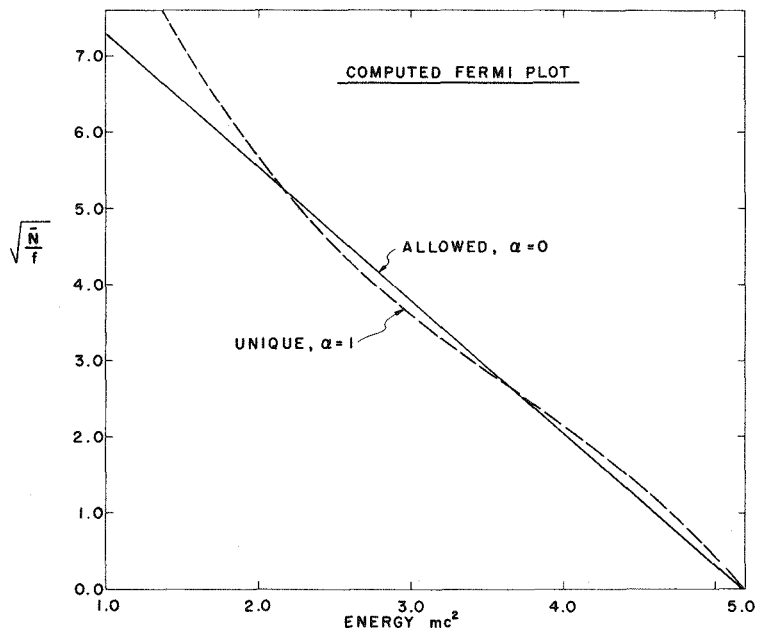

Fig. 3. Fermi Plot of a Beta-Ray Component with Pure Allowed Shape Contrasted with That of a Component of Pure Unique-First-Forbidden Shape Synthesized by the Use of Sense Switch 1. (No data actually being processed.)

REFERENCE

[1] M. E. Rose, C. L. Perry, and N. M. Dismuke, *Tables for the Analysis of Allowed and Forbidden Beta Transitions,* ORNL-1459.

(2-2) THE ROLE OF SMALL COMPUTERS IN THE ANALYSIS OF GAMMA-RAY SCINTILLATION SPECTRA

John W. Nostrand, Jr., and Martin L. Rossi
Research Department, Grumman Aircraft Engineering Corporation
Bethpage, New York

INTRODUCTION

Until a few years ago the vogue in data processing equipment was the large scale digital computer. Recently, a new market has developed for smaller computers. This market has expanded so rapidly that today the small computer represents a large percentage of total computer sales.

During this same time period, the feasibility of using digital computers for processing gamma-ray scintillation data has become firmly established. Many prototype programs have been written and evaluated for accuracy and practicability. Although the search for better methods of analysis and improved programs continues, the importance of automatic data processing as a routine tool in gamma spectral analysis is now fully accepted.

In this paper, we will investigate these coincident developments and indicate how small computers can contribute to the growth of routine analysis of gamma-ray scintillation spectra.

WHAT IS A SMALL COMPUTER?

Perhaps first, we should define what we mean by "small computer."

Today, practically every major computer manufacturer offers a small solid-state type computer. These machines are of a new breed, similar to the old IBM 650 but transistorized, less expensive, and with larger storage and faster operation time. The new machines have generated considerable interest both in small companies that cannot afford a larger machine and also in larger companies for use in individual departments as a supplement to their centralized facilities.

Table 1 lists some of the more popular small computers together with typical monthly rental prices, storage capacities, an indication of their operating speeds, and an estimate of the number of installations for each machine. For comparison with large scale computers, a similar listing is included for an IBM 7090. The monthly rental values given are rough estimates for the basic computer with the storage capacity listed. The cost will be higher for installations with more advanced input-output devices or extra storage capacity. Extended operations such as floating point capability or automatic division would also increase the cost.

In terms of sheer numbers, the small computer represents a sizable segment of the computer market. There are currently more than 5000 small solid-state computers in use as compared with less than 300 of the large 7090 class of transistorized machine. If we add to these figures the 300 vacuum tube computers of the 650 size or smaller still in use, we find that small size computers make up about 75% of the world computer population.

Table 1. Characteristics of Small Computers[a]

Type	Monthly Rental	Storage Locations	Word Size	Type of Storage	Cycle Time (μsec)	Add Time (μsec)	Number of Machines
Transistorized							
PB 250	$ 1,200	2.3–16K	22	Delay line	12–307	24	102
CDC 160	1,500	4K	12	Core	6.4	12.8	80
Recomp III	1,500	4K	40	Disk	1750–9300	1080	28
IBM 1620	1,600	20–100K	11	Core	20	560	1167
RPC 4000	1,900	8K	32	Drum	10,000	1000	69
Recomp II	2,500	4K	40	Disk	950–9000	1008	132
IBM 1401	2,500	1.4–4K	11	Core	11.5	230	2896
CDC 160A	4,000	8–32K	12	Core	6.4	12.8	115
Vacuum Tube							
LGP 30	1,500	4K	31	Drum	2,000	2260	433
Bendix G-15	2,000	2K	29	Drum	14,500	2700	354
IBM 650	9,000	4K	10	Drum	4,800	700	1173
Large Scale							
IBM 7090	64,000	32K	36	Core	2.2	4.4	183

[a]Compiled from data of [*1* and *2*].

CAPABILITIES OF A SMALL COMPUTER

Before we look at the problem of gamma spectral analysis, let us get a few facts straight about the capabilities of a small computer.

Its primary limitations are slow operation speed and restricted storage capability. The operation speeds and access time of a computer affect the machine time required to run a program. Large scale computers are vastly superior to small computers in both speed and storage capacity.

Assume, for example, that a program was available for which the same operations could be run on both a small and a large scale computer. The small computer would probably take from 50 to 150 times longer to run the program. This means that a program requiring 2 min on a large machine would need more than 2 hr on a small machine, and a program running 1 hr on the large computer would require 100 hr on the small computer!

Even these examples are being kind to the small computer because the same operations cannot always be used on the small machine. The large computer, in addition to being faster, has many more built-in operations. In order to perform the same job, the small computer would have to use more instructions and less efficient programming techniques.

In addition to this, for a lengthy program, time would be wasted in partitioning. Input-output operations are very time consuming, and dividing the program into parts which are read into fast storage individually greatly increases the running time of a program.

COST CONSIDERATIONS

Even on a cost basis, the small computer is at a disadvantage. The first venture into automatic data processing by a nuclear laboratory would probably be by renting time at a large computing facility. This assumes that no computer was available to the laboratory personnel within their own organization. Time on a 7090 currently rents for about \$550/hr or about \$10/min. The lowest monthly rate at which a company could hope to operate their own small computer would be about \$3000, if all the costs of operation are included. Considering a 176-hr standard shift, this would be

$$\frac{\$3000}{176} = \$17/\text{hr} .$$

The cost of running equivalent programs then, would be

large computer: $2 \text{ min} \times \$10/\text{min} = \$20$,
small computer: $2 \text{ hr} \times \$17/\text{hr} = \$34$.

Again, these figures are very conservative in the small computer's favor.

WHY HAVE A SMALL COMPUTER?

Having firmly established the limitations of small computers, we can well ask ourselves, why have a small computer? There is no doubt that gamma-ray spectral analysis can be performed with a small computer. Many current programs were developed on small or medium size machines. The least-squares fitting technique, which is receiving enthusiastic interest, was originally applied by Heath [3] to the IBM 650. Spectrum stripping methods have also been programmed for small or medium size computers.

The question we must ask, however, is whether it is practical to use small computers for this type of work? And if it is, what is the most effective way to use them?

By examining the relationships between the objectives of gamma spectral analysis and the capabilities of small computers, we can find answers to these questions and can show that the small computer as an integral part of a nuclear laboratory has at least four potential advantages over the large centralized computing facility. These are in the areas of (1) data handling, (2) "turn-around-time," (3) versatility, and (4) stimulation of ideas.

First of all, there are some problems for which the small computer is well suited, in particular, those requiring a large amount of data handling with very little processing. The time of such programs is limited by input-output speed. Since card input-output equipment is basically the same for large or small computers, time spent reading or punching cards could very rapidly eat into the large computer's advantage of

faster operation times. Of course, 7090's are usually fed from magnetic tape. However, time is consumed in the transfer of card data to tape.

For the moment, let us leave the cares of machine time and cost of operation to the computer operators and the accountants, and look at the problem of gamma spectral analysis from the experimentalist's point of view. He is interested, mainly, in the time interval between the collection of data and the return of meaningful answers – the so-called "turn-around-time."

The required turn-around-time varies in individual cases. In some medical applications and in monitoring of continuous flow lines, turn-around-time is critical. There are other applications for which a few days wait probably would not make much difference. But if turn-around-time is important, then a small computer as an integral part of the nuclear laboratory has distinct advantages.

When a program is run at a centralized computing facility, the turn-around-time would include travel time to and from the facility, handling time for logging in and preparing the deck, and the time spent waiting to get on the computer, in addition to the actual machine time. With a computer placed directly at the laboratory site, the experimenter could bypass all of the waiting times and have results within minutes of the end of an experiment.

The turn-around-time advantages of a small computer diminishes as the machine time of a program becomes longer. Figure 1 shows that for short programs or for only a few runs a day, the small computer has an advantage in turn-around-time. For longer programs, however, the centralized facility might be able to return the results sooner. This suggests that the most effective use of a small computer would be with short programs.

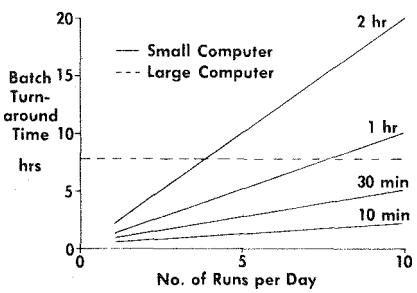

Fig. 1. Comparison Between the Turn-Around-Times of Small and Large Computers for Programs of Various Lengths.

Minimizing turn-around-time is tied directly to one of the most important advantages of having a small computer in the laboratory. That is the ability to control the scheduling and allocation of priorities. Even in the central computing facility of his own organization an experimentalist might have trouble establishing a priority. With a small computer at the lab site he can control his own schedule of experiments and data reduction. The advantages that are to be derived from such versatility would decrease, however, as the length of the program increased. If a single program tied up the computer for an entire day nothing would be gained by being able to control scheduling. Again, this suggests the effectiveness of shorter programs.

The final advantage that should not be overlooked when considering a small computer at the laboratory site is the stimulation of ideas. A centralized facility might

seem very remote to an experimentalist regardless of its real physical location. With a computer at the lab site, an experimentalist would be encouraged to think in terms of computer analysis and how it could permit him to perform a greater number of experiments or to gather more data from each run. This concept of stimulation, of course, is not limited to the small computer. It is the sustenance that all computer manufacturers thrive on. For sufficiently stimulated, you will probably need a larger computer to handle all the new work – and they will be happy to sell you one!

Up to this point we have seen, that if properly used, a small computer installed at the nuclear laboratory site could provide shorter turn-around-times and more versatility of operation. We have also determined that the positive capabilities of the small machine can be exploited by the use of short programs. In the remaining portion of this paper let us examine in more detail just what these short programs are and how they can be used most effectively.

PROGRAMMING CONSIDERATIONS

The programming of computers for gamma-ray spectral analysis is still an individualized process. Every laboratory has its own experimental methods and procedures; each may use a different type of equipment, and each requires a different final result. Since all of these factors must be considered in planning a data reduction system, each individual will probably want to develop his own special program. However, an experimenter can assemble his own program by using proven routines and techniques taken from existing programs and tailoring them to fit his own needs.

Until now, most of the development work in gamma-ray spectral programs has been on what we would like to call the "generalized" type of program. The aim of a generalized program is to reduce the multichannel analyzer data from an unknown gamma source completely without resorting to any human logic decisions. By the very nature of the problem, a generalized program is extremely complicated, requiring many tests and logic sequences. Currently, generalized programs are being developed on large scale computers. It is evident that these completely "automatic" programs are somewhat beyond the scope of the small computer.

But, the same solution that you would achieve with the generalized program, could be reached with a series of shorter special purpose programs of a type ideally suited for use with a small computer.

Consider first an easy case, a problem for which the number of possible solutions are limited. The simplest case would be one for which the identities of the isotopes were known and only the activities had to be calculated. In most experimental work, results are predictable, at least in part. The identity of the isotopes is known in most tracer studies, routine sampling operations, or searches for specified contaminants.

Once the multichannel pulse-height data has been accumulated, the analysis proceeds as follows (see Fig. 2): First, the experimenter examines the data and decides which method of analysis to use. He has a wide choice including any of the standard gamma spectral techniques of stripping-least-squares fit, total absorption peak, solution of simultaneous equations, or matrix solution. Having decided to use a least-squares fitting technique, he selects the correct object program deck from the

program file, and also picks out the response function decks corresponding to the isotopes known to be in the spectrum from another card file.

He then proceeds to the computer, reads in the pulse-height data, the response functions, and the object program. The computer then takes over, fits the data by the least-squares technique, and prints out the results and the residuals.

At this point, the experimenter can examine the results and decide whether a better fit is required. By this method, the reduction of data is performed quickly and the experimenter is then ready to compile additional data.

A more complicated analysis could be performed in the same stepwise manner. Let us consider another case of a simple spectrum, in which the identity of an isotope is not known. This would suggest the possibility of a decay curve analysis.

In this case a series of programs could be run (Fig. 3). The first program that the experimenter would choose would perform an integration under the decaying peak in each of a series of pulse-height spectra. Upon completion of that, a second program would be selected for the analysis of the decay curve. Once the isotope were identified by half-life, a third program might be chosen – perhaps a standard gamma spectral method such as a least-squares or stripping technique, to be run as a check on the validity of the identification.

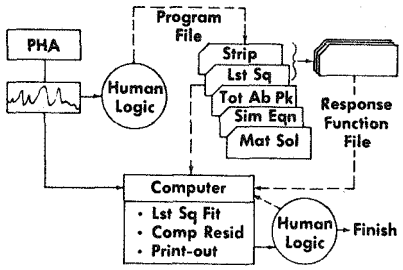

Fig. 2. Procedure for Spectrum Stripping with a Small Computer When the Isotope Identity Is Known.

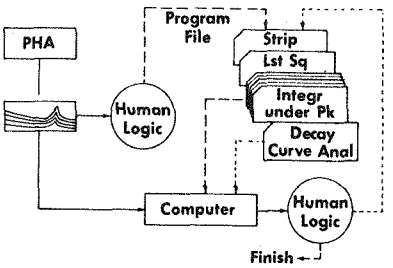

Fig. 3. Illustration of Possible Programs Which Might Be Used in the Analysis of a Series of Time-Dependent Gamma-Ray Spectra for Which the Identities of the Isotopes Are Not Known.

CONCLUSION

These examples are only two of an almost limitless number of ways in which small special purpose programs can be used. Only a few such programs have as yet been published. Blotcky, Watson, and Ogborn [4] have developed a matrix solution for gamma spectral analysis for an IBM 1620 that is an excellent example of the small computer program.

As more and more small laboratories enter the nuclear field and begin to consider automatic data processing, there will be an increasing need for proven small computer programs. We hope that in the next few years more of the small special purpose programs will be published, so that programming methods and ideas in this field can be shared.

Of course, the small computer will never replace the large scale machine in automatic gamma spectral analysis. The primary methods of computer analysis will continue to be developed on large machines. But, we feel that there is a definite place for the small computer in smaller laboratories, for installations requiring fast turnaround-time, and for people who just like to control their own computing. We feel that in the next few years there will be a marked increase in the use of small computers for gamma-ray spectral analysis as well as all types of experimental data analysis.

ACKNOWLEDGMENT

The authors wish to thank N. W. Johnson for his helpful discussions and suggestions.

REFERENCES

[1] "Computer Characteristics 1961," *Datamation* **7**(11), 88–92 (1961).

[2] "International Computer Census," *Datamation* **8**(8), 46–48 (1962).

[3] R. L. Heath, Phillips Petroleum Co., Idaho Falls, Idaho, private communication and *IRE (Inst. Radio Engrs.) Trans. Nucl. Sci.* **NS-9**(3), 294 (1962).

[4] A. J. Blotcky, B. T. Watson, and R. E. Ogborn, "Computer Applications In Neutron Activation Analysis," these *Proceedings*, paper (6-4).

(2-3) PRECISION DETERMINATION OF GAMMA-RAY ENERGIES WITH THE SCINTILLATION SPECTROMETER

Berol L. Robinson

Western Reserve University and

Israel Atomic Energy Commission Laboratories

This work was initiated with the intention of obtaining a precision value for the energy of the K^{40} gamma ray [1]. On account of the low specific activity of this material, scintillation spectrometry is the only practical means. In principle the problem is straightforward: one calibrates the scintillation spectrometer with gamma rays which have been accurately measured by the methods of electron spectrometry, and then observes the unknown and determines its energy from some sort of interpolation or extrapolation. Since the resolution of the scintillation spectrometer is so notoriously bad, one must use tedious and brute force methods to extract the maximum amount of information from the data. Recent publications and the program of this

symposium indicate that this has been pursued with considerable sophistication by a number of workers.

We begin by locating precisely the center of the pulse-height distribution corresponding to the total absorption of the gamma ray in the scintillation crystal, the so-called "full-energy peak." The full-energy peak is observed to be Gaussian on the high-energy side as well as for a good part of the low-energy side. We will assume that we have enough data so that the curve is reasonably smooth, with the general outlines already apparent. It is frequently suggested that the way to find the center of a Gaussian distribution is to make a least-squares fit of the logarithms of the data points to a power series, since a Gaussian appears as a parabola on a semilog plot. However, one really wants a least-squares fit to the data, not to their logarithms. Preliminary calculations on a desk computer showed that the former gives a better fit; that is, the residuals are smaller.

This nonlinear function is somewhat intractable, and we proceed to linearize it by guessing the central value and the width of the distribution. This guess can be made with fair accuracy from a rough look at the data. We then compute corrections by the method of least squares and iterate. The function is already linear in the amplitude of the pulse-height distribution, so nothing is gained by making an initial guess for the amplitude. An outline of the analysis is shown below.

The function to be minimized is

$$S = \sum_i w_i \{y_i - A \exp [-b_0^2 (c_i - c_0)^2]\}^2 .$$

Set

$$b_0 = b + \beta ; \qquad c_0 = c + \gamma ; \qquad \beta \text{ and } \gamma \text{ are small.}$$

Then,

$$b_0^2 (c_i - c_0)^2 = b^2 (c_i - c)^2 - 2\gamma b^2 (c_i - c) + 2\beta b (c_i - c)^2 + \text{higher-order terms.}$$

$$b_0^2 (c_i - c_0)^2 = p_i^2 - 2\gamma b p_i + 2 \frac{\beta}{b} p_i^2 + \text{higher-order terms,}$$

where $p_i \equiv b(c_i - c)$. Then

$$S = \sum_i w_i \left[y_i - A e^{-p_i^2} \left(1 + 2\gamma b p_i - 2 \frac{\beta}{b} p_i^2 \right) \right]^2 .$$

By using the approximation $e^x \approx 1 + x$,

$$S = \sum_i w_i \left[y_i - A e^{-p_i^2} - 2Ab\gamma p_i e^{-p_i^2} + \frac{2A\beta}{b} p_i^2 e^{-p_i^2} \right]^2 .$$

Let

$$F = 2Ab\gamma , \qquad \text{and } G = -2A\beta/b .$$

Then,

$$S = \sum_i w_i \left[y_i - Ae^{-p_i^2} - Fp_i e^{-p_i^2} - Gp_i^2 e^{-p_i^2} \right]^2 ,$$

$$\frac{\partial S}{\partial A} = 0 = \sum_i 2w_i \left[y_i - Ae^{-p_i^2} - Fp_i e^{-p_i^2} - Gp_i^2 e^{-p_i^2} \right] \left(-e^{-p_i^2} \right) ,$$

$$\sum_i w_i y_i e^{-p_i^2} = A \sum_i w_i e^{-2p_i^2} + F \sum_i w_i p_i e^{-2p_i^2} + G \sum_i w_i p_i^2 e^{-2p_i^2} ,$$

$$s_0 = At_0 + Ft_1 + Gt_2 \qquad \text{(definition of } s_i, t_j\text{)}.$$

Similarly, $\partial S/\partial F = 0$ leads to

$$s_1 = At_1 + Ft_2 + Gt_3 ,$$

and $\partial S/\partial G = 0$ leads to

$$s_2 = At_2 + Ft_3 + Gt_4 .$$

The actual computation is the solution of a set of three simultaneous equations in three unknowns, where the coefficients are the sums, s_i and t_j. We recover the corrections, β and γ, to the initial b and c and use the final results as new trial values for the iteration. Experience showed that a single iteration was sufficient unless a gross error was made in the initial choice of trial values. This work was programmed in machine language for the WEGEMATIC rotating drum computer of the Weizmann Institute of Science. In practice, data points were confined to the region above about 20% of the peak, after the subtraction of background.

Experiments based upon the alternation of standard sources of Na^{24} and the unknown K^{40} proved fruitless because of drifting. Frati and Rainwater [2] have shown how to overcome this problem, but these elaborate means were impractical for us; and we therefore tried a method in which the standard was mixed with the potassium itself. Since the low-energy line of Na^{24} at 1368 kev falls upon the Compton edge of the K^{40} line, Y^{88} was found to be a standard more suitable to this experiment. In the mixture of Y^{88} and K^{40}, the full-energy peaks fall on very flat portions of the Compton distributions of the higher energy lines. The Compton distribution may then be subtracted as a constant background without shifting the position of the full-energy peak. Table 1 shows a test of this subtraction and of overall stability and reproducibility of the results. These data were taken with a 3- by 3-in. Harshaw crystal and a TMC 400-channel analyzer. In this experiment the high-energy line of Y^{88} was compared with the two lines of Na^{24} by linear interpolation between the locations of the centers of the pulse-height distributions.

1. Under "accumulated data" in Table 1 the Compton distributions were subtracted as constant backgrounds under the full-energy peaks of the lower energy gamma rays. Under "difference data" the Y^{88} source was removed, the analyzer put in subtract mode, and the Na^{24} contribution was removed by pulse-height analysis. The differences are hardly significant at the level of precision sought in this work.

2. The reproducibility, as indicated by the fluctuations from the averages, was also quite adequate for the work at hand.

These data were taken at different base-line settings of the TMC 400-channel analyzer and therefore used different parts of the conversion ramp.

Table 1. Energy of a Y^{88} Gamma Ray Determined by a Linear Interpolation Based on the Energies of the Na^{24} Gamma Rays.[a] Counting Interval was 10 min

Accumulated Data (kev)	Difference Data (kev)
1831.34	1831.60
1831.62	1831.89
1831.62	1831.82
1831.78	1831.91
1831.88	1832.14
1831.69	1831.75
1831.65 ± 0.17[b]	1831.85 ± 0.16[b]

[a] Na^{24} lines taken as 1368.7 and 2755.7 exactly.

[b] rms fluctuations from averages.

Table 2 shows some very preliminary results on the energy of the K^{40} line, compared with the Y^{88} lines as standards. The source was about three kilograms of potassium chloride mixed with a roughly equal activity of Y^{88} and contained in an annular can surrounding the detector. The Y^{88} energies are taken from the results of Peelle and Love [3], and the first result is obtained by linear interpolation. Also shown are the results corrected for the nonlinearity of sodium iodide according to the work of Engelkemeir [4]; the correction is about 4.7 kev.

These results were not corrected for amplifier nonlinearity. In a study of the amplifier, the nonlinearity appeared to be of a "superproportional" nature. However, the quadratic term as determined by a least-squares fit, and the fluctuations of the data from the fit, and the least count of the mercury relay pulser used in the calibration were all three of the same size, and no definite conclusion could be drawn.

Table 3 shows the results of all these experiments, still uncorrected for amplifier nonlinearity. The first two lines are linear and nonlinear interpolations for the Y^{88} lines in terms of standards determined by beta-ray spectrometry. The third line is the nonlinear interpolation of the K^{40} line between the Y^{88} lines as just determined by nonlinear interpolation. Linear and nonlinear interpolations using

the results of Peelle and Love [3] appear on the last line of the table. It would be less than fair to the work and to the data not to point out that the Y^{88} results are all within the range of beta-ray spectrometer results for this activity, and that the energy of the K^{40} line is only slightly outside the combined errors of this measurement and the best previous result, the scintillation spectrometer work of Good [5].

Table 2. Gamma-Ray Energy for K^{40} Determined by Use of a Linear Interpolation Based on the Literature Values[a] for Y^{88}. Counting time was 40 min

Accumulated Data (kev)	Difference Data (kev)
1461.46	1461.95
1464.98	1465.47
1460.29	1461.02
1458.97	1459.19
1460.54	1459.00
Average and rms fluctuation	1461.3 ± 2.2
With uncertainties in Y^{88} energies	1461.3 ± 2.6
Corrected for NaI nonlinearity	1456.6 ± 2.7

[a] Y^{88} lines taken as 898.8 ± 1.2 and 1840 ± 2.

Table 3. Summary of Preliminary Results. Energies are in kev

Activity	Linear Interpolation	Corrected for NaI Nonlinearity	Standards	
Y^{88}	1831.7_5 ± 1.1	1828.8 ± 1.5	Na^{24}	1368.7 ± 1.0 2755.7 ± 1.0
Y^{88}	895.3 ± 1.3	892.8 ± 1.5	Na^{24} Cs^{137}	1368.7 ± 1.0 661.6 ± 0.2
K^{40}		1447.7 ± 3.0	Y^{88}	1828.8 ± 1.5 892.8 ± 1.5
K^{40}	1461.3 ± 2.2	1456.6 ± 2.7	Y^{88}	1840 ± 2 898.8 ± 1.2

In Table 3 the only energies which are known accurately are those of the Na^{24} and Cs^{137} standards. These lines have been measured by beta spectrometry, in instruments which have been proved linear by comparing sums with crossover energies; this is exactly the method used by Peelle and Love and others [6] to discover the nonlinearities in the scintillation spectrometer; in this connection, it should be pointed out again that there still exists a great need for precisely determined energy standards, especially isolated lines in the region between Bi^{207} and the thorium-active deposit. Some candidates are listed in Table 4; the energies shown are beta-ray spectrometer results, except for Cl^{38} which has not yet been studied in the beta-ray spectrometer.

Table 4. Suggested Gamma-Ray Line Standards

Activity	Gamma-Ray Energy[a] (kev)	Half-Life
Zn^{65}	1116 ± 5	250 d
Na^{22}	1277 ± 4	2.6 y
K^{42}	1530 ± 10	12.5 h
La^{140}	1596 ± 2	40 h
Y^{88}	1850 ± 40[c]	105 d
	908 ± 20	
Cl^{38}	(2160)[b]	37 min
	(1640)[b]	
$CePr^{144}$	695 ± 5[c]	284 d
	1480 ± 10	
	2185 ± 15	

[a] As measured by beta-ray spectrometry.

[b] Scintillation spectrometry value.

[c] See ref [7] for accurate interpolations with scintillation spectrometer.

It is proposed to complete the determination of the K^{40} line by making spectra of samples containing (1) K^{40} and Y^{88} and (2) Na^{24} and Y^{88}. The Y^{88} lines will be used as internal standards to control gain and base-line drifts. The position of the K^{40} line will be compared with that of the Na^{24} line at 1368.7 kev by interpolation and extrapolation over a relatively short interval of some 90 kev. Under these conditions, the uncertainties in the K^{40} line which arise from uncertainties in the energies of the Y^{88} lines and from the nonlinearities of the detector-analyzer system should be much reduced.

REFERENCES

[1] B. L. Robinson and R. W. Fink, *Revs. Modern Phys.* **32**, 117 (1960).

[2] W. Frati and J. Rainwater, *Phys. Rev.* **128**, 2360 (1962).

[3] R. W. Peelle and T. A. Love, ORNL-2790 (1959) (unpublished).

[4] D. Engelkemeir, *Rev. Sci. Instr.* **27**, 589 (1956).

[5] M. L. Good, *Phys. Rev.* **81**, 891 (1951).

[6] R. W. Peelle and T. A. Love, ORNL-2801 (1959) (unpublished); and *Rev. Sci. Instr.* **31**, 205 (1960); also, W. Managan and C. E. Crouthamel, "Extrinsic Variables," in *Applied Gamma-Ray Spectroscopy*, p 56, Pergamon Press, New York, 1960; J. Kantele and R. W. Fink, *Nucl. Instr. Methods* **13**, 141 (1961).

[7] Monahan, Raboy, and Trail, *Phys. Rev.* **123**, 1373 (1961).

(2-4) QUALITY CONTROL FOR THE GAMMA-RAY SCINTILLATION SPECTROMETER

D. F. Covell

U.S. Naval Radiological Defense Laboratory

San Francisco, California

INTRODUCTION

The range of applicability of the scintillation method of gamma-ray spectrometry has expanded in accordance with the rapid development of the pulse-height analyzer. At present, however, the form of the data from these instruments is such that interpretation is difficult, and the full potentialities of the method are not being utilized. The developing interest in applying digital computer techniques to the problem of interpretation should eventually make it possible to take greater advantage of these potentialities, and in so doing substantially broaden the range of applicability of the method.

In order to apply computer techniques to the problem of scintillation gamma-ray spectrometer data analysis, a calibration must be obtained for the spectrometer. The calibration consists of determining the channel-by-channel response of the spectrometer, as a function of gamma-ray energy over the energy range of interest. Once such a calibration has been obtained, however, drifts in the instrument may alter it, thereby introducing inaccuracies in attempted measurements. In this report, a method based on well-established quality-control techniques is described for both establishing and maintaining instrument stability over long periods of time.

The derivation of calibration data from theoretical considerations would be preferable to an empirical calibration if such data were accurate. Zerby [1] has shown that it is possible to approximate the crystal response characteristic of sodium iodide from theoretical considerations, but he also points out that definite discrepancies exist between theoretically derived pulse-height distributions and those actually observed. While possible explanations for these discrepancies have been advanced, Heath [2] does not believe there has been an adequate explanation to date and, further, stresses the importance of using the exact pulse-height distribution as actually observed in a given experiment. Even if the scintillator response could be obtained exactly from theoretical considerations, the response characteristic of a specific instrument assembly would depend upon such instrumental factors as (1) the conversion and optical efficiency of specific crystals, (2) photocathode conversion efficiency and dynode secondary-emission ratios, (3) linearity and stability of pulse-height analysis equipment, (4) detector-shield geometry, and (5) sample preparation and placement. It is for these reasons that an empirical calibration is considered to be essential.

The work of Bell [3] and Heath [4] shows that an empirical calibration is laborious to obtain. Once obtained, such a calibration may be invalidated by drifts or fluctuations or subtle performance abnormalities in the instrument. Even if such instrumental factors do not completely invalidate the calibration, they will lessen the precision of measurement. Therefore, in establishing high standards of precision and accuracy, it is important that fluctuations and drifts be minimized and that performance abnormalities be promptly recognized, corrected, and the likelihood of their further occurrence minimized.

Several methods for the correction of drifts, or the compensation of drift effects, have been proposed. These methods have consisted of applying feedback principles to the instrument, or normalization techniques to the resultant data. de Waard [5] considers the drifts in gain to be the principal problem in drift correction, and baseline drifts to be negligible by comparison. He has developed a method for gain stabilization in which there is generated an error signal proportional to the difference in the counting rate observed on the upper and lower amplitude slopes of a selected peak in the measured distribution. This error signal is applied directly in series with the phototube high voltage in such a manner as to correct the peak position.

Scherbatskoy [6] has used a method similar to that of de Waard for reducing gain drifts in the phototube. In Scherbatskoy's method, light pulses are introduced into the phototube along with the pulses from the main crystal. These pilot pulses are constant in magnitude and larger than any pulses within the spectrum of interest. An error signal is generated in accordance with shifts in the measured amplitude of the pilot pulses and this error signal is fed back to the phototube high voltage regulator.

Fite *et al.* [7] have used a technique which corrects for drifts in both gain and baseline. Two radionuclide sources are positioned near the crystal to provide two separate reference peaks, one in the lower channels where drift effects are primarily due to baseline shift and one in the upper channels. Based on deviations in the positions of these two peaks, both gain and baseline controls are adjusted by servo systems.

Chase [8] has also developed a method for stabilization of both gain and baseline. The objective was to achieve a degree of stabilization which would be compatible with the resolution capability inherent in the solid state detector. The method is

similar in principle to that of Fite *et al.* except that stable reference pulses from a pulse generator are used and are introduced at the preamplifier level.

Heath [2], in his computer program for spectrum unfolding, corrects for shifts in the gain or zero of the spectrometer by transforming the distribution in accordance with recognizable detail in the distribution. Such recognizable detail may be inherent in the measurement being made, or the source to be measured may have to have additional known material added to provide recognizable reference peaks.

Each of the above methods provides some degree of correction for drift. There are certain inadequacies in these techniques, however. In the methods where standard peaks or standard pulses are introduced, some loss of measurement capability results, especially if these pulses accompany the unknown pulses and are eventually stored in the memory of the instrument. In some of the above methods, possible changes in the crystal response are not being sensed, so that the correction for gain shifts is not complete. In addition, in the feedback systems of correction, an error signal is continually being generated and is subject to statistical fluctuation which may produce some line broadening in the measured pulse-height distribution. de Waard shows that under suitable conditions of measurement line broadening can be kept to a negligible value. In order to minimize such line broadening, it is necessary to have a peak sufficiently prominent and sufficiently free of underlying background or interference from other spectral detail. In practice, however, it may be difficult to keep line broadening to a negligible value on a routine basis, since spectral detail of sufficient quality cannot be assured.

None of the above methods, as they are currently applied, make provision for the early recognition of erratic performance, but tend rather to mask such performance. While erratic performance may be compensated by such stabilizing techniques so that peaks appear to be properly positioned, the greater the burden of correction, the greater the likelihood of distortion in the resultant pulse-height distribution.

Some of the above methods make the assumption that all peak displacements are due to drifts in gain. It has been our observation, in concurrence with Heath [2], Fite [7], and Chase [8], that baseline drifts are equally as important as gain drifts, and that the assumption that displacements are due to drifts in gain only, can lead to errors.

In seeking a method for instrument stabilization, we believe that both gain and baseline drifts should be corrected and, further, that any stabilization technique to be used should be augmented by a regular critical examination of selected instrument performance factors. The following procedure of quality control is proposed to satisfy these objectives.

QUALITY CONTROL

Quality control is a technique for maintaining the quality of the output product of a process or system at a prescribed level. It is not primarily concerned with the establishment of quality, although in the process of correcting system deficiencies as they are exposed, the level of quality may be raised. In establishing a quality control procedure, the characteristics of the output product which are to be controlled must first be

determined. Next, "normal" performance is determined by observing the central tendency (arithmetic mean) of the values for the selected characteristics, as well as observing the dispersion (usually expressed as the standard deviation) of these values. If the capabilities of the system as reflected in these properties of the output product are acceptable by the criteria established, then a procedure of periodic sampling may be instituted in which the values for individual output units are compared with the system norm. If the sampling is done in such a manner that the sample values can be considered representative of the output product generally, then an analysis of these values provides a periodic estimate, within the limits due to sampling errors, of the system performance. In order to expedite the analysis of such data, individual values are usually plotted on a chart on which the system norm and system dispersion are marked. From such a chart, referred to as a control chart, trends or excursions representing deviations from the central values or from the established standard deviation are readily detected and corrective action is initiated.

The response characteristic of the gamma-ray scintillation spectrometer is a composite of the transfer characteristics of the scintillation crystal, multiplier phototube, and pulse-height analyzer. The overall transfer characteristic, relating incident gamma-ray energy to mean storage channel number when the gamma-ray energy has been totally absorbed in the detector, can be considered as a straight line having an extrapolated zero intercept in gamma-ray energy at zero channel number. A primary system of standardization can be established by standardizing and stablizing the slope and intercept of this transfer characteristic. The slope is determined by (1) the conversion and optical efficiency of the crystal, (2) phototube gain, (3) amplifier gain, and (4) the clock frequency of the analog-to-digital converter. Drifts or changes in any of these factors will change the slope. The zero energy intercept will be determined by the acceptance threshold (or baseline) of the instrument, and baseline drifts will not only change the intercept point but will also displace uniformly the entire characteristic.

In specifying a quality control procedure, in addition to evaluation of the slope and intercept of the instrument transfer characteristic, it would also be desirable to make rudimentary evaluations of the linearity, resolution, and background counting rate of the instrument. In the procedure to be described, the assumption has been made that the quality of performance has been established at or near the desired level and that, ordinarily, deviations will be small. A further consideration is that the entire quality control procedure (sampling, data evaluation, logging and estimation of control status) should be as brief as possible consistent with efficacy.

PROCEDURE

The procedure was originally developed as a possible aid in stabilizing an Argonne-type, 256-channel analyzer as manufactured by Radiation Counter Laboratories (Mark 20, Model 2603). This instrument was installed as a permanent laboratory facility to be used on a routine basis for radionuclide determination and estimation to augment existing radiochemical techniques. The analyzer was used in conjunction with an RCL Model A-61 linear amplifier and an RCL Model 21 precision high voltage

supply. The instrument was left energized on a continuous basis. During the period of development of the procedure, the detector consisted of a 3 × 3 in. NaI(Tl) crystal (Harshaw Chemical Company), in conjunction with a Dumont type 6363 phototube.

Several modifications were made on this equipment, of which the most significant were the following: (1) substitution of a 10-turn Helipot for the standard carbon potentiometer used as a fine voltage control in the phototube high voltage supply; this control provides an incremental adjustment of the phototube voltage of approximately 100 mv, and thus constitutes a vernier on the system gain; (2) inclusion of an auxiliary scaler to count all "store" pulses generated during a counting period so that a total gamma count could be readily obtained for each sample to be counted; (3) removal of the upper level trigger, V-718, so that a "store" pulse would be generated for overflow pulses, thereby making it possible to interpret the total gamma count in the usual sense (i.e., the total number of pulses above a given acceptance threshold).

The procedure consisted of making a count once each day, or more often if additional standardization appeared necessary, with a Zn^{65} standard. Zinc-65 was selected since its decay characteristics give rise to a pair of readily discernible peaks with energies of 1.12 Mev and 0.51 Mev in the pulse-height distribution (see Fig. 1).

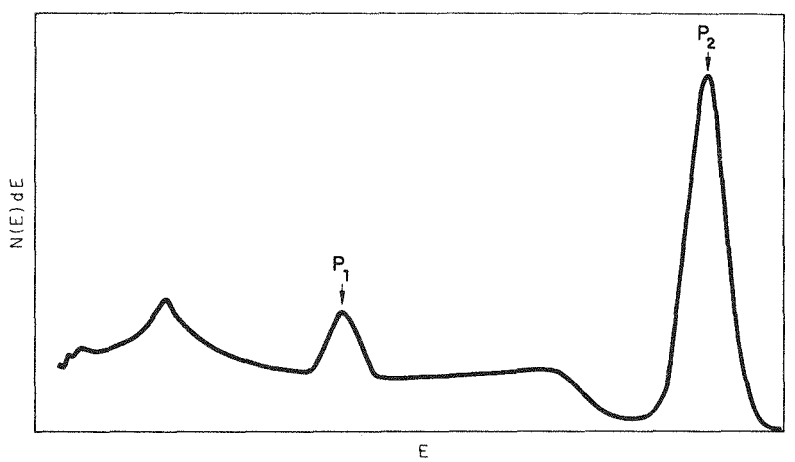

Fig. 1. Typical Pulse-Height Distribution for Zn^{65}, Showing the Relative Positions and Intensities of the Two Reference Photopeaks, $p_1 : E_{\gamma_1}$ = 0.51 Mev, and $p_2 : E_{\gamma_2}$ = 1.12 Mev.

The half-life of Zn^{65} is relatively short for a standard (245 days) but in this application, Zn^{65} has a useful life of at least one year.[1] In the pulse-height distribution, peak positions relative to specific reference channels yield information regarding deviations in the settings of the gain and baseline controls. In the present case, with

[1] We have recently been studying the possible use of Ti^{44} as a standard. This radionuclide has a half-life on the order of 1000 years, so that no half-life correction would be necessary. In addition to gamma rays having energies of 0.072 Mev and 0.160 Mev from the Ti^{44} decay, the 4-hr Sc^{44} daughter would provide additional peaks at 1.16 Mev, and 0.51 Mev. Such qualities are ideal for a general purpose gamma-ray spectrometer standard, and would be of particular interest in a standard for use with the present quality control procedure.

a standard setting of 5 kev equivalence per channel, the 2 reference photopeaks should be symmetrical about channels 102 (E_γ = 0.51 Mev) and 224 (E_γ = 1.12 Mev). When this condition exists, the counts in corresponding channels on either side of the reference channel are equal. In order to minimize errors, the counts in several channels on either side of the reference channel are summed and compared. Thus a ratio, k_{p_j}, is defined for a photopeak, p_j, as follows:

$$k_{p_j} = \sum_{a_{p_j}+1}^{a_{p_j}+l} n_i \Big/ \sum_{a_{p_j}-l}^{a_{p_j}-1} n_i , \qquad (1)$$

where

n_i = counts contained in channel i ,

a_{p_j} = reference channel number corresponding to photopeak p_j ,

l = number of channels which are to be summed on either side of the reference channel.

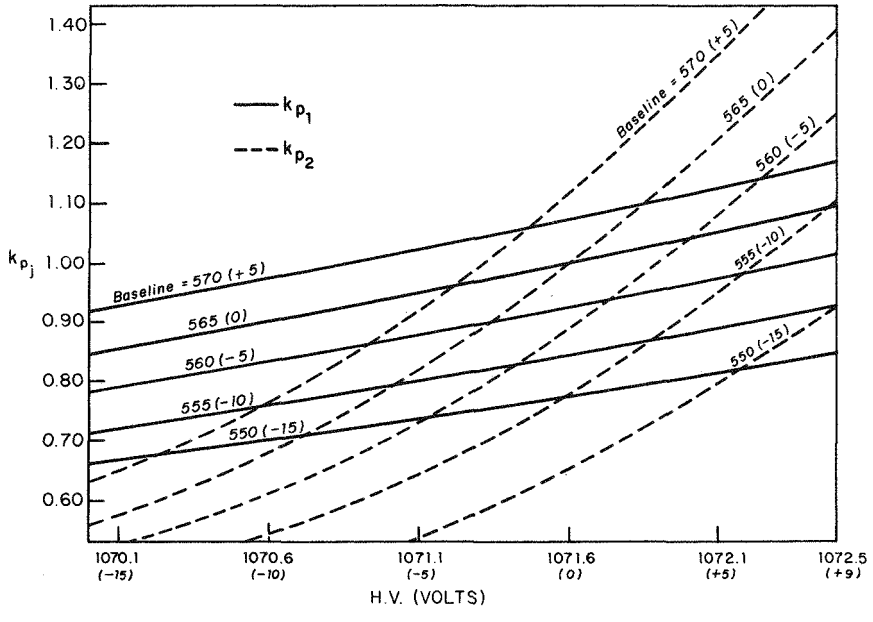

Fig. 2. Relationship of the k_{p_j} Ratios with Respect to Voltage Applied to the Detector for the Two Observable Peaks in the Zn^{65} Distribution ($p_1 : E_{\gamma_1}$ = 0.51 Mev, a_{p_1} = Channel 102; $p_2 : E_{\gamma_2}$ = 1.12 Mev, a_{p_2} = Channel 224). The relationships are shown for several settings of the baseline control. The values in parentheses represent deviations from a normal (0) setting in units of minimum increment on a ten-turn Helipot dial. These increments correspond to approximately 0.1 v on the detector voltage control, and approximately 0.032 v on the baseline control.

The photopeak is considered to be correctly positioned when $k_{p_j} = 1.00$ and deviations from the correct position will give values of k_{p_j} that will be less than or greater than 1.00.

In order to relate k_{p_j} values to deviations in gain and bias adjustments, quantitative correlations are obtained by a process of calibration in which k_{p_j} values are determined for specific settings of these controls. Such empirical data can be represented as families of curves, as shown in Fig. 2, where k_{p_j} values for the two reference photopeaks of Zn^{65} are plotted as a function of the high voltage (gain) setting for each of several bias settings. From Fig. 2, it is seen that for either family of curves, any of several combinations of bias and gain (H.V.) settings satisfy the condition that $k_{p_j} = 1.00$. By considering both families of curves, however, it is seen that only one combination of bias and gain settings satisfies the condition that $k_{p_j} = 1.00$ for both peaks, and these will be considered to be the correct settings.

The numerical values indicated for the high voltage and baseline controls on Fig. 2 correspond to specific settings of the respective controls. Once the correct settings are determined, the values can be converted to units of deviation, plus and minus, as shown by values in parentheses on the figure. Figure 2 could then be used directly in determining the extent of deviations in gain and baseline by routine determination of the k_{p_j} values. The curves of Fig. 2 however, do not provide the most convenient form for making the required estimates of deviation in the control settings. From these curves, a nomograph (Fig. 3) has been constructed from which the required estimates of deviation are easily obtained by drawing a straight line between the computed k_p values and observing the points of intersection of this line when extrapolated to the H.V. and baseline scales.

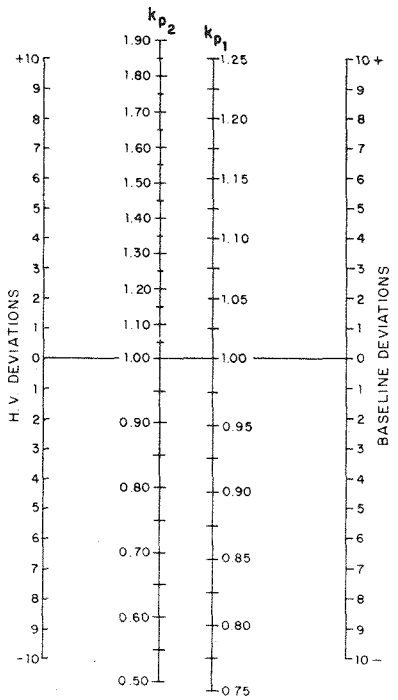

Fig. 3. Nomograph Prepared from Relationships Such as Shown in Fig. 2.

Figure 4 shows an excerpt from a typical control record on which various parameters of the data obtained by this procedure are logged. The data are normally plotted on K & E 350-142L graph paper (1 year by days), so that an entire year's record for each of the several parameters being plotted for a given instrument can be included on one sheet. A mean value and standard deviation for each of the parameters are estimated from the first 10 values for each year (provided instrument performance seems to be representative during the period that these values are obtained). Mean values are indicated by solid lines, and the one-standard-deviation values are indicated by dashed lines above and below the solid lines. On line 1 of the chart is plotted the day-to-day observed count rate (N_0) of the standard, corrected for half-life and background. N_0 is determined by summing all conversions taking place in the analog-to-digital converter in an auxiliary scaler during the counting period, and correcting this gross sum (n_0) for background and half-life. On line 2 is plotted the day-to-day background rate (B_0) which has been computed from the sum (b_0) of all conversions taking place in the analog-to-digital converter during a background counting period. N_0 was kept between 100,000 and 200,000 counts/min, and 5-min counting periods were used for both the standard and the background counts. On line 3 is plotted the ratio of the counts contained in a standard fraction of the photopeak to the total net count. This ratio,[2] f_p, is computed as follows (see ref [9]):

$$f_p = \frac{\sum_{a_p - l}^{a_p + l} n_i - (l + 1/2)\left[n_{(a_p - l)} + n_{(a_p + l)}\right]}{n_0 - b_0} .$$

The ratio, f_p, is computed only for the upper energy peak (E_γ = 1.12 Mev) of the standard, and a value of 10 has been arbitrarily selected for l. On lines 4 and 5 of the chart shown in Fig. 4 are plotted the day-to-day deviations in the control settings as determined from Fig. 3. These lines provide an indication of instrument stability.

Deviations in the baseline and high voltage (gain) controls should be uniformly dispersed around zero. If they show a tendency to be predominantly positive or negative, a long-term drift is indicated, as might accompany a gradual degeneration of elements in the instrument, such as the detector, preamplifier, amplifier, etc. If the dispersion of points is large, it is an indication of excessive short-term drifts. The dashed lines above and below lines 4 and 5 indicate deviation values in the baseline and gain controls which would correspond to a shift in the upper energy peak (E_γ = 1.12 Mev, a_p = 224) of one full channel.

No explanation is offered regarding the significance of the specific patterns which can be readily seen in the plots of Fig. 4. The plots are part of a cumulative history of a particular instrument and have been of value, both in establishing confidence in the instrument as well as in improving the performance of the instrument. They are

[2]The ratio, f_p, bears a correspondence to peak resolution and has been used as a figure of merit at this laboratory in making evaluations of detection assemblies. The routine logging of f_p values, as derived from the upper energy peak (E_γ = 1.12 Mev), has on two occasions exposed degenerating elements in the system. In both instances, the difficulty was a departure from linearity for the larger pulses. In one case, the phototube was determined to be at fault and in the other case the preamplifier was at fault. In both of these cases, the irregularities were exposed by the data on the control chart and were corrected before the effects were noticeable in the experimental data being taken.

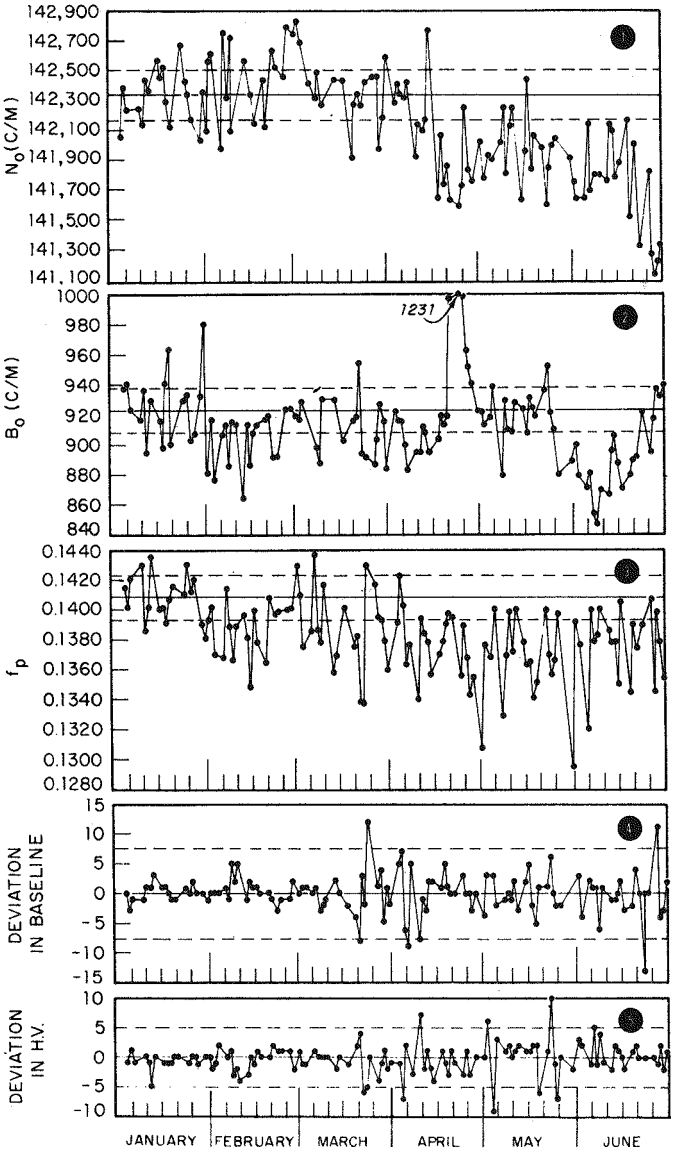

Fig. 4. Excerpt from a Typical Control Chart. N_0 **is the observed count rate of the standard, corrected for half-life and background.** B_0 **is the background rate.** f_p **is the ratio of the counts contained in a standard fraction of the photopeak to the total net count, and bears a correspondence to peak resolution. On lines 4 and 5 are plotted the day-to-day deviations in the control settings. The dashed lines associated with lines 1, 2, and 3 indicate the one-standard-deviation values as estimated from the first 10 values to be plotted on the respective lines. The dashed lines associated with lines 4 and 5 indicate deviations in the control settings (Baseline and H.V.) which would cause a one-channel shift in the upper energy peak (**E_{γ_2} **= 1.12 Mev,** a_{p_2} **= Channel 224).**

presented here merely to demonstrate the types of patterns which may develop, and the ease with which such patterns can be recognized when viewed in this perspective.

RESULTS

The early results of such a program tend to be discouraging, apparently yielding nothing more than a demand for an inordinately large amount of effort devoted to correction of irregularities that were not apparent before. However, persistent adherence to this discipline, once imposed, has paid large dividends in instrument reliability and improved quality of measurement. The procedure has been used over a period of several years on each of two gamma-ray spectrometers in use at this laboratory and has made it possible to achieve and maintain, on a long-term basis, a channel stability of better than 0.25%, based on the apparent stability of the upper energy peak (E_γ = 1.12 Mev, a_p = 224) as inferred from Fig. 4.

During the period that this method has been in use, it has helped to expose certain manufacturing flaws (e.g., improperly soldered connections), and design inadequacies (e.g., excessive current flow in a voltage reference tube in one of the power supplies) in the instrument. It has also helped to establish the level of regulation required for the power line as well as the stability to be maintained for the ambient temperature. Calls for special maintenance assistance have been reduced, and when such calls are made, they are based on more objective observation.

CONCLUSIONS

This method of analyzer standardization has the following desirable features:

1. The entire measurement system, including the phototube and crystal, is corrected for drift.
2. The method provides correction on both baseline and gain settings.
3. A history of performance is established so that unusual or persistent drifts can be easily spotted and corrective action taken before major difficulties develop.
4. The method does not introduce extraneous "background" or additional spectral detail which may complicate the interpretation of measurement spectra.
5. The method is simple and easy to perform, even by unskilled technicians; for two instruments, approximately 30 min/day of technician time is required for the data taking, computing and logging.
6. The method provides a more objective basis for instrument repair and maintenance.
7. Adherence to the procedure assures a regular objective inspection of the instrument, so that irregularities are spotted early.
8. Periodic examination of the chart may show correlations with ambient effects which may either be eliminated or compensated, thus providing a basis for the gradual improvement of measurement quality.

This method has the disadvantage of not being continuous, that is, corrections are made only once each day. From the charts, however, an estimate of the magnitude of short-term deviations can be obtained, thereby establishing a basis for the

study and eventual minimizing of these deviations. Another feature is that a certain experimental and statistical error is associated with the determination of the k_p values. These errors will tend to increase the dispersion of the points on lines 4 and 5 of the control chart (Fig. 4). The magnitude of these errors has not been examined, but the errors are part of the data of Fig. 4, which shows that the total deviation in the upper energy peak ($a_p = 224$) (including effects due to drift and errors in the determination of the k_p values) can be maintained at less than $\frac{1}{2}$ channel. The method described does not correct for drifts that may result directly from the measurement of specific samples (e.g., drifts in the detector as a result of counting high activity samples), but these sources of drift have been examined collaterally. The examination and proposed method for the reduction of the major source of such drifts (i.e., gain shifts as related to sample activity levels) has been reported separately [*10*].

The level of stability achieved by this method has been adequate for much of the measurement work done on our instruments. As the requirements for higher quality measurements become greater, however, it appears that greater stability may be required. Such improvement might be achieved by making second-order corrections with respect to those demonstrated here, possibly by combining elements of this method with other methods (either utilizing feedback principles, or computer compensation), in which case this technique could serve to assure that such corrections would be small and meaningfully applied.

REFERENCES

[*1*] C. D. Zerby and H. S. Moran, *Calculation of the Pulse Height Response of NaI(Tl) Scintillation Counters*, ORNL-3169 (1962).

[*2*] R. L. Heath, "Data Analysis Techniques for Gamma-Ray Scintillation Spectrometry," IDO-16784 (1962); *IRE Trans. Nucl. Sci.* **NS-9**(3), 294 (1962).

[*3*] P. R. Bell, "The Scintillation Method," *Beta- and Gamma-Ray Spectroscopy* (ed. by K. Siegbahn), Interscience, New York, 1955.

[*4*] R. L. Heath, *Scintillation Spectrometry Gamma-Ray Spectrum Catalogue*, IDO-16408 (1958).

[*5*] H. de Waard, "Stabilizing Scintillation Spectrometers with Counting Rate-Differences Feedback," *Nucleonics* **13**(7), 36–41 (1955).

[*6*] S. A. Scherbatskoy, "Stabilized Scintillation Counter," *Rev. Sci. Instr.* **32**, 599 (1961).

[*7*] L. E. Fite, D. Gibbons, and R. E. Wainerdi, "A System for the Control of Drift in a Multi-Channel Gamma Ray Spectrometer," *Proceedings of the 1961 International Conference on Modern Trends in Activation Analysis, held at Texas A. & M. College, December 15-16, 1961*, Texas A. & M. College, College Station, 1962.

[8] R. L. Chase, "A Servo Stabilized Analog-to-Digital Converter for High Resolution Pulse Height Analysis," *IRE Trans. Nucl. Sci.* **NS-9**(1), 119 (1962).

[9] D. F. Covell, "Determination of Gamma-Ray Abundance Directly from the Total Absorption Peak," *Anal. Chem.* **31**, 1785 (1959).

[10] D. F. Covell and B. A. Euler, "Gain Shift vs Counting Rate in Certain Multiplier Phototubes," *Proceedings of the 1961 International Conference on Modern Trends in Activation Analysis, held at Texas A. & M. College, December 15-16, 1961*, Texas A. & M. College, College Station, 1962.

(2-5) EVALUATION AND CALIBRATION OF PULSE-HEIGHT ANALYZER SYSTEMS FOR COMPUTER DATA PROCESSING

D. F. Crouch and R. L. Heath
National Reactor Testing Station, Phillips Petroleum Company
Atomic Energy Division, Idaho Falls, Idaho

INTRODUCTION

If data coming from several analyzers is to be used in the same computer programs, a precise knowledge of the operating characteristics of each system must be known. Furthermore, it is particularly convenient if the analyzer systems can be standardized to a performance level which is readily reproducible. This paper is a report of tests developed and used to evaluate and calibrate performance parameters of various analyzer systems. The performance parameters specifically covered by this report are:

1. Analog-to-digital converter (ADC) accuracy and stability,
2. ADC integral and differential linearity,
3. Zero and bias shift due to counting rate,
4. Live-timer accuracy,
5. Effect of pulse shape on performance of the ADC.

In addition, initial calibration and routine checking of calibration will be briefly discussed.

LINEAR TEST PULSE GENERATOR

A stable, linear, pulse generator greatly facilitates the evaluation of analyzer systems. In particular, it is very helpful if the relative pulse height can be read

directly from the vernier on the amplitude control. Since no generator was commercially available with precise amplitude control, a simple, inexpensive pulser was constructed. Total cost of parts for the pulse generator is estimated at $200. A schematic of the pulse generator is shown in Fig. 1.

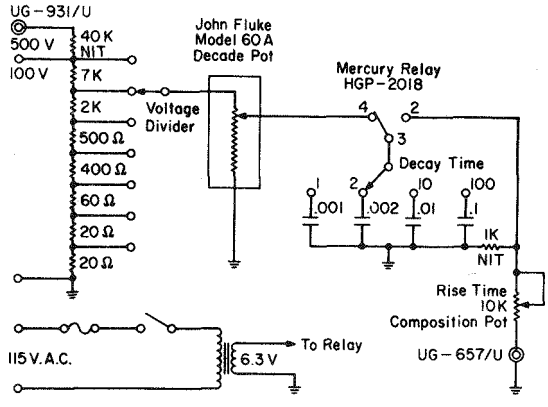

Fig. 1. Precision Pulse Generator.

Precise, linear voltage control was attained by using a John Fluke model 60A High Resolution Decade Potentiometer as the pulse amplitude control. Specifications for the potentiometer include a resolution of better than 0.0002% and linearity of 0.005%. Excellent voltage stability was attained by attenuating a 500-v power supply voltage down to 200 mv for a maximum output from the pulser. High voltage for the pulse is externally supplied by one of the high voltage power supplies normally used for photomultiplier high voltage. The power supply is always allowed to warm up for several hours before being used with the pulser.

Selection of one of four capacitors permits adjustment of the decay time of the outgoing pulse. A 10,000-ohm composition pot determines the pulse rise time.

To check linearity of the pulser, dc voltages between the Fluke Potentiometer arm and ground were measured with a Leeds and Northrup No. 7552 Slide-Wire Potentiometer as a function of pulser amplitude vernier settings. On the scale used to check the pulser, the slide-wire bridge was accurate to, and could be read to, 0.00001 v. Typical calibration points are given below:

Pulse Amplitude Setting	Voltage
911.00	0.91100
511.00	0.51100
199.50	0.19951
49.50	0.04951

In addition, relay timing and RC constants were verified with an oscilloscope to ascertain that no charge buildup was occurring.

PERFORMANCE TESTING OF ANALYZER

Testing of ADC Accuracy and Stability

In conjunction with checking the ability of the analyzer ADC to consistently store pulses of the same height into the same channel, this test also permits the sharpness of channel edges and the associated adjacent channel overlap to be determined. All of the tests to be described were performed by using an Oak Ridge model A-8 linear amplifier [*1*] in place of the amplifier normally supplied with the analyzer.

The pulser is fed through a 33-pf coupling capacitor into the A-8 preamplifier. (Unless a 33-pf capacitor is used for coupling into the A-8 preamplifier, peculiarities in the preamplifier feedback circuit will cause a nonlinear output.) After the pulse height is adjusted to fall into some convenient region with respect to readout ease, the analyzer is switched to the analyzer mode for a short time interval (usually 100 sec in our laboratory). It is most accurate to let the live timer stop the analyzer. The counts in all adjacent channels, the corresponding channel numbers, and the pulser setting are recorded. The analyzer memory is cleared, the pulse amplitude increased by a small increment, and the new pulse height analyzed for the same time interval as the former run. This procedure is continued until the pulse has been incrementally advanced through three or four channels. A sufficient number of evenly spaced experimental points should be taken in each channel so that channel edges and center will be clearly defined. A semi-log plot of channel counts vs pulser setting permits a "channel profile" to be sketched. Where channels overlap, at least two channel counts will appear on the graph for each pulser setting. A "channel profile" is shown in Fig. 2.

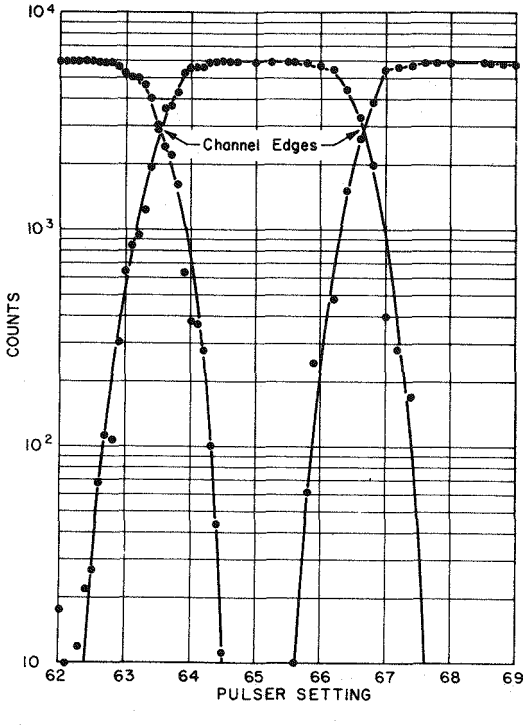

Fig. 2. Channel Profile.

Of course, the most accurate ADC will be one which shows the least amount of adjacent channel interference. Sources of noise that may cause channel overlap are pulser noise, ADC jitter, and pulse amplifier noise.

Test of Integral Linearity

The characteristic curve, for a particular analyzer, indicates the channel number into which a pulse of any amplitude will be recorded. Ideally, this should be a straight line. Departure of this characteristic curve from a straight line is a measure of non-linearity. Integral linearity is the ratio of departure at any point to the pulse amplitude corresponding to full scale. Generally, the term integral linearity is intended to mean the ratio defined above at the worst part of the characteristic.

A good working definition for integral linearity of an analyzer system is the maximum deviation in any channel from a straight line plot of channel position vs input pulse amplitude. The following test is based on the latter definition.

Initially, the pulser is adjusted until pulses are being recorded equally in adjacent channels, for example, channels 249 and 250. The final pulser amplitude setting is noted along with channel number 250. With the pulses being recorded equally in channels 249 and 250, one can assume that the pulse is precisely on the lower edge of channel 250. If the pulses were being recorded entirely within channel 250, the exact location of the pulses inside the channel would be uncertain. This assumption can be verified by examining the channel profile and noting the sharpness of the channel edges.

The procedure described above is usually repeated in the vicinities of channels 200, 150, 50, 25, and for all channels below number 10. All channels below number 10 are plotted because deviations in integral linearity are usually greatest in these channels.

A plot of channel number vs pulser setting is made from the resulting data and is shown in Fig. 3. Analyzer *A* is an old vacuum tube analyzer; deviations in linearity are apparent at both the low channel and high channel ends of the curve. Analyzer *B* is a transistorized analyzer and appears to be linear.

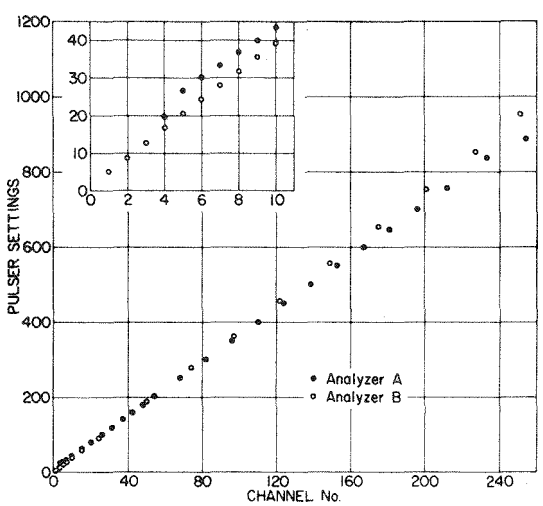

Fig. 3. Linearity Plots.

A more sensitive method of presenting the same information is to plot deviation in pulse height vs pulse height. For this plot, the analyzer zero control and pulse-height gain control were adjusted until relative pulse heights of 9.5 and 199.5 are recorded on the leading edges of channels 10 and 200, respectively. (The reasons for using pulse heights of 9.5 and 199.5 are explained in detail in the calibration section of this report.) These two points are assumed to be lying on a theoretical straight line characteristic curve. Positions of the leading edges of other channels are measured in the same manner as described in the preceding paragraphs. The measured pulse height of channel position is subtracted from what the pulse height would be if the channel were on the theoretical straight line. The difference in these two pulse heights represents the deviation from linearity of the ADC for that particular channel. In Fig. 4 the deviations were changed to percentages of a channel width and plotted against channel number. Once again, the curve labeled "Analyzer *A*" represents the performance of an old vacuum tube analyzer, while the curve for "Analyzer *B*" represents the performance of a newer transistorized model. Of course, the analyzer zero control could be adjusted to split the worst deviation. For example, the zero control of Analyzer *B* could be adjusted such that channel 130 has ± 0.25 channel deviation instead of +0.5 channel deviation. The integral linearity, by the usual definition, would then become 0.25 channel (maximum deviation) divided by 200 channels (full scale amplitude) or 0.13%.

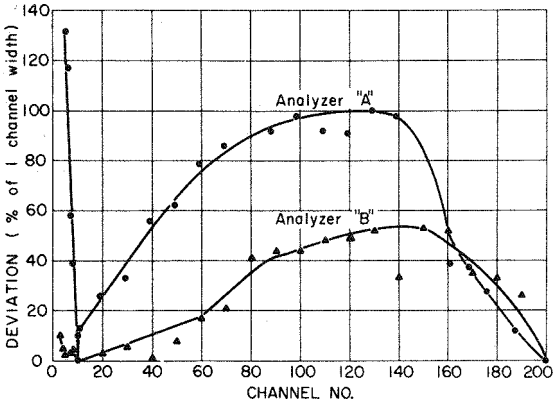

Fig. 4. Plot of Deviation from Linearity.

Differential Linearity

Differential linearity is a term used to describe uniformity in channel widths over the entire analyzer range. Thus, a differential linearity of 1% means that no channel departs by more than 1% from the average channel width for all channels. Generally, a sliding pulse generator is used to check differential linearity. An adequate description of this method is given by Chase [2]. Most of the recent model analyzers have good differential linearity above the first five channels.

Test of Counting-Rate Shift

A shift in analyzer zero or a shift in ADC bias due to a high counting rate is highly undesirable if computer processing is to be used. Counting-rate shift is usually caused by pulse pileup; that is, the count rate is so high that circuit capacitance does not have time to discharge completely and succeeding pulses appear to have a pulse height larger than their actual height. In this laboratory, counting-rate shift in the amplifier system is avoided by using a double-differentiating A-8 amplifier [*1*]. The negative portion of the amplifier's bipolar pulse discharges circuit capacitance immediately after charging by the positive portion. Thus, there is no residual charge to distort the height of ensuing pulses. Tests on the A-8 amplifiers in this laboratory have indicated no counting-rate or bias shift (<0.05%) for rates up to 40,000 counts/sec.

Photomultiplier tubes usually contribute the major portion of the observed counting-rate shift. Therefore, if a test is used to evaluate counting-rate shift in an analyzer, the test should be of such a nature as to isolate counting-rate shift due to the photomultiplier from shift due to the analyzer itself. The usual method involves the simultaneous measurement of radioactive source and a pulser to indicate the degree of counting-rate shift.

The pulser is connected to the preamplifier in parallel with the scintillation detector. With no input to the detector, the pulser is adjusted until an equal number of pulses are being recorded by adjacent channels in the high channel number end of the analyzer memory. The channels should be high enough that coincident pulses from the "hot" source will not interfere with pulses from the pulser.

Finally, the "hot" source is placed on the detector, and the resultant spectra are recorded. (A Cs^{137} source of 30,000 counts/sec is commonly used in our laboratory.) Any counting-rate or bias shift in the analyzer system will be indicated by the pulser pulse moving off the channel edge where it was originally placed. The sensitivity of this measurement is directly proportional to the sharpness of the channel edges. Referring back to the channel profile (Fig. 2) will give an idea of the minimum amount of counting-rate shift that can be detected.

Live-Timer Check

The live-timer check is based on the following reasoning: If the live timer works accurately for a particular setting, the analyzer will be "alive" – that is, in readiness to accept incoming pulses – for the same total time regardless of counting rate. Therefore, if a weak source and a hot source were counted simultaneously, the total counts of the weak source recorded should be the same as if the weak source were being counted by itself. A hot low energy source and a weak high energy source are used for the live-timer test. Typical sources used are Hg^{203} (15,000 counts/sec) and Zn^{65} (200 counts per sec).

First, the hot source and weak source are counted simultaneously. Next, the weak source is counted alone. The counts in the photopeak of the weak source are totaled for both runs. A comparison of the totals indicates the accuracy of the live timer. A pulser could be used in the place of the weak source and, thereby, eliminate the uncertainty due to the error in integration of the peak due to the weak source. However, consideration should be given to the possibility of errors due to lock-in of the pulser with

the analyzer live timer and pulser pulses occurring in coincidence with the hot source pulses. Live timers of transistorized analyzers evaluated by our laboratory have had inaccuracies ranging from 12% down to less than 0.5%.

Pulse Shape

The peak detector of an analyzer requires a finite time to decide that a pulse entering the ADC has reached its peak and is ready to be stretched. This decision time becomes critical and can cause nonlinearities for large pulses. For small pulses, the change in voltage per unit time is low and a small error in peak detector time will have little effect on the stretched pulse height. But the large pulses have a high rate of voltage change, and a small error in decision time can cause a nonlinearity of two or three channels in the uppermost part of the analyzer range. Many peak detectors require approximately 1.25 μsec to make a decision; however, most A-8 amplifiers come from the factory with 1-μsec delay lines. Increasing A-8 delay lines by 25% will greatly improve the linearity of the uppermost channels. As would be expected, the random sum coincidences will increase by about 25%.

CALIBRATION AND ROUTINE CHECKING OF CALIBRATION

Pulse-Height Scale Considerations

If the nonlinearity of sodium iodide crystal light output is to be taken into account by computer programs, some pulse-height scale must be established. Due to the nonlinearity of sodium iodide and the uncertainty of locating photopeak maxima within a channel, radioisotopes cannot readily be used to establish an accurate pulse-height scale. For this reason an absolute pulse-height scale based on electrical calibration must be employed.

Since a channel represents a band of pulse heights from V to $V + \Delta V$, a plot of counts vs pulse height should be a histogram with each bar representing the width of one channel. If a point plot is to be used, consideration should be given as to where the point representing a channel belongs. If the analyzer system characteristic curve intersects the pulse-height axis at zero, and a Gaussian distribution of pulse heights within a channel is assumed, a point representing channel counts should properly appear as a point in the middle of the channel; for example, a point representing counts in channel 50 should be plotted at 49.5, because channel 50 represents a band of pulse heights whose mean height is 49.5. However, if the characteristic curve intersects the pulse-height axis at -0.5 channel, a relative pulse height of 50 would fall in the middle of channel 50 and could legitimately be plotted as a point on the 50 division line. This is the basis for the absolute scale as used in our laboratory.

Method of Initial Zero Alignment

Analyzer zero control and pulse-height gain control are varied until relative pulse heights of 199.5 and 9.5 are recorded on the lower edges of channels 200 and 10. Thus a channel number represents the mean of the pulse heights stored in that channel.

Routine Checks of Calibration

Analyzer system performance and calibration are checked daily by laboratory assistants. Routine procedure is to adjust photomultiplier high voltage so that the maximum of the Cs^{137} photopeak is positioned in channel 66.2. Live-timer, linearity, and zero shift are checked with a Bi^{207} standard. After the standard source has been analyzed, its spectrum is superimposed over that of a Bi^{207} standard read into the analyzer from tape. A comparison of heights and positions of photopeaks will point out any changes in performance parameters. This method has been established to be accurate to 0.01 of one channel for the zero setting.

As a check of system stability, an analyzer system was allowed to go for one month without adjustment. The amount of gain drift was determined by daily least-squares fitting of the 0.57- and 1.06-Mev peaks of Bi^{207}. Zero drift would be indicated by a change in the ratio of the 0.57-Mev peak position to the 1.06-Mev peak position. The 1.06-Mev peak drifted 1.5 channels during the first five days of the test and remained within 0.5 channel of the same value for the remainder of the month. No zero shift (<0.1 channel) was detected over the 30-day period.

REFERENCES

[1] G. G. Kelley, *IRE Natl. Conv. Record* **9**, 263 (1957).

[2] R. L. Chase, *Nuclear Pulse Spectrometry*, p 281, McGraw-Hill, New York, 1961.

Session 3

Chairman: J. E. Monahan

Argonne National Laboratory, Argonne, Illinois

(3-1) SCINTILLATION SPECTROMETRY – THE EXPERIMENTAL PROBLEM[1]

R. L. Heath

National Reactor Testing Station, Phillips Petroleum Company, Atomic Energy Division, Idaho Falls, Idaho

INTRODUCTION

Prior to the many detailed descriptions of sophisticated analysis techniques which will be presented during the course of this meeting, it would seem useful to review the problems associated with the experimental acquisition of data with scintillation spectrometers. It was felt that this would be particularly appropriate at this conference because several disciplines are represented. Among these are the nuclear spectroscopists who originated the experimental techniques presently being utilized, experimental scientists from many other fields who are interested in applying gamma-ray spectrometry to problems in their own field, and – most welcome – the applied mathematicians who are becoming more and more involved in the development of methods for the analysis of data.

This paper is intended to summarize, briefly, the areas of experimental interest, to define the experimental variables, and to indicate the present limitations imposed by experimental procedures and equipment. A restatement of the experimental problems should aid in the evaluation of particular methods of analysis and their limitations.

The basic problem in the analysis of data obtained with scintillation spectrometers is the rather complicated relationship between the photon spectrum incident upon the detector and the pulse-amplitude spectrum produced by the interaction of photons with the detector. This relationship is illustrated in Fig. 1, which shows a line photon spectrum consisting of four gamma rays of 0.060, 0.320, 0.830, and 1.92 Mev of equal intensity. Above this are the pulse-amplitude spectra produced by a 3- by 3-in. NaI(Tl) detector for each of these monoenergetic gamma rays. At low energies the pulse spectrum is essentially characterized by a symmetrical peak which is in fact nearly Gaussian in shape. This feature is attributed to interaction by the

[1]Work performed under the auspicies of the U.S. Atomic Energy Commission.

photoelectric process. As the gamma-ray energy increases, the pulse distribution becomes more complicated. In addition to the so-called photopeak there is also a continuous distribution of pulses all the way down to zero amplitude. This distribution is attributed to the Compton process. At even higher energies numerous little satellite peaks appear which are attributed to interaction of the photons by the pair process. Although the detailed shape to be expected from a detector for a gamma ray of a given energy may vary with different types of detectors, it will always contain the major features described. The essential information contained in an experimental spectrum is contained in the photo or full-energy peak. Its median position on the pulse-amplitude scale is related to energy and its area to the intensity of the associated gamma ray.

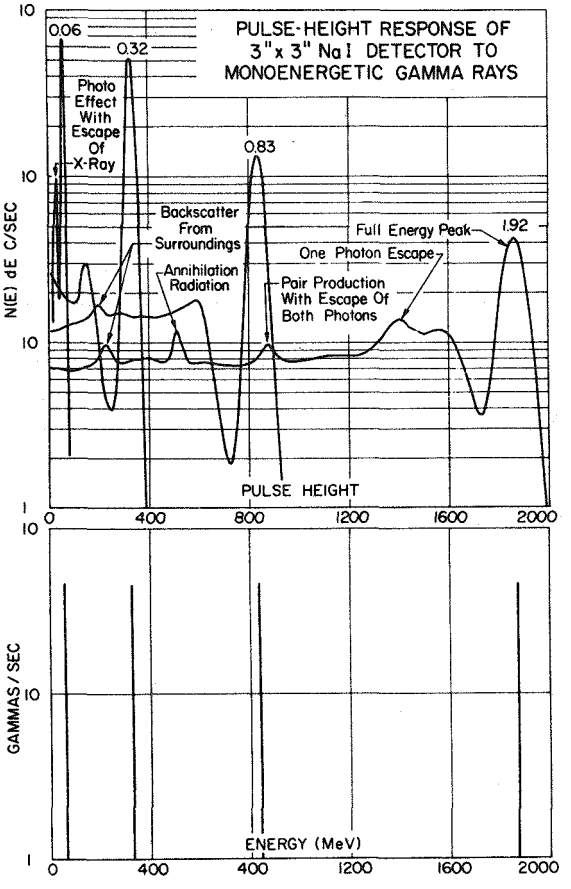

Fig. 1. Typical Pulse-Height Spectra of Monoenergetic Gamma Rays.

It should be recalled that the measured pulse spectrum is really an electron energy spectrum resulting from the loss of energy by the photon resulting from interaction with electrons in the detector by one or more processes. Figure 2 illustrates this conversion. This figure shows the theoretical electron spectrum to be expected as a result of the detection of a gamma ray of approximately 0.50 Mev. Interaction by the photo process produces the monoenergetic line representing essentially full-energy loss by the photon. The distribution of electrons from zero to a maximum at

an energy less than the full energy of the photon results from interaction of the photons by the Compton process. Above this is shown the measured pulse-height distribution observed from a 3- by 3-in. NaI detector. We see that, aside from what appears to be a near-Gaussian smearing of the data, the general features of the electron spectrum are preserved. The major difference is in the relative magnitude of the Compton distribution and the photopeak. The increase in the relative number of photo events is due to a rather high probability for the occurrence of multiple events which result in total loss of energy in a detector of this size. As the dimensions of the detector increase, the relative probability for total energy loss will increase.

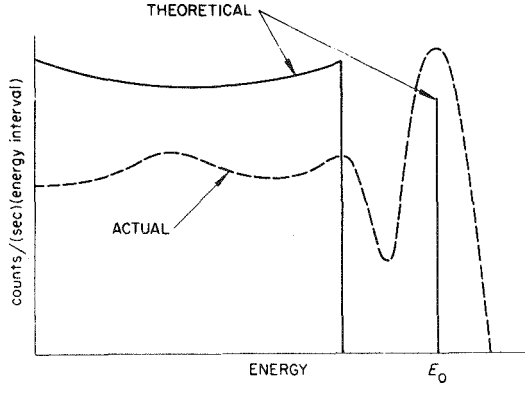

Fig. 2. Theoretical Electron-Energy Distribution (Single Events) for 0.50-Mev Gamma Ray in NaI Compared with Observed Pulse-Height Distribution Obtained on 3- by 3-in. Detector.

EFFECT OF ENVIRONMENT ON DETECTOR RESPONSE

If we could isolate the source and detector from all surrounding material, the shape and magnitude of the observed pulse-amplitude spectrum would be dependent only upon the energy of the gamma ray, the physical properties of source and detector, and the geometrical arrangement. Unfortunately, this cannot be achieved. In practice, the shape of the observed pulse-amplitude distribution is influenced by many factors. Since the response of the detector to its experimental environment must be understood in any attempt to analyze data, let us examine the many experimental variables which can influence the response of the detector. Figure 3 shows the experimental pulse-height spectrum resulting from the detection of a monoenergetic gamma-ray source (0.478 Mev) by a 3- by 3-in. NaI detector. This spectrum was taken under experimental conditions which have been optimized to reduce extraneous effects to a minimum. The spectrum has been measured with and without a 670 mg cm^2 polystyrene absorber which is normally interposed between detector and source to prevent the entry of beta particles from beta decay sources into the detector. Extraneous contributions appear in the spectrum which do not represent the response of the detector to gamma radiation directly incident on the detector.

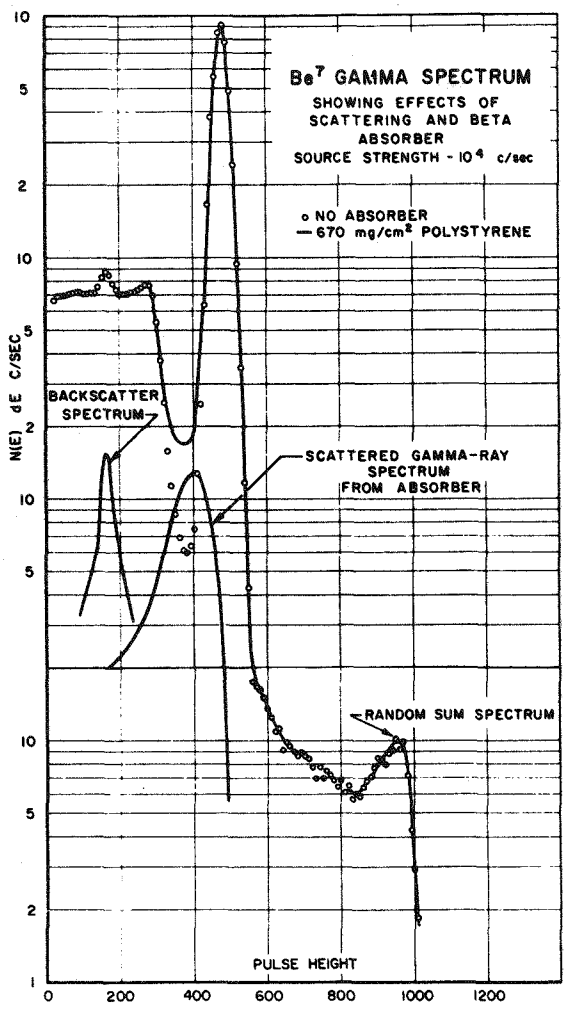

Fig. 3. Experimental Response of 3- by 3-in. NaI Detector to Monoenergetic Gamma Ray Showing Extraneous Effects.

BACKSCATTER SPECTRUM

The small peak appearing on the Compton distribution results from gamma rays Compton-scattered from the surrounding materials in the detector shield, air, source, and source mount.

The magnitude and shape of the contribution from scattered radiation is dependent upon the geometrical arrangement. Figure 4 shows the pulse-height spectrum for an 0.835-Mev gamma ray measured in the three different shield configurations shown in Fig. 5. Inspection of the scatter spectrum shows that the intensity and shape of the distribution of pulses attributable to scattering is inversely proportional to the size of the shield and to the Z of the absorbing material. The reduction in scattering from lead as opposed to iron is due to the relatively high photoelectric absorption cross section of the high Z material. It is of interest to inspect the shape of the scattered spectrum from the small iron shield. Note the presence of two distinct peaks in this

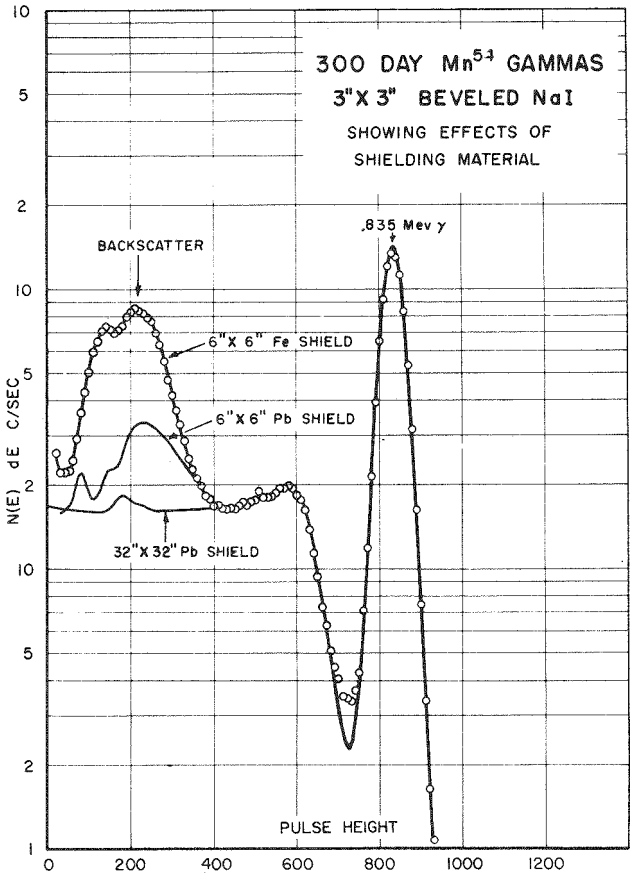

Fig. 4. Effect of Detector Shield Geometry on Pulse-Height Distribution.

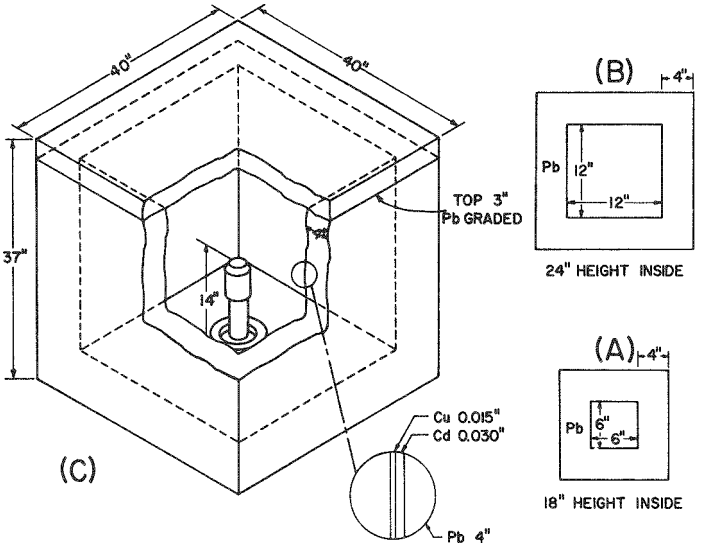

Fig. 5. Shield Configurations Used for Data Shown in Fig. 4.

distribution. These correspond to 180° single scattering and to processes involving two successive large-angle Compton events before striking the detector. An important deduction from these measurements is that appreciable scattering from surrounding material considerably degrades the quality of the spectrum. The presence of a large contribution to the pulse spectrum from scattering will reduce the "uniqueness" of the energy response. For this particular case the ability to detect gamma rays in the energy range from 100 to 400 kev would be reduced by a factor of ten if measurements were made in the small iron field.

X-RAY PRODUCTION

Figure 6 illustrates one additional effect of scattering from surrounding material. If high Z materials are used in the construction of detection shields to lower ambient background, the high probability of photoelectric interaction will result in the production of considerable quantities of x rays characteristic of the shielding material. This

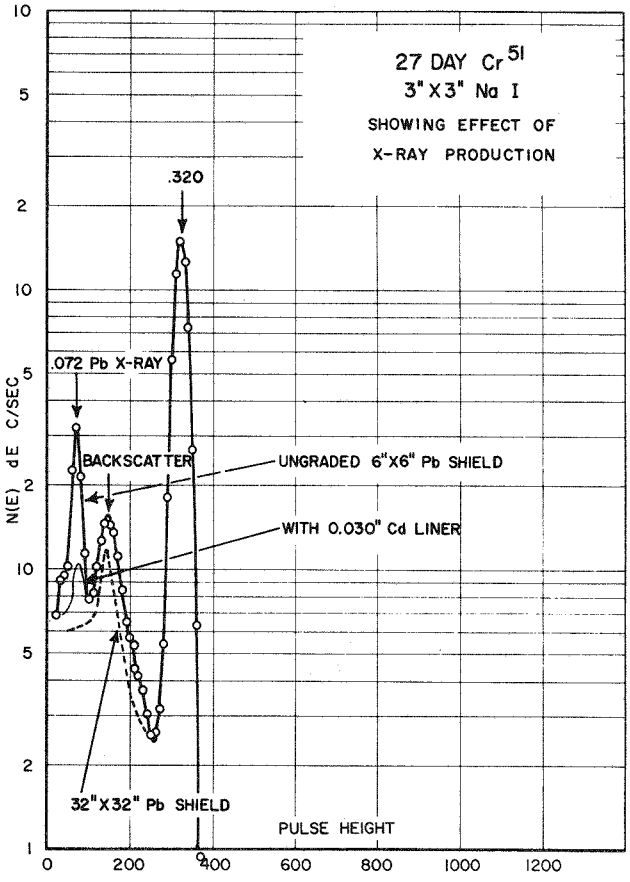

Fig. 6. Effect of X-Ray Production Following Photoeffect in Shield Material.

component in the scattered spectrum can be effectively eliminated by lining the shield with selected materials which have a high probability of selectively absorbing the characteristic x rays produced in the lead shield. This technique, known as "graded shielding," is generally recommended for high quality spectrometry.

EFFECT OF BETA ABSORBERS AND SELF-ABSORPTION

Generally speaking, nature does not provide us with convenient sources which emit only photons. The decay of the usual radioactive source has associated with it the emission of charged particles (either positrons or electrons). Since NaI is quite efficient as a detector of charged particles, it is necessary to prevent their entry into the detector. The presence of these charged particles introduces several complications. Figure 7 shows the pulse spectra resulting from the measurement of radiation emitted from the decay of 3.6-hr Y^{92}. This isotope, which decays by beta emission, emits very energetic beta particles (3.6 Mev) and several gamma rays. The upper curve results from a measurement made with no absorbing material between the source and detector. The particular detector employed is surrounded by only 0.005 in. of aluminum. We see that under these conditions the gamma-ray spectrum is almost completely obscured by the high energy beta-ray continuum. The second curve represents a measurement made with a 1.6-g beryllium absorber interposed between source and detector. The third curve was obtained by surrounding the sides of the cylindrical detector with 0.7 g/cm^2 of polystyrene. The difference observed between

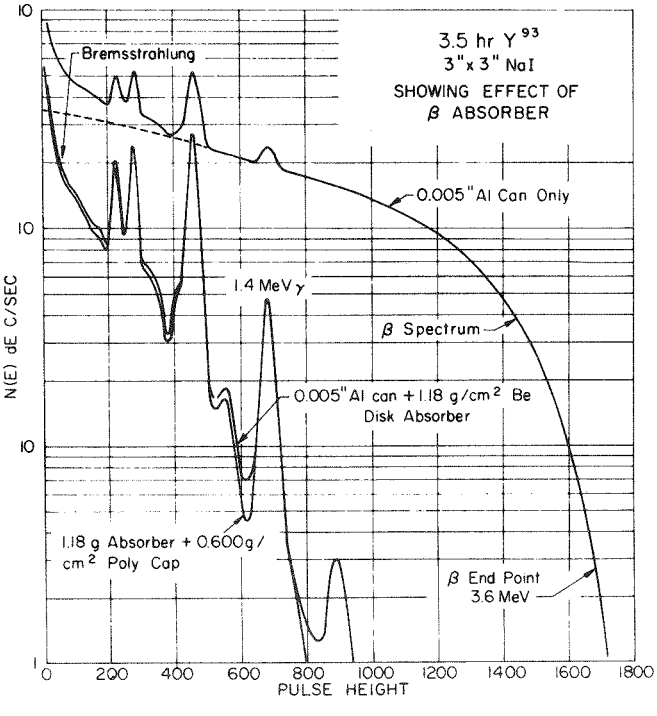

Fig. 7. Illustration of Use of Beta Absorber.

these two curves in the high energy portion of the spectrum is the result of beta particles scattered from the air and surrounding material into the sides of the detector. Thus we must be particularly careful to exclude all electrons from the detector if the pulse spectrum is to represent only the response of the detector to photons emitted by the source.

If we observe the low energy portion of the "gamma-ray spectrum" of Y^{92} we observe a continuum of pulses rising with decreasing pulse amplitude. This contribution to the spectrum is not due to the response of the detector to gamma radiation emitted in the decay of the source, but is a bremsstrahlung spectrum produced in the slowing-down of the beta particles by the surrounding material and the absorber. Such continuous spectra of photons are associated with all sources of radiation which emit charged particles. The shape and magnitude of these spectra will be a function of the beta spectrum and the material in which the electrons expend their energy. The magnitude of this effect can be minimized by proper experimental design.

Finally, now that we have admitted the necessity for using absorbing materials in certain experimental cases, what effect does this absorbing material have on the photon spectrum of interest? Figure 8 shows the pulse spectrum obtained from a

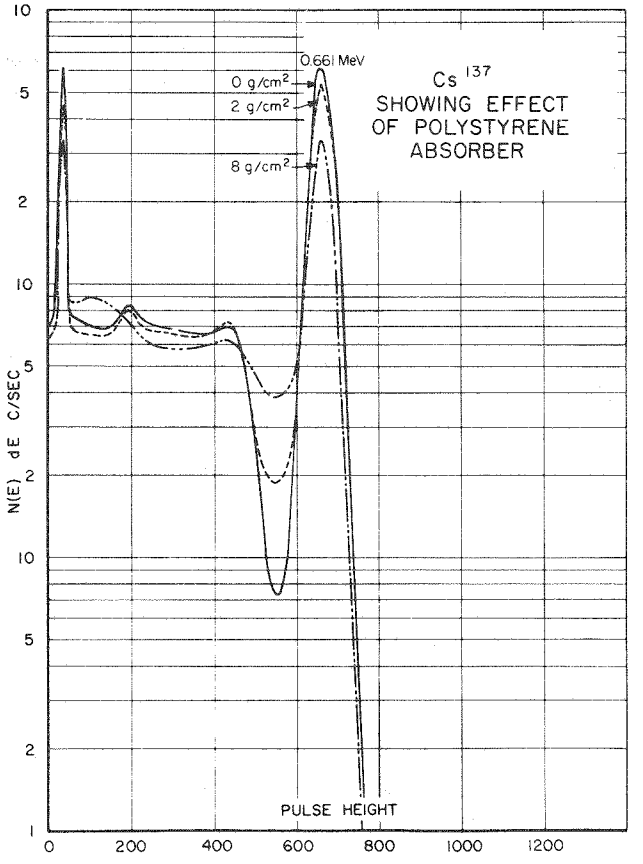

Fig. 8. Effect of Beta Absorber on Shape of Pulse-Height Distribution Resulting from Compton Scattering.

photon source with no absorber and the effect of adding increasing thickness of beta absorber. In addition to increasing attenuation of the entire spectrum, the shape of the pulse-amplitude distribution is seen to change materially. This results from the detection of photons which are Compton scattered in the forward direction following interaction by the Compton process in the absorbing material. The same effect would occur if the source were sufficiently thick to produce appreciable scattering. For this reason source preparation can also affect the quality of the spectrum.

SUMMATION EFFECTS

If we again examine Fig. 3 in the region above the photopeak, we see a continuous distribution of pulses which extend up to approximately twice the amplitude of the full-energy peak. This contribution to the monoenergetic energy response of the detector results from random time-coincidence between pulses. Since radiations emitted from a radioactive source are randomly distributed in time, there is a finite chance that two events may occur in the detector within the resolving time of the electronic circuitry. If this occurs, then the amplitude of the resultant pulse will be the sum of the amplitudes of the two separate events. The magnitude of this "random sum spectrum" will be related to the source intensity and the system resolving time by the following simplified relationship:

$$I_{\text{r.s.s.}} = N^2 2\tau , \tag{1}$$

where N is the input pulse rate, τ is the resolving time of the electronic system for pulse pairs, and I is the total number of pulses appearing in the sum spectrum. Pulses in this sum spectrum represent the detection of photons directly incident upon the detector and so must be considered as part of the energy response of the detector. This random sum spectrum should not be confused with the so-called "coincidence sum spectrum" which is illustrated in Fig. 9. This figure shows the spectrum of radiation emitted by Nb^{94m}. In the decay of this isotope two gamma rays are emitted simultaneously in the decay of each nucleus. In addition to the response of the detector to the two gamma rays individually, we also see a distribution of pulses which results from the simultaneous detection of both coincident gamma rays. The resultant sum spectrum is really a convolution of the two response functions for the individual gamma rays. The most prominent feature of this spectrum is the so-called sum peak which results from the coincident detection of pulses from the photopeaks of the two coincident gamma rays. The probability for the detection of pulses in this summation spectrum is given by the following expression:

$$N_{\text{c.s.s.}} = N_0 \epsilon_1 \epsilon_2 \overline{W}^0 , \tag{2}$$

where N_0 is the decay rate of the source, ϵ_1 and ϵ_2 are the detector efficiencies for the detection of gamma rays 1 and 2, respectively, and $\overline{W}^0$ is a factor to account for the angular distribution of the coincident gamma rays. The shape and magnitude of such coincident spectra can be successfully calculated using a computer program [*1*].

Comparison of expressions (1) and (2) indicates that the magnitude of the random summing effect is rate dependent while the real coincidence sum spectrum intensity is a function of the detector-source geometry. With the addition of these effects we see that when more than one gamma ray is emitted in the decay of a single nucleus,

the shape of the spectrum can become quite complex. Such a case is shown in Fig. 10, which illustrates the observed pulse-height spectrum from the decay of Pm^{148} with its associated sum spectrum. In this case there are many coincident gamma rays emitted in the decay of each nucleus.

To summarize, we have seen that the shape of the pulse-height spectrum resulting from the detection of monoenergetic gamma rays may be influenced by many parameters. These include source preparation, source-detector geometry, size and shape of the detector, input count rate to the spectrometer, and the environment in which the experiment is performed. In addition, other radiations emitted by the source and the time relationships between emitted radiations may produce extraneous effects which must be considered in any analysis of the data. For this reason it is most important that serious thought be given to the design of the experimental arrangement. In addition it should be quite obvious at this point that standard measurement conditions are necessary to the development of any precise method of data analysis since it is not possible to predict the effect of a change in any experimental variable.

Aside from the experimental parameters discussed above, the detailed shape of the observed pulse-amplitude spectrum will depend very strongly upon the various elements of the scintillation spectrometer. Each element of the spectrometer and its contribution to the experimental problem will be discussed briefly.

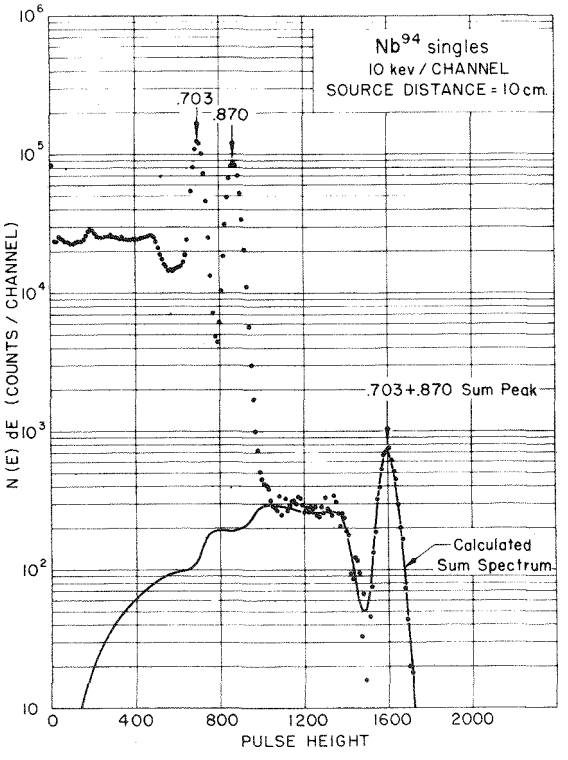

Fig. 9. Coincidence Sum Spectrum.

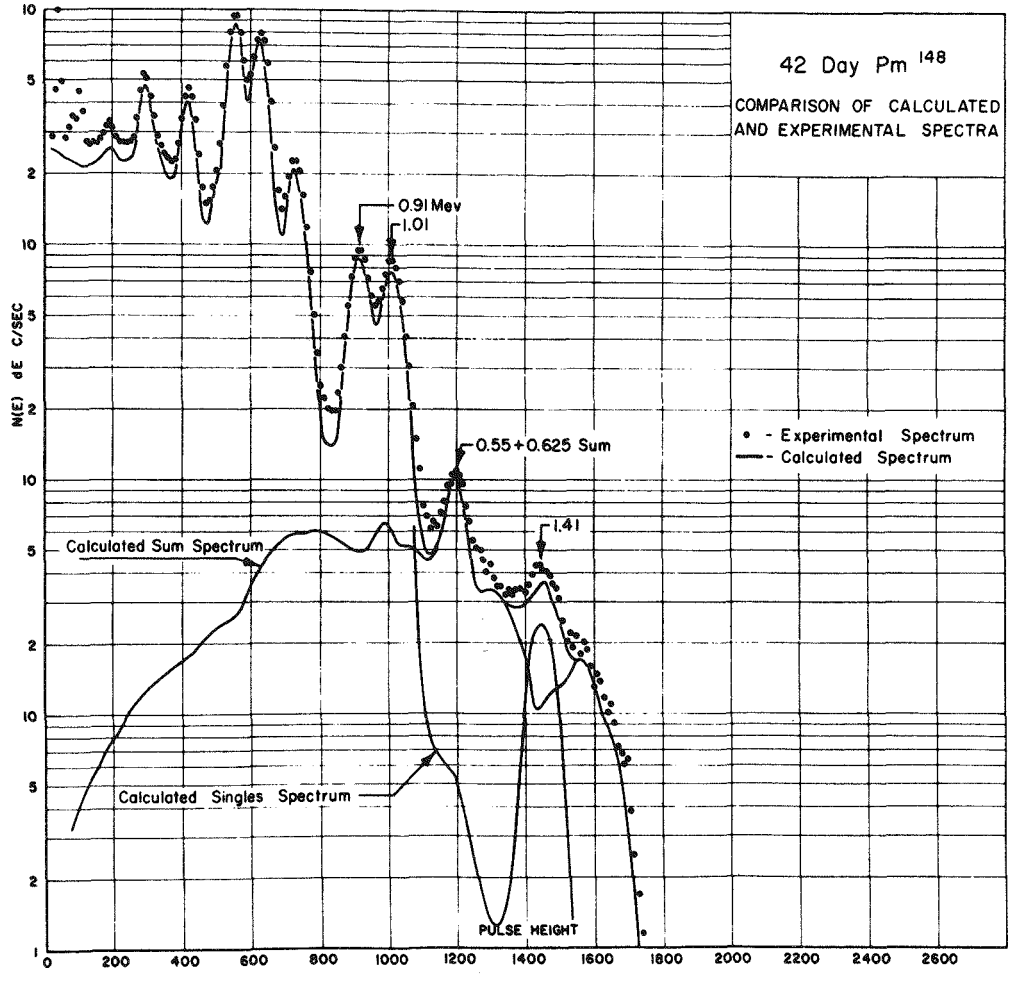

Fig. 10. Complex Coincidence Sum Spectrum.

DETECTOR

Both the phosphor and photomultiplier tube have inherent properties which complicate the experimental problem. The most important variables affecting the experimental data are detector linearity, resolution, and stability of output pulse amplitude.

NaI Linearity

In the analysis of pulse-height spectra to obtain precise gamma-ray energies, the pulse height vs energy response of the detector is most important. It has been well established that NaI(Tl) is not linear, particularly in the energy region below 0.50 Mev. Figure 11 shows the relationship between pulse height and energy for NaI(Tl) as determined by three experimenters [*1*–*3*]. Fractional change in pulse

height is plotted as a function of gamma-ray energy. The ordinate is normalized to a light output of 1.00 for the 661-kev line of Cs^{137}.

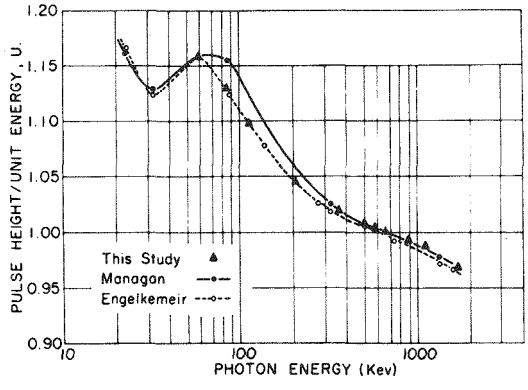

Fig. 11. Pulse-Height vs Energy Response for NaI Detector.

The observed nonlinearity is attributed to a variation of phosphor light-conversion efficiency with secondary electron energy. In general it should be the same for all NaI detectors, although some deviation has been found between crystals for energies below 100 kev – presumably attributable to the optical properties of the detector.

It should be noted that this nonlinearity is attributable to the detector alone and does not include any defects which may exist in the electronic system. If data from a given system is to be analyzed to obtain gamma-ray energies, the overall response of the spectrometer must be experimentally determined by a calibration against known energy standards.

Detector Resolution

The resolution of the detector is usually defined as the relative width of the full-energy peak or photo-line in the response of the spectrometer to a source of monoenergetic gamma radiation. The width, or more specifically, the shape, of this line as a function of gamma-ray energy is determined by the statistical nature of the processes involved. These include the production of light in the scintillator, the collection of this light at the photocathode of the multiplier phototube, the subsequent production of electrons by the photocathode, the collection of electrons at the first dynode of the multiplier, and the multiplication in the dynode structure. The relative contributions of each of these factors will vary with each detector and the conditions of the experiment. Many detailed descriptions of detector resolution and the many factors affecting it have appeared in the literature [4, 5].

The considerations of importance to this discussion are the effects of conditions external to the detector upon the experimental data. The first of these effects is the temperature dependence of the light output from the phosphor. NaI has a temperature coefficient of $-0.1\%/^{\circ}C$. This requires rather stable temperature conditions during a given measurement. In some detectors the resolution is observed to vary

with source-detector geometry. This is attributed to nonuniformities in the optical system which produce differences in the transfer variance. This effect can result from defects in either the reflector system or the photocathode of the photomultiplier tube. A third effect which can be troublesome is variation in the resolution of detector with count rate. This effect is observed in large detector packages employing more than one photomultiplier tube for light collection. Such detectors may exhibit change in resolution with counting rate due to differing characteristics of the phototubes, that is, counting-rate shift. This effect will be discussed in a later section.

PHOTOTUBE

Gain of phototube is of course highly dependent upon voltage impressed upon the dynode string. For usual phototube operating voltages, approximately 0.1% change in voltage produces a 1% change in gain. To obtain 0.1% gain stability which is considered the best that can be obtained with current electronic systems, this implies a voltage supply with long-term voltage regulation of ±0.01%.

The most troublesome type of gain variation produced by the phototube is a change in gain as a function of input counting rate. The magnitude of this gain change is proportional to phototube current which is related to both pulse amplitude and counting rate. It generally takes the form of an increase in gain with increased counting rate. The time constant for this shift can vary from a few minutes to several hours for different phototubes. Although some types of tubes exhibit much less shift than others [6], selection of tubes and appropriate operating conditions are necessary to obtain satisfactory performance. All phototube manufacturers are aware of this problem and are working toward a solution. At the present time, selection of phototubes and operating conditions can produce detectors which exhibit a gain shift of less than 0.5% for a change of counting rate from 100 to 10,000 counts/sec. For a given measurement this effect can be minimized by calibration with standard sources of approximately the same counting rate as the source to be measured. An alternative is to include a calibration source with a line of known energy. It should be noted that a change of gain during the course of a measurement will result in degradation of the resolution of the detector. For this reason the system must be allowed to stabilize prior to the start of the measurement. In the measurement of the decay of short-lived activities, this problem can become particularly troublesome.

ELECTRONIC SYSTEM

Two parameters are important in an analysis of the performance of the electronic system. These are linearity and system stability. These parameters must remain constant with changing temperature, line voltage fluctuations, and changing experimental conditions, for example, counting rate, gain, etc. Experimental methods for investigating these parameters were discussed in papers (2-4) and (2-5).

One of the most troublesome problems is zero or bias shift with counting rate. This is generally a problem of the amplifier and results from improper dc restoration or "pulse pile-up" at high count rates. This problem can be eliminated by the use

of an amplifier which produces an output pulse which is symmetrical about the voltage axis. These so-called "double-differentiated" amplifiers are commercially available both in vacuum tube or transistor types. Such amplifiers exhibit no measurable bias shift for counting rates up to 50,000 input pulses/sec. The integral linearity of these amplifiers is considerably better than 0.1%. Their gain stability against normal variation in temperature and line voltage is better than 0.1%. At the present time no multichannel analyzer available commercially utilizes such amplifiers as internal equipment.

Another parameter which can measurably affect the quality of data is random noise appearing at the output of the electronic pulse amplifier. This random noise will produce an additional fluctuation in the amplitude of pulses produced by the detector. High quality electronic amplifiers have a noise level less than ±0.2% of full output in the normal operating range. A noise level of this magnitude will have negligible effect on the observed detector resolution. It should be stressed, however, that difficulties in the electronic system which produce variation of the random noise level could cause serious fluctuation in the resolution of the system. For this reason stability of the signal-to-noise ratio is very important.

ANALYZER

Important considerations in the performance of the pulse-height analyzer which can influence analysis of data include the stability of gain and zero of the analogue-to-digital converter with counting rate and changes in ambient operating conditions (temperature and line voltage). These requirements appear to be met by most of the multichannel machines available today. Some analyzers have an overall stability of conversion gain of better than ±0.2% per day with no measurable zero shift for input counting rates up to 50,000/sec.

A more subtle requirement for precision data analysis is that the detailed shape of the pulse-height spectrum from a known source of radiation be independent of counting rate. In a good modern system this can be achieved. In view of the complexity of equipment of this type, malfunctions can occur which will produce errors in the shape of the distribution. For this reason extreme care should be exercised to ensure proper circuit operation. In evaluating this criterion, it should be pointed out that one must be aware of the rate and geometry-sensitive changes in spectrum shape due to real or random pulse summing. These effects were previously discussed.

LIVE TIMER

All of the multichannel machines presently available use the amplitude-to-time conversion principle. This implies that the time required for analysis is proportional to input pulse amplitude. Absolute measurement of source intensity requires that

the time for analysis be accurately determined. Since a measurement of the analyzer dead time is somewhat complicated, all analyzers of this type incorporate circuitry which automatically corrects for this loss. The precision of any quantitative determination will be dependent upon the accuracy of this circuitry. Methods for checking the accuracy of the so-called live timer were described in paper (2-5). A good live timer is capable of accuracies better than ±0.2% for input count rates up to 50,000 input pulses/sec.

To summarize the effects of all experimental parameters, we see that many variables are present in each experiment which can influence the quality of data obtained from a scintillation spectrometer. These include experimental design, source material, and the quality and stability of the electronic equipment used. Any successful method of data analysis must include adequate treatment of these variables if one is to obtain an estimate of the error involved in the analysis. Because of the complex relationships which exist between all variables which can influence the response of a spectrometer to a given source of radiation, it is impossible to treat these variables analytically. This implies that it is not possible to compute the response of the spectrometer for a given set of experimental conditions. For this reason an empirical method must be used. This requires that the response of the system must be thoroughly investigated under a rigidly controlled set of "standard" experimental conditions. The success of any attempt to do a detailed analysis of pulse-height spectra will depend very strongly on the quality of the experiment.

REFERENCES

[1] R. L. Heath, "Recent Developments in Scintillation Spectrometry," in *IRE Trans. Nucl. Sci.* **NS-9**(3), 294 (1962).

[2] D. Engelkemeir, *Rev. Sci. Instr.* **227**(8), 589 (1956).

[3] W. C. Kaiser *et al.*, "Response of NaI(Tl) to Low Energy Gamma Rays," in *IRE Trans. Nucl. Sci.* **NS-9**(3), 22 (1962).

[4] C. D. Zerby, A. Meyer, and R. B. Murray, *Nucl. Instr. Methods* **12**, 115 (1961).

[5] P. Iredale, *Nucl. Instr. Methods* **11**, 340 (1961).

[6] L. A. Webb and R. F. Johnson, *Phys. Rev.* **98**, 234 (1955).

(3-2) ITERATIVE UNFOLDING

N. E. Scofield
U. S. Naval Radiological Defense Laboratory
San Francisco 24, California

INTRODUCTION

The widespread use of multichannel analyzers and automated data recording in gamma-ray scintillation spectrometry has placed an emphasis upon computer data reduction methods. At the same time there has been a tendency to write computer programs to reduce data in the same manner in which it has been hand-corrected in the past. Where the spectra to be observed consist of a sum of gamma-ray lines, a stripping process which depends upon the ability to resolve distinct peaks for each line may be satisfactory, but where there are many lines or even a continuous gamma-ray distribution, then some type of approach is needed which will solve a set of simultaneous linear equations. These equations arise from a linear super-position principle that the pulse-height distribution from one gamma line is unaffected by the presence of other gamma lines and that the resultant pulse-height distribution from n_1 gamma rays of energy E_1 and n_2 gamma rays of energy E_2 is given by n_1 times the E_1 pulse-height distribution plus n_2 times the E_2 pulse-height distribution. This of course may be extended to many components. Now the solution of large sets of simultaneous equations has a long history dating back at least to Gauss. We will most likely not be making discoveries or innovations in this field but rather rediscovering techniques that were old before we were born. One new element that has been added is that of automatic computing devices, which make possible calculations that would not even have been attempted in the past. For an excellent collection of papers on the solution of simultaneous linear equations and an index and categorization scheme, see ref [*1*].

There are two main reasons to turn to iterative methods of solution. The first is the difficulty in constructing a square response matrix of high order and the second is the approximate nature of the pulse-height vector and response matrix elements.

The simplest solution to the matrix equation $RN = C$ is $N = R^{-1}C$, but this presupposes that R is a nonsingular $n \times n$ square matrix. This in turn necessitates measurement and/or interpolation to find n different response distributions. It is quite difficult to find more than, say, ten relatively monoenergetic gamma-ray sources in the region from 0 to 2 Mev and even these will, in general, not be uniformly distributed over this range. This means that the approximate numbers obtained experimentally will be used to interpolate even more approximate matrix elements.

Historically the solution of large numbers of simultaneous linear equations with approximate coefficients has been accomplished by iterative methods because of their self-correcting properties. These methods depend for their successful use upon the convergence properties of the iterative algorithm. These in turn can be shown to depend upon the nature of the response matrix. In general the stronger the principal diagonal of the matrix is, the better the convergence will be. The reason for the application of these methods to "total absorption" crystal spectrometer data with its large peak to total ratio and hence the strong principal diagonal in its response matrix is obvious.

A brief description will be given of the type of gamma-ray measurements we were doing at NRDL in order to show the type of problem we had to solve. Some of our early

experiences in unfolding will be described and the kind of thinking that led to a usable method will be sketched. Some tests and examples of this method will be shown; in addition, we will mention some remaining problems and the direction in which we are heading at present in this field.

EXPERIMENTAL PROBLEM

For some years now there has been a continuing program of gamma-ray scintillation spectrometry in connection with the fundamental shielding studies at NRDL. In these studies the angular distribution of the spectra of scattered gamma rays emerging from various thicknesses of structural materials has been measured.

The sources used to irradiate the slabs have been Cs^{137} and Co^{60} and the geometry has been distant and broad beam so as to approximate plane parallel incidence (see Fig. 1). Note that the source distance has been compressed to facilitate presentation. The detector was a 4- by 4-in. NaI(Tl) crystal and the split collimator was effectively $\frac{3}{4}$ in. in diameter and 25 in. long, giving an angular resolution of 1.5°.

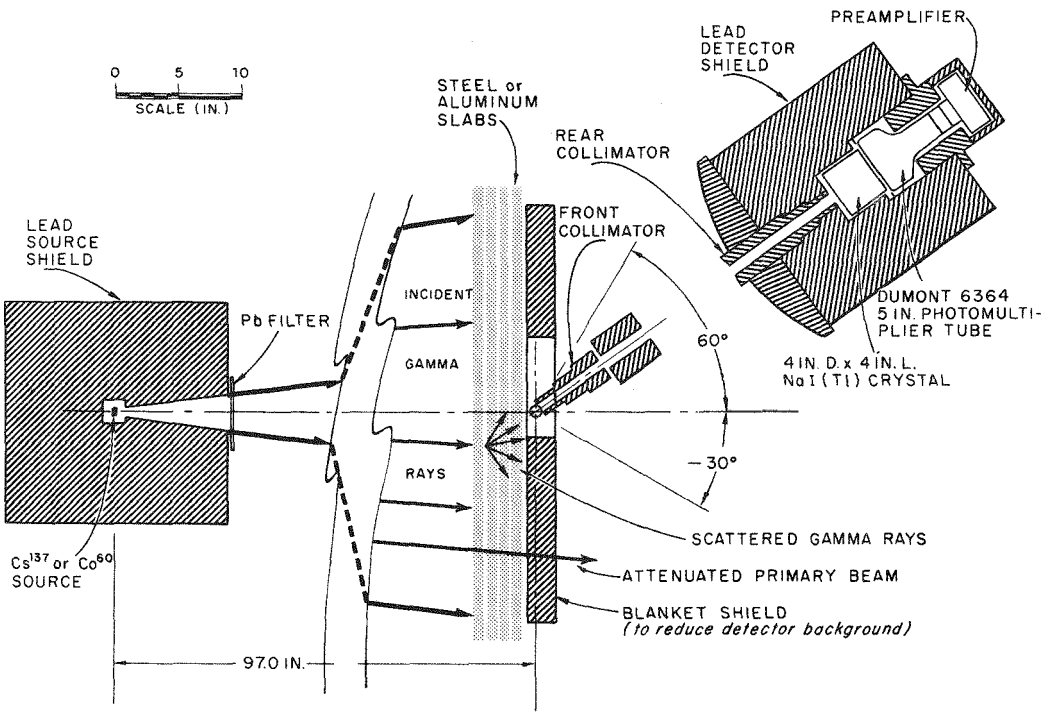

Fig. 1. Experimental Geometry.

Under these conditions the type of pulse-height distribution obtained at a detection angle of 20° is indicated in Fig. 2, where counting-rate as a function of pulse height is shown for five different thicknesses of steel irradiated by Co^{60} gamma rays. Under these experimental conditions for the 1 in. of steel the calculated first plus second scattered gamma-ray spectrum is shown in Fig. 3 as curve *A*, while the corresponding calculated

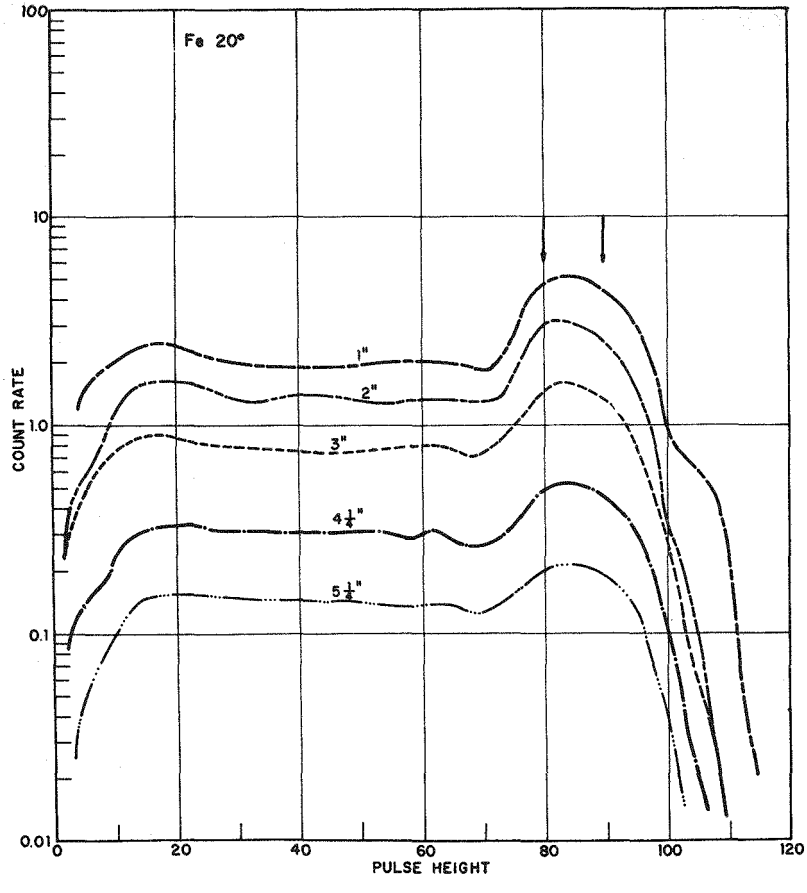

Fig. 2. Experimental Pulse-Height Distribution.

pulse-height distribution is given by curve *B*. Actually, higher order scattering cannot be ignored even for 1 in. iron but the point I would like to make is that the gamma spectra we wished to unfold from the experimental pulse-height distributions were a mixture of lines and continuous and discontinuous spectra. As we shall see later this discouraged us from using either inverse matrix or stripping methods.

A typical response curve for Cs^{137} is shown in Fig. 4, where the Gaussian total absorption peak, the Compton tail, and the usual unwanted features such as x-ray peaks and backscatter distributions are indicated. A somewhat cleaner spectrum is shown in Fig. 5, where the semi-log and histogram presentation serves to emphasize the discrete and statistical nature of even the best response spectra.

Figure 6 shows the photofraction and resolution curves of the total absorption peaks as a function of source energy and shows that we are willing to lose a little resolution by using a 4- by 4-in. crystal in order to obtain a more unique response.

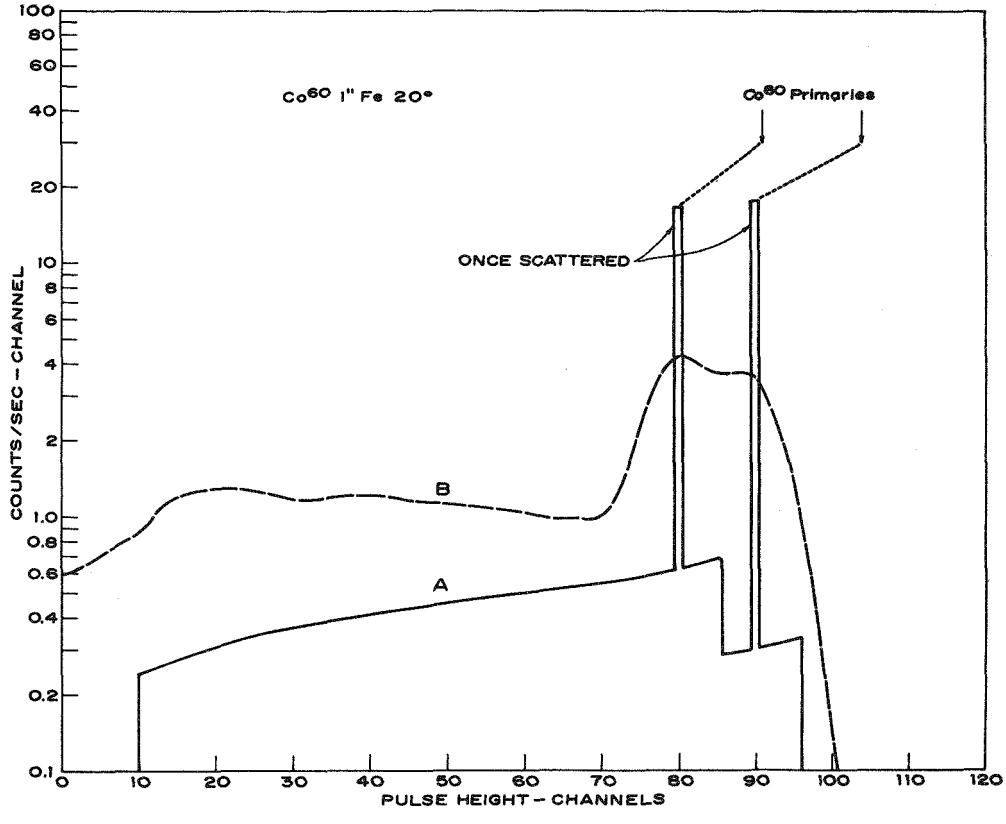

Fig. 3. Curve *A*: Calculated First and Second Scattered Gamma-Ray Spectrum Penetrating Slab; Curve *B*: Pulse-Height Distribution Obtained by Folding Curve *A* with the Experimental Spectrometer Response.

DETAILS OF THE INSTRUMENTAL RESPONSE

Perhaps at this point it would be a good idea to express a little more precisely what the relationships between these various entities are. In Fig. 7, Eq. (1) is a mathematical expression of the distortion by the spectrometer response, $R(V,E)$, of the gamma spectrum, $N(E)$, incident upon the crystal face to give the observed pulse-height distribution $C(V)$.

The spectrometer response function is shown in Eq. (2) to consist of a Gaussian smearing,

$$\int_0^\infty g(V,E,V')\left\{\quad\right\}dV',$$

times a response kernel which consists of the crystal detection efficiency, $\epsilon(E)$, times the weighted sum of the total absorption lines, $\delta(aE-V')$, and the Compton tail function $aK(E,V')$; the weighting factors are the photofraction $p(E)$ and Compton tail fraction $c(E)$. In Eq. (3) we show the relation between a pulse-height distribution, C_k, resulting from an incident number of photons, N_k, all of energy E_k.

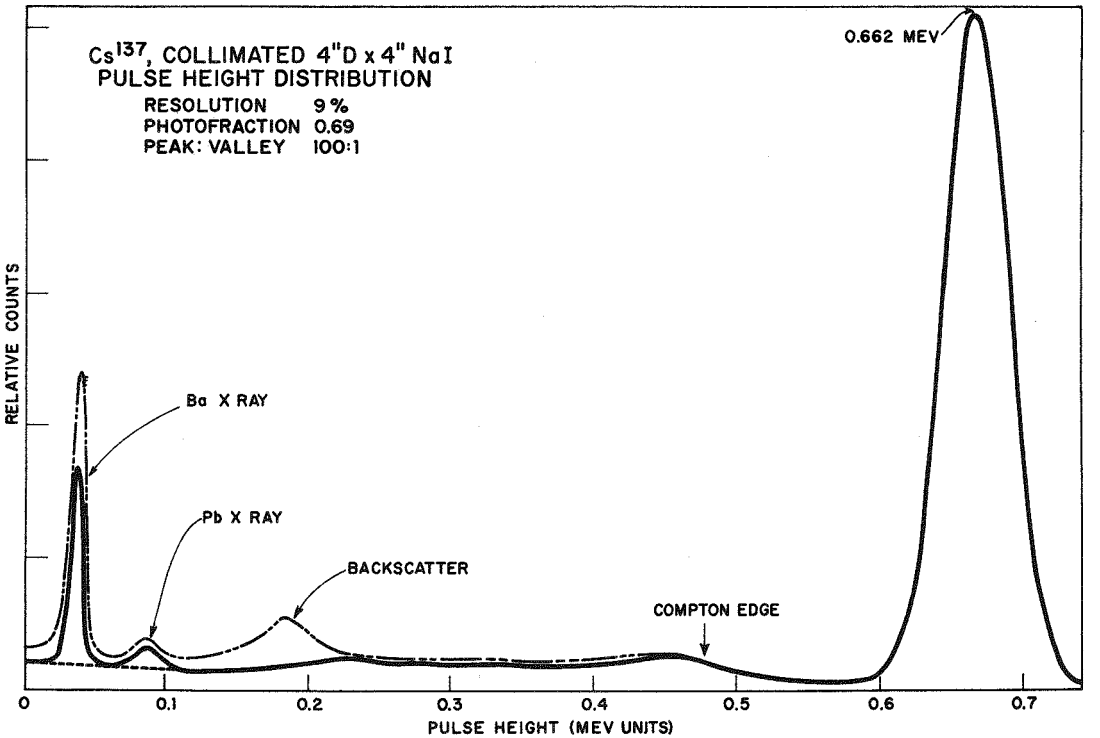

Fig. 4. Cs^{137} Response Curve.

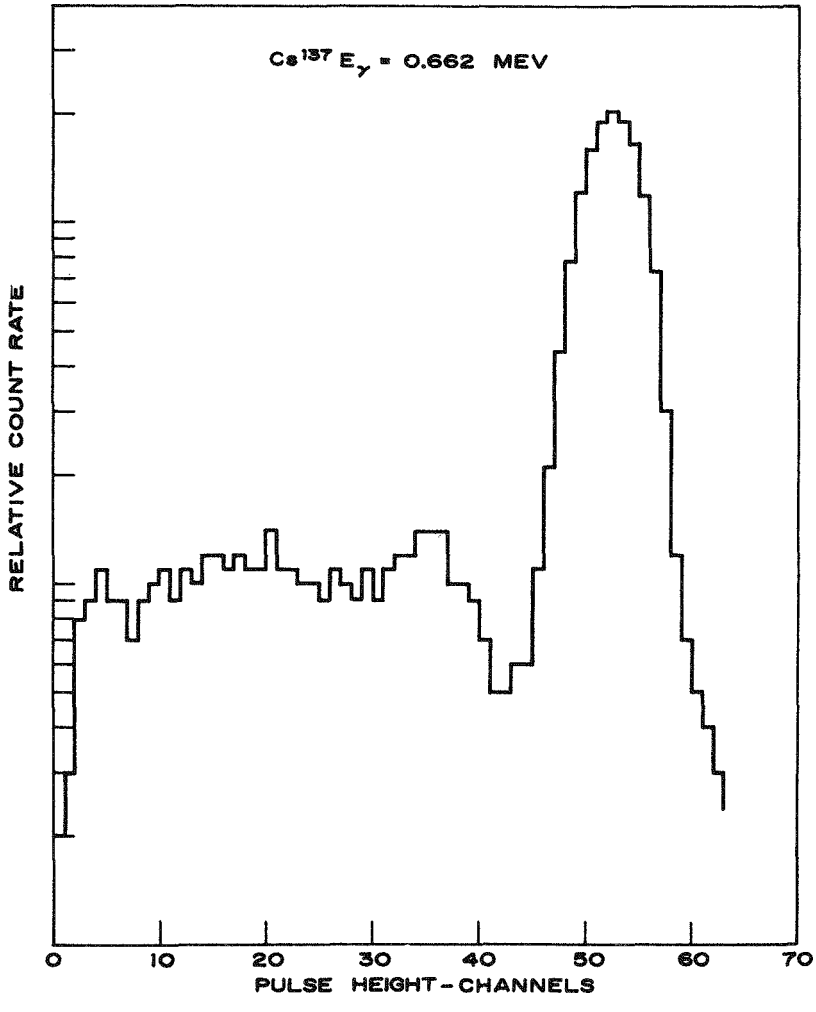

Fig. 5. Cs^{137} Response Pulse-Height Distribution.

Finally Eqs. (4) and (5) show the matrix representation of (1) and the inverse operation, respectively.

Here the matrix element r_{ij} of the response matrix, R_{ij}, is to be interpreted as the probability of observing a pulse height between $V_i - \Delta V$ and V_i given one photon incident upon the crystal of energy E_j. N_i is to be interpreted as the number of photons incident upon the crystal with energies between $E_j - \Delta E$ and E_j. Finally C_i is the number of counts with pulse-height falling between V_i and $V_i - \Delta V$.

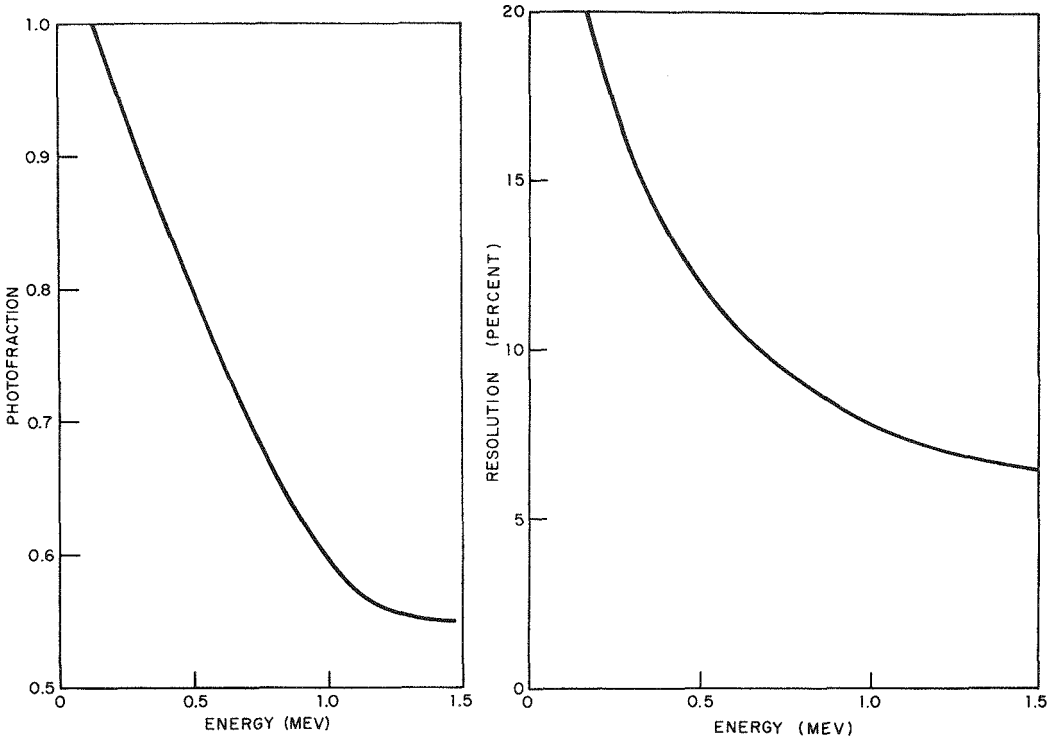

Fig. 6. Photofraction and Resolution Curves for the 4- by 4-in. NaI(Tl) Scintillation Detector.

$$C(V) = \int_0^{E_{max}} R(V,E)N(E)dE \quad (1)$$

$$R(V,E) = \int_0^{\infty} g(V,E,V')\epsilon(E)\{c(E)\alpha K(E,V') + p(E)\delta(\alpha E - V')\}dV' \quad (2)$$

$$C_K(V) = N_K R(V,E_K) \quad (3)$$

Fig. 7. Response Function Expressions.

$$R_{ij}N_j = C_i \quad \textit{(FOLDING)} \quad (4)$$

$$R^{-1}{}_{ji}C_i = N_j \quad \textit{(UNFOLDING)} \quad (5)$$

ATTEMPTED SOLUTIONS

Equation (5) is the obvious solution for Eq. (4). However, unfortunately, it does not always work. The reason is that, for matrices as large as those encountered with modern multichannel analyzers (50×50, 128×128, 256×256, 400×400, etc.), special methods have to be used to obtain the inverse even when the response matrix elements are without error. For a 100×100 matrix, for example, double precision arithmetic must be used to avoid roundoff errors. When in addition there is imposed the condition of statistical fluctuations in the elements of the response matrix which have been interpolated from experimentally measured quantities, it may be realized that even with extraordinary care the inverse may be violently unstable. Table 1 shows a portion of

Table 1. A Portion of the Inverse Matrix $||R||^{-1}$

Energy Bins	Pulse-Height Channels									
	18	19	20	21	22	23	24	25	26	27
21	−2.41423	4.58224	−8.09134	12.02740[a]	−8.90633	5.45649	−2.72097	0.54618	1.36009	−2.82737
22	1.68851	−3.23438	5.92633	−10.16500	14.61770	−11.67800	7.53477	−4.22349	1.61839	0.27309
23	−1.09792	2.10925	−3.90993	6.99745	−11.73780	17.19920	−14.06030	9.59245	−6.23354	3.66594

[a]Main diagonal elements have been underlined.

an inverse matrix when near the main diagonal which illustrates the oscillating positive and negative values developed. The net effect of using such a matrix to unfold experimental spectra is shown in Fig. 8.

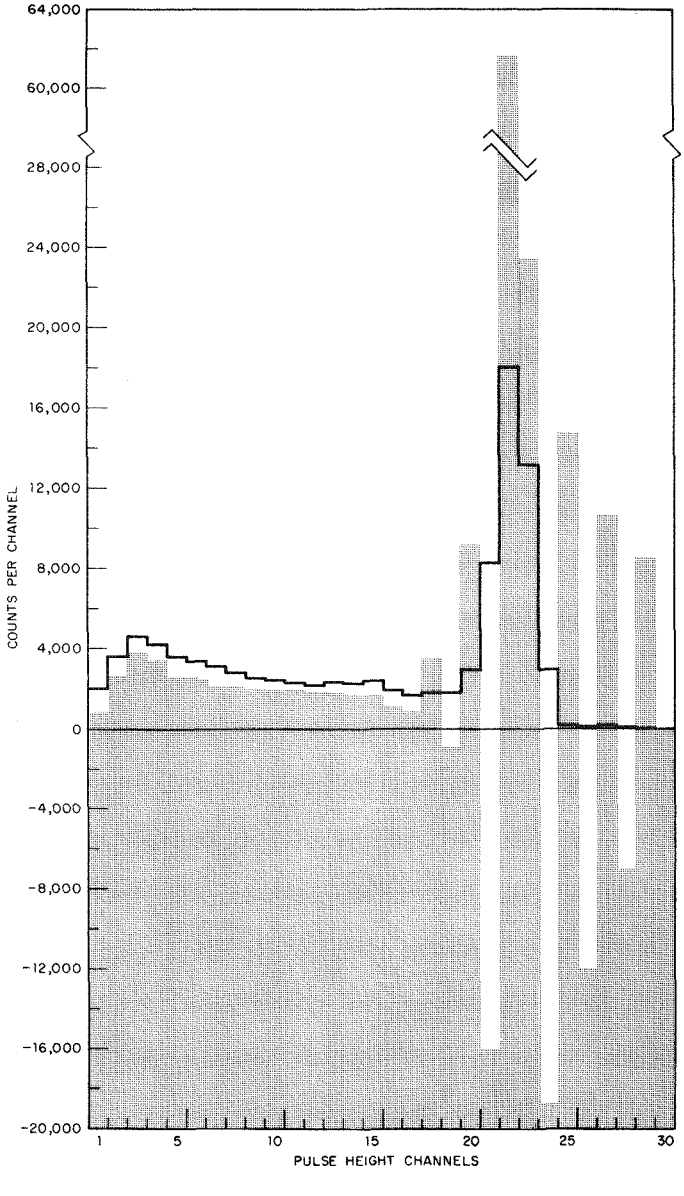

Fig. 8. Experimental Spectrum Unfolded by Inverted Response Matrix.

The seriousness of the above instability was not fully appreciated by us in our early unfolding work since we were working with bremsstrahlung spectra. These spectra are characteristically smooth curves asymptotically approaching zero at the high-energy end and hence tend to smooth out the effect of the alternating inverse matrix

elements noted above. When, however, the application of an inverse matrix to unfold slab penetration spectra produced the results shown here, we started to reexamine other possible methods.

OTHER METHODS OF UNFOLDING

When attempting to unfold a spectrum by hand one is immediately led to "cut and try" methods. The most straightforward of these methods is that of stripping, whereby a series of identifiable peaks are fitted and subtracted out along with their accompanying Compton tails starting from the high-energy end.

Many machine-stripping programs have been written and several have or will be presented at this symposium. These stripping methods break down, however, when no discernible peaks are present in the pulse-height distribution. The next type of calculation that suggests itself is actually a type of iterative procedure in which a first guess at the gamma spectrum is folded by the response matrix and compared to the experimental pulse-height distribution. On the basis of this comparison one then modifies the first guess and compares again, etc. Villforth [2] did just the above and since the method we have adopted is a modification of his method we will describe it briefly. In Table 2 Villforth's method (which he adapted from Freedman [3]) is shown as method II while a "standard" [4] iteration scheme is shown as method III. Actually II and III are the same, since, by expanding the right side of the basic equation in III, we get $N^{(m)}-(RN^{(m)}-C)=N^{(m)}-(C^{(m)}-C)=N^{(m)}-\Delta^{(m)}$ in the notation of method II. The general method, however, leaves open the choice of $N^{(o)}$.

Table 2.

I. Correction Factor	
Basic Equation:	$N^{(m+1)}=(D^{-1})^{(m)}C$
Auxiliary Equations:	$N^{(o)}=C$
	$C^{(m)}=RN^{(m)}$
	$(D^{-1})^{(m)}=\left\| \delta_{ij}n_j^{(m)}/C_i^{(m)} \right\| = \left\| d_{ij}^{-1} \right\|$
	where $\delta_{ij}=1 \longleftrightarrow i=j$
	$\delta_{ij}=0 \longleftrightarrow i\neq j$
II. Incremental Correction	
Basic Equation:	$N^{(m+1)}=N^{(m)}-\Delta^{(m)}$
Auxiliary Equations:	$N^{(o)}=C$
	$C^{(m)}=RN^{(m)}$
	$\Delta^{(m)}=C^{(m)}-C$
III. "Standard"	
Basic Equation:	$N^{(m+1)}=(I-R)N^{(m)}+C$

CORRECTION FACTOR METHOD

General Remarks

The modification that we have made to Villforth's iteration method was suggested by the work of Starfelt and Koch [5]. They obtained an unfolded spectrum by use of an inverse matrix and determined a correction factor curve as a function of pulse height from the ratios of corresponding elements of the unfolded and experimentally observed pulse-height distribution. This correction factor curve was then used to "unfold" all of the distributions having the same end point and a similar shape.

Our thought was to combine the correction factor method of Starfelt with the iteration scheme of Villforth. This we were able to do. The principal advantage of this modification is that if one starts with only nonnegative elements in the pulse-height vector and the response matrix, then the modified iteration method will guarantee only nonnegative gamma components in the unfolded spectrum. We next present the correction factor method more formally and in greater detail.

Iteration Method

It is assumed that a square response matrix R_{ij} has been fabricated, that pulse-height distributions C_i have been recorded and that it is desired to determine that gamma line spectrum, N_j, which might have produced C_i. That is, we wish to solve the matrix equation: $R_{ij}N_j = C_i$.

Now $i_{max} = j_{max} = q$ may be a large number ($50 \rightarrow 400$), and the elements of both R_{ij} and C_i are only approximate numbers. For this reason we cannot push the solution to its exact limit by using $N_j = R_{ij}^{-1}C_i$. Rather, we use an iterative or successive approximation method and stop the process when the residual error has reached a minimum or after a predetermined maximum number of iterations.

Before presenting the iterative algorithm a few remarks should be made about the vector elements C_i. In general the numbers C_i represent the net registration of pulses falling in an interval ($V_i - \Delta V$ to V_i) for a counting time of t seconds. Each one of these pulses results from the (single or multiple) interaction of an incident gamma photon with the scintillation crystal. In order to eliminate unwanted gamma rays which enter the crystal from directions other than through the collimator, "background" spectra are taken with lead plugging up the collimator opening. Thus, if we denote by S_i the "foreground" counting rate in the ith channel, t_f the foreground counting time, B_i the background counting rate, and t_b the background counting time:[1]

$$C_i = \left((S_i t_f) - (B_i t_b)\frac{t_f}{t_b} \right) \pm 0.6745 \sqrt{(S_i t_f) + (B_i t_b)\left[\frac{t_f^2}{t_b^2} + \left(B_i \frac{\langle t_f \rangle + \langle t_b \rangle}{t_b} \right) \right]},$$

where $\langle\ \rangle$ means "variance of."

[1] The use of a multichannel analyzer is assumed, so that $t_{fi} = t_{fi+1} = t_f$ and $t_{bi} = t_{bi+1} = t_b$; however, t_f may not $= t_b$. A "true" (or "live") timer was used which counted 1-kc pulses whenever the analyzer was not gated off.

Under our usual operating conditions $t_b = t_f$ and $\langle t \rangle \ll t$ so that, if we replace t_f/t_b by one and neglect the counting time variances, we have

$$C_i = (S_i t - B_i t) \pm 0.6745 \sqrt{S_i t + B_i t} .$$

Now it is evident from the above formula and it is also observed experimentally that as $C_i \to 0$ so $S_i t \tilde{=} B_i t$, occasional negative values of C_i will pop up, although the average value for a large number of observations would be zero. Since we wish to avoid any negative photon outputs from our unfolding program, we do not calculate C_i values beyond the last nonnegative one. The span of the multichannel analyzer is usually adjusted to extend above the pulse height of the maximum gamma energy present, so the above procedure effectively sets an i_{max} and determines the rank of the necessary portion of the response matrix.

In Table 3, condition (1) restricts the elements of N to the class of finite, nonnegative numbers while (2) excludes $N = 0$. Equation (3) is to guarantee that the response matrix is not singular while (4) and (5) state that the matrix diagonal elements must be positive and finite while the off-diagonal elements may be positive or zero but also finite. Finally, (6) states that the elements of the pulse-height vector C must be finite and positive.

Table 3.

Given:	$R \equiv \left\| r_{ij} \right\|$	$C \equiv \left\| c_i \right\|$
	and $RN = C$	
To find:	$N \equiv \left\| n_j \right\|$	
With the following conditions:		
(1)	$\infty > n_j \geqq 0$	$j = 1, 2, \ldots, q$
(2)	$\infty > \Sigma n_j n_j > 0$	
(3)	$\lvert R \rvert \neq 0$	
(4)	$\infty > r_{ii} > 0$	$i = 1, 2, \ldots, q,$
(5)	$\infty > r_{ij} \geqq 0$	$i, j = 1, 2, \ldots, q, \; i \neq j$
(6)	$\infty > C_i > 0$	$i = 1, 2, \ldots, q$

We wish to find N without explicitly determining the inverse R^{-1}. Suppose $N^{(m)}$ to be an approximation to N. That is, the vector $N^{(m)}$ is a point in phase space near to N. Then R is a transformation that takes $N^{(m)}$ to the point $C^{(m)}$ in the same space. We assume that $C^{(m)}$ will be near C. Furthermore as $C^{(m)} \to C$, then $N^{(m)} \to N$.

Now for any pair of vectors $N^{(m)}$, $C^{(m)}$ we assert that the transformation R may be represented by a diagonal matrix, D. That is:

$$RN^{(m)} = C^{(m)} = D^{(m)} N^{(m)} . \qquad (1)$$

What is more, we may now solve our equation for $[D^{-1}]^{(m)}$ and use it as an approximate inverse of R to find N:

$$R^{-1} C \tilde{=} D^{-1} C \tilde{=} N . \tag{2}$$

We now require a method of determining $D^{(m)}$, given $C^{(m)}$ and $N^{(m)}$. Since the inverse of a diagonal matrix is easily found by forming a diagonal matrix, each of whose elements is the reciprocal of the corresponding element in the first matrix:

$$D^{-1} = \left\| d_{ii} \right\|^{-1} = \left\| \frac{1}{d_{ii}} \right\| . \tag{3}$$

Examining Eq. (1) we note that if this were a matrix equation we could postmultiply by $N^{(m)-1}$ and obtain

$$D^{(m)} N^{(m)} [N^{(m)}]^{-1} = C^{(m)} [N^{(m)}]^{-1} = D^{(m)} . \tag{4}$$

However, N and C are column vectors and do not have an inverse. We may get around this, however.

We define a unit column vector:

$$E = \left\| \begin{matrix} 1 \\ 1 \\ 1 \\ \vdots \end{matrix} \right\|$$

and two diagonal matrices, D_N and D_c, where each diagonal element of D_N is equal to the corresponding component of the vector N and similarly for D_c and C. Thus, $N = D_N E$ and $C = D_c E$. Replacing C and N in (1) by their equivalents, as shown above, we have:

$$D D_N E = D_c E . \tag{5}$$

We now premultiply (5) by D_c^{-1}:

$$D_c^{-1} D D_N E = D_c^{-1} D_c E = E . \tag{6}$$

Since D_N^{-1}, D and D_N are all diagonal matrices the order of multiplication may be changed without affecting the result:

$$D D_N D_c^{-1} E = E , \tag{7}$$

or

$$D D_N D_c^{-1} = I;$$

thus

$$D_N D_c^{-1} = D^{-1} . \tag{8}$$

We see that the diagonal matrix D^{-1} approximately equivalent to R^{-1} for the pair of vectors $N = \left\| n_j \right\|$ and $C = \left\| c_i \right\|$ has elements

$$d_{ij}^{-1} = \delta_{ij} \frac{n_j}{c_i} ,$$

where

$$\delta_{ij} = 0,\ i \neq j$$

$$\delta_{ij} = 1,\ i = j\ .$$

Then it is evident that we have the following matrix equation:

$$N = D^{-1}\, C \tag{9}$$

for

$$n_k = d_{kk}^{-1}\, c_k = \frac{n_k}{c_k}\, c_k = n_k\ .$$

We note that although $N = R^{-1}C$ we *cannot* say that $D^{-1} = R^{-1}$. The term D^{-1} is a function of C and will not work for a different C', while R^{-1}, once determined, will be true for any C arising from:

$$C = RN\ . \tag{10}$$

We next replace N in (9) by C to find the zero order approximation:

$$N^{(0)} = C = [D^{-1}]^{(0)}\, C\ .$$

Thus

$$[D^{-1}]^{(0)} = I \tag{11}$$

where I is the identity matrix. Next we apply (10) to $N^{(0)}$:

$$C^{(0)} = RN^{(0)} \tag{12}$$

We next find

$$[d_{kk}^{-1}]^{(1)} = \frac{n_k^{(0)}}{c_k^{(0)}} \qquad k = 1, 2, \ldots q\ , \tag{13}$$

and thus $[D^{-1}]^{(1)}$. Now we calculate $N^{(1)}$, the first order approximation of N:

$$N^{(1)} = [D^{-1}]^{(1)}\, C\ . \tag{14}$$

Note that we always revert to the original C vector at this point rather than to an approximate value $C^{(m)}$. This is to minimize cumulative errors and help assure convergence. Next we find

$$C^{(1)} = RN^{(1)},\ [d_{kk}^{-1}]^{(2)} = \frac{n_k^{(1)}}{c_k^{(1)}},\ N^{(2)} = [D^{-1}]^{(2)}\, C,\ \text{etc.}$$

To demonstrate this method we have detailed the steps of applying the above algorithm to a simple 3×3 matrix and three-component vector in Table 4. In Table 5 is shown a comparison of each step of two different iteration methods applied to this same problem. We see that there is not much difference in this simple example but the correction factor

Table 4. Correction Factor Iteration

An Example

Given: $R = \begin{Vmatrix} .9 & .1 & 0 \\ .2 & .7 & .1 \\ .2 & .2 & .6 \end{Vmatrix}$ $C = \begin{Vmatrix} 1.0 \\ 1.1 \\ 1.6 \end{Vmatrix}$ $N = \begin{Vmatrix} n_1 \\ n_2 \\ n_3 \end{Vmatrix}$

To find N when $RN = C$

Algorithm $N^{(m+1)} = (D^{-1})^{(m)} C$

$(D^{-1})^{(m)} = \left\| (d_{jj}^{-1})^{(m)} \right\| = \left\| \delta_{ij} n_j^{(m)} / C_i^{(m)} \right\|$

$C^{(m)} = RN^{(m)}$

$N^{(o)} = C$

First Iteration

$N^{(o)} = C = \begin{Vmatrix} 1.0 \\ 1.1 \\ 1.6 \end{Vmatrix}$.

$C^{(o)} = RN^{(o)} = RC = \begin{Vmatrix} .9 & .1 & 0 \\ .2 & .7 & .1 \\ .2 & .2 & .6 \end{Vmatrix} \begin{Vmatrix} 1.0 \\ 1.1 \\ 1.6 \end{Vmatrix} = \begin{Vmatrix} 1.01 \\ 1.13 \\ 1.37 \end{Vmatrix}$

$(D^{-1})^{(o)} = \left\| \delta_{ij} n_j^{(o)} / C_i^{(o)} \right\| = \begin{Vmatrix} 1.0/1.01 & 0 & 0 \\ 0 & 1.1/1.13 & 0 \\ 0 & 0 & 1.6/1.37 \end{Vmatrix} = \begin{Vmatrix} .99 & 0 & 0 \\ 0 & .97 & 0 \\ 0 & 0 & 1.17 \end{Vmatrix}$

Second Iteration

$N^{(1)} = (D^{-1})^{(o)} C = \begin{Vmatrix} .99 & 0 & 0 \\ 0 & .97 & 0 \\ 0 & 0 & 1.17 \end{Vmatrix} \cdot \begin{Vmatrix} 1.0 \\ 1.1 \\ 1.6 \end{Vmatrix} = \begin{Vmatrix} .99 \\ 1.07 \\ 1.87 \end{Vmatrix}$

$C^{(1)} = RN^{(1)} = \begin{Vmatrix} .9 & .1 & 0 \\ .2 & .7 & .1 \\ .2 & .2 & .6 \end{Vmatrix} \cdot \begin{Vmatrix} .99 \\ 1.07 \\ 1.87 \end{Vmatrix} = \begin{Vmatrix} .998 \\ 1.134 \\ 1.533 \end{Vmatrix}$

$(D^{-1})^{(1)} = \left\| \delta_{ij} n_j^{(1)} / C_i^{(1)} \right\| = \begin{Vmatrix} .99/.998 & 0 & 0 \\ 0 & 1.07/1.134 & 0 \\ 0 & 0 & 1.87/1.533 \end{Vmatrix} = \begin{Vmatrix} .992 & 0 & 0 \\ 0 & .944 & 0 \\ 0 & 0 & 1.22 \end{Vmatrix}$

$N^{(2)} = (D^{-1})^{(1)} C =$ etc. ---

method is, if anything, slightly faster than the other one, which is the incremental correction method of Freedman.

Now we have little to say about the convergence properties of this method except to say that the strength of the principal diagonal of the response matrix, R, relative to the off-diagonal elements is the governing factor. It may also help to normalize the sum of all matrix elements since many of the indicators of convergence depend upon some function (a norm) of the matrix elements having an absolute magnitude less than unity [4].

In Table 6 we show two unfolded spectra from the slab penetration experiment. The first spectrum was printed out after only 13 iterations because the sum of the squared residual test had reached a minimum.

On the other hand the other spectrum was printed out after reaching the programmed maximum number of iterations – 70. We observe a much closer fit (i.e., $\Delta C \to 0$) to the channels in the second case. Finally, Fig. 9 shows the same unfolded spectrum and the effect of smoothing.

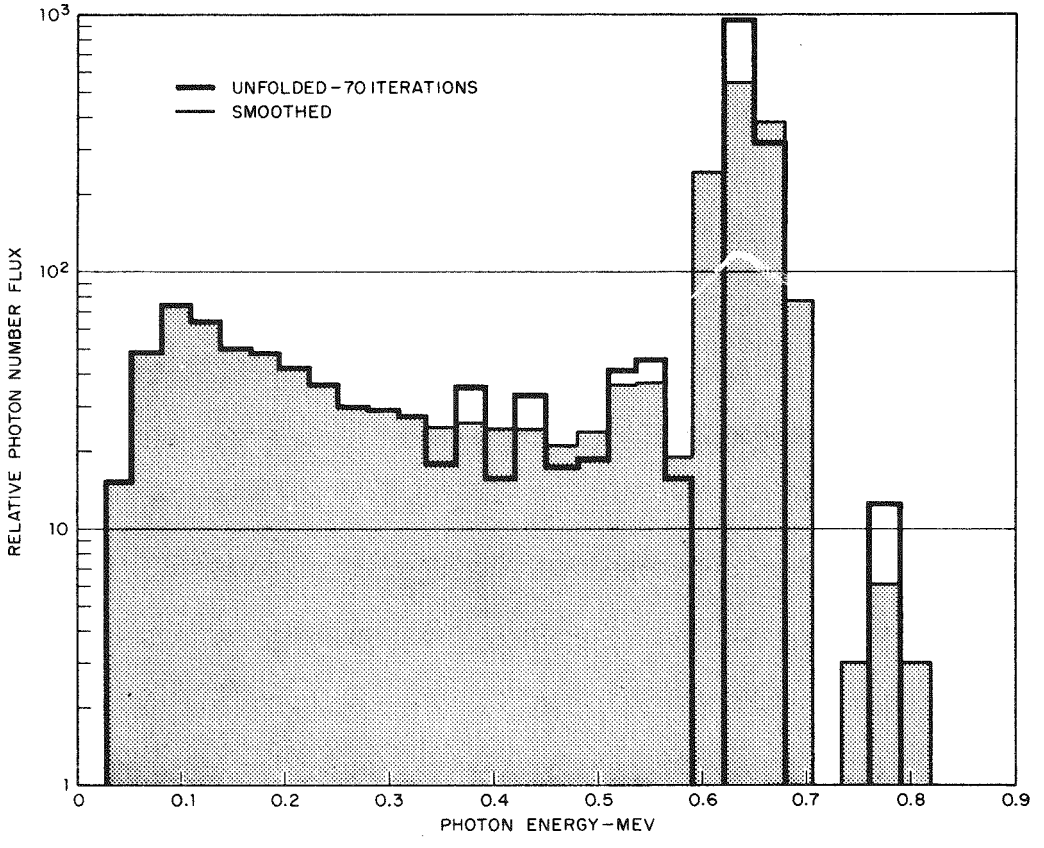

Fig. 9. Cs^{137}, 2-in. Al Unfolded Spectrum.

Table 5. Iteration Method Comparison

	$N^{(m)}$			$C^{(m)}$		
m	n_1	n_2	n_3	c_1	c_2	c_3
0^a	1	1.1	1.6	1.01	1.13	1.37
0^b	1	1.1	1.6	1.01	1.13	1.37
1^a	0.99	1.07	1.87	0.998	1.134	1.533
1^b	0.99	1.07	1.83	0.998	1.130	1.510
2^a	0.992	1.038	1.950	0.9965	1.1202	1.5760
2^b	0.992	1.040	1.920	0.9968	1.1184	1.5584
3^a	0.9954	1.0196	1.9795			
3^b	0.9952	1.0216	1.9616			
	1.0000	1.0000	2.0000	1.0000	1.1000*	1.6000
		N			C	

[a]Correction factor method.
[b]Incremental correction method.

FUTURE DEVELOPMENTS

The iterative program we have been describing was written several years ago for a Burroughs Datatron. Since that time we have replaced this by an IBM 704 and have only recently had a need to use the unfolding program. We are now rewriting this program in FORTRAN. Such a program, utilizing the correction factor iteration method, has already been written at another laboratory [6].

We are incorporating the least-squares fitting in our new program, following the lead of Rose [7], Trombka [8], and Salmon [9]. It should be noted that this involves solving the matrix equation, $R^T\omega RN = R^T\omega C$, where ω is a diagonal weighting function matrix. If we redefine the response matrix $R' \equiv R^T\omega R$ and the count vector $C' \equiv R^T\omega C$, then we again have the matrix equation $R'N = C'$, which may be solved iteratively.

There are several attractive features about this modification. Our original response matrix, R, no longer needs to be square since it automatically becomes so upon multiplication by its transpose. Furthermore the rank of the resultant matrix R' is the smaller of the two matrix dimensions. One unexpected bonus is that the matrix is symmetrized which has favorable implications concerning its convergence properties. Lastly, with the requirement for a square response matrix eliminated we are now able to unfold, by a least-squares method, a small number of gamma lines or any mixture of lines and continuous spectra.

We finally come to the matter of error or uncertainty to be assigned to the unfolded values. Certainly one attraction that the least-squares methods have is the ability to

Table 6. Examples of Unfolding

Cs^{137}, 2-in. Al, 20° (m = 13)					Cs^{137}, 2-in. Al, 30° (m = 70)				
Channel No.	C	$RN^{(m)}$	ΔC	$k_1^* N^{(m)}$	Channel No.	C	$RN^{(m)}$	ΔC	$k_2^* N^{(m)}$
1	2606	2604	−2	219	1	2366	2366	0	155
2	4561	4560	−1	542	2	4701	4701	0	464
3	5648	5647	−1	742	3	5822	5822	0	627
4	5033	5032	−1	656	4	5326	5326	0	582
5	4483	4482	−1	564	5	4345	4345	0	434
6	3974	3973	−1	482	6	4054	4054	0	410
7	3598	3597	−1	421	7	3666	3666	0	352
8	3231	3230	−1	358	8	3298	3298	0	301
9	2947	2945	−2	317	9	3032	3032	0	260
10	2698	2699	1	267	10	2901	2901	0	250
11	2588	2581	−7	261	11	2773	2773	0	213
12	2578	2589	−11	237	12	2817	2817	0	235
13	2664	2645	−19	306	13	2403	2403	0	174
14	2448	2484	−36	161	14	2072	2073	1	167
15	2232	2216	−32	238	15	2248	2247	−1	312
16	1968	1953	−15	250	16	2414	2415	1	279
17	1997	2011	−14	270	17	3248	3247	−1	409
18	2309	2316	−7	424	18	8580	9384	804	1
19	3696	3636	−60	421	19	18456	18456	0	5590
20	7983	11173	3190	26	20	13392	13392	0	2084
21	19335	19262	−73	8803	21	2895	3976	1081	0
22	11077	11614	537	914	22	358	540	182	0
23	1977	2606	629	1	23	145	145	0	53
24	209	335	126	0	24	31	85	54	0
25	156	154	−2	70	25	37	37	0	11
26	99	105	6	17					
27	40	41	1	1					
28	22	21	−1	5					
29	3	27	24	0					
30	37	37	0	22					
31	26	34	8	0					
32	26	26	0	15					

*Source normalization and conversion factors to yield gamma flux.

assign error limits to their results. In their expressions for error however, the diagonal elements of the inverse matrix, R'^{-1} or $(R^T \omega R)^{-1}$ appear. If we solve the modified matrix equation by an iterative method we do not get an inverse. However, the diagonal D^{-1} is operating as an inverse for the two vectors under consideration so we may assign

an error, e_j, to the element n_j of the unfolded gamma-ray vector N by the following expression:

$$[e_j^{(m)}/0.6745]^2 = \text{variance}\,[n_j^{(m)}] = \frac{\epsilon^2}{p-q}\, d_{jj}^{-1}\,,$$

where

$$\epsilon^2 \equiv \sum_{i=1}^{p}\left[C_i - \sum_{j=1}^{q} R_{ij}N_j\right]^2$$

is the sum of the squared residuals, n is the maximum number of pulse-height channels and m is the number of energy bins or gamma lines.

Note added in proof: Gold [10] has shown that the necessary and sufficient condition for the convergence of this iteration scheme (for exact vector and matrix elements) is that the response matrix, R or R' be positive-definite.

REFERENCES

[1] Simultaneous Linear Equations and the Determination of Eigenvalues, *Nat. Bur. Std. Appl. Math. Ser.*, **29** (1953).

[2] J. C. Villforth, R. D. Birkhoff, and H. H. Hubbell, Jr., *Comparison of Theoretical and Experimental Filtered X-Ray Spectra*, ORNL-2529 (1958).

[3] M. S. Freedman, T. B. Novey, F. T. Porter, and F. Wagner, "Correction for Phosphor Backscattering in Electron Scintillation Spectrometry," *Rev. Sci. Instr.* **27**, 716 (1956).

[4] V. N. Faddeeva, *Computational Methods of Linear Algebra*, Dover, New York, 1959.

[5] Starfelt and Koch, "Measurements of Thin Target Bremsstrahlung," *Phys. Rev.* **102**, 1598 (1956).

[6] J. F. Mollenauer, *A Computer Analysis for Complex Sodium Iodide Gamma Spectra*, UCRL-9748 (August 1961).

[7] M. E. Rose, "The Analysis of Angular Correlation and Angular Distribution Data," *Phys. Rev.* **91**, 3 (1953).

[8] J. I. Trombka, *On the Analysis of Pulse Height Spectra,* thesis, University of Michigan, No. 56662 (1961).

[9] L. Salmon, "Analysis of Gamma-Ray Scintillation Spectra by the Method of Least Squares," AERE-R-3640, Harwell, Berkshire (1961).

[10] R. Gold and N. Scofield, "An Iterative Solution of the Matrix Representation of Detection Systems," to be published.

(3-3) A STUDY OF THE ERRORS ASSOCIATED WITH SPECTRAL ANALYSIS METHODS

Walter R. Burrus and Dixon Bogert[1]
Oak Ridge National Laboratory[2]
Oak Ridge, Tennessee

INTRODUCTION

It is a platitude that every experimentally determined quantity ought to be accompanied by an indication of its reliability. Most persons will grant that the computation of errors justifies as much time and effort as the computation of answers. Hence, a paper on errors, as opposed to a paper on answers, appears to be appropriate.

The problem of unfolding a gamma-ray spectrum can be approached by setting up a system of equations relating the unknown spectrum to the observed pulse-height distribution. These equations might then be solved by matrix inversion or least squares. The solution to systems of equations and the associated error analysis is well understood. The trouble is that the errors come out too large if there are many unknown components. The same comments also apply to the problem of analyzing decay curves in terms of the half-lives and numbers of atoms of several components.

The key to resolving the error problem, in the case of spectrum unfolding, is to use some of the additional physical knowledge about the spectrum which is ignored in the ordinary inversion or least-squares problems. For example, gamma-ray spectra cannot be negative, yet negative solutions are produced with abandon when inversion and least-square methods blow up. The importance of incorporating the a priori knowledge into the formulation is attested to by several other papers given here which are concerned with techniques of reducing the errors in conventional equation solving methods by the use of nonnegativity.

ERRORS IN UNFOLDING

We will introduce some problems associated with errors by means of several examples. The case we will be interested in is illustrated by Fig. 1, which shows a pulse-height distribution obtained with a large NaI crystal. The error bars shown for a few points are the usual errors of ± one standard deviation. The appearance of this pulse-height distribution strongly suggests that there are several discrete gamma rays producing the peaks, but it is also clear that any fine details in the spectrum have been considerably obscured by the lethal combination of resolution and statistics.

If we really knew that there were exactly four gamma rays, then we could carry out a least-squares fitting analysis and obtain a fairly straightforward solution with errors. But if there are a large number of possible gamma rays – or worse, if the gamma-ray spectrum is continuous – then we will have trouble with large errors.

---

[1]Summer employee from Yale University.

[2]Operated by Union Carbide Nuclear Company for the United States Atomic Energy Commission.

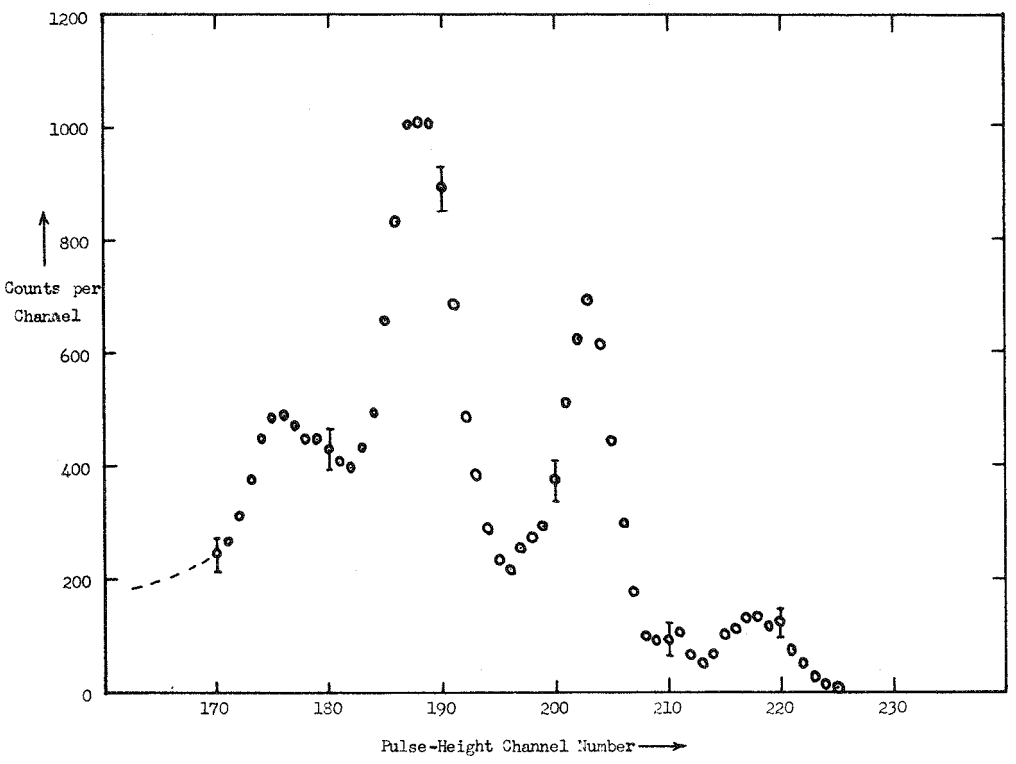

Fig. 1. Typical Pulse-Height Distribution.

If we are unwilling (or unable) to make any assumptions about the form of the gamma-ray spectrum, then we should not expect to unfold the actual gamma-ray spectrum. Instead we can partially unfold the data by removing the effects of Compton tails, escape peaks, etc. which complicate the direct analysis of the pulse-height distributions. Then the result will still show only the effects of the Gaussian-type resolution of the spectrometer. It apparently has not been sufficiently emphasized in the past that large errors are inevitable in solving a system of equations if the energy interval chosen is much less than the natural instrumental resolution width and no provision is made for reintroducing a resolution or "smoothing" type function in the solution.

Figure 2 shows the results of an analysis of the pulse-height distribution. A certain amount of broadening was intentionally introduced into the analysis. The broadening which was left in was determined in advance of the calculation. If results from a theoretical calculation of this spectrum were available, they would first have to be broadened by folding in the prescribed broadening function before they could be compared with this graph. In addition to the broadening, which we do not try to completely eliminate, this figure illustrates another type of error. Namely, because of statistical fluctuations and because we must start with a finite discrete pulse-height distribution and end up with a continuous gamma-ray spectrum, we can only specify a confidence region for our result (shown on the figure by a shaded area).

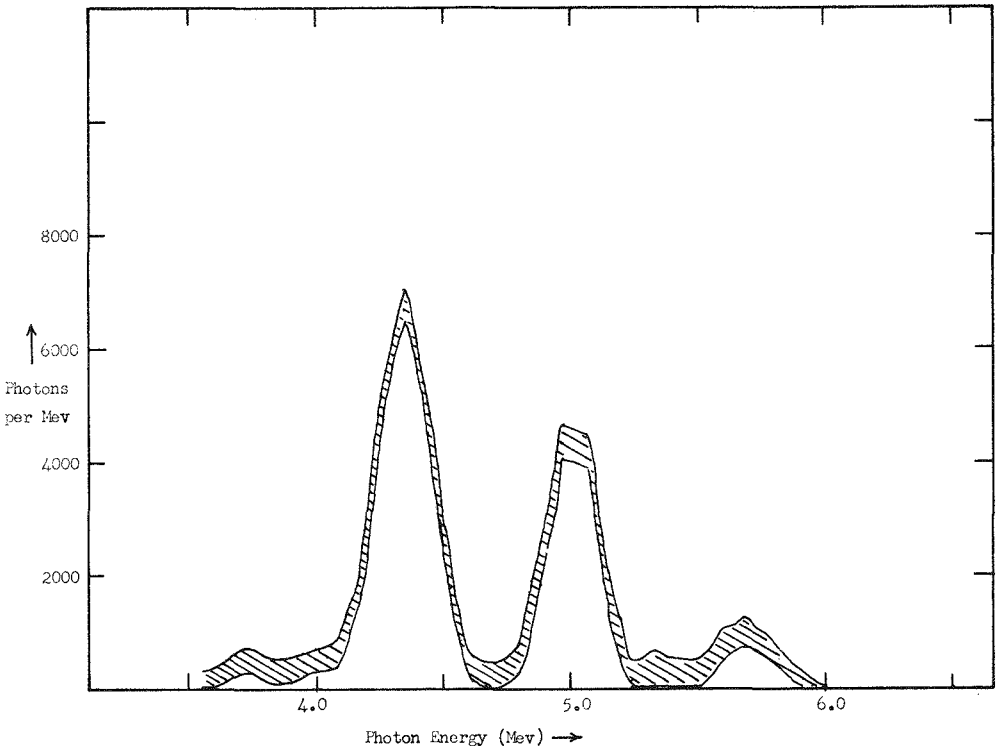

Fig. 2. Unfolded Gamma-Ray Spectrum.

If we fail to formulate the problem so that a broadened spectrum is obtained as the result (that is, if we solve for the true spectrum directly), then we will obtain a very large, nearly trivial confidence interval for the result. A quite reasonable rule of thumb is that the size of the confidence region increases rapidly when the prescribed broadening function becomes much narrower than the inherent instrumental resolution of the spectrometer. Thus, we need a more general formulation of the unfolding problem which allows us to unfold some prescribed function of the spectrum (that is to say, a broadened spectrum) instead of the true spectrum itself.

Some methods automatically leave in a certain amount of broadening (such as linear iterative methods which are terminated before convergence), but then it becomes part of the error analysis problem to find out how much broadening has been introduced by the analysis method. We prefer to prescribe the broadening we expect before the computation begins and to calculate the error with the prescribed broadening in mind. Then, if the errors are too large, we can change the prescribed broadening and try again.

Now we will illustrate another aspect of the error problem. Suppose we have reason to suspect that the spectrum must consist of monoenergetic gamma rays. Then we might try to fit the pulse-height distribution of Fig. 1 by, say, four discrete gamma rays. An analysis of the pulse-height distribution using this assumption is shown in Fig. 3. Note that four gamma rays, at positions marked γ_1, γ_2, γ_3, and γ_4 seem to result in small residuals in the upper half of the distribution, but that there are fairly large residuals

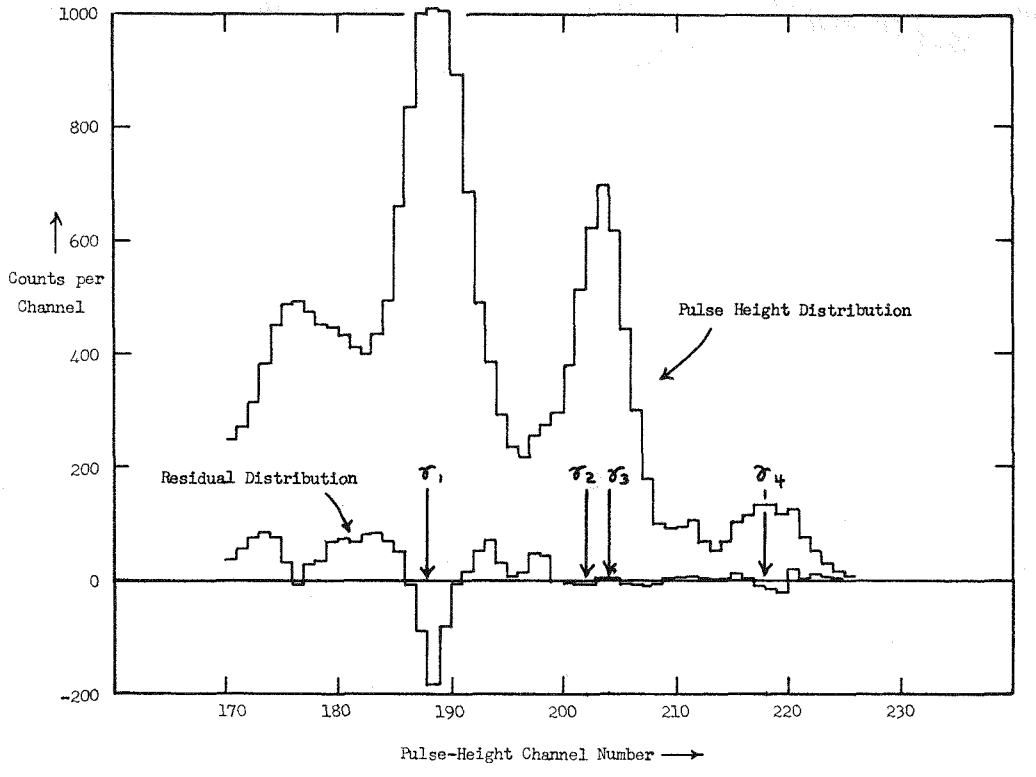

Fig. 3. Least-Squares Fit to Pulse-Height Distribution with Four Gamma Rays.

in the lower half. Thus, we probably need an additional gamma ray somewhere near channel 185. But it is also clear that even where the residuals are small, there might really be three gamma rays instead of two.

We have shown two different kinds of unfolded solutions for the same pulse-height distribution. The unfolded spectrum of Fig. 2 is much the safer of the two, since no assumptions about the nature of the spectrum had to be made. However, the price we paid for no assumptions was that we had to prescribe a certain amount of broadening in order to obtain a small confidence interval.

One way to deal with this problem (or to avoid it) is to state the computed errors with respect to the set of initial assumptions. Thus, in Fig. 2 we can state that the computed errors depend only on the stated resolution function and not on any arbitrarily assumed facts. But the calculated errors based on Fig. 3 depend on the assumption that there are exactly four monoenergetic gamma rays. Both methods are useful, and, in fact, we frequently unfold the same set of data using different sets of initial assumptions. The calculated errors for the weakest assumption set involve the least risk. Of course, the set of initial assumptions ought to be motivated by good physical reasons. The assumption set may be empty, or the assumptions may rest on very solid ground, but the veracity of the assumption set is not part of the numerical problem (although the computation sometimes indicates that there are no solutions consistent with the assumption set).

USE OF A PRIORI INFORMATION

We now turn to the problem of how the assumption set may be utilized to reduce the errors over those produced in the ordinary inversion or least-squares techniques. We do not mean to imply that the classical mathematicians – Gauss, Markov, and Legendre – have been disproved. We merely propose to use additional information which is usually ignored in the classical linear regression analysis. Doubtless, had the scintillation spectrometer existed in the days of Gauss, we would not have had to wait so long for good unfolding methods!

A somewhat simplified and small set of equations $Ax = b$ that we might set up for an unfolding calculation is shown in Fig. 4. The matrix is a broadening type of matrix so that the right-hand side b has about a two-channel resolution width. Now, since the unknown gamma-ray spectrum x in a real problem is continuous and really requires an infinite number of components to represent it, we have tried to approximate this condition (within the limitations of the size of a slide) by taking 13 unknowns for x and only 9 knowns for b. We have also put the extra four components (x_1, x_2, x_{12}, and x_{13}) on the edges, where we frequently run into trouble in real problems because we do not know how to stop gracefully.

For a given right-hand side b, this set of equations has no unique solution since it is underdetermined. Yet we will show how we can obtain an adequate solution by use of the fact that a gamma-ray spectrum with negative photons is impossible. But first, the conventional approach to this problem would be to eliminate the edge problems somehow and to omit or combine enough components of x so that the number of unknowns was equal to the number of knowns. Then we could employ ordinary matrix inversion to obtain the solution, and, with a little extra calculation, also obtain the standard deviations of the solution components.

Figure 5 shows the results of the standard matrix inversion methods applied to a particular right-hand side. We first synthesized a possible right-hand side by computing the distribution which would result from a spectrum x with the 6th and 8th elements

$$\begin{bmatrix} .1 & .4 & .6 & .4 & .1 & & & & & & & & \\ & .1 & .4 & .6 & .4 & .1 & & & & & & & \\ & & .1 & .4 & .6 & .4 & .1 & & & & & & \\ & & & .1 & .4 & .6 & .4 & .1 & & & & & \\ & & & & .1 & .4 & .6 & .4 & .1 & & & & \\ & & & & & .1 & .4 & .6 & .4 & .1 & & & \\ & & & & & & .1 & .4 & .6 & .4 & .1 & & \\ & & & & & & & .1 & .4 & .6 & .4 & .1 & \\ & & & & & & & & .1 & .4 & .6 & .4 & .1 \end{bmatrix} \begin{bmatrix} x_1 \\ x_2 \\ x_3 \\ x_4 \\ x_5 \\ x_6 \\ x_7 \\ x_8 \\ x_9 \\ x_{10} \\ x_{11} \\ x_{12} \\ x_{13} \end{bmatrix} = \begin{bmatrix} b_1 \\ b_2 \\ b_3 \\ b_4 \\ b_5 \\ b_6 \\ b_7 \\ b_8 \\ b_9 \end{bmatrix}$$

Fig. 4. A 9 by 13 System of Equations Used in the Example. A truncated 9 by 9 system is shown within dotted lines.

	x_j	b_i	$\sigma[b_i]$	$\sigma[x_j]$
1	0.	0.	0.	- -
2	0.	1000.	32.	- -
3	0.	4000.	63.	1920.
4	0.	7000.	84.	4826.
5	0.	8000.	89.	7798.
6	10000.	7000.	84.	9995.
7	0.	4000.	63.	10799.
8	10000.	1000.	32.	9995.
9	0.	0.	0.	7798.
10	0.			4826.
11	0.			1920.
12	0.			- -
13	0.			- -

Fig. 5. Errors in Solution of the Truncated 9 by 9 System Obtained by Matrix Inversion for a Particular Right-Hand Side b.

equal to 10,000. The edges of the x vector were intentionally taken as zero so that we could stay out of trouble with the components we dropped from the matrix. Thus, we are giving the matrix inversion method every possible advantage. In order to calculate plausible errors in x, we took the standard deviation of the right-hand side elements b_i to be the square root of b_i. Then we inverted the matrix and computed the statistical errors in the solution. In Fig. 5, we see that the magnitude of the calculated errors is just about as large as the initial values of the unknown that we used, and, hence, using a right-hand side b with statistical errors, we should not expect the solution to come out very close to 10,000 in the 6th and 8th component and to be zero elsewhere.

What can we do to improve matters? Consider the first two equations in the system of equations:

$$A_{11}x_1 + A_{12}x_2 + A_{13}x_3 + \ldots = b_1 ,$$

and

$$A_{21}x_1 + A_{22}x_2 + A_{23}x_3 + \ldots = b_2 . \qquad (1)$$

If all the A_{ij}'s are nonnegative and if all the x_j's are nonnegative, then we can determine a very simple upper bound to the solution. Looking at the first row only, we see that x_1 must be less than b_1/A_{11}, since that is the largest value it could take if all the other x_j's are zero. Similarly, from the second row only, we can say that x_1 must be less than b_2/A_{21}. Since we can obtain an upper bound for x_1 from any row, we pick the row which gives the smallest value. Generalizing to the x_j component, we obtain the relation:

$$0 \leqq x_j \leqq \min_i (b_i/A_{ij}) , \qquad j = 1, 2, \ldots . \qquad (2)$$

Namely, x_j is greater than zero and less than b_i/A_{ij} for whatever row i gives the best result.

Figure 6 shows the computed upper and lower bounds for our 13 by 9 system of equations using the previous inequality relations. We see that all but three components have been found to be exactly zero. We can then solve for the remaining three components by inversion or least-squares methods and obtain the solution with standard errors shown in the $\sigma(x_j)$ column. In the next column we have copied from Fig. 5 the standard errors obtained by matrix inversion. Note that the new errors are much less than the matrix inversion errors.

	XLO	XUP	$\sigma[x_j]$	$\sigma[x_j]$ "inversion"
1	0.	0.	0.	- -
2	0.	0.	0.	- -
3	0.	0.	0.	1920.
4	0.	0.	0.	4826.
5	0.	0.	0.	7798.
6	0.	10000.	320.	9995.
7	0.	13333.	260.	10799.
8	0.	10000.	320.	9995.
9	0.	0.	0.	7798.
10	0.	0.	0.	4826.
11	0.	0.	0.	1920.
12	0.	0.	0.	- -
13	0.	0.	0.	- -

Fig. 6. Errors in the Solution of the 9 by 13 System of Equations Obtained by Use of a Priori Information Compared with Errors Obtained by Matrix Inversion of the Truncated 9 by 9 System.

A useful point of view for understanding the implications of this result is to consider that the solution vector $\hat{x}$ in the above example can be expressed by means of an

unfolding matrix U in the form $\hat{x} = Ub$ as follows:

$$\begin{bmatrix} x_1 \\ x_2 \\ x_3 \\ x_4 \\ x_5 \\ x_6 \\ x_7 \\ x_8 \\ x_9 \\ x_{10} \\ x_{11} \\ x_{12} \\ x_{13} \end{bmatrix} = \begin{bmatrix} 0 & 0 & 0 & 0 & 0 & 0 & 0 & 0 & 0 \\ 0 & 0 & 0 & 0 & 0 & 0 & 0 & 0 & 0 \\ 0 & 0 & 0 & 0 & 0 & 0 & 0 & 0 & 0 \\ 0 & 0 & 0 & 0 & 0 & 0 & 0 & 0 & 0 \\ 0 & 0 & 0 & 0 & 0 & 0 & 0 & 0 & 0 \\ 0 & 10 & 0 & 0 & 0 & 0 & 0 & 0 & 0 \\ 0 & -20/3 & 0 & 0 & 5/3 & 0 & 0 & -20/3 & 0 \\ 0 & 0 & 0 & 0 & 0 & 0 & 0 & 10 & 0 \\ 0 & 0 & 0 & 0 & 0 & 0 & 0 & 0 & 0 \\ 0 & 0 & 0 & 0 & 0 & 0 & 0 & 0 & 0 \\ 0 & 0 & 0 & 0 & 0 & 0 & 0 & 0 & 0 \\ 0 & 0 & 0 & 0 & 0 & 0 & 0 & 0 & 0 \\ 0 & 0 & 0 & 0 & 00 & 0 & 0 & 0 & 0 \end{bmatrix} \begin{bmatrix} b_1 \\ b_2 \\ b_3 \\ b_4 \\ b_5 \\ b_6 \\ b_7 \\ b_8 \\ b_9 \end{bmatrix}$$

The elements in the U matrix were obtained by solving for the three variables x_6, x_7, and x_8 in terms of b_2, b_5, and b_8. But the unfolding matrix U is not unique and we could have used any other three elements of b for which the matrix A had independent columns. The smallest statistical errors for the three solution components (x_6, x_7, x_8) would have resulted if the matrix U were obtained by solving the overdetermined 9 by 3 system of equations by the method of weighted least squares.

Even though the results of the usual matrix inversion or least-squares method may be written in the form $\hat{x} = Ub$, there is an important difference in the new method. Suppose that b is known without any statistical errors. Then $b = Ax$, and the above unfolding equation becomes $\hat{x} = UAx$. Thus the solution $\hat{x}$ is related to the true value x by the matrix product UA. In inversion or least squares, this product UA is the identity matrix I which means that the solution $\hat{x}$ and the true value $\hat{x}$ agree if b is obtained exactly. But in the new method UA is not equal to the identity. In fact, for the example given above,

$$UA = \begin{bmatrix} 0 & 0 & 0 & 0 & 0 & 0 & 0 & 0 & 0 & 0 & 0 & 0 & 0 \\ \vdots & \vdots & \vdots & \vdots & \vdots & \vdots & \vdots & \vdots & \vdots & \vdots & \vdots & \vdots & \vdots \\ 0 & 0 & 0 & 0 & 0 & 0 & 0 & 0 & 0 & 0 & 0 & 0 & 0 \\ 0 & 1 & 4 & 6 & 4 & 1 & 0 & 0 & 0 & 0 & 0 & 0 & 0 \\ 0 & -2/3 & -8/3 & -4 & -5/2 & 0 & 1 & 0 & -5/2 & -4 & -8/3 & -2/3 & 0 \\ 0 & 0 & 0 & 0 & 0 & 0 & 0 & 1 & 4 & 6 & 4 & 1 & 0 \\ 0 & 0 & 0 & 0 & 0 & 0 & 0 & 0 & 0 & 0 & 0 & 0 & 0 \\ \vdots & \vdots & \vdots & \vdots & \vdots & \vdots & \vdots & \vdots & \vdots & \vdots & \vdots & \vdots & \vdots \\ 0 & 0 & 0 & 0 & 0 & 0 & 0 & 0 & 0 & 0 & 0 & 0 & 0 \end{bmatrix}.$$

The fact that UA is not diagonal (except for the 6th, 7th, and 8th positions) was not detrimental to the solution because we knew from a priori considerations that the elements of x corresponding to the nondiagonal elements were exactly zero. In a real problem where the knowledge of the a priori bounds are not as sharp, usually some uncertainity is introduced into the solution by obtaining an unfolding matrix for which $UA \neq I$, but we can use the a priori knowledge to evaluate the maximum uncertainty due to this source. We call this type of error "bias error" since it is not present in so-called "unbiased methods." If we just traded one kind of error for another, we would not have gained anything. But by allowing a very small amount of bias error, we can greatly decrease the amount of overall error. The overall improvement is a consequence of the fact that if the solution is known to lie in the positive region of "solution space" of dimension n, then only $(\frac{1}{2})^n$ of the total space is available to the solution.

UNFOLDING METHODS

Several of the methods discussed at this symposium, such as the Trombka method [1] and the vector analysis method [2], can be understood as methods for producing an unfolding matrix U which does not yield $UA = I$. The a priori information which they use is the nonnegativity of the gamma-ray spectrum. Others such as the Scofield-Gold method [3] do not produce a full unfolding matrix directly and will have to be treated in a more general manner.

Two codes have been written at the Oak Ridge National Laboratory for unfolding spectra which allow the incorporation of nonnegativity into the formulation of the problem. One called the SLOP code [4] uses the inequality relation in Eq. (2) to derive an additional term added to the sum of squares in the usual least-squares method. The other, known as the OPTIMO code [5], deals directly with the inequalities by means of linear programming. Both codes have provisions for solving for a broadened spectrum and for imposing certain a priori information in addition to nonnegativity.

GENERAL ERROR ESTIMATE

Thus far, we have discussed the types of errors we encounter in unfolding and have indicated by means of a simple example how the use of a priori information can reduce the conventional errors. We have also indicated how the use of this additional information may result in another type of "bias error" in addition to the usual statistical error, although resulting in a much smaller overall error.

Here we will outline an error analysis which is more general than that we have discussed up to now. In particular, we will not assume that the unfolding method produces an unfolding matrix U. Thus the error analysis is applicable to graphical and other methods for which definite rules can be formulated. First we summarize the formulae needed concisely, and then elaborate further in the text.

Model:

$$Ax = b \tag{3}$$

$\hat{b}$ has mean b (4)

$\hat{b}$ has variance matrix V (5)

x satisfies certain a priori constraints (6)

Wanted:

estimates $\hat{p}_k$ of the quantities

$p_k = \sum_j W_{kj} x_j$ (or in matrix notation $p = Wx$) (7)

and their errors

Estimation Method:

produces estimates $\hat{p}_k$ of p_k for $k = 1, 2, \ldots$ (8)

$$D_{kj} = \partial \hat{p}_k / \partial b_i |\hat{b} \tag{9}$$

Errors:

$$e^{(s)} = \hat{p}^{(s)} - Wx = [\hat{p} - D\hat{b}] + D[\hat{b}^{(s)} - b] + [DA - W]x \tag{10}$$

Equation (3) expresses the relation between the true solution x and the mean b of the observed pulse-height distribution. Of course, we never know b exactly because of statistical fluctuations. Equations (4) and (5) characterize the assumed statistical properties of the observed pulse-height distribution $\hat{b}$. Equation (4) states that the mean of a large number of experiments made under identical conditions will converge to the true mean value b. Further, Eq. (5) states that the variance matrix V of $\hat{b}$ is known. Usually, a sufficient approximation is to take the variance matrix as diagonal with elements equal to the estimated variance of the $\hat{b}_i$'s.

In line with our previous discussion, we allow the solution $\hat{p}$ to be an estimate of functions of the spectrum rather than restricting it to the actual spectrum x. Thus we must concentrate our attention (and computations) on finding estimates of the quantities $p_k = \sum_j W_{kj} x_j$, where the coefficients W_{kj} are the elements of a broadening matrix. (Actually the coefficients W_{kj} can be a conversion from gamma-ray spectra to any quantity of interest which is linearly related to the unknown spectrum – such as the dose.) Finally, we may know some a priori information. We generally always know that the gamma-ray spectrum is nonnegative. In addition, we sometimes know that the gamma-ray spectrum has been smoothed by Doppler shift – as with gamma rays from moving fission fragments.

A conceptual way to approach the problem of obtaining errors for the estimates $\hat{p}_k$ is to think of a degenerate confidence region obtained by linear regression, which covers the point p with a prescribed probability. However, if the matrix A is underdetermined (more unknowns than knowns), singular, or nearly singular, then certain axes of the confidence region will be degenerate and have infinite length (or very large length) unless the W_{kj} coefficients are chosen to be exactly orthogonal to the

degenerate directions. But we know with certainty that only those values of $\hat{p}_k$ are jointly possible which are consistent with the a priori information. Thus the intersection of the linear regression confidence region and the a priori constraint region for p yields the best possible composite confidence region which incorporates all the information available.

The trouble with the above conceptual idea is that the resulting composite confidence region does not have a simple mathematical description (such as an ellipse) and cannot be found analytically. Instead one must resort to numerical methods to find specific features of the composite confidence region of interest. Most simply, we solve only for the univariate confidence intervals for each of the quantities p_k, for $k = 1, 2, \ldots$.

Equations (8) and (9) characterize the unfolding method. We suppose that the method yields an estimate of the components of p, and that the matrix of coefficients D_{kj} can somehow be obtained which relates the estimates to small changes in the components of b. Usually the D matrix can be calculated as a by-product of the unfolding calculations, but we can always compute it numerically by varying the elements of b in turn, and repeating the entire unfolding process each time.

The final formula for errors is obtained by considering an ensemble of imagined experiments performed under identical conditions. Usually we perform only one experiment and obtain a pulse-height distribution $\hat{b}$. Then we want to deduce the properties of the ensemble from this one observation. Denoting $\hat{p}^{(s)}$ as the estimate for p obtained by employing the unfolding process on the sth member of the ensemble of b, we can express $\hat{p}^{(s)}$ in terms of the observed $\hat{b}$ to first order in the derivatives by the relation:

$$\hat{p}^{(s)} = \hat{p} - D[\hat{b} - b^{(s)}] . \tag{11}$$

Adding and subtracting the term Db to the right-hand side of Eq. (11) and rearranging, we obtain

$$p^{(s)} = \hat{p} - D[b - b^{(s)}] - D\hat{b} + Db . \tag{12}$$

The substitution of Ax for b in the last term of Eq. (12) finally yields the results shown in Eq. (10).

Returning to Eq. (10), the second term is just the usual statistical error term. The average of the square of the bracket in this term is the variance matrix V. But the first and third terms are peculiar to methods which utilize a priori information. In the conventional matrix inversion and least-square methods, both the first and last term drop out – the first term because the method is linear, and the last term because the method is unbiased. Indeed, in methods which do not utilize a priori information, there is no way to ensure that the last term is not infinity without requiring the expression in brackets to be identically zero. But if some weak a priori information is known at the start about the maximum size of the true value of x, as could be obtained from the inequalities of Eq. (2), then we no longer need to insist that the term vanish identically, but can concentrate our efforts on minimizing the sum of all the different contributions to the error. By allowing some error of the "bias" type, we achieve much smaller overall results.

CONCLUSIONS

The problems in utilizing all the information known about the problem are far from solved. In fact there is not even general agreement that the Eqs. (3 – 7) constitute the core of the general problem. In addition, the present codes either do not calculate the errors at all, or as in the case of the Oak Ridge codes, are more inefficient in time and performance than they need be. Also certain basic problems involved when the number of unknown components increases without limit have not been rigorously overcome in practice, although the answers to all these questions appear to be in sight.

We intend to continue working on such problems at Oak Ridge for the indefinite future and would very much like to encourage others to do so. As our main problem is shortage of manpower, and as the spirit of a particular solution is often impossible to communicate formally, we prefer to exchange ideas by direct collaboration.

REFERENCES

[1] J. I. Trombka, these *Proceedings*, paper (4–3).

[2] D. L. Summers and D. D. Babb, these *Proceedings*, paper (3–5).

[3] cf., N. E. Scofield, these *Proceedings*, paper (3–2).

[4] V. D. Bogert and W. R. Burrus, "The SLOP Code for the Unfolding of Instrument Response," *Neutron Phys. Div. Ann. Progr. Rept. Sept. 1, 1962,* ORNL-3360, pp 22–34.

[5] W. R. Burrus, "Unscrambling of Scintillation Spectra," *Neutron Phys. Div. Ann. Progr. Rept. Sept. 1, 1961,* ORNL-3193, pp 44–52.

(3-4) COMPUTER ANALYSIS OF COINCIDENT GAMMA-RAY SPECTRA

A. H. Wapstra and J. Oberski

Instituut voor Kernphysisch Onderzoek, Amsterdam

INTRODUCTION

Present-day pulse analyzers often contain a provision for counting in four groups of 100 or 128 channels. This makes possible rapid collection of great numbers of coincidence spectra. Working them out by hand is very laborious; use of a computer in analyzing them is of great help.

In our case these coincidence data fall into two groups. With purely conventional apparatus, one can obtain angular correlations by measuring four angles simultaneously (see Fig. 1). A gamma ray is selected by a fifth counter provided with a single-channel

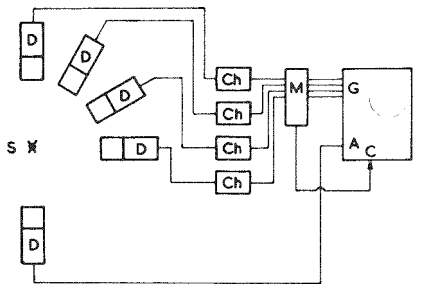

Fig. 1. Simultaneous Measurement at Four Angles of Angular Correlation Between Gamma Rays Selected in a Single-Channel Analyzer and Gamma Spectra Measured in Four Groups of a Multichannel Pulse Analyzer. *S* = source, *D* = detector, *Ch* = single channel, *ACG* = pulse-height analyzer with analysis, coincidence, and grouping pulse inputs.

analyzer, and the four coincidence spectra are recorded in the pulse analyzer. In principle, one could also display the spectrum in the fifth counter in four groups each in coincidence with pulses from single-channel analyzers selecting the same part of the spectrum in the four detectors at the different angles (see Fig. 2). This would have the advantage that the spectra in the four groups would be completely identical except for mostly small differences in the intensities of the components. Thus, in the analysis, only one set of calibration lines would be necessary. But we think that it will be very hard to make corrections for the fact that the regions selected by the four single-channel analyzers always contain slightly different collections of gamma-ray intensities. And anyhow, in order to determine the composition of these collections, we will have to analyze the spectra in each of these four counters.

The second group of coincidence results consists of those that are obtained if the experimental arrangement is provided with four single-channel analyzers as shown in Fig. 3. Thus, the scintillation spectrum in one detector can be displayed in four groups, each in coincidence with another region in the spectrum in a second detector selected by these channels.

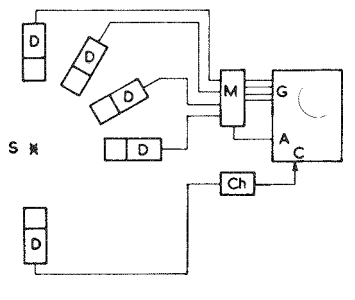

Fig. 2. Simultaneous Measurement of Angular Correlations; Alternative Scheme to That in Fig. 1.

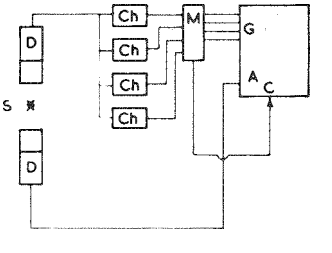

Fig. 3. Simultaneous Measurement of Scintillation Spectra in One Detector in Coincidence with Several Channels in Another One. For explanation of the symbols see Fig. 1.

The first case is, computationally, the most simple. One starts by unscrambling so many spectra (coincidence and single) that one knows with sufficient accuracy the positions of the different components in the four spectra; thereafter, one makes a least-squares analysis in which only the intensities of the lines are variable. It seems rather easy to extend the program in such a way that the computer at once analyzes the angular correlation, thus giving as its output not (only) four intensities (at each angle) for each gamma ray but the angular correlation parameters A_2 and A_4. Of course, the experimental setup should then be calibrated with some standard nuclide like Co^{60}, and the results of this calibration run should belong to the input data of the computer.

The resulting A_2 and A_4 often will not correspond to simple cascade but to mixtures, since the single-channel analyzer may have selected a mixture of gamma rays. Thus, a complete interpretation will require analysis of the spectrum measured in the fifth counter and, quite probably, angular correlations measured at a few channel positions. In making programs for this part of the problem, one encounters the difficulties to be discussed now.

The second problem, coincidence measurements with different channels, offers a few unusual problems. In principle, one wants to determine a matrix of coincidence results $N_{ik} = \mathbf{N}_{ik}/\epsilon_i \epsilon'_k$. Here, $\mathbf{N}_{ik}$ is the number of measured coincidences between two gamma rays γ_i and γ_k and ϵ_i and ϵ'_k are the efficiencies for counting these gamma rays in the two detectors (efficiency per photopeak, or per channel, or any appropriate definition).

If we now assume that the counters are seen at such large solid angles that there is no serious effect from angular correlations, and that the level fed N_i times by γ_i is fed $(n_i - N_i)$ times by other α, β or γ transitions and decays N_b times to the level which emits γ_k with an intensity N_k and emits other radiations with an intensity $(n_k - N_k)$ (see Fig. 4; if the two levels are identical, $n_i = n_b = n_k$), then, $N_{ik} = (N_i/n_i)(N_k/n_k)n_b$.

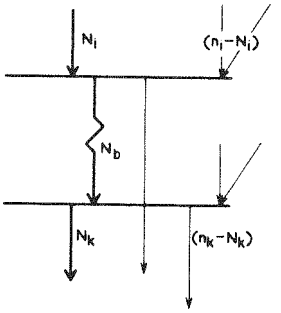

Fig. 4. Relations Between Coincident Gamma Rays; N_b Stands for all Transitions Leading from the Upper Level to the Lower One.

Thus, comparison of the experimental value with that computed from a suggested decay scheme can help in determining its correctness. For instance, N_{ik} can at most be equal to the smallest of N_i and N_k; and $N_{ik} = N_i$ proves that $N_k = n_k$ and $n_b = n_i$.

METHOD OF ANALYSIS

At first sight, one would think that analysis of a coincidence spectrum should be as straightforward as that described above: one could take the gamma line positions from the single spectrum and then make a least-squares evaluation of the intensities in

the coincidence spectrum. Or even better, one could simultaneously analyze a set of at least as many coincidence spectra as there are gamma rays in the spectrum. One could then even imagine a program, probably iterative, that would automatically correct for the occurrence of summing in each of the two detectors, which can be a very serious complication especially in the analysis of coincidence spectra.

A serious handicap in the above analysis is the occurrence of gamma rays not visible in the single spectrum but prominent in coincidence spectra, or of pairs of gamma rays of nearly the same energy. They may cause new peaks in the coincidence spectra, or shifts in the apparent positions of known peaks. The first handicap necessitates single analysis of all coincidence spectra before a final least-squares calculation can be made.

The occurrence of peaks at apparently different positions in different coincidence spectra due to the second effect gave us an idea for what appears to be a novel approach to the problem of unscrambling gamma scintillation spectra which we hope will offer considerable advantages, especially at the often somewhat limited statistics obtained in coincidence spectra. First, the approximate positions P_k of the photolines of clearly present gamma rays are obtained by visual inspection (later, we may try also to automate this part of the procedure). Then, a set of corresponding line shapes $n_i(P_{ko})$ is obtained by an interpolation procedure outlined below. A least-squares adjustment of this set of gamma lines is made in which both their intensities and their positions are variable; for the last purpose, the line shapes are assumed to be of the form

$$N_i(P_k) = n_i(P_{ko}) + \frac{i}{2}(n_{i+1} - n_{i-1})(P_k/P_{ko} - 1) .$$

Of course, this formula is only useful if the relative shift is sufficiently small; if it is larger than a few percent the procedure has to be repeated with improved estimates for P_{ko}.

We have tried this procedure using the X1 computer at the Mathematical Center in Amsterdam, with a program written in Algol 1960. A spectrum containing 11 lines needed 6 min per iteration; only two iterations were necessary. This time could be decreased considerably by using a machine code program; also, faster computers are available.

If positions of important lines have been missed in the first part of the program, no proper result can be obtained. By analysis of the residuals, positions of missing lines can be obtained for further iterations. Presently this part of the program is done by visual inspection; we will try to automate this too.

Our line shapes are also obtained by an apparently somewhat unorthodox approach. A set of standard lines is measured and normalized to the same photopeak height. For each required line shape, standard spectra for the four most nearby gamma energies are stretched in such a way that prominent features fall at approximately the same place as the similar features in the spectrum to be constructed (photopeak, escape peak, Compton edge, pair peaks, and backscattering peak). This is done by shifting channel positions to new positions which then, almost always, do not coincide with the channel positions on the line to be constructed. The corresponding intensities at the lost channel positions are obtained by cubic interpolation. Cubic interpolation of these four intensities (one for each stretched standard line) then gives the required line shape.

The above procedure was again programmed in Algol for use on the X1. On the average, 1 min was necessary for each line shape. To show the performance of this procedure, the procedure was applied to obtain a set of line shapes at various energies, and then the last shapes were used in their turn as standard lines to compute line shapes at the energies of the original standard lines. Fig. 5 compares the final results with the original one for an average case; Fig. 6 shows in the same way the worst possible case where one interpolated line lies completely outside the energy region of the standard lines, so that one should properly speak of a combination of interpolation and extrapolation. Even here, the results will be sufficient for several applications.

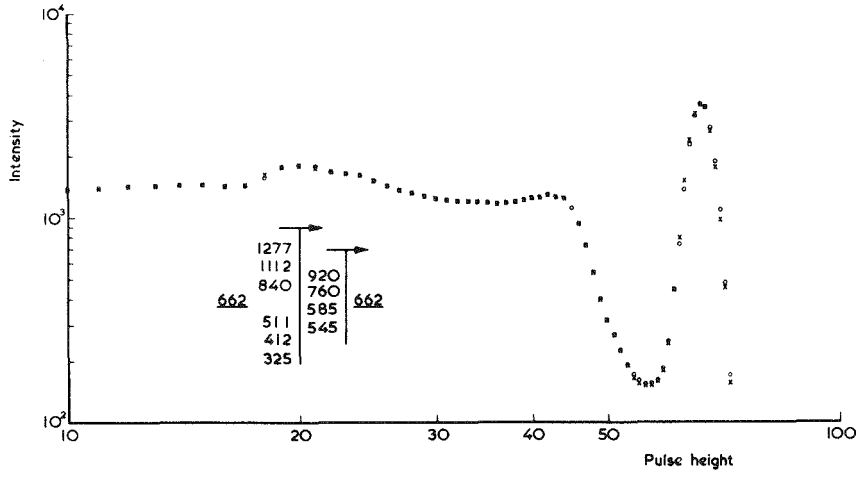

Fig. 5. Comparison of a Standard Line with a Computed Line Shape Obtained by a Double Interpolation Procedure.

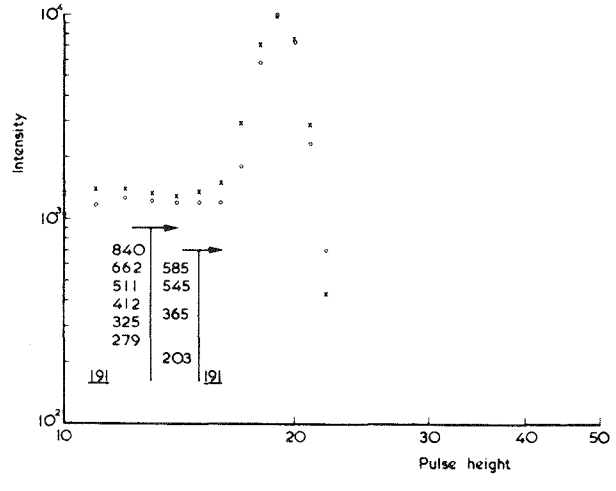

Fig. 6. Same as Fig. 4 for a Case in Which an Intermediate Line Shape Had To Be Obtained by Extrapolation.

ACKNOWLEDGMENT

We thank Prof. Dr. P. C. Gugelot for this interest in this work, and Prof. Dr. H. R. van Wijngaarden for his permission to use the facilities of the Mathematical Centre. Also many thanks are due to Dr. G. J. Nijgh for many useful discussions. This work is part of the research program of the Foundation for Fundamental Research of Matter (FOM) of the Dutch Organization for Pure Scientific Research.

APPENDIX

The Interpolation Procedure

The calibration lines are divided into three energy regions. Each region is stretched linearly in such a way that the energy positions of prominent features in the calibration spectra coincide with those of the same features in the response curve to be constructed, or nearly so. In doing this, we took care of three points:

1. the stretched regions should touch again,
2. the derivatives at the region limits should be continuous (this is done by choosing these limits at places where the spectra are horizontal, or nearly so),
3. the stretching procedure should be continuous as a function of energy, or again nearly so.

For gamma rays in the region above 1600 kev, one limit is chosen slightly below the lower pair peak; the upper part of the spectrum is shifted without stretching so that the pair peak and the photopeak positions coincide (and the Compton shoulder very nearly, too) with those on the line shape to be constructed. For gamma rays between 400 kev and 1600 kev, a limit is chosen slightly below the Compton shoulder, and the stretching procedure adjusted to get photopeak and Compton edge at the correct positions.

For all gamma rays above 400 kev, another limit is chosen just above the escape peak, and the lower part of the spectrum stretched to make the lower edge of the escape peaks coincide. The parts in between the above region, containing the relatively flat part of the Compton continuum, are stretched between the limits mentioned above.

In the region 200–400 kev, one limit is used slightly above the backscattering peak, and the upper region is stretched to get the photoline and the Compton edge at the right place. For energies between 40 kev and 200 kev, a limit is taken slightly below the escape peak, and the photopeak and escape peak are stretched to the right place.

All calibration lines with energy higher than the energy of the line to be constructed are stretched by the procedures of the region in which the line to be constructed is situated. For every calibration line with lower energy the stretching procedures of the region of this line itself are used.

(3-5) UNFOLDING PULSE-HEIGHT DISTRIBUTIONS BY VECTOR ANALYSIS[1]

D. L. Summers
and
D. D. Babb
The Dikewood Corporation
Alburquerque, New Mexico

I. INTRODUCTION

There are several possible approaches to the solution of the problem of unfolding pulse-height distributions. One of these approaches has resulted in the development of a vector-analysis method of solving the problem that is quite satisfactory.

A pulse-height distribution is considered to be an n-dimensional vector where n is the number of channels in the pulse-height analyzer used. The problem is to represent a given pulse-height distribution, referred to as the unknown vector and denoted by $\mathbf{C}$, as a unique sum of fractions, P_i, of other given pulse-height distributions of known significance, referred to as the standard vectors, $\mathbf{S}_i$. The sum of the fractions of the standard vectors is denoted by

$$\mathbf{F} = \sum_{i=1}^{m} P_i \mathbf{S}_i$$

for m standards, and is called the representation vector. The nonrepresentable part of the pulse-height distribution is called the residue vector and is denoted by $\mathbf{R}$. The unknown vector is therefore given by Eq. (1).

$$\mathbf{C} = \sum_{i=1}^{m} P_i \mathbf{S}_i + \mathbf{R} . \tag{1}$$

The main objectives are to find the proper P_i's in Eq. (1) and to keep $|\mathbf{R}|$ as small as possible. To accomplish this, the standard vectors must be linearly independent so that the solution is determinate.

The P_i's are determined by projecting the unknown vector onto a set of basis vectors constructed from the set of standard vectors. Then these components are projected back onto the set of standard vectors. This second process is defined as reprojection.

II. EXPLANATION OF THE VECTOR-ANALYSIS MODEL

For simplicity, consider the hypothetical case of a two-channel analyzer. Assume that the observed gamma radiation is composed of two components having energies E_1 and E_2, and that there are also available monoenergetic sources (standards) having each of these energies. It is desired to determine the number of counts, x_1 and x_2, that are due to each of the energies from a knowledge of the number of counts, C_1 and

[1]This work was sponsored in part by the Advanced Research Projects Agency and Air Force Special Weapons Center, Kirtland AFB, N.M., under Contract AF 29(601)-4569.

C_2, that occur in each of the two channels of a pulse-height analyzer. A count of the first standard at energy E_1 yields S_{11} and S_{12} counts in channels one and two, respectively; the second standard at E_2 gives counts of S_{21} and S_{22}. The following equations relate the quantities.

$$\frac{S_{11}x_1}{S_{11}+S_{12}} + \frac{S_{21}x_2}{S_{21}+S_{22}} = C_1 , \tag{2a}$$

and

$$\frac{S_{12}x_1}{S_{11}+S_{12}} + \frac{S_{22}x_2}{S_{21}+S_{22}} = C_2 . \tag{2b}$$

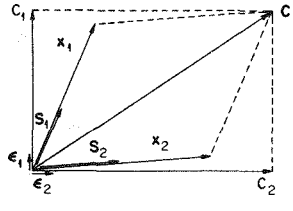

Fig. 1. Vector Diagram for Two-Channel Case.

A nonconventional approach to the solution of these equations arises when it is recognized that this problem is mathematically identical to a simple problem in vector analysis. Consider the problem of resolving a vector **C** into its components along two other vectors $\mathbf{S}_1$ and $\mathbf{S}_2$ when the three vectors all lie in a single plane described by the orthogonal unit basis vectors, $\boldsymbol{\epsilon}_1$ and $\boldsymbol{\epsilon}_2$, as shown in Fig. 1. The vectors are defined by the following relations.

$$\mathbf{C} = C_1\boldsymbol{\epsilon}_1 + C_2\boldsymbol{\epsilon}_2 , \qquad \mathbf{x}_1 = x_{11}\boldsymbol{\epsilon}_1 + x_{12}\boldsymbol{\epsilon}_2 ,$$

$$\mathbf{S}_1 = S_{11}\boldsymbol{\epsilon}_1 + S_{12}\boldsymbol{\epsilon}_2 , \qquad \mathbf{x}_2 = x_{21}\boldsymbol{\epsilon}_1 + x_{22}\boldsymbol{\epsilon}_2 ,$$

$$\mathbf{S}_2 = S_{21}\boldsymbol{\epsilon}_1 + S_{22}\boldsymbol{\epsilon}_2 .$$

More precisely, it is desired to determine the scalar sum of the components, x_1 and x_2, of the vectors $\mathbf{x}_1$ and $\mathbf{x}_2$.

Let $\qquad x_1 = x_{11} + x_{12} , \qquad x_2 = x_{21} + x_{22} .$

Note that $\qquad x_{11} + x_{21} = C_1 , \qquad x_{12} + x_{22} = C_2 ,$

where $\qquad x_{11} = \dfrac{S_{11}x_1}{S_{11}+S_{12}} , \qquad x_{12} = \dfrac{S_{12}x_1}{S_{11}+S_{12}} ,$

$$x_{21} = \frac{S_{21}x_2}{S_{21}+S_{22}} , \qquad x_{22} = \frac{S_{22}x_2}{S_{21}+S_{22}} .$$

This set of equations is the same as the set previously arrived at for the physical problem when the x_{ij} are replaced by their formulas in terms of S_{ij} and x_i.

The usual way to resolve a vector $\mathbf{C}$ into a set of nonorthogonal vectors, $\mathbf{S}_1$ and $\mathbf{S}_2$, is to first form an orthogonal set that spans the same space as the set of vectors. In the hypothetical case considered, the set of ϵ vectors, corresponding to a single count in a single channel with no counts in any other channel, was such a set. However, if there are fewer standard vectors than there are channels, the space spanned by the standard vectors will be a unique vector subspace of the vector space spanned by the channels. In the vector-analysis approach to the general unfolding problem, it is first necessary to obtain a set of orthogonal vectors that just span the subspace of the standard vectors. Consider the case of m standards and n channels where $n > m$. The required orthogonal basis can be obtained by the so-called Gram-Schmidt orthogonalization process, which consists of accepting the first standard vector as the first basis vector, subtracting the component of the second standard vector along the first standard vector from the second standard vector to obtain the second basis vector, and continuing to subtract the components of the following standard vectors along all previous basis vectors from the standard vector to obtain the next basis vector. Thus, the standard vectors must be linearly independent for such a process to yield a set of useful basis vectors. The previously described process can be expressed mathematically as follows, where $\mathbf{B}_k$ is the kth basis vector:

$$\mathbf{B}_1 = \mathbf{S}_1 ; \qquad \mathbf{B}_k = \mathbf{S}_k - \sum_{j=1}^{k-1} \frac{B_j \cdot S_k}{B_j \cdot B_j} \mathbf{B}_j . \tag{3}$$

This process is illustrated for two standard vectors, regardless of the number of channels, by using the vector diagram of Fig. 2.

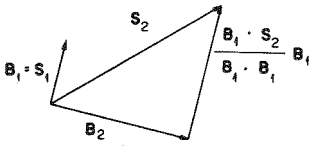

Fig. 2. Construction of the Orthogonal Basis Vector.

The indicated dot products are evaluated in terms of the channel basis; that is, if

$$\mathbf{S}_k = \sum_{i=1}^{n} S_{ki} \epsilon_i \text{ and } \mathbf{B}_j = \sum_{i=1}^{n} B_{ji} \epsilon_i ,$$

then

$$\mathbf{S}_k \cdot \mathbf{B}_j = \sum_{i=1}^{n} S_{ki} B_{ji} .$$

Having obtained an m-dimensional (m standard vectors) orthogonal basis, the vector component of the unknown, $\mathbf{C}$, projected along the basis vector, $\mathbf{B}_j$, is

$$\mathbf{V}_j = \frac{\mathbf{B}_j \cdot \mathbf{C}}{\mathbf{B}_j \cdot \mathbf{B}_j} \mathbf{B}_j .$$

It is then necessary to reproject the vector $\mathbf{V}_j$ onto the original set of standard vectors. This is done by computing the components of a basis vector along all standard vectors of higher indices, since, by construction, $\mathbf{B}_j$ is orthogonal to all $\mathbf{S}_k$ vectors with $j > k$. Actually, it is more direct to solve now for the ratio of the length of the component of $\mathbf{C}$ along $\mathbf{S}_k$ to the length of $\mathbf{S}_k$, rather than for the component itself. Some vector algebra produces the result that

$$P_m = \frac{x_m}{S_m} = \frac{\mathbf{B}_m \cdot \mathbf{C}}{\mathbf{B}_m \cdot \mathbf{B}_m} \tag{4}$$

for the fraction of the last standard vector. For the jth standard vector $j < m$ one obtains

$$P_j = \frac{\mathbf{B}_j \cdot \mathbf{C} - \sum_{k=j+1}^{m} (\mathbf{B}_j \cdot \mathbf{S}_j) P_k}{\mathbf{B}_j \cdot \mathbf{B}_j}.$$

Note that the intermediate projection vector $\mathbf{V}_k$ was eliminated so that the evaluation of the P_j's can immediately follow the determination of the orthogonal basis.

The relationships of Eq. (4) are not easy to derive directly for the general n-dimensional case, but can readily be verified for the two-dimensional case shown in the vector diagram of Fig. 3. The ratio of the length of $\mathbf{x}_2$ to the length of $\mathbf{S}_2$ is equal to the ratio of the length of $\mathbf{B}_2$ to the length of $\mathbf{V}_2$; thus

$$P_2 = \frac{|\mathbf{x}_2|}{|\mathbf{S}_2|} = \frac{\mathbf{B}_2 \cdot \mathbf{C}}{\mathbf{B}_2 \cdot \mathbf{B}_2}.$$

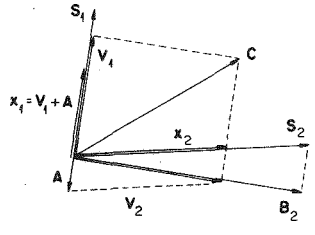

Fig. 3. Projection and Reprojection of the Unknown.

The vector $\mathbf{x}_1$ is the vector sum of $\mathbf{V}_1$ and $\mathbf{A}$. The ratio of the lengths of $\mathbf{A}$ to $\mathbf{S}_1$ is equal to the ratio of the projection of $\mathbf{S}_2$ onto $\mathbf{S}_1$ times the ratio of $\mathbf{x}_2$ to $\mathbf{S}_2$. Therefore,

$$P_1 = \frac{|\mathbf{V}_1|}{|\mathbf{S}_1|} - \frac{|\mathbf{A}|}{|\mathbf{S}_1|} = \frac{\mathbf{B}_1 \cdot \mathbf{C}}{\mathbf{B}_1 \cdot \mathbf{B}_1} - \left[\frac{\mathbf{S}_1 \cdot \mathbf{S}_2}{\mathbf{S}_1 \cdot \mathbf{S}_1} \frac{|\mathbf{x}_2|}{|\mathbf{S}_2|}\right].$$

But

$$\mathbf{S}_1 = \mathbf{B}_1$$

and

$$\frac{|\mathbf{x}_2|}{|\mathbf{S}_2|} = P_2.$$

Therefore

$$P_1 = \frac{\mathbf{B}_1 \cdot \mathbf{C} - (\mathbf{B}_1 \cdot \mathbf{S}_2) P_2}{\mathbf{B}_1 \cdot \mathbf{B}_1} .$$

The difficulty in proving the general case is that a series of vector identities must be used to convert the dot products of the standard vectors which appear in the denominator of the correction terms to the dot products of basis vectors.

In general, the unknown vector will have a component orthogonal to the subspace spanned by the standard vectors. This will be the residue vector, **R**, evaluated from Eq. (1). Since the representation, **F**, is in the subspace spanned by the standard vectors, it is also orthogonal to the residue. Thus, **R**, **C**, and **F** form a right triangle. Now if $|R| \ll |C|$, as it must be for the representation to be valid, a measure of the error due to representing **C** by **F** is

$$1 - \frac{|\mathbf{F}|}{|\mathbf{C}|} = 1 - \left[1 - \frac{|R|^2}{|C|^2}\right]^{1/2} \cong \frac{|R|^2}{2|C|^2} .$$

Such a measure has been employed in a large number of runs, and it appears to be a fairly reasonable estimate of the overall accuracy of the analysis.

Another problem is that in real physical measurements one does not have negative quantities of radioactive material. It is therefore often desirable to attempt to remove any negative coefficients, P_i. To date two reasonable methods have been employed that are compatible with the vector-analysis approach and give acceptable results. The first method is approximate. Those subspace basis vectors which were derived from standard vectors that resulted in negative coefficients, P_i, are omitted in the process of projection and reprojection. This procedure is continued until all standard vectors associated with negative coefficients are eliminated from the answers. Mathematically this method is not as satisfactory as the reconstruction of a new set of basis vectors excluding those standard vectors whose associated coefficients were negative. This is because, among other reasons, it destroys the orthogonality of the residue vector, **R**, to the representation vector, **F**. However, the first method has the advantage of computing speed since the subspace basis vectors are not recalculated each time a standard vector or series of standard vectors associated with negative coefficients is deleted. Normally, in experience so far, it has been rarely necessary to resort to the more rigorous method of eliminating negative answers to obtain satisfactory results.

Another difficulty that frequently presents itself is a gain shift between the unknown vector and standard vectors or perhaps among the standard vectors themselves. This problem is dealt with in a straightforward manner by shifting the standard vector photopeak into the channel demanded by the relative gain employed for the unknown vector. The basic equations involved in this process are

$$N' = \frac{g_o'}{g_o} N ; \qquad C_{N'} = C_N \frac{g_o}{g_o'} ,$$

where

g_o is the relative gain used for the original photopeak line shape ,

g_o' is the relative gain desired for the new photopeak line shape ,

N' is the channel number of the channel in which the number of counts is computed ,

N is the number of the channel that corresponds to N' in the original spectrum ,

C_N is the number of the counts in channel N, and

$C_{N'}$ is the number of counts in channel N'.

Linear interpolation is used to arrive at the number of counts in each channel for the new line shape.

III. EQUIVALENCE TO THE LEAST-SQUARES ANALYSIS APPROACH

The vector-analysis solution of the gamma spectrum unfolding problem mathematically yields the same numerical quantities (answers) as the least-squares analysis approach. To verify this, recall that the residue vector, $\mathbf{R}$, is orthogonal to each standard vector, $\mathbf{S}_i$, individually. Now if the least-squares analysis yields the same result for the residue then the identity of the results of the two methods will be established since from the equation $\mathbf{F} = \mathbf{C} - \mathbf{R}$, the representation must also be identical for the two methods.

One obtains as the minimal condition for the least-squares method using Eq. (1),

$$\frac{\partial}{\partial P_j}\left[\sum_{k=1}^{n}\left(C_k - \sum_{i=1}^{m} P_i S_{ik}\right)^2\right] = 0 \text{ for } j = 1, 2, \ldots, m .$$

The result of the differentiation is

$$\sum_{k=1}^{n}\left(C_k - \sum_{i=1}^{m} P_i S_{ik}\right) S_{jk} = 0 \text{ for all } j .$$

Applying Eq. (1) again,

$$\sum_{k=1}^{n} R_k S_{jk} = 0 \text{ for all } j .$$

Or, in vector language, $\mathbf{R} \cdot \mathbf{S}_j = 0$ for all j. This is the vector analysis condition on the residue.

Hence, the mathematical equivalence of the answers for the least-squares analysis and the vector-analysis methods is established. Consequently, all statements regarding errors or other facts of interest concerning the results of the vector-analysis method are equally valid for the results obtained by a least-squares analysis and vice versa. The mathematical equivalence of the results has been demonstrated on several computer runs with the same inputs to the two different methods of analysis. The results agree to within the computer roundoff error.

Comparison with Other Methods

Equations (2*a*) and (2*b*), which define the problem for the two-dimensional case, become for the general case:

$$\sum_{i=1}^{m} \frac{S_{ij}}{\sum_{j=1}^{n} S_{ij}} X_i = C_j \text{ for all } j = 1, 2, \ldots n .$$

This may be written in vector-matrix form as $\mathbf{X}\, M = \mathbf{C}$, where

$$M_{ij} = \frac{S_{ij}}{\sum_{j=1}^{n} S_{ij}},$$

and M is an $(m \times n)$ matrix. Usually $n > m$ and the solution is overdetermined. Methods differ principally in the way in which this overdetermination is eliminated. In both the vector-analysis and least-squares methods, this is done by concerning oneself only with the components of the unknown along the standards. Mathematically, this is done by multiplying each side of the equation by an $(n \times m)$ matrix, S, with elements S_{ji}, yielding $\mathbf{X}M' = \mathbf{C}'$, where $M' = MS$ and $\mathbf{C}' = \mathbf{C}S$. M' is an $(m \times m)$ matrix and $\mathbf{X}$ and $\mathbf{C}'$ are both m-dimensional vectors. The fact that the vector-analysis method corresponds to this set of equations is one of the consequences of the fact that it yields the same answer as the least-squares method. Other matrix methods combine the n equations into m equations by other arbitrary prodecures suited to the nature of the problem being solved, such as adding several equations with adjacent values of the index j. In any case the resulting set has the form $\mathbf{X} = \mathbf{C}'M'^{-1}$, and the problem is reduced to the problem of finding the inverse of a matrix, M'. Actually, for the least-squares and vector methods, it is more convenient to consider the

$$P_i = \frac{X_i}{\sum_{j=1}^{n} S_{ij}}$$

as the variables; the matrix elements are then

$$M^*_{ij} = \sum_{k=1}^{n} S_{ik} S_{jk} = \mathbf{S}_i \cdot \mathbf{S}_j$$

in the equation $\mathbf{P} = \mathbf{C}'M^{*-1}$. Once the inverse of the matrix or its equivalent is determined, the problem is essentially solved, for then only one matrix multiplication remains to arrive at the desired coefficients, P_i.

The matrix formed by the least-squares analysis consists of elements that are referred to from the vector-analysis viewpoint as dot (scalar) products. Because of the symmetry in the least-squares matrix, only $m(m + 1)/2$ dot products must be evaluated to obtain the entries in the matrix.

At this point, one is in position to examine the relative merits of the vector-analysis and the matrix-inversion methods. Each is a solution of approximately the same set of equations, as explained previously. Although the solution is arrived at by different mathematical steps, the results, especially of the least-squares analysis and the vector analysis, are essentially the same. For the purposes of the following discussion, m is still the number of standards and n the number of channels in the analyzer, and also $n > m$.

The process of finding the inverse of a matrix, M, consists of setting up the equation $MI = M$ where I is the identity matrix, and then operating on the right side of the equation from the right in such a manner as to reduce it to the identity matrix. The same operations are applied to modify the identity matrix, thus producing an equation of the form $MM^{-1} = I$. This system then requires $2m^2$ storage locations where m is the order of the matrix. In the vector-analysis method it is usually required to store both the standards and the basis vectors, requiring $2mn$ storage locations. Depending on the order in which the calculations are executed and whether negatives are eliminated rigorously, the amount of storage used for either method varies considerably. But, generally, it is easier to conserve memory capacity using the matrix method than it is using the vector-analysis method.

The bulk of the elementary operations in the inversion process consists of dividing a row of the matrix by a number, multiplying by another number, and subtracting another row to produce a zero in one of the off-diagonal elements on the right side of the equation. This must be done $m(m - 1)$ times so that there are $m^2(m - 1)$ divisions and a like number of subtractions and multiplications. In the vector-analysis method the part of the calculation analogous to the determination of the inverse matrix is the determination of the basis vectors. This requires the calculation of $m(m - 1)/2$ dot products necessary for Eq. (3), and involves $nm(m - 1)/2$ multiplications and additions. The actual evaluation of Eq. (3) requires $m(m - 1)/2$ divisions and $nm(m - 1)/2$ multiplications and subtractions. Thus, the number of divisions is less than that required for matrix inversion by a factor of $2m$, but the ratio of the number of multiplications and subtractions or additions is $2(m/n)$. If a least-squares analysis is to obtain the matrix M, then an additional $m(m + 1)$ dot products must be evaluated. This means $nm(m + 1)/2$ additional multiplications and additions are performed. Hence, in this case, the total number of multiplications and subtractions or additions is $m/2\ (2m^2 - 2m + nm + n)$. Thus, if $m \gg 1$, this implies that the ratio of the total number of multiplications and subtractions or additions for the vector analysis is approximately equal to $n/2m + n$ at this stage in the discussion. Since usually $n > 2m$, this implies that the two approaches have about the same number of multiplications and subtractions or additions in their respective compilations, but that the vector-analysis method requires a factor of $2m$ fewer divisions. The exact comparison with other matrix-inversion approaches is more difficult to specify since the exact formulation of the elements in the matrix can be arrived at in a large variety of ways.

The evaluation of the desired coefficients, P_i, in the matrix method possessing the inverse matrix, is simply a multiplication of a vector by the inverse matrix involving m^2 multiplications and additions. For both the vector-analysis and least-squares approach there are m additional dot products to be executed before the evaluation of the desired coefficients, P_i, can commence. The evaluation of m dot products requires nm multiplications and additions indicating that the matrix-inversion methods and the vector-analysis method require about the same number of operations to accomplish

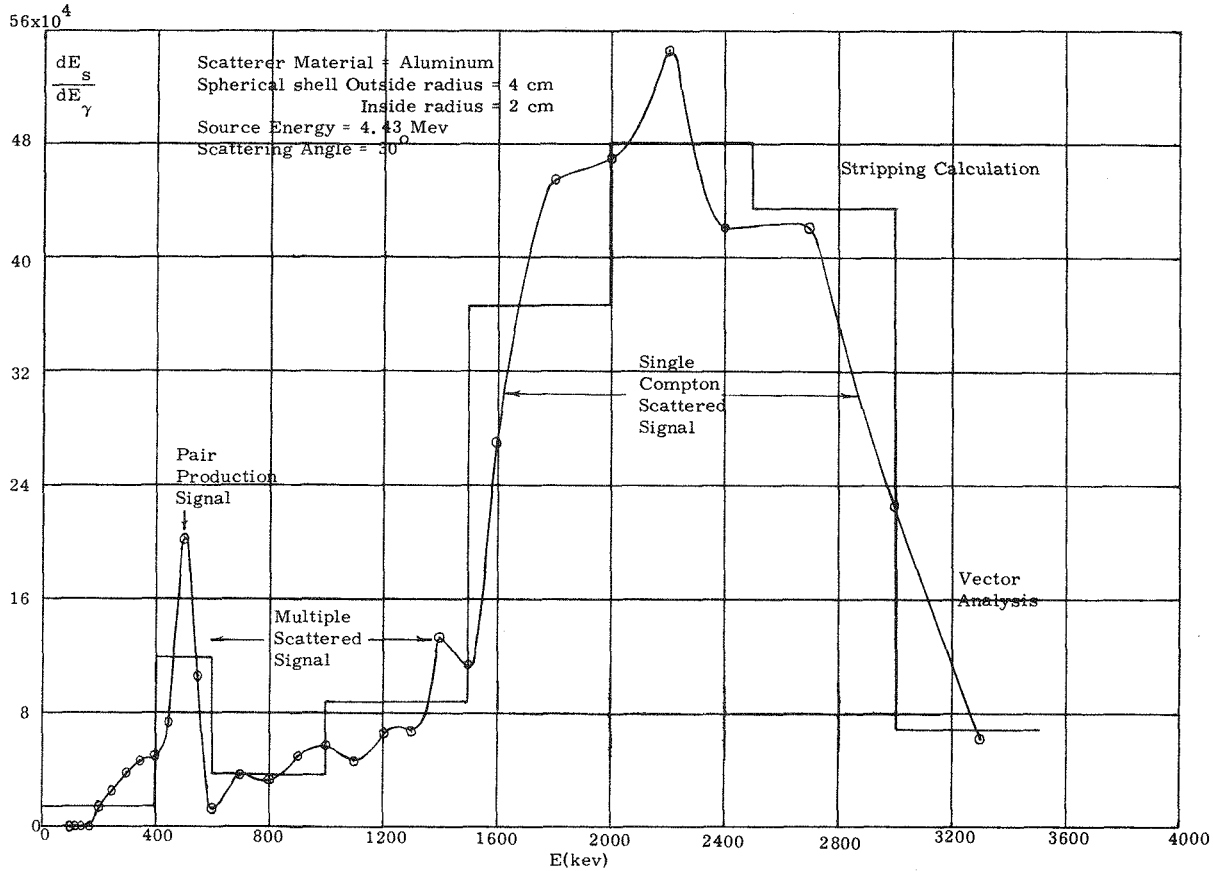

Fig. 4. Comparison of Hand Stripping and Vector Analysis of a Pulse-Height Spectrum.

this step in the solution. The vector-analysis method requires $m(m-1)/2$ multiplications and subtractions as is seen by Eq. (4). Thus, once again assuming $m \gg 1$, one arrives at the conclusion that the vector-analysis method is about twice as fast in this portion of the solution. However, since the evaluation of the required m dot products generally takes much longer (usually $n \gg m$), the overall computational times of the matrix-inversion methods and vector-analysis method are almost the same.

Another popular method for unfolding a pulse-height distribution is generally referred to as a stripping method. Because of the variety of the so-called stripping codes in use today and because of their inherent differences from the vector-analysis method, a computational time analysis as is given above for the matrix-inversion methods will not be given here. However, a crude comparison between the results of the vector-analysis method and a simple hand-stripping procedure is given in Fig. 4. Note that the hand-stripping process employed only eight different standards and the vector-analysis method employed 30 different standards over the same region. Thus, the results are not strictly comparable in fineness of detail, but are of interest in the light of the general overall comparison of fit. The spectrum shown is the scattered signal from 4.43-Mev gamma rays incident on a 4-cm radius, 2-cm wall aluminum shell observed at a scattering angle of 30°.

IV. EXPERIMENTAL RESULTS

Results of several runs employing 30 monoenergetic sources covering the entire energy range of the analyzer set up for particular continuous spectra scattering experiments yielded the energy-vs-energy curves given by Figs. 5–7. These curves are in good agreement with the expected results of the physical experiments which were performed. Furthermore, these curves appear to be as good as or better than the results obtainable by other methods. These represent the results of the same experimental arrangement as the previous figure except that the scattering angle is varied.

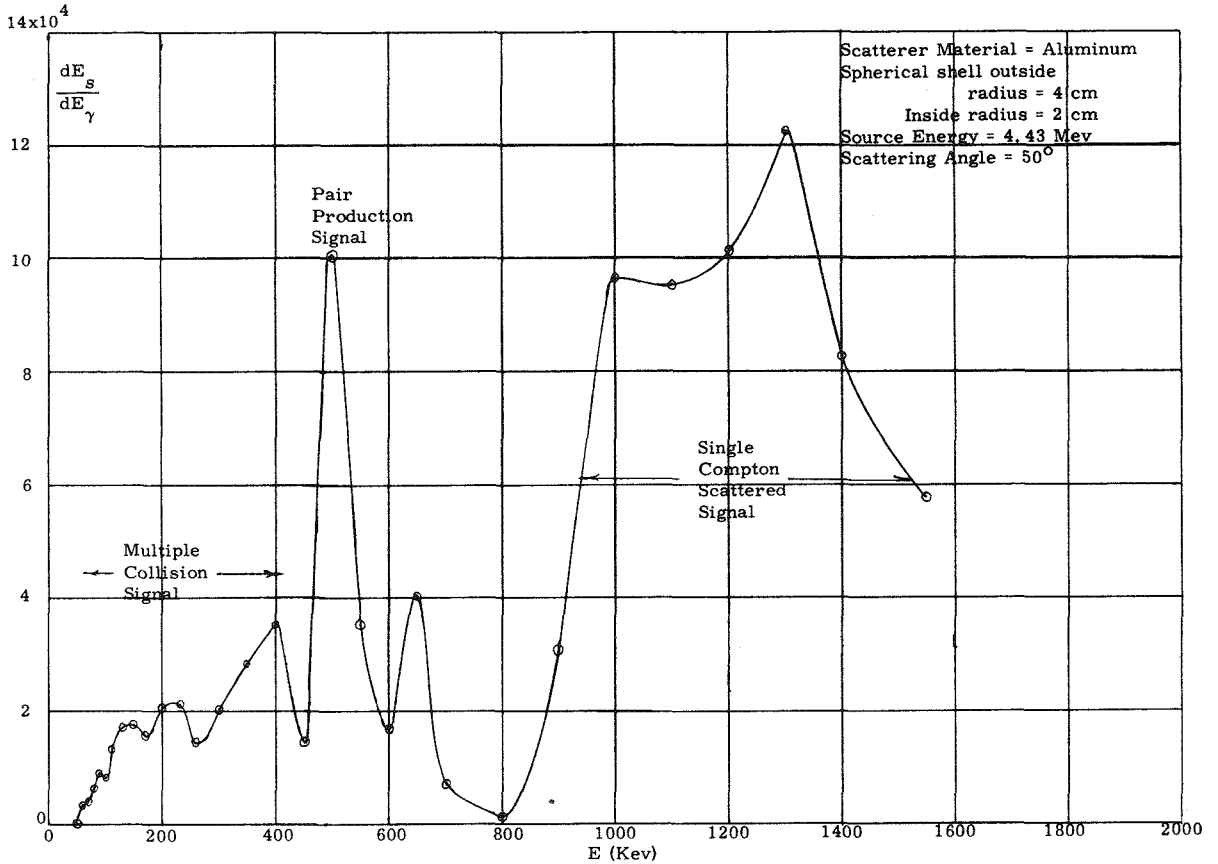

Fig. 5. Aluminum-Scattered Signal at 50° Scattering Angle.

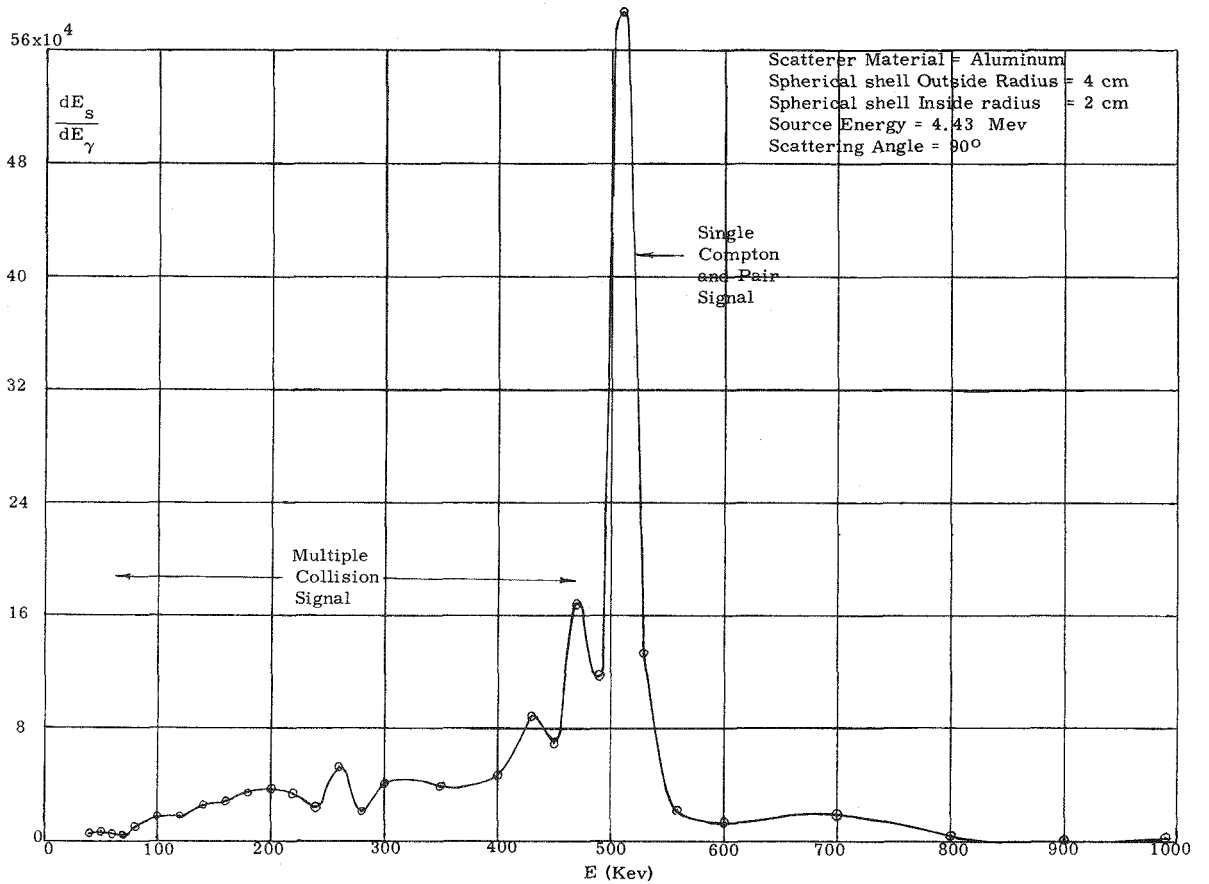

Fig. 6. Aluminum-Scattered Signal at 90° Scattering Angle.

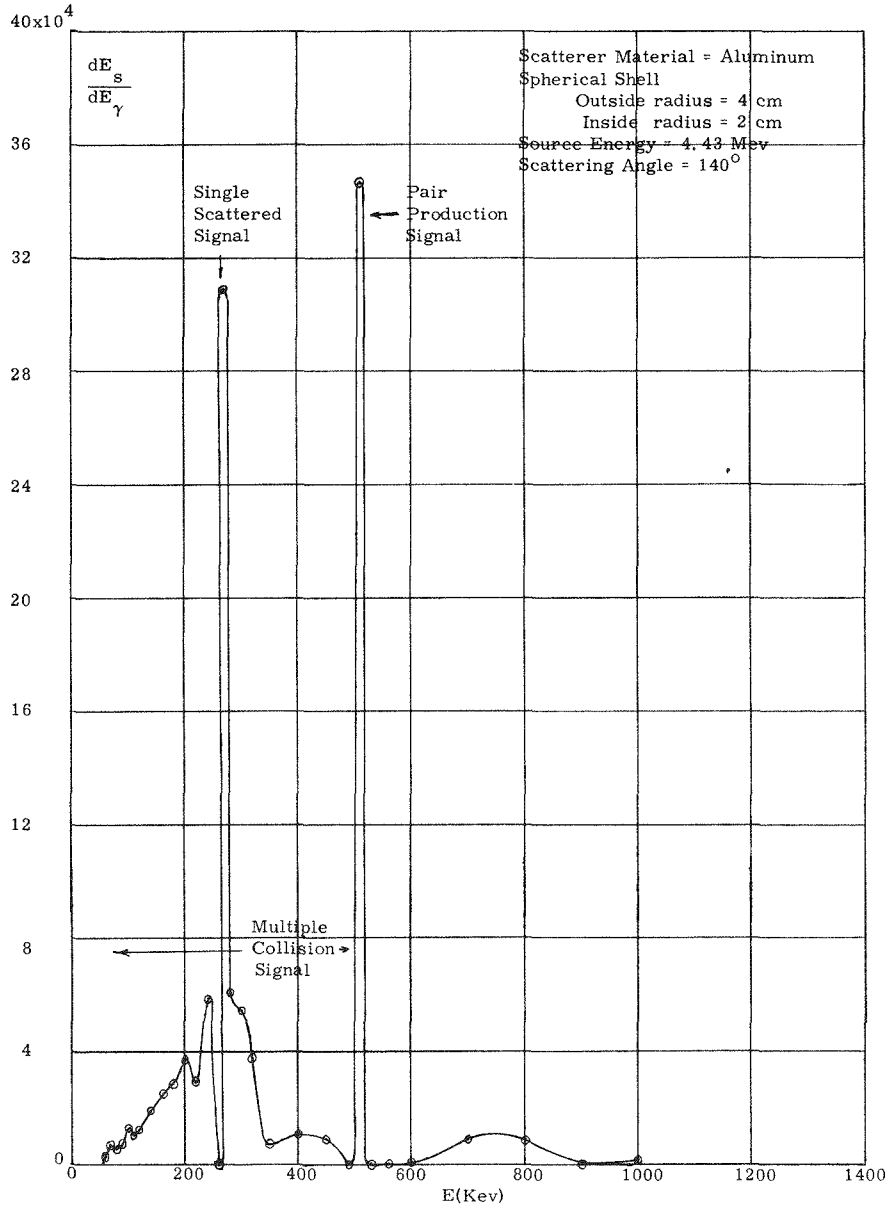

Fig. 7. Aluminum-Scattered Signal at 140° Scattering Angle.

Session 4

Chairman: R. L. Heath

Phillips Petroleum Company,
Atomic Energy Division,
Idaho Falls, Idaho

(4-1) A LEAST-SQUARES COMPUTER PROGRAM FOR THE ANALYSIS OF GAMMA-RAY SCINTILLATION SPECTRA

A. J. Ferguson
Atomic Energy of Canada, Ltd.,
Chalk River, Canada

The computer program for unfolding gamma-ray scintillation spectra which will be described has been in use at Chalk River for several years. It uses the method of least squares and is designed to handle numbers of components up to 15 and numbers of channels up to 100. Similar programs have been written by Heath, Salmon, Trombka, and others. The present program is described briefly in Chalk River report CRP-1055. It is able to find the intensities of components of specified energy, or both the energy and intensity using the specified energy as a first approximation. A novel feature is that the weights used in the fitting, instead of being the reciprocals of the recorded counts in the channels, as is conventional, are instead the reciprocals of the computed contributions in the channels. This was adopted when it was found that the conventional weighting produced a low bias to the fits, especially when the spectra contained small numbers of counts. It is compatible with the Poisson distribution if the computed count can be identified with the mean count in a channel. The line shapes of the component gamma rays are computed by polynomial approximations derived from sources of pure lines which are assumed to be available.

The program consists of two parts. The first is a preliminary one which computes the polynomial constants required to represent the spectra. A number, not exceeding six, of spectra of pure gamma rays must be available, which have been measured in the same experimental setup and whose energies cover the region of interest. These spectra are smoothed, integrated from the top down, normalized, and then transformed to the polynomial representation. The smoothing is necessary to obtain good approximations from the statistically fluctuating measured spectra. A method described by Whittaker and Robinson [*1*] is used here which essentially replaces each channel count by a special average of the seven channels which extend three channels to either side. The integration takes care of the analyzer resolution. The contribution in any channel is found by subtracting the value of the integral at the bottom of the channel from the value of the top, and it is readily seen that this accounts correctly for the finite channel widths. The normalization is necessary because we are going to represent the variation with gamma ray energy by a polynomial, so

that the spectra must vary smoothly from energy to energy. Smoothness is the essential requirement here, and can be achieved in a number of ways, for example, by making the integrals at the position of the second escape peak uniform, or by making all photopeak heights equal, etc.

The spectra are then subdivided into four portions, each of which is represented by a 9th degree polynomial. The technique of getting polynomial representations is described by Lanczos [2]. The spectral intensity, $S(x)$, is assumed represented by a Chebychev polynomial series

$$S(x) = 1/2\ a_0 + a_1\ T_1\ (x) + \ldots + 1/2\ a_n\ T_n\ (x)\ , \tag{1}$$

where $T_k(x)$ is a Chebychev polynomial.

The coefficients a_k are given by

$$a_k = \frac{2}{n} \sum_{0}^{n} S(x_r) \cos\ (rk\pi/n)\ , \tag{2}$$

where $x_r = \cos\,(r\pi/n)$, and x is a linear function of the channel energy which ranges between -1 and $+1$ in each portion. It is convenient and practical to determine the a_k by matrix methods. Thus after the integrating, a 10×4 matrix consisting of the $S(x_r)$ for the 4 regions is found using an interpolation subroutine. The $2/n$ cos $(rk\pi/n)$ terms are stored as a permanent matrix and the 10×4 matrix of an a_k is obtained by a matrix multiplication. To ensure continuity between regions, each one terminates at the points where the fit is exact, that is, $x = \pm 1$. A further matrix transformation converts the Chebychev series into one in powers of x.

This leads to 40 constants to represent each spectrum. Each such constant is next represented by a polynomial approximation in the gamma-ray energy. Actually not the gamma-ray energy, E_γ, but a derived quantity, ξ, is used which varies between -1 and $+1$ as E_γ ranges from 0 to ∞; ξ is defined by

$$\xi = 1 - 2[(E_\gamma/E_0) + 1]^{-1}\ . \tag{3}$$

E_0 is a somewhat arbitrary energy chosen near the center of the range of interest. Introduction of ξ avoids the rapid fluctuations characteristic of polynomial approximation near the ends of the range. Capacity for 5th degree polynomials in ξ have been allowed for, although a lower degree will be used if fewer than 6 standard lines are available.

Figure 1 shows a computed line shape for a 4.24-Mev gamma ray in which the divisions of the spectrum are illustrated. The gamma ray is identified by E_γ which we always assume to correspond to the top of the photopeak. A linear relation between channel energy and channel number is also assumed. The four divisions are defined by E_{max}, E_1, E_2, E_3, and E_{min} which is below the bottom of the graph here.

Although primarily intended to cover the regions of the photopeak, 1st and 2nd escape peaks, and Compton tail as shown, the boundary regions are somewhat arbitrary and can be altered to deal with spectra with lower energies.

A flow chart showing the overall operation of the program for generating polynomial constants is shown in Fig. 2. After the start, a pilot card is read which specifies the number, N, of standard spectra to be used, E_0 and other parameters. Then a spectrum together with constants which define its energy scale is read. The spectrum is smoothed, integrated, normalized, and its polynomial representation found as described before. After N spectra have been treated in this way, the ξ representation is found for the constants and also for E_{max} and E_{min}. This gives 252

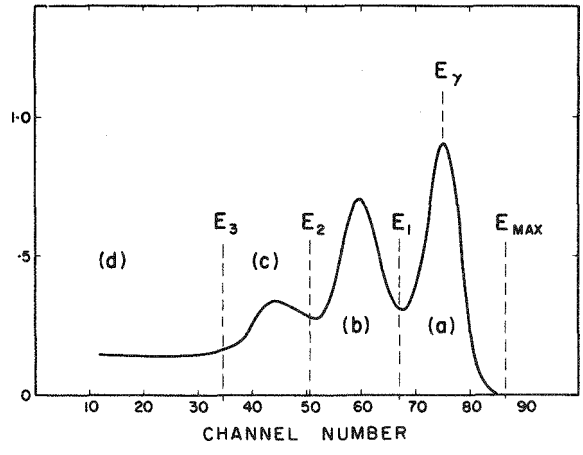

Fig. 1. Computed Line Shape for a 4.24-Mev Gamma Ray on a 5- by 4-in. NaI(Tl) Crystal Without Collimation. The energy of the gamma ray E_γ is assumed to be defined by the position of the top of the photopeak. The spectrum is divided into regions (*a*), (*b*), (*c*), and (*d*) for the purpose of a polynomial approximation whose boundaries are indicated by the dashed lines marked E_{max}, E_1, E_2, and E_3. The lower boundary of region (*d*) is off scale below channel zero.

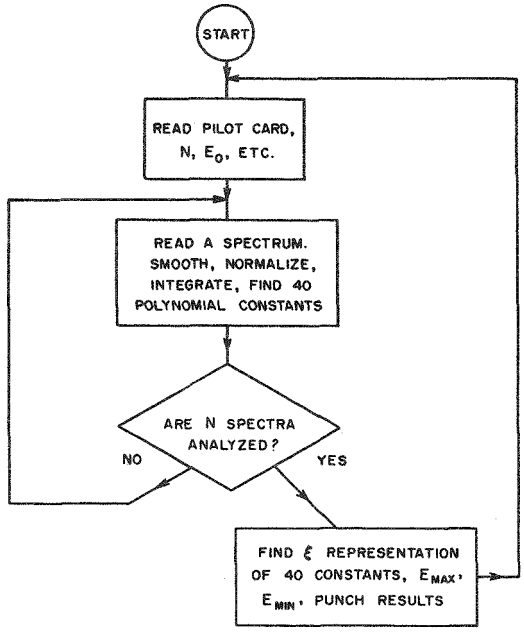

Fig. 2. Flow Diagram for the Polynomial Constant Program.

parameters which are punched out in a form suitable for the main fitting program. This phase of the calculation is quite rapid, typically about 15 min on our Burroughs 205 computer. We have found it a good policy to check new polynomial constants by calculating a number of line shapes with a small program written for this purpose.

Figure 3 shows again the 4.24-Mev spectrum as a solid line and its derivative, which is necessary to adjust the energy of the component, as a dashed line. Some irregularities can be seen in the dotted line which are due to imperfections in the polynomial representation that are accentuated in the derivative.

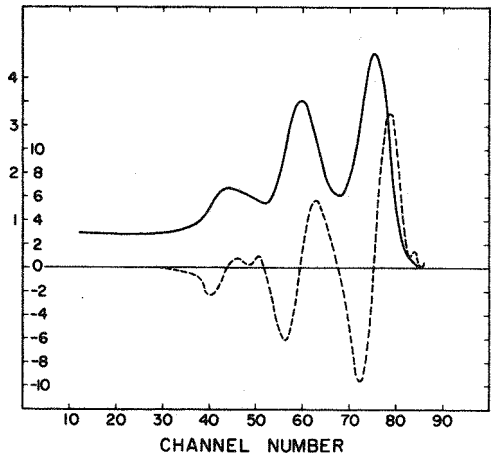

Fig. 3. The Spectrum of a 4.24-Mev Gamma Ray (Solid Line) Compared with Its Derivative (Dashed Line).

An unacceptable computed line shape for a 2.30-Mev gamma ray is illustrated in Fig. 4. The "wiggles" which appear here are due to lack of smoothness of the measured line shape and to an E_{max} which is much too high. It is always important to assign E_{max} to a point not far above the steep front of the curve. A flat section cannot be well represented by a polynomial.

Gamma rays which have been used as standard line shapes are: 2.31 Mev coincident with the first excited state proton group from $C^{12}(He^3,p,\gamma)N^{14}$; 4.43 Mev coincident with 12.14 Mev from $B^{11}(p,\gamma)C^{12}$; 12.14 Mev with a small admixture of 4.43 Mev from $B^{11}(p,\gamma)C^{12}$ in coincidence with 4.43 Mev; 6.14 Mev from $F^{19}(p,\alpha,\gamma)O^{16}$ at the 0.34-Mev resonance. A catalog of suitable lines has been given by Nordhagen [3].

Figure 5 is a general flow diagram for the main least-squares fitting program. The fact that energies can be adjusted and also the method of weighting described earlier require an iterative procedure. A pilot card is first read which instructs the program how to proceed. A code number zero or a blank card indicates the end of the problem, and the computer stops. Code number 1 indicates that the polynomial constants together with the spectrum must be read. Code number 2 indicates that the spectrum and its parameters only are to be read, the polynomial constants needed being left from the previous case. A preliminary fit using unit weight is first made and then the iterative program is entered. Iterations continue until the sum of the squares of the fractional corrections is less than some initially specified number, generally 10^{-6}. Convergence

is always very rapid if intensities only are being adjusted. When the energies are also being fitted more iterations are required, and some cases have not converged at all. These were ones in which an attempt was made to find several gamma energies from a single unresolved peak. The results are then punched out and a new case is read in.

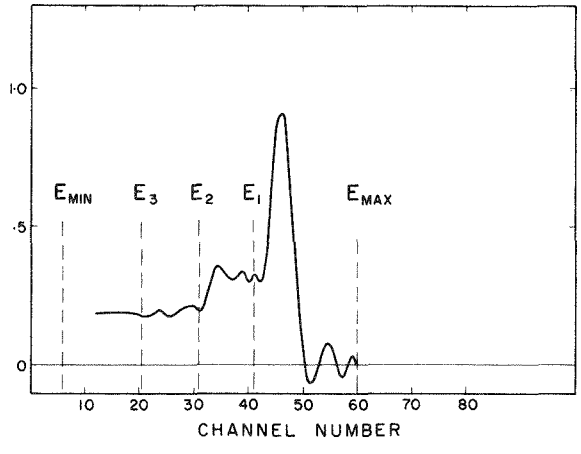

Fig. 4. An Unacceptable Computed Line Shape for a 2.30-Mev Gamma Ray in an Uncollimated 5- by 4-in. NaI(Tl) Crystal. The "wiggles" which occur result from irregularities in the measured spectrum and from a choice of E_{max} which is too high.

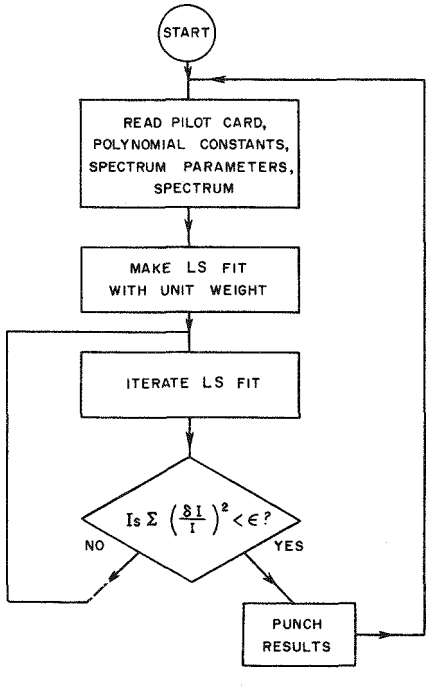

Fig. 5. Flow Diagram for the Least-Squares Fitting Program.

The output consists of the final values of the variables, their internal and external errors, the χ^2 for the fit, the spectrum with the fitted values, and finally the "reference integrals." These last are the integrals of the pure line shapes used in the fit from energies specified in the input for each component to the top of the spectrum. These can be used as parameters to normalize the intensities found.

The program makes use of a general nonlinear least-squares subroutine which is part of our library. The principal operating time is in computing the contribution of each component in each channel. This requires $\frac{1}{2}$ sec and must be repeated a minimum of four times for a fit. An additional $\frac{1}{2}$ sec is required per component per channel for the derivatives when the components are being fitted in energy.

A typical time is $\frac{1}{2}$ hr to fit 5 components in intensity only to 80 channels. No spectrum may be used below E_{min}, and a programmed stop occurs if such a point is required. A maximum weight must be specified with each spectrum which is used wherever the computed weight exceeds it.

A point worth remarking is that with the method of weighting used here the integrated areas under the fitted curve and the measured spectrum are equal, which seems a natural requirement. This will not be true for other methods of weighting.

Figure 6 shows a spectrum from the $Li^7(\alpha,\gamma)B^{11}$ reaction at the 0.96-Mev resonance. The solid line is the computed fit using the components indicated by the arrows. Four of the line shapes used in the fit on the previous slide are shown in Fig. 7. Some irregularities are evident at the low end of the 2.52-Mev component, but these are below the region of the fit.

A least-squares fit using the reciprocal of the channel counts as weights is shown in Fig. 8. These are gamma rays in coincidence with the proton group to the 4th excited state of B^{11} which had to be resolved with a magnetic spectrometer, so that a very small yield was obtained. The low bias of the fit is obvious which is clearly due to the fact that low counts have much bigger weights than large ones.

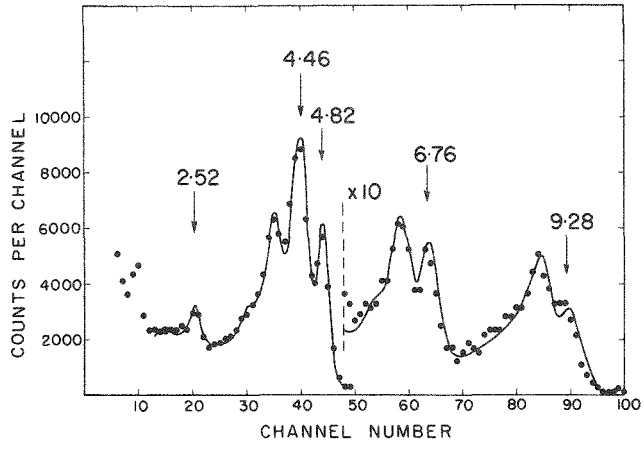

Fig. 6. A Fit to the Gamma-Ray Spectrum from the Reaction $Li^7(\alpha,\gamma)B^{11}$ at an Alpha-Particle Energy of 0.96 Mev. The measured spectrum is indicated by dots and the computed fit by the solid line.

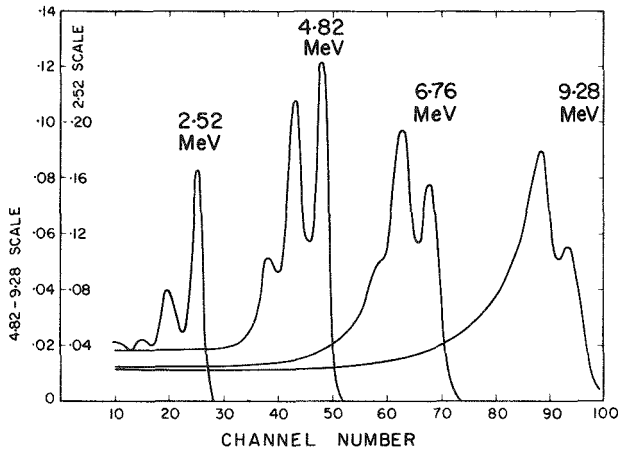

Fig. 7. Four of the Line Shapes Used in the Analysis of Fig. 6.

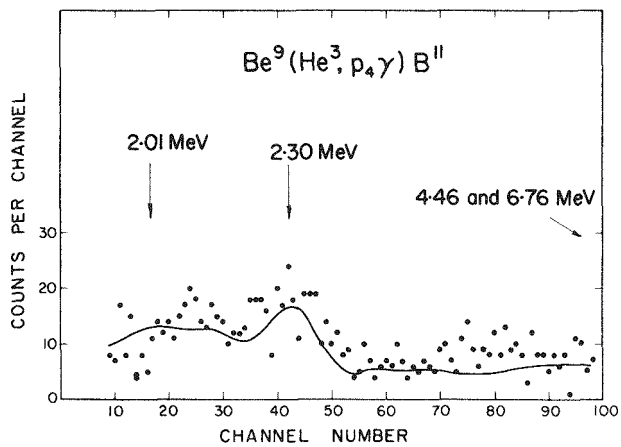

Fig. 8. Least-Squares Fit to a Gamma-Ray Spectrum with a Small Number of Counts, Illustrating the Low Bias of the Fit Obtained by Using the Reciprocals of the Channel Counts as Weights.

In Fig. 9 is shown a fit made by G. A. Bartholomew to a spectrum from slow neutron capture in Nd^{143}. This illustrates a difficulty which may sometimes arise, namely that the computed lines are sharper than those of the measured spectrum. The measured peaks have been spread out here by drifts of photomultiplier gain in the course of the experiment. Figure 10 shows a fit to a spectrum from this same reaction which does not suffer from this difficulty. The individual components are also shown here in their computed intensities.

The program has been used by a number of experimenters at Chalk River, generally with satisfactory results. Experience has suggested some minor improvements. The use of more divisions of the spectra, represented by polynomials of lower degree would probably lead to fewer troubles with wiggles. A better method

of smoothing would probably be useful and a suggestion of Lanczos [2] for using Fourier series in this regard merits consideration. The program could be substantially speeded in the usual problems where only intensities are required by storing the component line shapes, possibly on magnetic tape, and avoid the repetition of this time consuming part of the calculation.

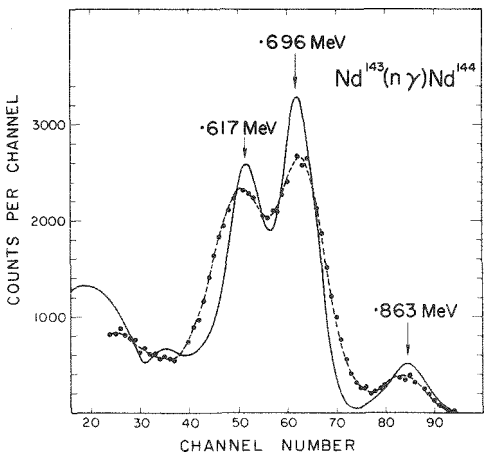

Fig. 9. Comparison Between the Computed Spectrum (Solid Line), and a Measured Spectrum (Dashed Line) Which was Broadened by Instrumental Drift.

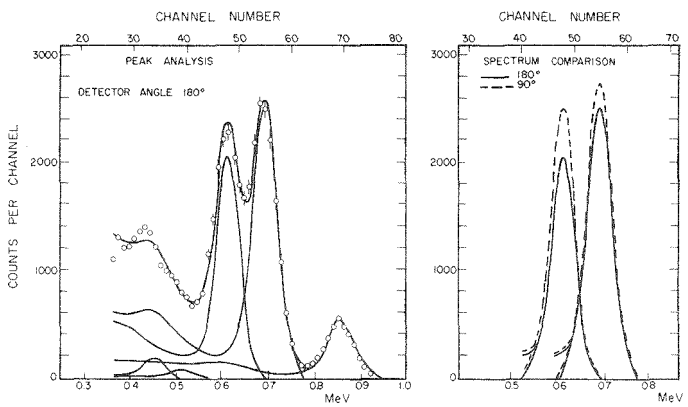

Fig. 10. Fits to Gamma-Ray Spectra from Neutron Capture in Nd^{143} as in Fig. 9, Except That the Instrumental Drift Was Eliminated.

REFERENCES

[1] E. T. Whittaker and G. Robinson, *The Calculus of Observations,* Blackie and Sons, Ltd., London and Glasgow, 1925.

[2] C. Lanczos, *Applied Analysis*, Prentice Hall, Englewood Cliffs, N.J., 1956.

[3] R. Nordhagen, *Nucl. Instr. Methods* **12**, 291 (1961).

(4-2) COMPUTER ANALYSIS OF GAMMA-RAY SPECTRA FROM MIXTURES OF KNOWN NUCLIDES BY THE METHOD OF LEAST SQUARES

L. Salmon
Health Physics and Medical Division,
Atomic Energy Research Establishment, Harwell

INTRODUCTION

Considerable interest is currently being shown in least-squares analysis of gamma-ray spectra [*1–6*] as an alternative to the more usual technique of "stripping," that is, successive subtraction of individual components of the spectrum after normalizing each peak with an appropriate standard spectrum.

The purpose of this paper is to discuss the validity of the least-squares method of analysis and to present some results indicating the accuracy and the sources of error that arise.

It will be seen that many of the examples chosen involve the measurements of radioactive debris from nuclear explosions, since this is the particular field for which the method was introduced into this laboratory.

THE LEAST-SQUARES METHOD

The least-squares method is an extension of the most general case of analysis of spectra usually referred to as the "incremental method."

The pulse-height analyzer is considered to have n channels numbered $1 \ldots i \ldots n$ and the midpoint of each channel represents a gamma-energy E_i. The response function of the system for each value of E_i can be found, at least in principle, experimentally; this results in an $n \times n$ matrix A. An experimental spectrum, a vector $\mathbf{y}$, resulting from a mixture of up to n gamma rays each corresponding to the energies E_i results in a set of linear simultaneous equations

$$\underset{(n \times n)}{A} \quad \underset{(n \times 1)}{\mathbf{x}} = \underset{(n \times 1)}{\mathbf{y}} ,$$

where the vector $\mathbf{x}$ represents the unknown intensity of each gamma ray in the mixture considered. The solution of these equations by inverting the matrix A, $\mathbf{x} = A^{-1}\mathbf{y}$, yields the desired information.

This method, described by Childers [7] and elaborated by Chester and Burrus [8], is intended for analysis of mixtures of unknown composition. Its practical disadvantages lie in obtaining satisfactory values of the large matrix A, and the necessity of applying smoothing corrections to nullify the effect of small inaccuracies and statistical counting fluctuations in an ill-conditioned matrix.

In the more restricted case considered here, it is assumed that the spectrum to be analyzed is from a mixture of known nuclides of number m and that standard spectra of these nuclides are available.

The spectra of these standards form the matrix A with dimensions $n \times m$. Thus the equations

$$\underset{(n \times m)}{A} \quad \underset{(m \times 1)}{\mathbf{x}} \quad = \quad \underset{(n \times 1)}{\mathbf{y}}$$

have $(n - m)$ redundancies or degrees of freedom.

It would be simple to sum the counts over appropriate areas of the spectrum thus reducing n to m. Such a method, however, deliberately reduces the information available by effectively using an analyzer of m channels.

Alternatively if it is assumed that the only errors encountered are statistical fluctuations in $\mathbf{y}$, then the principle of least squares may be applied. By minimizing the sum of the squares of errors in $\mathbf{y}$ it can be shown from the simple theory of multilinear regression that the resulting normal equations derived are [9]

$$\underset{(m \times n)}{A^T} \quad \underset{(n \times m)}{A} \quad \underset{(m \times 1)}{\mathbf{x}} \quad = \quad \underset{(m \times n)}{A^T} \quad \underset{(n \times 1)}{\mathbf{y}}$$

The application of the principle of least squares requires that the variance of each observation shall be the same. Since the variance of each element in $\mathbf{y}$ is not constant, a diagonal weighting matrix W must be introduced. Here each diagonal element is the inverse of the estimated variance of the channel count it represents. This variance is not represented exactly by the magnitude of the count but must allow for the background count also.

The resulting equations are represented by

$$\underset{(m \times n)}{A^T} \quad \underset{(n \times n)}{W} \quad \underset{(n \times m)}{A} \quad \underset{(m \times 1)}{\mathbf{x}} \quad = \quad \underset{(m \times n)}{A^T} \quad \underset{(n \times n)}{W} \quad \underset{(n \times 1)}{\mathbf{y}}$$

simplified as $S\mathbf{x} = \mathbf{z}$. The solution of these equations $\mathbf{x} = S^{-1}\mathbf{z}$ yields the quantity of each nuclide.

It can further be shown [9] that the variance/covariance matrix for the vector $\mathbf{x}$ is S^{-1} provided the errors observed are attributable only to statistical counting fluctuations. Thus the uncertainties in the determination of $\mathbf{x}$ are known.

The advantages of this system of analysis may now be summarized:

1. The method is free from subjective errors.
2. It is amenable to computer calculation.
3. It should be particularly suited to spectra whose statistical variations in counting are large.
4. All data in a spectrum can be used and not restricted to that in the region of the photopeaks.
5. It should be possible to analyze spectra where peaks are superimposed.
6. Estimates may be made of the variance, and the uncertainty of the variance, associated with each result.

COMPUTATION AND EXPERIMENTAL METHOD

In the present work calculations have been performed using a FORTRAN program written for an IBM 7090 computer.

The program makes the necessary corrections (octal-decimal conversion, background subtraction, etc.) to the spectrometer data obtained from sources of mixed gamma emitting nuclides. Corrected data are fitted by least squares to standard spectra of nuclides comprising the mixture to be analyzed. Facilities are also available in the program for a simple stripping procedure to be used if desired, and correction may be made for decay. Additions to the program to overcome certain difficulties encountered are mentioned later in this paper.

Some results mentioned have been obtained from a simpler program written in AUTOCODE for a Ferranti "Mercury" computer, where unit weighting was used.

The spectrometer used consisted of a 3- by 3-in. sodium iodide detector coupled to a photomultiplier and shielded by a lead "castle" 4 in. thick. The output of a stabilized amplifier system was fed to a 100-channel analyzer. The contents of the analyzer store (in octal representation) were copied automatically onto punched cards suitable for input to the computer.

The incorporation of a live-time integrating unit precluded the need for paralysis correction.

VALIDITY OF THE LEAST-SQUARES METHOD APPLIED TO SPECTRAL ANALYSIS

If it is accepted that analysis of spectra is best carried out by some form of curve fitting procedure, then it follows that the best results (not necessarily ideal) are likely by application of the principle of least squares. To quote Birge's classical article on the subject [*10*]:

"Except in especially favourable cases, least squares' results and their computed probable errors are not as reliable as indicated by theory ... , but alternative methods are, without exception, inferior."

Data to be subjected to least-squares fitting should satisfy the requirement that errors of observations follow the Gaussian error curve if statements regarding the accuracy of the results are to be made. Thus the observations should have a common variance, and their errors should have a zero mean. Since the observations result from radioactive decay, this criterion is satisfied except that the variance of each observation will not be constant but be approximately equal to the magnitude of the observation. As already pointed out, this results in the necessity of suitable weighting. It also follows that the spectra of the standards to be used in the fitting procedure must be exact in the sense that (*a*) the standards truly represent the constituents of the mixture to be analyzed, (*b*) the spectra have been obtained under conditions identical with the sample (the same counting geometry, gain, bias threshold, etc.), and (*c*) that the statistical counting fluctuations of the standards are negligible in comparison with the sample.

The validity of the fit is tested by comparing the differences between the observed and fitted spectrum with the expected uncertainties predicted from statistical considerations.

For a mixture of m nuclides the array of observations is $y_i (i = 1, n)$ and the fitted spectrum is y_i'; then

$$\frac{\chi^2}{(n - m \text{ degrees of freedom})} = \sum_{i=1}^{n} (y_i - y_i')^2 / [\text{var}\,(y_i')] \,.$$

The term $m - n$ is large; hence

$$R = \frac{\chi^2}{n - m} \approx 1 \ .$$

The ratio R of observed to predicted errors should always be calculated to check that the fit is valid. If R is significantly greater than unity, then the standards either (*a*) do not represent all the nuclides present in the sample; (*b*) have not been counted for a sufficient period to make statistical uncertainties insignificant; (*c*) do not correspond with the sample in terms of physical shape, counting geometry, etc.; or (*d*) have not been measured at the same gain or bias threshold values as the sample.

In ideal circumstances R will approximate to unity but in most practical cases it will be somewhat larger. If this increase can be ascribed to random (i.e., Gaussian) errors such as (*b*) above or small changes in gain, then the least-squares fit can still be regarded as valid though the variance/covariance matrix should then be multiplied by the scalar quantity R.

Experiments have been performed to observe the validity of least-squares fitting in practical cases. The accuracy has been measured; the ability of the system to resolve spectra from nuclides of similar gamma-ray energy has been tested; and the errors resulting from gain drift and from the presence of unpredicted nuclides have also been examined.

Accuracy

A series of synthetic mixtures were analyzed by least squares to observe the accuracy obtained by such a method. The nuclides used are listed in Table 1 and the results in Table 2. The spectrum of a six component mixture is shown in Fig. 1. Depending on the complexity of the mixture, it will be seen that accuracies of

Table 1. Sources Used in Experiments

Nuclide	Gamma Energies (Mev)		Total Gamma Counting Rate (counts/min)
Cs^{137}	0.66		2640.9
Sc^{46}	0.89	1.12	8506.9
Mn^{54}	0.84		1183.7
$Zr\text{-}Nb^{95}$	0.72	0.76	4568.4
Co^{60}	1.17	1.33	6100.4
$Ru\text{-}Rh^{106}$	0.51	0.62	1330.4
Background			380.0

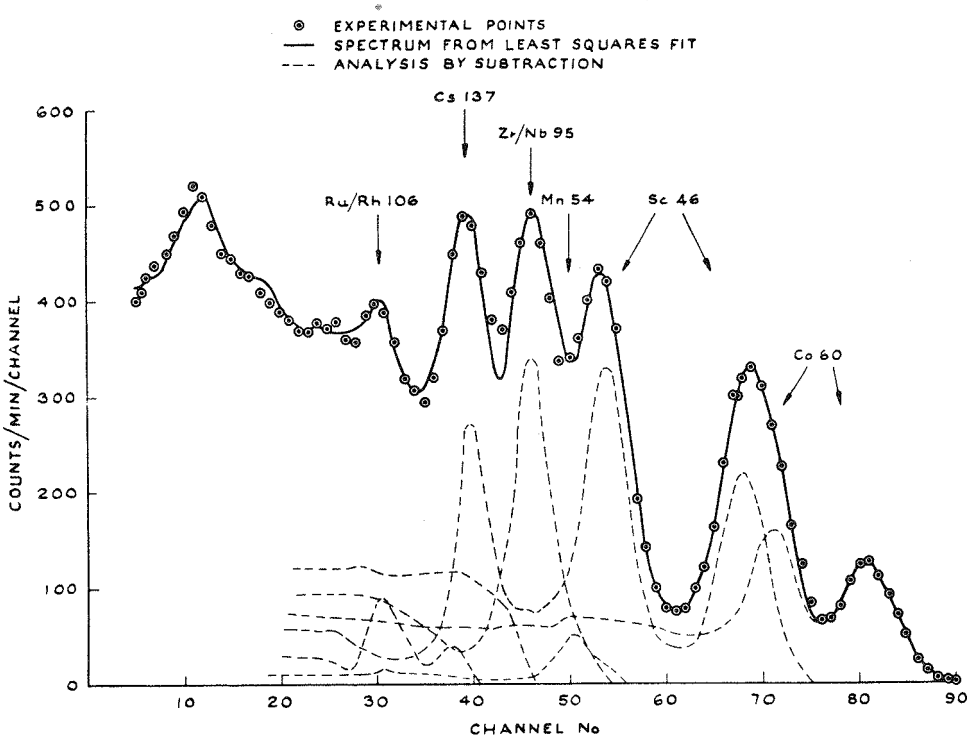

Fig. 1. Analysis of Gamma-Ray Spectrum of 6 Nuclides.

0.5–2% are general, and correspond reasonably with the calculated standard deviations. A greater degree of accuracy is obtainable with more active samples than those illustrated, as was demonstrated by Heath [5] and Hallett [9].

The results obtained in the tables are not very greatly superior to graphical fitting and subtraction but are independent of subjective errors; calculated standard deviations are obtained and measurements are performed on nuclides whose photopeaks superimpose on others. Results from the analysis of a synthetic mixture showing very poor counting statistics are given in Table 3 and illustrated in Fig. 2.

Sensitivity

To test the sensitivity of the method for a typical case, known quantities of Cs^{137} were added to a mixture of Zr^{95}-Nb^{95} and Ru^{103} (see Fig. 3). The percentage of Cs^{137} added plotted against the amount found by least-squares analysis is shown in Fig. 4. Although the total number of counts measured in each case did not exceed 2×10^4, the results are adequate for Cs^{137} concentrations of less than 1% of the total activity.

Two measurements made on samples containing no cesium gave results of $Cs^{137} = 0.18\%$ ($\sigma = 0.36$) and -0.30% ($\sigma = 0.48$).

Table 2. Analysis of 2, 3, 4, and 6 Component Mixtures by Least-Squares Fit and by Successive Subtraction[a]

Nuclide	True Counting Rate (%)	Least-Squares Fit				Successive Subtraction		
		Calcd Counting Rate (counts/min)	Calcd Counting Rate (%)	Std Dev (%)	Error (%)	Calcd Counting Rate (counts/min)	Calcd Counting Rate (%)	Error (%)
Cs^{137}	23.67	2697.4	24.21	0.26	0.54	2746.5	24.53	0.86
		2694.2	24.01	0.33	0.34			
		2705.6	24.23	0.26	0.56			
Sc^{46}	76.31	8443.9	75.79	0.83	0.52	8447.3	75.47	0.84
		8526.5	75.99	0.48	0.32			
		8461.0	75.77	0.38	0.54			
Cs^{137}	21.42	2665.4	21.20	0.26	0.22	2720.1	21.68	0.26
		2682.0	21.38	0.26	0.04			
		2705.1	21.67	0.31	0.25			
Sc^{46}	68.98	8620.8	68.56	0.52	0.42	8464.4	67.47	1.51
		8639.7	68.85	0.52	0.13			
		8584.3	68.76	0.62	0.22			
Mn^{54}	9.60	1288.6	10.24	0.40	0.64	1361.3	10.85	1.25
		1226.3	9.77	0.40	0.17			
		1194.5	9.57	0.45	0.03			
Cs^{137}	15.63	2880.4	16.69	0.38	1.06	2651.4	16.19	0.58
		2793.8	16.30	0.40	0.67			
		2793.2	16.16	0.39	0.53			
Sc^{46}	50.34	8923.7	51.71	0.75	1.37	8549.4	52.21	1.87
		8816.6	51.44	0.80	1.10			
		8976.4	51.95	0.77	1.61			

Mn^{54}	7.00	809.6	4.69	0.40	2.31	898.4	5.49	1.51
		859.0	5.01	0.43	1.99			
		808.6	4.68	0.41	2.32			
$Zr\text{-}Nb^{95}$	27.03	4643.7	26.91	0.47	0.12	4276.0	26.11	0.92
		4671.6	27.25	0.50	0.22			
		4701.7	27.21	0.48	0.18			
Cs^{137}	10.86	2898.9	11.51	0.37	0.65	2891.7	11.46	0.60
		2974.7	11.82	0.41	0.96			
		2995.0	12.15	1.13	1.29			
Sc^{46}	34.96	9173.8	36.43	0.85	1.47	8906.7	35.29	0.33
		9344.2	37.13	0.94	2.17			
		8700.0	35.28	2.38	0.32			
Mn^{54}	4.87	850.7	3.38	0.38	1.49	710.2	2.81	2.06
		883.0	3.51	0.40	1.36			
		1485.1	6.02	1.82	1.15			
$Zr\text{-}Nb^{95}$	18.77	4825.1	19.16	0.49	0.39	4568.4	19.82	0.05
		4779.9	18.99	0.56	0.22			
		4489.9	18.21	1.24	0.44			
Co^{60}	25.07	6102.2	24.23	0.86	0.84	6100.4	24.66	0.41
		5891.0	23.41	0.84	0.66			
		5443.5	22.07	2.38	3.00			
Ru^{106}	5.47	1330.8	5.23	0.50	0.19	1330.4	5.96	0.49
		1291.3	5.13	0.50	0.34			
		1547.0	6.27	1.63	0.80			

[a]Background = 380 counts/min; counting time = 10 min.

Table 3. Analysis of 3 Component Mixture with Large Statistical Variations by Least-Squares Fit and by Successive Subtraction[a]

Nuclide	Counting Rate (counts/min)	True Counting Rate (%)	Least-Squares Fit				Successive Subtraction		
			Calcd Counting Rate (counts/min)	Calcd Counting Rate (%)	Std Dev (%)	Error (%)	Calcd Counting Rate (counts/min)	Calcd Counting Rate (%)	Error (%)
Cs^{137}	112.3	6.97	107.2	6.73	2.16	0.24	183.5	12.63	5.66
			121.4	7.50	2.44	0.53	172.4	11.11	4.13
			127.0	7.72	2.23	0.75	224.6	12.42	5.45
			131.5	8.10	2.10	1.13	222.5	12.59	5.62
Ru^{106}	509.2	31.61	494.6	31.07	2.75	0.54	269.9	18.59	13.02
			507.3	31.36	3.07	0.25	371.7	23.93	8.68
			541.7	32.92	2.81	1.31	575.4	31.80	0.19
			491.9	30.30	2.66	1.31	458.2	25.90	5.71
$Zr\text{-}Nb^{95}$	989.2	61.42	990.4	62.20	2.58	0.78	999.0	68.78	7.36
			989.0	61.14	2.88	0.28	1009.0	64.96	3.54
			976.5	59.36	2.64	1.06	1009.0	55.78	5.64
			1000.0	61.60	2.46	0.18	1088.1	61.51	0.09

[a]Background = 1831.6 counts/min; time of count = 10 min.

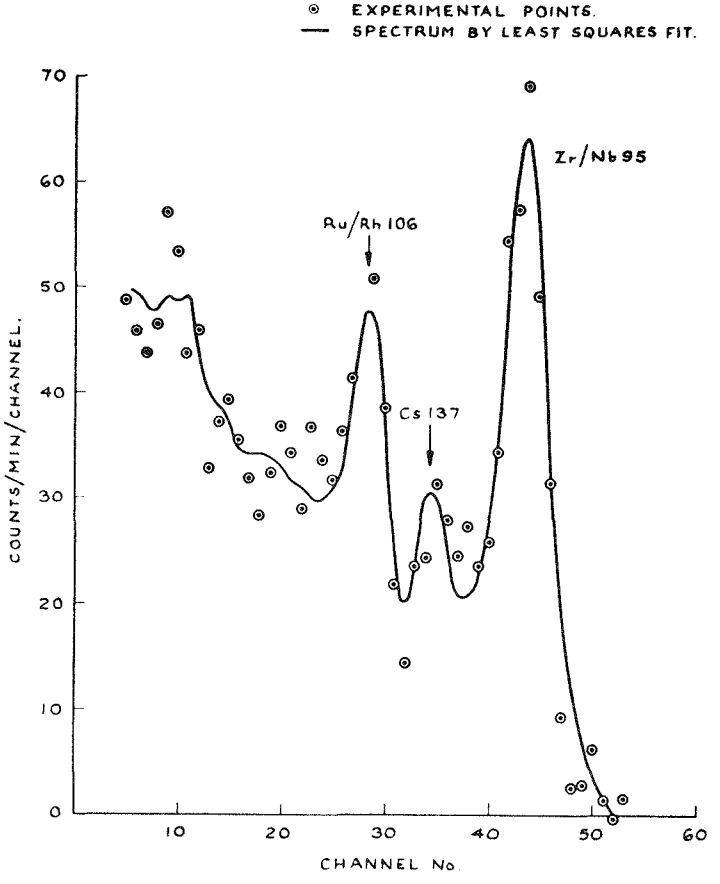

Fig. 2. Analysis of a Three-Component Gamma-Ray Spectrum with Large Statistical Variations.

Resolving Power

Although the resolving power of a sodium iodide spectrometer is frequently quoted in terms of the width of a particular photopeak (usually the 0.662-Mev peak from Cs^{137}), it is always possible in principle to separate two superimposed photopeaks, even in very close proximity, provided ideal counting conditions are maintained and a sufficiently large number of counts are taken. For example, the nuclides Ru^{103} and Ru^{106} emit photons of energies 0.50 and 0.61 Mev and 0.51 and 0.62 Mev respectively [Fig. 5(*c*)].

When analyzed by least squares, a spectrum of a mixture gave for unit values of these nuclides 1.03 ($\sigma = 0.06$) and 0.98 ($\sigma = 0.03$) respectively, using a total count of only 2×10^4.

Since in this case the major difference in the two spectra lies in the relative abundance of the 0.61 and 0.62 lines, the analysis was repeated using the spectra

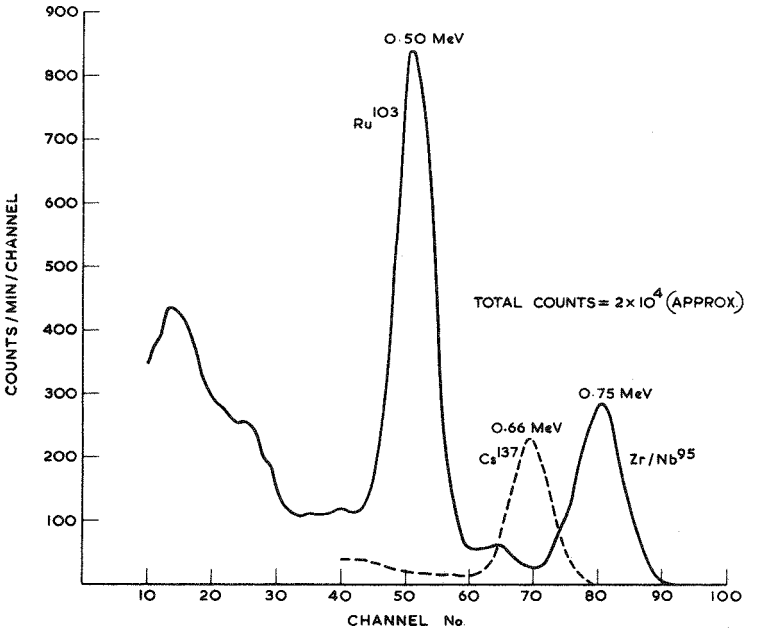

Fig. 3. Gamma-Ray Spectrum of Mixture Analyzed for Varying Quantities of Cs^{137}.

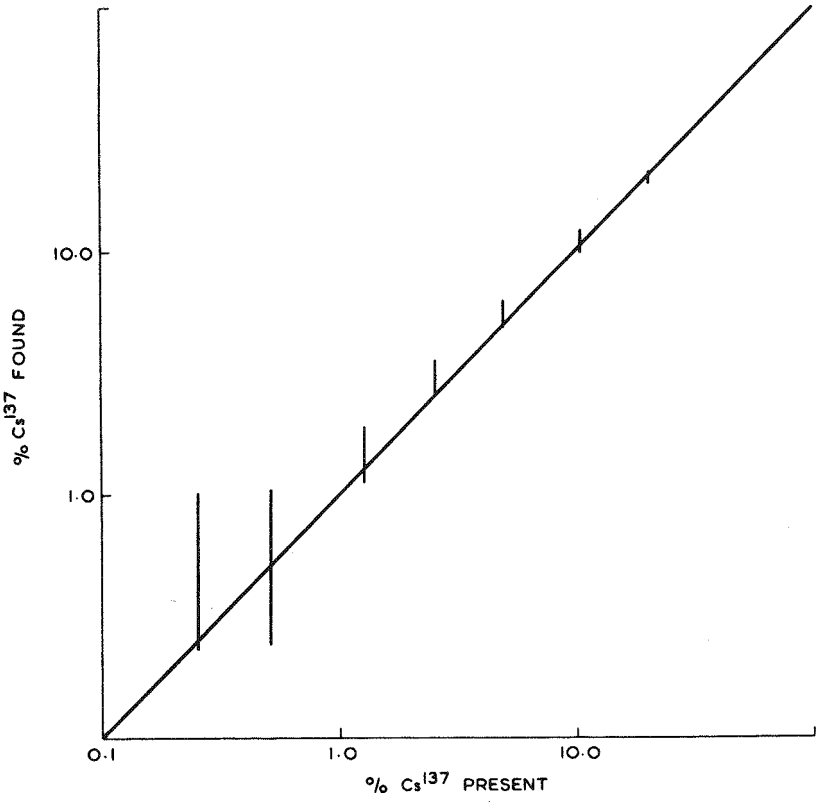

Fig. 4. Estimation of Varying Quantities of Cs^{137} in a Mixture of Ru^{103} and Zr^{95}-Nb^{95}.

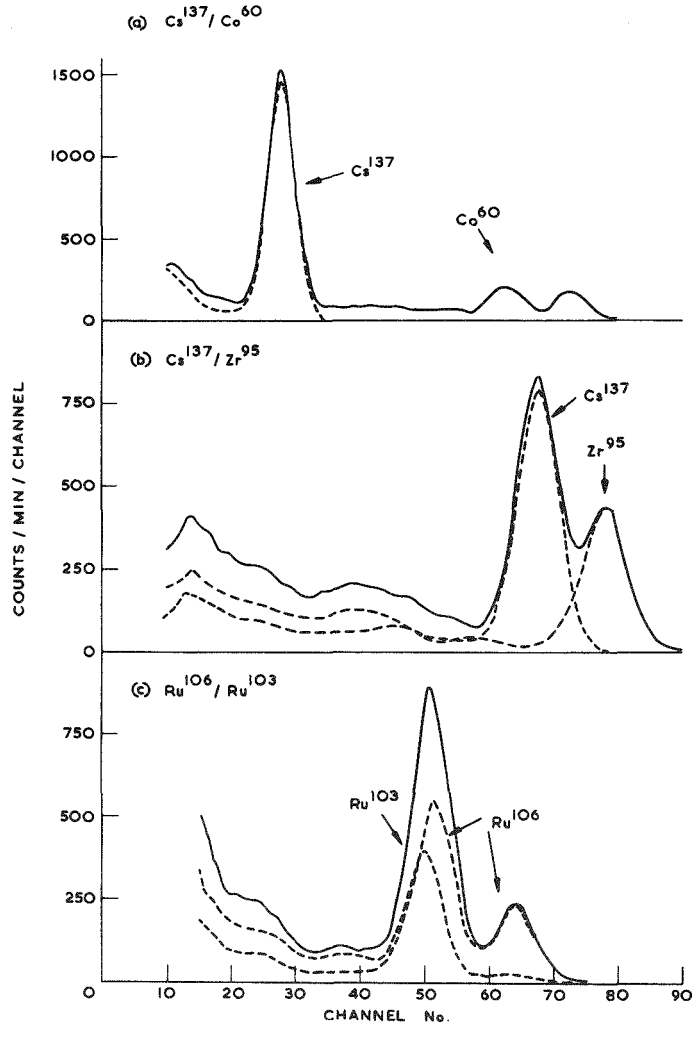

Fig. 5. Gamma-Ray Spectra of Some Two-Component Mixtures.

restricted to the 0.50/0.51-Mev peak. The values then obtained for unit quantities of Ru^{103} and Ru^{106} were 0.96 (σ = 0.11) and 1.03 (σ = 0.06).

These results are generally superior to those normally expected by subjective examination of a spectrum.

Effect of Gain Drift

It is very difficult to predict mathematically the effect of poor stabilization of the counting system on the least-squares analysis. Consequently a number of controlled experiments were performed to observe empirically the magnitude of this effect upon different mixtures of nuclides.

Individual standard sources were measured and synthetic mixtures prepared from these, each constituent being of unit activity. The mixtures were measured under the same physical conditions as the standards but with changing bias threshold values.

This system was used to simulate changes of gain since in this way a fine control was possible. For a 100-channel analyzer the addition of one channel bias is approximately equivalent to a change in gain of $100/n$ percent for channel n.

From the spectrum of Co^{60} and Cs^{137} shown in Fig. 5(*a*), little change would be expected in the results for appreciable gain changes. In fact, Fig. 6(*a*) shows that the results are reasonable up to about one channel bias change. Where the gamma energies are similar, as in a mixture of Cs^{137} and Zr^{95}-Nb^{95} [Fig. 5(*b*)] the system is far less tolerant of gain changes [Fig. 6(*b*)], while in the case of the

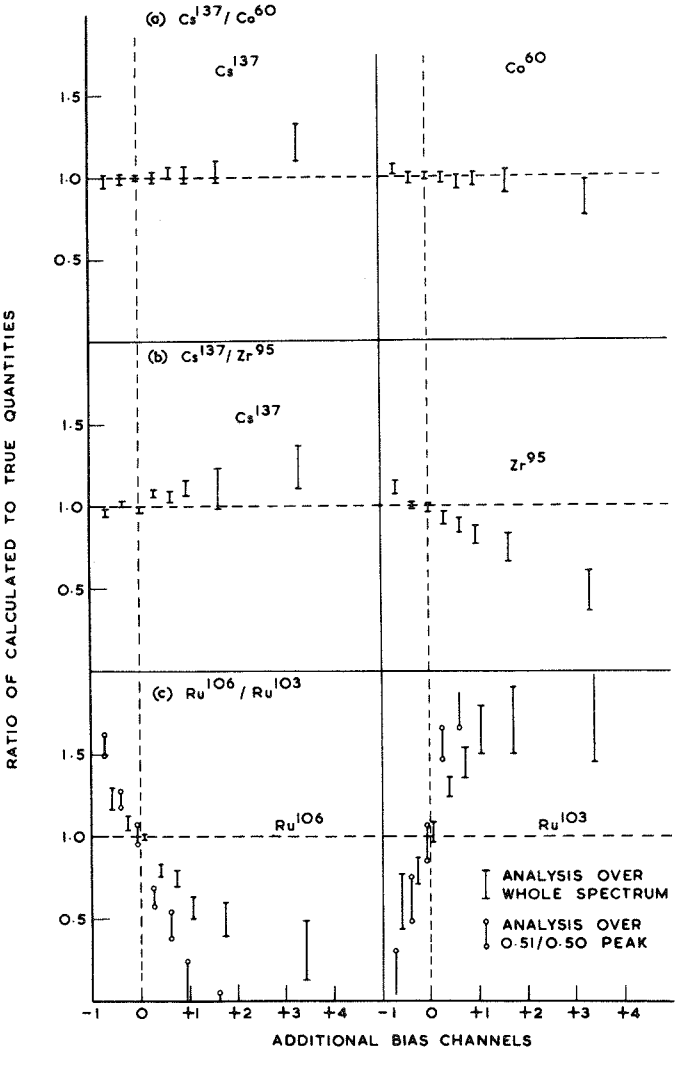

Fig. 6. Effect of Bias Change on the Analysis of the Two-Component Mixtures of Fig. 5.

two ruthenium nuclides [Figs. 5(*c*) and 6(*c*)] it is evident that a very high degree of stability is needed.

In this latter case two sets of results are given in Fig. 6(*c*), one for fits over the whole spectrum shown and the second restricting the fit to the major photopeaks. As would be expected, the latter case is the least tolerant of gain change.

Finally a mixture of four nuclides is shown in Fig. 7 with the effect of gain change in Fig. 8. It will be seen that the nuclide least affected by gain change (Cs^{137}) is that which is present in greatest quantity.

From all these results it is evident that small changes in gain are self-compensating to some extent in favorable cases, but overall, a very high degree of stability is necessary to obtain wholly reliable results.

In practice one finds that good stability is difficult to attain over long periods of a day or more. Stabilizing of power supplies and thermostating of the detector system do not completely solve this problem. Probably the best technique is an automatic form of stabilization of the type described by Wainerdi [*11*] and Dudley [*12*] where an alpha-emitting nuclide is implanted within the sodium iodide crystal itself, and the position of the resulting high energy peak used to control the overall gain of the system.

As an alternative a computational method can be used in many cases. Such a system is used in this laboratory. It is confined to those spectra where a predominant peak is present to allow precise measurement of its position.

The center position of the peak is found by fitting the top of this peak to a Gaussian function. The fitting is performed by nonlinear least squares using the iterative Newton-Raphson method. A similar calculation is performed on the corresponding standard spectrum and any change of channel is thus found. It is assumed that any change observed in the peak position is due to gain drift and not to change in threshold level. A new spectrum is then computed channel by channel on the basis of this change.

This method has shown itself to be very satisfactory for suitable spectra.

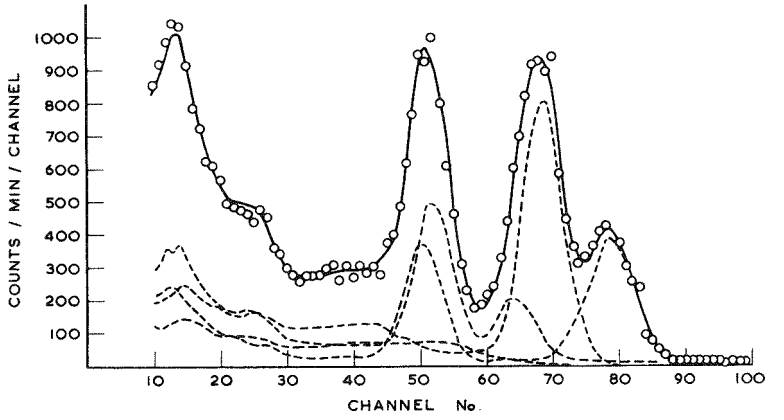

Fig. 7. Analysis of a Four-Component Gamma-Ray Spectrum, as Used for Testing the Effect of Bias Change.

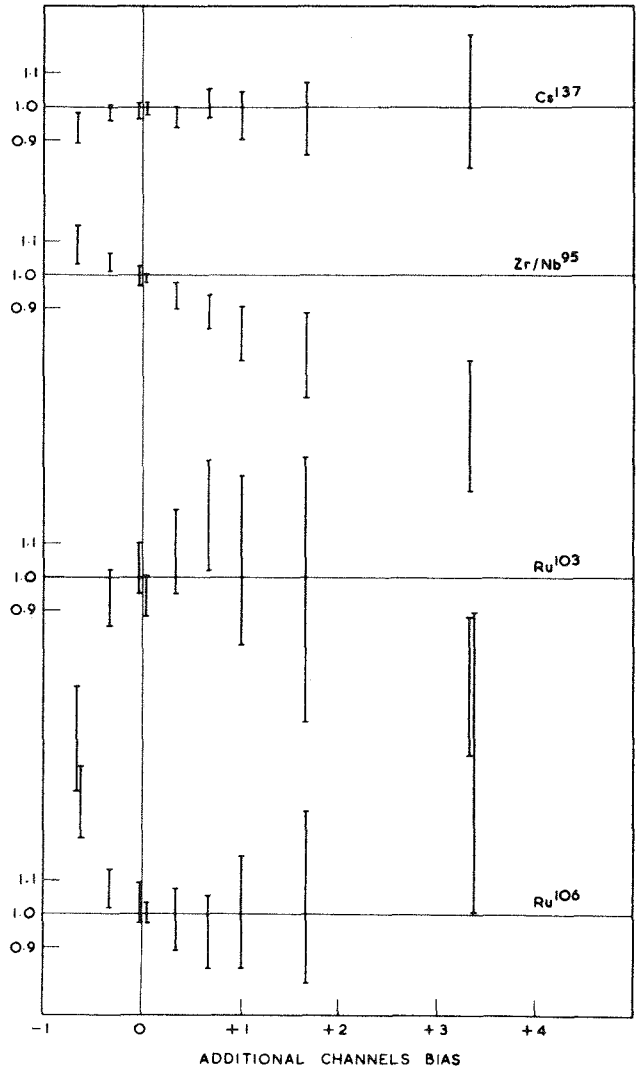

Fig. 8. Effect of Bias Change on the Analysis of the Four-Component Mixture Illustrated in Fig. 7.

The Effect of Unpredicted Nuclides

The theoretical basis of least-squares fitting will not accommodate nuclides other than those for which standards are provided. While one could include standards of all nuclides which could possibly occur, needless uncertainties would arise in the calculated amounts of the major nuclides present.

However, if unpredicted nuclides do occur in a mixture to be analyzed, the system should be made to cope with this situation. Assuming that other eventualities are accounted for (gain drift, etc.), then the presence of an unpredicted nuclide will be shown by a high value of χ^2. Least-squares fitting may then be repeated but by

using an arbitary method of weighting. Here the weights used are the inverse of the square of the differences between the observed and the originally fitted spectra. Such a system has no true mathematical justification but is merely an empirical system to minimize the effect of those points of the spectrum where the contribution of an unpredicted nuclide is greatest. It is not claimed that this system completely negates the effect of unpredicted nuclides, but it does allow identification of them. Thus Fig. 9 is the *difference* spectrum between an observed spectrum and the final fitted spectrum obtained as described above. The spectrum is of a mixture of Ru^{103}, Zr^{95}-Nb^{95}, and Cs^{137}, the analysis being performed for the first two nuclides only. The Cs^{137} in this case represented ~10% of the total activity present.

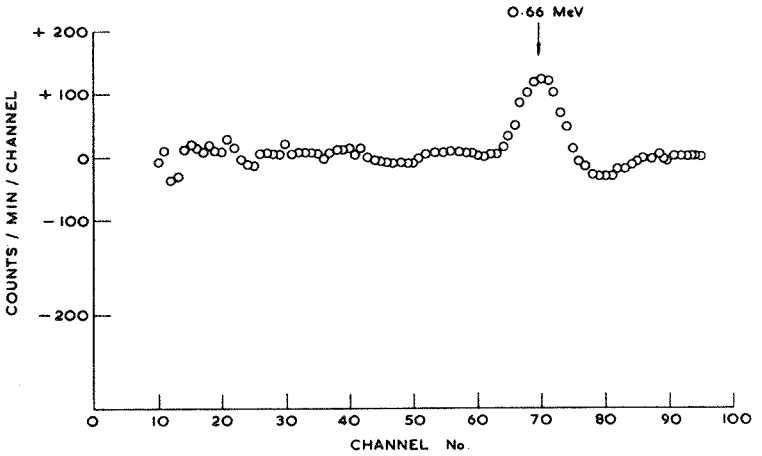

Fig. 9. Difference Between Observed and Predicted Spectra Using Arbitrary Weighting.

EXAMPLES OF LEAST-SQUARES FITTING IN GAMMA SPECTROMETRY

The method of analysis described is particularly suited to experiments where large numbers of similar samples are to be analyzed. In health physics work this is exemplified in large-scale tracer experiments and in measurement of fallout debris from nuclear explosions.

Figure 10 shows the spectrum of a mixture of Br^{82} and Cs^{137}. These and other pairs of nuclides were introduced into a river to measure the relative absorption rate of the two nuclides on the river bed, for studies related to economic effluent disposal. Hundreds of samples of water were collected and examined by gamma spectrometry. Analyses were performed computationally as described and resulted in saving many man-hours of labor.

Similarly much labor was saved in analyzing mixtures of iodine isotopes (Fig. 11). Here experiments were being performed to observe the difference in chemical behavior of gaseous iodine produced under two different physical conditions.

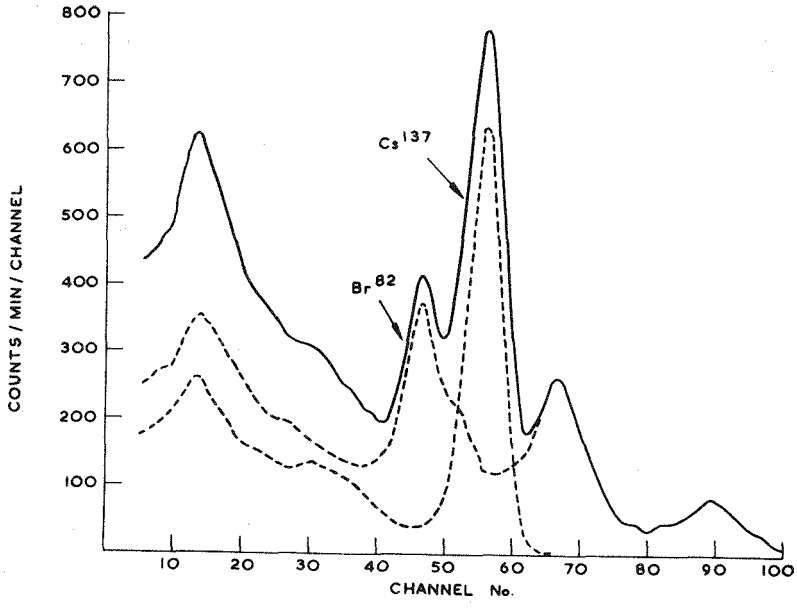

Fig. 10. Gamma-Ray Spectrum of River Water in Absorption Rate Study.

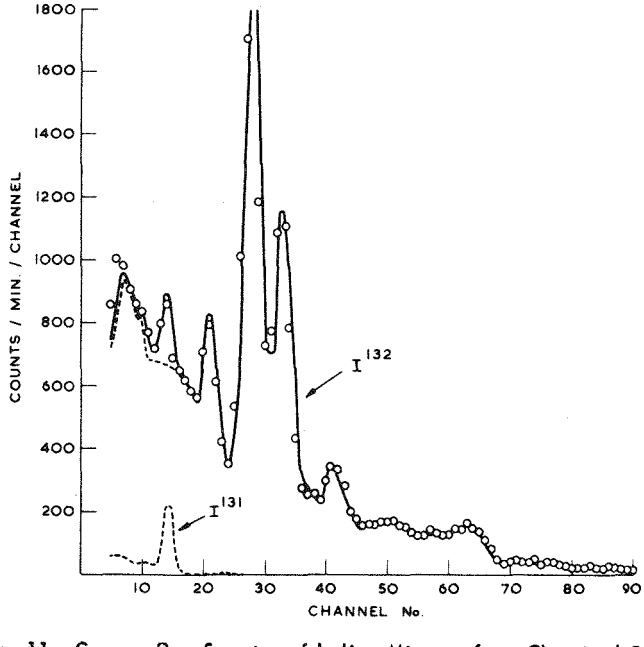

Fig. 11. Gamma-Ray Spectra of Iodine Mixture from Chemical Study.

Figure 12 shows the spectrum of fission-product activity in a typical air filter. The nuclides shown here are readily determined by the least-squares method. An analysis for similar nuclides is shown in Fig. 13, which displays the spectrum of the feeble radioactivity from a sample of fecal ash. Finally, an interesting spectrum is that of a human being with the lungs slightly contaminated with U^{235}. A very good fit is obtained to the standard sources used. These consisted of whole body phantoms of Cs^{137} and K^{40} and chest phantoms of U^{235} and Zr^{95}-Nb^{95} made to simulate activity in the lung (see Fig. 14).

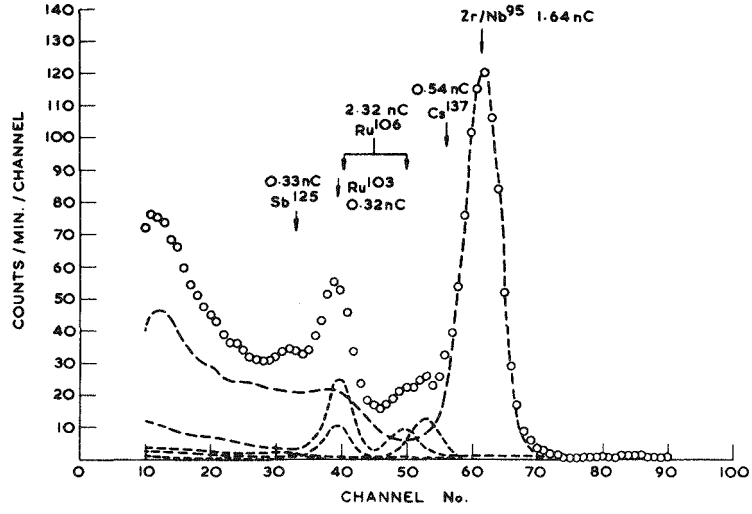

Fig. 12. Analysis of Gamma-Ray Spectrum of Debris from Nuclear Explosions.

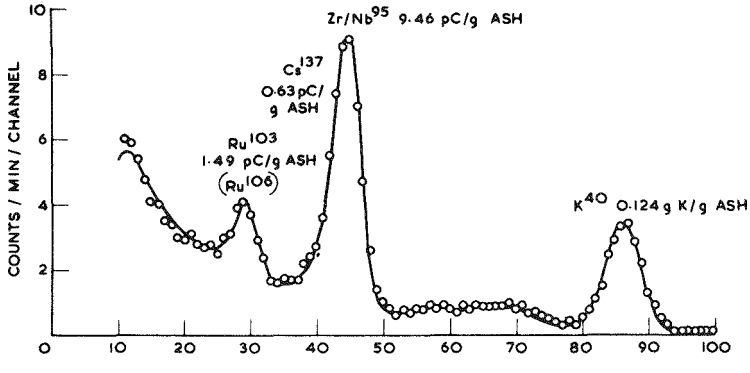

Fig. 13. Analysis of Gamma Radioactivity in 17.7 g of Fecal Ash.

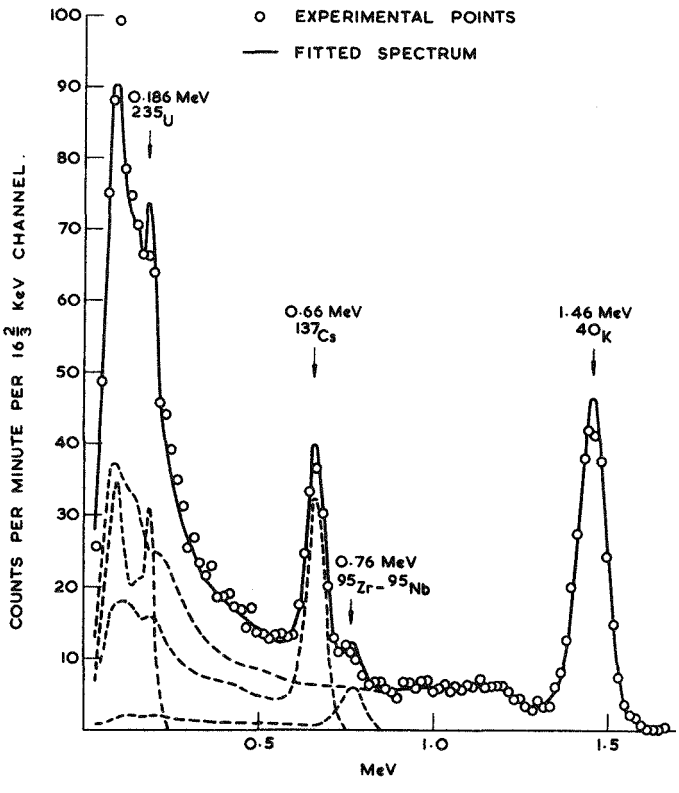

Fig. 14. Analysis of Whole-Body Spectrum.

CONCLUSIONS

The method of least squares is a suitable computational method for the routine analysis of gamma-ray spectra of known constitution. It is more accurate than previously used methods and makes maximum use of the resolving power of the sodium iodide spectrometer. Ideally, it is necessary to maintain very stable conditions of counting and all contributions to the activity of a sample must be known, but computational methods have been devised to allow some latitude on these conditions.

ACKNOWLEDGMENTS

The author is grateful to Dr. J. Rundo for the last two examples quoted in the paper and to Mr. E. York whose FORTRAN subroutine for nonlinear least-squares fitting is incorporated in the program described.

REFERENCES

[1] J. C. Reynolds, ANL-5829 (1958).

[2] L. Salmon, *Nucl. Instr. Methods* **14**, 193 (1961).

[3] R. E. Bentley, *Strahlentherapie* (in press).

[4] A. J. Ferguson, AECL-1398 (1961).

[5] R. L. Heath, IDO-16784 (1962); *IRE Trans. Nucl. Sci.* **NS-9**(3), 294 (1962).

[6] B. Pasternack, *Technometrics* (in press).

[7] H. M. Childers, *Rev. Sci. Instr.* **30**(9), 810 (1959).

[8] R. O. Chester and W. R. Burrus, ORNL-3016, p 249 (1960).

[9] O. Kempthorne, *The Design and Analysis of Experiments*, p 55, Wiley, New York, 1952.

[10] R. T. Birge, *Phys. Rev.* **40**, 207 (1932).

[11] L. E. Fite, R. E. Gibbons, and R. Wainerdi, *Proceedings of the 1961 International Conference on Modern Trends in Activation Analysis, Held at Texas A. & M. College*, Texas A. & M. College, College Station, 1962.

[12] R. H. Dudley and R. Scarpatti, *Radioact. Man, Symp. Chicago, Ill., 1962.*

(4-3) LEAST-SQUARES ANALYSIS OF GAMMA-RAY PULSE-HEIGHT SPECTRA[1]

J. I. Trombka

Jet Propulsion Laboratory, California Institute of Technology, Pasadena, California

INTRODUCTION

A least-squares fitting technique for the analysis of complex gamma-ray pulse-height spectra has been developed. In this analysis, the pulse-height spectrum due to a polyenergetic distribution of gamma rays is synthesized by using a series of normalized pulse-height distributions due either to the monoenergetic components in the incident beam or to the pulse-height characteristic of various possible nuclear species

[1]This paper presents one phase of research supported by the Michigan Memorial Phoenix project and the Atomic Energy Commission, and submitted in partial fulfillment of the requirements for the Ph.D. degree at the University of Michigan, Ann Arbor, Michigan. This research is now continuing under sponsorship of the National Aeronautics and Space Administration Contract NAS 7-100.

in the source. Each of these pulse-height distributions is weighted so that their sum is a best fit, based upon a least-squares criterion, to the experimentally determined polyenergetic pulse-height distribution.. There is difficulty in the application of least-squares techniques to the analysis of pulse-height spectra, because the problem is nonlinear in energy. In the technique described here, this difficulty has been overcome by using linear methods of solution, but applying the constraint that only positive or zero values be allowed for the intensities or amplitudes of the various monoenergetic components. .

APPLICATION OF THE PRINCIPLE OF LEAST SQUARES

Formulation

When a number of gamma rays are incident upon an NaI(Tl) crystal, the measured pulse-height spectrum is made up of a summation of the photopeaks and Compton continua of the various monoenergetic components; that is, if ρ_i is the total number of counts in channel i, then

$$\rho_i = \sum_n B_{in} , \tag{1a}$$

where B_{in} is the number of counts occurring in channel i due to the interactions of gamma rays of energy E_n with the crystal. This also can be written as

$$\rho_i = \sum_n \beta_n A_{in} , \tag{1b}$$

where A_{in} is the normalized number of counts occurring in channel i due to the interaction of gamma rays of energy E_n with the crystal and

$$\beta_n = \frac{B_{in}}{A_{in}} . \tag{2}$$

The A_{in}'s can be obtained, for example, by measuring monoenergetic emitters placed in the same geometrical configuration as that of the polyenergetic emitter used to measure ρ_i.

Due to the variance in the determination of ρ_i and $\beta_n A_{in}$, $\beta_n A_{in}$ cannot be simply determined from an inversion of Eq. (2). Therefore, the most probable values of $\beta_n A_{in}$ are determined based on the least-squares criteria, that is,

$$\sum_i \omega_i \left(\rho_i - \sum_n \beta_n A_{in} \right)^2 \Longrightarrow \text{Minimum} , \tag{3}$$

where ω_i is the statistical weight and $\omega_i \sim 1/\sigma_i^2$. In the simplest case $\sigma_i^2 \sim \rho_i$, if the counting time in each channel is constant and if it is assumed that there is no variance in A_{in}. The summation is over all channels i and all energies n.

Method of Obtaining Minimum for Least-Squares Fit

Incident Gamma Flux Discrete in Energy (Energy Distribution Known and Intensities Required). – A number of algorithms can be used to obtain the minimum required in Eq. (3), but the method of solution used depends on how much is known about the incident flux. The simplest case is considered first. In this case, the gamma-ray energy distribution is known, and it is desired to determine the intensity.

Now, ρ_i is measured, and since the energy distribution is known, the monoenergetic components (A_{in}'s) are known. The minimum is therefore obtained by taking the partial derivative with respect to β_k for each of the p monoenergetic components. Each derivative is then set equal to zero. Thus

$$\frac{\partial M}{\partial \beta_k} = -2 \sum_i \omega_i (\rho_i - \sum_n \beta_i A_{in}) A_{ik} = 0 , \tag{4}$$

for $k = 1, 2, \ldots, p$. Thus, there are p linear equations to be solved for the β's. Relation (4) can be expressed in matrix notation [*1*], as follows:

$$A^T \omega \rho - (A^T \omega A)\beta = 0 , \tag{5}$$

where β is vector of the β_k's; A is a p by n matrix of the pulse-height spectra; n is the maximum pulse height; A^T is the transpose of A; and ω is a diagonal matrix of the ω_i's.

Solving for β, it is found that

$$\beta = (A^T \omega A)^{-1} A^T \omega \rho . \tag{6}$$

The calculation described in Eq. (6) has been programmed for the IBM 7090 computer and can handle up to 40 monoenergetic pulse-height spectra and up to 250 values for each pulse-height spectrum.

An application of this method will now be considered. The energy distribution of a gamma-ray emitter is known, but the problem is to determine the relative intensities of these energy components. The emitter chosen is I^{131}. The gamma-ray energies in the spectrum of I^{131} are 0.722 Mev, 0.637 Mev, 0.634 Mev, and 0.284 Mev. Another gamma ray which is a possible contaminant is also noticed at 0.5 Mev. The measured pulse-height spectrum is shown in Fig. 1. A point source of I^{131} was placed 10 cm from the top of a 2- by 2-in. NaI(Tl) crystal. The shapes of the monoenergetic pulse-height spectra were determined using monoenergetic sources and extrapolating from these spectra the pulse-height spectra for the energies desired. These spectra were normalized so that the area under the photopeak is unity. The curves were normalized in this manner so that the β's obtained would equal the area under the photopeak. Thus it is only necessary to divide by the absolute peak efficiency to determine the intensity. A least-squares fit is made using Eq. (6). The results are shown in tabular form in Table 1 and graphically in Fig. 1. Results for I^{131} determined by other investigators [*2, 3*] are also presented to show the close agreement with the results obtained using the least-squares fitting technique.

The errors were determined by a method described later in this paper. It was also assumed that the intrinsic peak efficiencies are known to within ± 5%. This assumed error was confirmed by comparing theoretical and experimental results obtained for the efficiencies of 2- by 2-in. NaI(Tl) crystals [*4–7*].

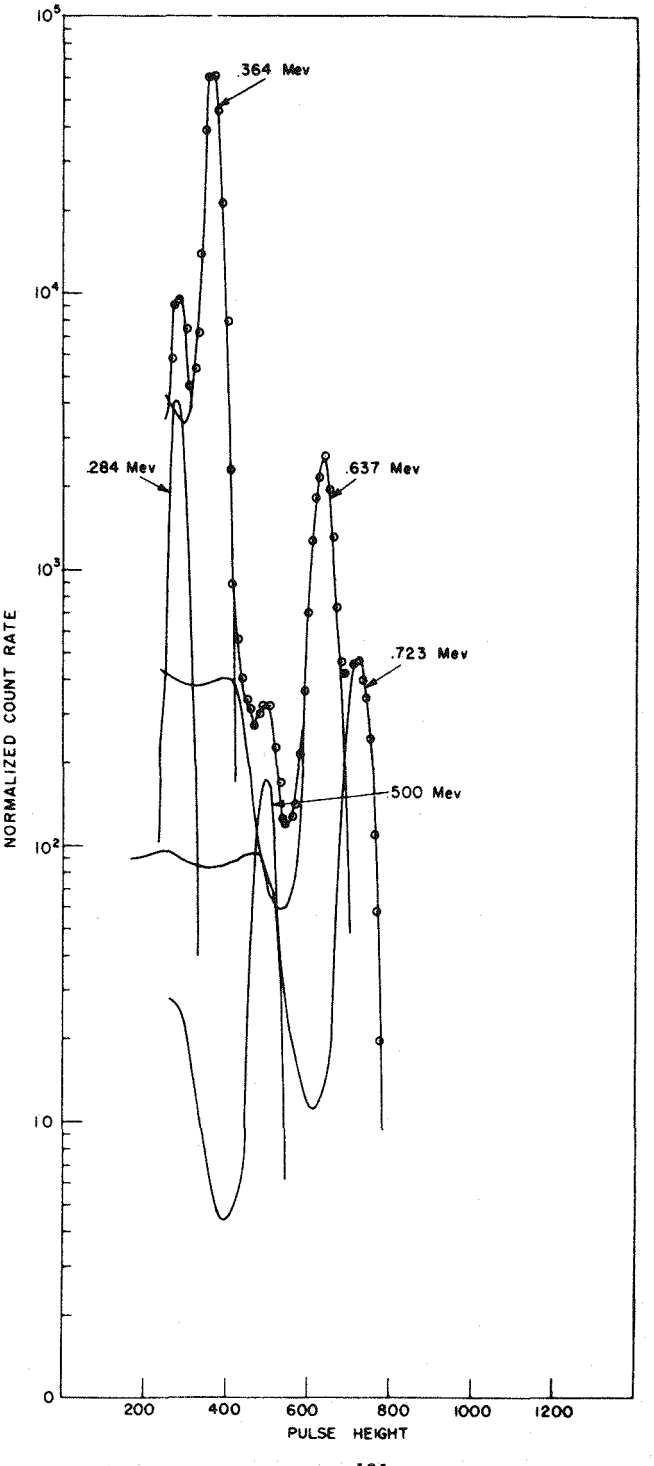

Fig. 1. Pulse-Height Spectrum of a Source of I^{131} Placed 10 cm from a 2- by 2-in. NaI(Tl) Crystal.

Table 1. I^{131} Gamma-Ray Spectra

Energy (Mev)	Least Mean Square	Bell *et al.*[a]	Haskins and Kurbatov[b]
0.284	5.2 ± 0.7	6.0	4.2
0.364	100 ± 9	100	100
0.500[c]	0.5 ± 0.1		
0.637	10.2 ± 1.2	10	7.2
0.722	2.4 ± 0.3	3	2.4

[a]Bell *et al.*, ref [2].
[b]Haskins and Kurbatov, ref [3].
[c]Possible contaminant.

Discrete Incident Energy Spectrum (Both the Energy Distribution and Intensity of the Incident Beam Unknown). – The difficulty in the application of the technique lies in the method of obtaining the minimum. The minimization should be made with respect to both β_n and A_{in}. The term A_{in} is a function of both pulse height and energy, while β_n is only a function of energy. Since the pulse-height spectra (A_{in}) are not known analytically as a function of pulse height and energy, it is extremely difficult to attempt to minimize Eq. (3) with respect to the A_{in} (i.e., numerical methods would introduce large errors in the calculation). Therefore, the following method was used.

The energy spectrum under consideration is divided into discrete increments. A monoenergetic pulse-height distribution corresponding to each increment is included. The energy components or increments will be chosen depending on the photopeaks observed in the measured distribution, and in those regions where the photopeaks are not obvious, the energy region is divided up depending upon the energy resolution of the system. Ideally, one can use relation (6) to obtain the values β_n for the various energy components. If a given energy component m is not present, β_m should be zero or the statistical variance in β_m should be greater than β_m itself. The presence of these zeros in the inverse transformation leads to the possibility of obtaining negative solutions, which in turn leads to oscillating components in the solution of Eq. (6). This problem is treated in detail in a work by Burrus [8]. In this paper it is pointed out that the source of error in unscrambling scintillation data by the incremental technique [i.e., simple inversion of Eq. (1)] can be attributed to an error amplification when the basic equations are solved exactly. As is stated in this paper, this amplification is caused by an attempt of the exact solution to restore rapidly fluctuating components in the original gamma-ray spectrum which have been attenuated below the statistical error level by the instrumental response. A first attempt to smooth out this fluctuation was made by this author using the least-squares technique described above. A further smoothing can be obtained by requiring not only that Eq. (3) lead to a minimum but that the solution for the β's be positive or zero.

Let us now consider a problem wherein this difficulty can be demonstrated. The problem is to determine the energies and intensities in the single-crystal spectrum of

W^{187}. The measured pulse-height spectrum is shown in Fig. 2, in which certain energies are easily identified from the resolved photopeaks. In Table 2 the various energies that were assumed present are tabulated. Also four iterations using the least-squares fitting technique are presented in Table 2.

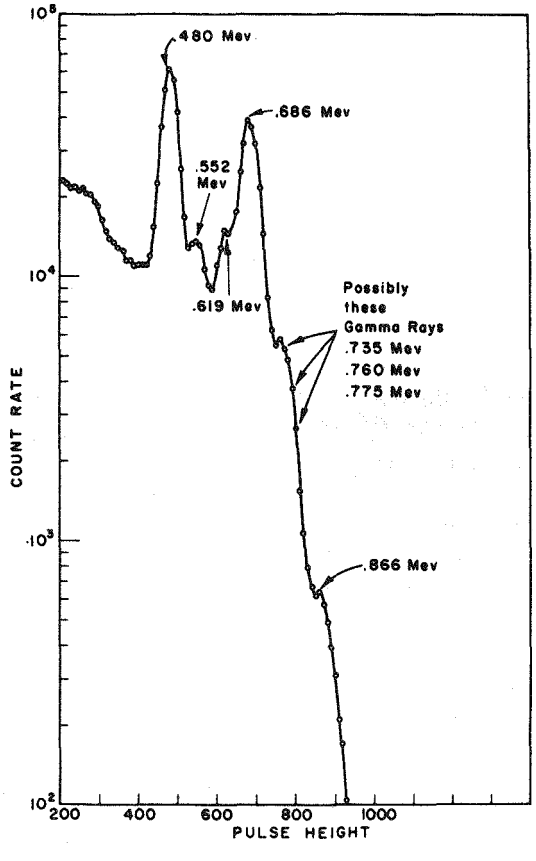

Fig. 2. Pulse-Height Spectrum of a W^{187} Source on a 2- by 2-in. NaI(Tl) Crystal at a Source-to-Crystal Distance of 10 cm.

A negative β is obtained for the 0.440-Mev gamma ray. In terms of the decay scheme of W^{187} it is found from other experimental and theoretical calculations that its intensity relative to the other gamma rays present is almost zero [9] and thus is lost in the background.

An interesting result to be noted is that a variation in the choice of energy components in one region does not seem to affect the values of β in the other energy regions. Further, an important result is obtained in the region of the 0.730- to 0.866-Mev peaks. In this region the energies cannot be resolved as separate (i.e., there is loss of resolution due to the smearing out of the information by the detector), but the results obtained show that the number of gamma rays in this region remain constant, although the distribution in the region changes depending upon the components chosen to represent the region. These results seem to hold for other cases investigated. Thus, it seems that when one cannot resolve the energy spectrum in a given region because of the finite resolution of the detection system, only the total number of gamma

Table 2. Results of Least-Squares Analysis of W^{187} Spectrum

Energy	For Data 731	For Data 741	For Data 733	For Data 743
0.866	0.464 ±0.008	0.462 ±0.008	0.438 ±0.007	0.437 ±0.007
0.775	1.93 ±0.06	1.94 ±0.06	2.95 ±0.02	2.94 ±0.04
0.760	1.72 ±0.09	1.69 ±0.09		
0.735	0.0245 ±0.0615	0.0383 ±0.0615	1.11 ±0.03	1.11 ±0.03
0.686	22.7 ±0.06	22.5 ±0.06	21.8 ±0.05	21.7 ±0.05
0.619	7.36 ±0.03	7.33 ±0.03	7.42 ±0.03	7.40 ±0.03
0.552	6.02 ±0.03	6.02 ±0.03	6.17 ±0.03	6.18 ±0.03
0.480	25.9 ±0.06	25.6 ±0.06	26.1 ±0.06	26.0 ±0.06
0.440	−0.601 ±0.035		−0.223 ±0.036	
0.301	0.112 ±0.032	0.136 ±0.032	0.115 ±0.032	0.123 ±0.032
0.256	0.867 ±0.040	0.850 ±0.040	0.806 ±0.040	0.799 ±0.040

rays in the region can be determined; however, the exact energy distribution in that region cannot be determined. The ability to resolve two energies can be related to the width of the photopeak at a half-maximum counting rate. This problem has been considered theoretically by Burrus [8]. There seems to be a minimum separation in the choice of monoenergetic components to be used in a given region depending on the width at half-maximum of the photopeak. This choice will also depend greatly on how well (i.e., to how many significant figures) the monoenergetic pulse-height spectra are known or can be known, for the least-squares analysis depends on differences in these numerical values.

The results obtained in this calculation for W^{187} agree well with other experimental and theoretical calculations. The results of this calculation and the decay scheme of W^{187} are discussed in a paper by Arns *et al.* [9].

A more general method of solution of this problem has been developed to handle such problems. Before outlining the method of solution for these cases, an example is presented to help clarify the discussion. The method described above and the method to be discussed below are applied to a simple problem.

A measurement is made with a three-channel pulse-height analyzer. The following data are obtained:

Channel i	Counts
1	3
2	2
3	3

It is known that the measured spectrum is some linear combination of the following functions:

Channel i	Normalized Count		
	A_{i1}	A_{i2}	A_{i3}
1	1	1	1
2	1	1	0
3	1	0	0

The following matrices are formed according to previous definitions:

$$A = \begin{pmatrix} 1 & 1 & 1 \\ 1 & 1 & 0 \\ 1 & 0 & 0 \end{pmatrix}, \tag{7}$$

$$A^T = \begin{pmatrix} 1 & 1 & 1 \\ 1 & 1 & 0 \\ 1 & 0 & 0 \end{pmatrix}, \tag{8}$$

$$\omega = \begin{pmatrix} 1/3 & 0 & 0 \\ 0 & 1/2 & 0 \\ 0 & 0 & 1/3 \end{pmatrix}, \tag{9}$$

$$\rho = \begin{pmatrix} 3 \\ 2 \\ 3 \end{pmatrix}.$$

Then,

$$(A^T \omega A) = \begin{pmatrix} 7/6 & 5/6 & 1/3 \\ 5/6 & 5/6 & 1/3 \\ 1/3 & 1/3 & 1/3 \end{pmatrix}, \tag{10}$$

$$(A^T \omega A)^{-1} = \begin{pmatrix} 3 & -3 & 0 \\ -3 & 5 & -2 \\ 0 & -2 & 5 \end{pmatrix}, \tag{11}$$

$$(A^T \omega A)^{-1} A^T \omega = \begin{pmatrix} 0 & 0 & 1 \\ 0 & 1 & -1 \\ 1 & -1 & 0 \end{pmatrix}. \tag{12}$$

The β's, or intensities, of each component vector can be determined from Eq. (6):

$$\beta = (A^T \omega A)^{-1} A^T \omega \rho ,$$

and

$$\beta = \begin{pmatrix} 0 & 0 & 1 \\ 0 & 1 & -1 \\ 1 & -1 & 0 \end{pmatrix} \begin{pmatrix} 3 \\ 2 \\ 3 \end{pmatrix} = \begin{pmatrix} 3 \\ -1 \\ 1 \end{pmatrix} . \tag{13}$$

That is, the sum of the vectors (1,1,1), (1,1,0) and (1,0,0) which yields the best fit to the experimental data using the least-squares criteria is 3(1,1,1) – 1(1,1,0) + (1,0,0) = (3,2,3). The residual is zero.

Now if it is known that the intensities must be positive, the least-squares fit must be made so as to require Eq. (3) to be a minimum with the constraint $\beta_1 \geqq 0$, $\beta_2 \geqq 0$, and $\beta_3 \geqq 0$. One could proceed by eliminating the negative element and then reevaluating Eq. (6). That is, the following matrices are now formed:

$$A = \begin{pmatrix} 1 & 1 \\ 1 & 0 \\ 1 & 0 \end{pmatrix} , \tag{14}$$

$$A^T = \begin{pmatrix} 1 & 1 & 1 \\ 1 & 0 & 0 \end{pmatrix} , \tag{15}$$

and ω remains the same.

Then

$$(A^T \omega A) = \begin{pmatrix} 7/6 & 1/3 \\ 1/3 & 1/3 \end{pmatrix} , \tag{16}$$

$$(A^T \omega A)^{-1} = \begin{pmatrix} 6/5 & -6/5 \\ -6/5 & 21/5 \end{pmatrix} , \tag{17}$$

$$(A^T \omega A)^{-1} A^T \omega = \begin{pmatrix} 0 & 3/5 & 2/5 \\ 1 & -3/5 & -2/5 \end{pmatrix} . \tag{18}$$

Using these matrices, β is found to be

$$\beta = (A^T \omega A)^{-1} A^T \omega \rho = \begin{pmatrix} 0 & 3/5 & 2/5 \\ 1 & -3/5 & -2/5 \end{pmatrix} \begin{pmatrix} 3 \\ 2 \\ 3 \end{pmatrix} = \begin{pmatrix} 12/5 \\ 3/5 \end{pmatrix} . \tag{19}$$

These results indicate that the best fit requiring only a positive or zero value of β is 2.4(1,1,1) + 0(1,1,0) + .6(1,0,0) = 3,2.4,2.4.

The method just completed is rather simple but one must be careful in the method of eliminating the negative components. A method for minimizing quadratics subject to various constraints is described by Beale [12]. The following is an application to the above problem, and is a simplification of the work found in Ref. [12]. The simplification is possible, since when applying the technique to pulse-height analysis, the only constraint required is that of a positive solution for the β's when minimizing the quadratic.

In this method one forms the quadratic given in Eq. (3). For the conditions in the problem discussed above, Eq. (3) can be written as

$$M = 8 - 6\beta_1 - 4\beta_2 - 2\beta_3 + \frac{7}{6}\beta_1^2 + \frac{5}{6}\beta_2^2 + \frac{1}{3}\beta_3^2 + \frac{5}{3}\beta_1\beta_2 + \frac{2}{3}\beta_1\beta_3 + \frac{2}{3}\beta_2\beta_3 . \quad (20)$$

M is to be minimized and also the constraint and $\beta_1 \geqq 0$, $\beta_2 \geqq 0$, $\beta_3 \geqq 0$ is to be applied.

A geometric solution of the problem can be considered with reference to Fig. 3. The method of solution proceeds in the following manner. Start at point 0 (Fig. 3); that is, assume the solution $\beta_1 = \beta_2 = \beta_3 = 0$. Keep $\beta_2 = \beta_3 = 0$, and increase β_1 in a positive direction. As β_1 increases along this direction, M will decrease until we reach point A. Point A is determined by taking the derivative of M with respect to β_1 and setting the derivative equal to zero with $\beta_2 = \beta_3 = 0$. Then

$$\frac{\partial M}{\partial \beta_1} = -6 + \frac{7}{3}\beta_1 + \frac{5}{3}\beta_2 + \frac{2}{3}\beta_3 = 2u_1 . \quad (21)$$

Then for

$$u_1 = \beta_2 = \beta_3 = 0, \ \beta_1 = 18/7 .$$

The coordinates of A are (18/7, 0, 0). The plane $u_1 = 0$ in the space described by β_1, β_2, and β_3 contains all points β_1 for which M is a minimum given any values of β_2 and β_3.

Continuing the solution, it is found that increasing β_1 any further will only increase M. A change of basis is now made. By using Eq. (21), β_1 is found in terms of u_1, β_2, and β_3.

$$\beta_1 = \frac{6}{7}\left(u_1 + 3 - \frac{5}{6}\beta_2 - \frac{1}{3}\beta_3\right) . \quad (22)$$

This substitution is now made in (19) and

$$M = \frac{2}{7} + \frac{2}{7}\beta_2 = \frac{2}{7}\beta_3 + \frac{6}{7}u_1^2 + \frac{5}{21}\beta_2^2 + \frac{5}{21}\beta_3^2 + \frac{4}{21}\beta_2\beta_3 . \quad (23)$$

Now, keep $u_1 = \beta_3 = 0$ and change β_2 while attempting to decrease M; that is, β_2 is increased or decreased by moving along the line of intersection of the $u_1 = 0$ plane and $\beta_3 = 0$ plane. This intersection is along the line $\overline{AKL}$ indicated in Fig. 3. The problem is to determine in which direction a point should be moved along $\overline{AKL}$ so that M decreases. This can be done by taking the derivative of M [cf., Eq. (20)] with respect to β_2:

$$\frac{\partial M}{\partial \beta_2} = \frac{2}{7} + \frac{10}{21}\beta_2 + \frac{4}{21}\beta_3 + \frac{10}{7}u_1 \quad (24)$$

at

$$\frac{\partial M}{\partial \beta_2} = \beta_3 = u_1 = 0, \ \beta_2 = -\frac{3}{5} .$$

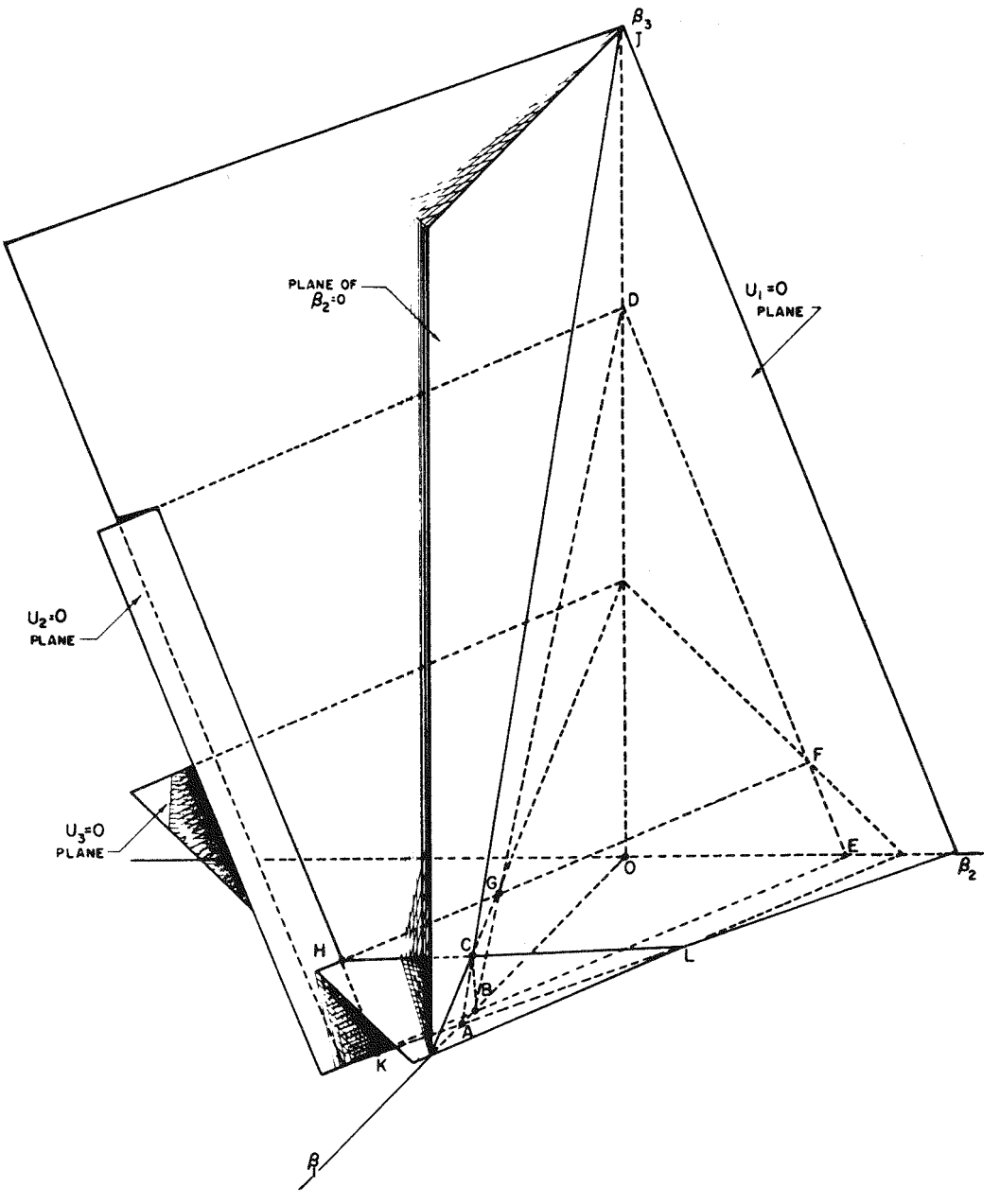

Fig. 3. Geometric Solution of Least-Squares Fitting Problem.

β_2 must go negative to decrease M. This cannot be allowed because of the constraints; therefore β_2 must be made zero. In this case $\beta_2 = u_2'$ and again substitution is made in Eqs. (20) and (21). The plane $u_2' = 0$ is the plane of all values of β_2 given any β_1, β_3 for which M is a minimum within the constraints of the problem. Of course, because of Eq. (24) $\beta_2 = 0$ for all values of β_1 and β_3.

Again we start at point A, and an attempt is made to minimize M by increasing β_3 from zero; β_3 is increased along line $\overline{ACJ}$, the intersection of the $u_1 = 0$ and $u_2' = 0$ planes. This ensures that β_1 and β_2 will have values which will yield a minimum value of M within the constraint $\beta_1 \geqq 0$, $\beta_2 \geqq 0$ for any value of β_3. By using Eq. (20) and by taking the partial derivative of M with respect to β_3, the direction of increase or decrease of β_3 (and also the value of β_3) can be determined so as to minimize M:

$$\frac{\partial M}{\partial \beta_3} = -\frac{2}{7} + \frac{10}{21}\beta_3 + \frac{4}{21}u_2 + \frac{4}{7}u_1 = 2u_3 \tag{25}$$

for $u_3 = u_2' = u_1 = 0$, $\beta_3 = 3/5$. This value of β_3 along with the value $\beta_2 = u_1 = 0$ can be substituted in Eq. (22) to determine the value of β_1:

$$\beta_1 = \frac{6}{7}\left[3 - \left(\frac{1}{3}\right)\left(\frac{3}{5}\right)\right] = \frac{12}{5}.$$

This is point C on Fig. 3 and corresponds to the intersections of the $u_1 = 0$, $u_2' = 0$, and $u_3 = 0$ planes. Thus the values of β_1, β_2, and β_3 required to minimize Eq. (20) within the constraints that $\beta_1 \geqq 0$, $\beta_2 \geqq 0$, and $\beta_3 \geqq 0$ are, respectively, 12/5, 0, and 3/5. This is the same result as that obtained in Eq. (19). If the solution is contained ignoring the constraints, the absolute minimum (3, –1, 1) is obtained. This is the point H, the intersection of the $u_1 = 0$, $u_2 = 0$, and $u_3 = 0$ planes. The solution will be independent of the path taken to reach the solution.

The method applied to a case where there are n values of β_n to be determined can be outlined as follows:

1. Using Eq. (3), form the quadratic $M = M(\beta_1, \beta_2, \ldots, \beta_n)$.
2. Take the partial derivative of M with respect to β_1, and let $2u_1 = \partial M/\partial \beta_1$.
3. Let $u_1 = \beta_2 = \beta_3 = \ldots = \beta_n = 0$ and solve for β_1. If $\beta_1 > 0$, then solve for β_1 in terms of $u_1, \beta_2, \ldots, \beta_n$. Substitute this value of β_1 into the equation for M. Now, $M = M(u_1, \beta_2, \ldots, \beta_n)$. In this first time around the β_1 chosen will always be positive.
4. Now using the quadratic M found in step 3, the partial derivative of M is taken with respect to β_2. Let $2u_2 = \partial M/\partial \beta_2$.
5. Let $u_1 = u_2 = \beta_3 = \ldots = \beta_n = 0$ and solve for β_2. If $\beta_2 > 0$, then solve for β_2 in terms of $u_1, u_2, \beta_3, \ldots, \beta_n$ and substitute this value in the equation for M (step 3). If $\beta_2 \leqq 0$, then let $\beta_2 = u_2'$ and substitute this value of β_2 into M (step 3).
6. The above procedure is continued for all β's. At each step the values for all the β's considered up to that point are determined. If any of these β's are negative, one makes the change of variable $\beta_k = u_k'$. Further, if a previous change of variable was made introducing a $u_j = \partial M/\partial \beta_j$, u_j must be eliminated from the function M by using the relations $u_j' = \beta_j$ and $u_j = \partial M/\partial \beta_j$ before continuing the iterative process.
7. The n values of β are found after the last iteration by setting all u and u' equal to zero.

This solution is equivalent to the following matrix approach: Assume the measured distribution is made up of only two components (e.g., the A_{i1}'s and A_{i2}'s). One can use least-squares fitting to obtain the β_1 and β_2 from Eq. (6). It has been assumed that the $\beta_3 = \beta_4 = \ldots = \beta_n = 0$. If $\beta_1 > 0$ and $\beta_2 > 0$, then one adds a third

component (e.g., A_{i3}'s) and solves (6) for β_1, β_2, and β_3. If any of these β's are negative, one sets that given β_i equal to zero by eliminating the A_{ij} components from the matrix calculation involved in Eq. (6). In this way, the n components are added one at a time, the β's determined for each addition and if any one of the β's determined is negative, that β is set equal to zero and its corresponding component eliminated from the matrix A before adding another one of the n components to A. The solution for the β's after all n components have been added in the manner prescribed above will give the values for the β's for which M is a minimum and $\beta_1 \geqq 0$, $\beta_2 \geqq 0, \ldots, \beta_n \geqq 0$.

The number of monoenergetic pulse-height spectra used in performing the above will depend upon the energy resolution of the system. If the energy distribution of the incident flux in some region is such that the energy separation between the various energy components is less than some fraction of the half-widths of the photopeaks in this region, it may be only possible to determine the total number of gamma rays in this region without being able to determine uniquely the energy distribution in this region. The half-width of the photopeak is a measure of the energy resolution of system.

A FORTRAN program has been written for the IBM 7090 computer which makes use of the solution described above. The following options are available: The weighting function matrix ω can be set equal to the unity matrix, set equal to $1/\rho$, or read in as input. The calculation can be performed with or without iteration. So that only the fast memory of the computer is used, the following limitation on the size of the A matrix (i.e., matrix of monoenergetic or monoelemental pulse-height spectra) has been set: The maximum number of channels or numbers describing a given component spectrum is 250, and the maximum number of component spectra is 40. When the iterative process is used, there is no limit on the number of component spectra, but it is necessary to impose the restriction that no more than 40 components be used in a given iteration. There is always the limitation that no more than 250 channels or numbers be used for a given component. It should be emphasized that these size limitations are due to the computer's memory capacity and are not due to the mathematical method.

ERROR IN THE CALCULATION

Once the β's in Eq. (6) have been determined, it is possible to determine the mean square deviation in β. If it is assumed that the A_{ij}'s (i.e., the pulse-height spectra) are known without error this calculation is rather simple. Then, due to the variation in the measurement in ρ_i, there will be a corresponding mean square deviation [1] in the determination of the β's. Using Eqs. (4) and (6),

$$\beta_\lambda = \sum_i \sum_\nu C^{-1}_{i\lambda} A_{i\nu} \omega_i \beta_i . \tag{26}$$

The following definitions are used: the matrix $C = (A^T \omega A)$ is a symmetric matrix and the elements $C_{\nu\gamma}$ of C are given by

$$C_{\nu\gamma} = \sum_i \omega_i A_{i\nu} A_{i\gamma} ; \tag{27}$$

C^{-1} is the inverse of the matrix of C. The elements of C^{-1} are written as $C^{-1}_{\lambda\gamma}$. Thus, $CC^{-1} = I$, where I is the identity matrix with elements $I_{\nu\lambda}$ and

$$I_{\nu\lambda} = \sum_{\gamma} C_{\nu\gamma} C^{-1}_{\gamma\lambda} ; \tag{28}$$

recall that both C and C^{-1} are symmetric matrices. Further,

$$\begin{aligned} I_{\nu\lambda} &= 1 \qquad \text{if } \nu = \lambda , \\ I_{\nu\lambda} &= 0 \qquad \text{if } \nu \neq \lambda . \end{aligned} \tag{29}$$

From Eq. (6) it is seen that β_λ is a linear homogeneous function of the counts, under the assumption that there is no error in the A_{ij}'s. Thus the mean square deviation $\sigma^2(\beta_\lambda)$ corresponding to the variation in ρ_i can be written as

$$\sigma^2(\beta_\lambda) = \sum_i \sum_\nu \sum_\gamma C^{-1}_{\nu\lambda} C^{-1}_{\gamma\lambda} A_{i\nu} A_{i\gamma} \omega^2 \sigma^2(\rho_i) ,$$

where $\omega_i = 1/\sigma_i^2(\rho_i)$. Then

$$\sigma^2(\beta_\lambda) = \sum_i \sum_\nu \sum_\gamma C^{-1}_{\nu\lambda} C^{-1}_{\gamma\lambda} A_{i\nu} A_{i\gamma} \omega_i$$

or

$$\sigma^2(\beta_\lambda) = \sum_\nu \sum_\gamma C^{-1}_{\nu\lambda} C^{-1}_{\gamma\lambda} \sum_i \omega_i A_{i\nu} A_{i\gamma} .$$

Then from Eq. (27):

$$\sigma^2(\beta_\lambda) = \sum_\nu \sum_\gamma C^{-1}_{\gamma\lambda} C_{\gamma\lambda} C_{\nu\gamma} ,$$

or

$$\sigma^2(\beta_\lambda) = \sum_\nu C^{-1}_{\nu\lambda} \sum_\gamma C_{\nu\lambda} C^{-1}_{\gamma\lambda} ,$$

and from Eqs. (28) and (29),

$$\sigma^2(\beta_\lambda) = C^{-1}_{\lambda\lambda} ; \tag{30}$$

that is, $\sigma^2(\beta_\lambda)$ can be found from the diagonal elements of the C^{-1} matrix. The mean square deviation $\sigma^2(\rho_i)$ in the simplest case is

$$\sigma^2(\rho_i) = \rho_i . \tag{31}$$

Depending on the experimental situation, the corresponding σ_i's can be determined and used as above. The probable error can then be determined from the mean square deviation.

The above considerations are only true if it is assumed that the A_{ij}'s are known without error, that the set of A_{ij}'s chosen are the correct set, and that the set of pulse-height spectra are linearly independent (i.e., there is no interference between various

components). Further calculations are therefore carried out in an attempt to determine whether these problems contribute a significant error in the calculations.

A factor indicating percent interference can be calculated as follows:

$$\text{In} = \frac{(C^{-1}_{\lambda\gamma})^2}{C^{-1}_{\lambda\lambda}\, C^{-1}_{\gamma\gamma}} \times 100\% \,. \tag{32}$$

It was shown above that $C^{-1}_{\lambda\lambda}$ is the variance on β_λ, and it can be shown (ref [10]) that $C^{-1}_{\lambda\gamma}$ is the covariance of the λ and γ component. Then Eq. (32) is a measure of interference between the λ and γ component (ref [10], [11]).

ANALYSIS OF A COMPLEX GAMMA-RAY SPECTRUM

The following experiment was designed to test the analytic method described above. A mixture of ten different elements was activated in a thermal-neutron flux for a given length of time and the pulse-height spectrum of the activated sample was measured as a function of time. Then a known amount of each element in the mixture was activated in the same neutron flux for the same length of time as the mixture, and the pulse-height spectrum of each of these elements was measured in the same geometrical configuration as that for the mixture. A 3- by 3-in. NaI(Tl) crystal with a 200-channel pulse-height analyzer was used for the measurement. A pulse-height distribution recorded soon after irradiation is shown in Fig. 4. The background spectrum was included as a separate pulse-height distribution. Furthermore, it was noticed that due to the presence of some air in the sample, argon gas had been activated and

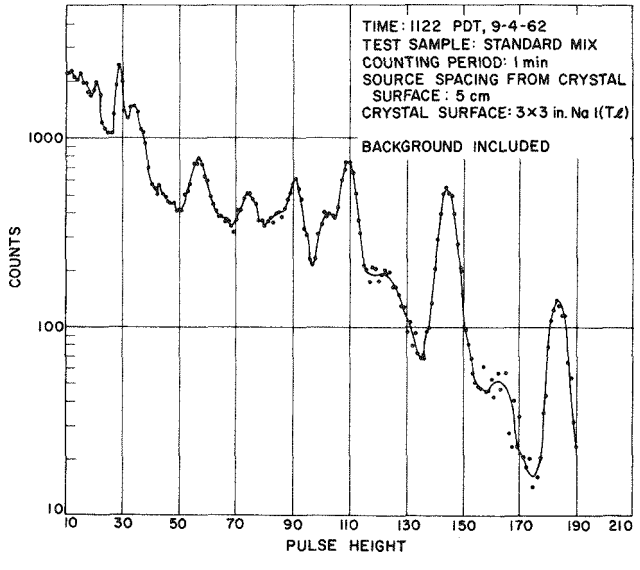

Fig. 4. Pulse-Height Distribution for a Test Sample Containing 10 Different Elements Which Had Been Irradiated with Thermal Neutrons.

tended to perturb the measurement of the pulse-height spectra of the various other elemental spectra. A pure argon pulse-height spectrum was measured and an attempt was made to subtract this effect from the spectra of the various other nuclear species. The argon spectrum was included in the analysis of the mixture spectrum. Finally, it was noticed that a significant amount of sodium was present in the supposedly pure chromium spectrum. The contribution of the sodium spectrum to the chromium spectrum was subtracted out, and a "pure" chromium spectrum was obtained.

Since the mixture and each of the various nuclear species were activated in the same neutron flux for the same length of time, and since the standard spectra used in the analyses were those due to the activation of the various nuclear species, the results of the least-squares analysis were in terms of relative abundance of the nuclear species in the mixture to the amount in the standard. Because there is radioactive decay of the standards and mixture, decay time corrections must be made to determine the absolute abundance from the relative abundance. The relative abundances obtained from the least-squares analysis are given in Table 3. The zeros indicate that the given nuclear species has been rejected in the fit

Interferences between the various component spectra were then calculated. Some of those interferences which were found to be significant are plotted in Fig. 5. From curves of this type it was apparent that significant errors would be expected in the calculation of the intensities due to background, La, K, Na, and Sc. At certain times the interference may be great, but if one nuclear species decays away, the interference will become negligible.

After correcting for decay, the analysis of the mixture was obtained. The results are given in Table 4 and compared with the actual composition of the mixture. The calculated errors indicated in the table do not include interference effects.

The calculation for sodium seems to be rather poor but it must be remembered that sodium was detected in the chromium standard; this may partially explain the discrepancy. Further, it should be noted that in those cases wherein there was significant interference, one element would be overestimated while the other with which there was interference would be underestimated. Otherwise, the results seem to be in rather good agreement within the statistical variance involved in the experiment.

The interference effect may be greatly reduced by breaking up the various standard spectra into monoenergetic components and using these monoenergetic components for the analysis. This group of monoenergetic spectra should be a linearly independent group.

It can further be seen that there is a very significant interference by background. Therefore, it seems best to subtract background and perform the analysis. In this problem, the background was very small compared to the counts above background so that when the analysis was redone with the background subtracted, there were no significant differences from those reported in Table 4.

Finally, it should be pointed out that the analysis is only as good as the set of fitting spectra available. Spectra such as those due to bremsstrahlung should be included in the library of functions used for analysis. At the present, a chi-square test is being prepared for inclusion in the analysis for testing the goodness of fit. This test, plus the calculation of interference, should indicate whether such difficulties as the shifting of gain and the lack of a complete library of functions have perturbed the analysis.

Table 3. Relative Intensities of Various Nuclear Species in Mixture Obtained Using Least-Squares Analysis[a]

Nuclear Species	Oct. 4 1122	Oct. 4 1146	Oct. 4 1259	Oct. 4 1633	Oct. 5 0827	Oct. 5 1641	Oct. 6 0900	Oct. 7 1329	Oct. 11 0914
Background	9.44	9.55	33.6	3.66	4.72	4.86	5.86	6.87	1.91
Na^{24}	19.9	19.1	15.2	17.1	7.22	3.86	2.12	0.0	0.0
Cl^{38}	0.68	0.466	0.133	0.0	0.0	0.0	0.0	0.0	0.0
K^{42}	8.78	7.67	5.59	6.5	3.28	2.34	0.0630	0.0	0.0
Mn^{56}	0.0691	0.0669	0.0382	0.0166	0.00173	0.0048	0.0	0.0	0.0
Sc^{46}	0.0340	0.0340	0.0422	0.0442	0.0488	0.0466	0.0360	0.0431	0.0413
A^{41}	0.0	0.0	0.0	0.0	0.0	0.00806	0.0	0.0	0.0
As^{76}	10.6	12.5	11.3	9.75	6.04	4.52	3.54	1.65	0.363
Cu^{64}	4.45	3.49	1.94	2.91	1.77	1.38	0.183	0.148	0.0493
Cr^{51}	4.00	3.93	3.60	4.81	5.0	4.94	4.12	4.39	4.13
I^{128}	18.1	9.6	0.0	0.0	0.138	0.0274	0.0	0.0	0.132
La^{140}	5.68	4.79	4.41	3.98	2.30	1.91	1.57	0.989	0.199

[a]Mixture removed from reactor Oct. 4, 1962 at 1055.

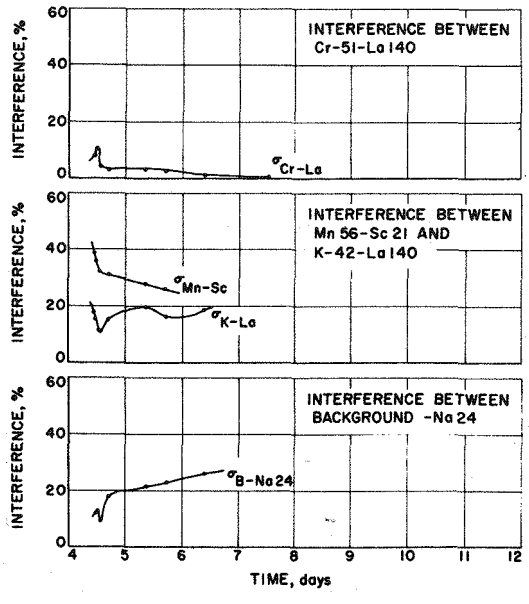

Fig. 5. Typical Plots of Interference as a Function of Time for a Few of the Components in Fig. 4.

Table 4. Experimental Determination of Composition

Element	Prepared Sample	Experimental Determinations
Sodium	5.00 μgm	7.7 ±1 μgm
Chlorine	36.8 μgm	38.0 ±3.8 μgm
Potassium	0.404 mgm	0.301 ±0.011 mgm
Manganese	0.101 μgm	0.0904 ±0.0018 μgm
Scandium	14.2 μgm	12.2 ±2.5 μgm
Arsenic	5.00 μgm	4.98 ±0.11 μgm
Copper	2.23 μgm	2.11 ±0.16 μgm
Chromium	1.82 mgm	1.56 ±0.24 mgm
Iodine	2.49 μgm	2.68 ±0.08 μgm
Lanthanum	2.19 μgm	3.02 ±0.04 μgm

REFERENCES

[1] M. E. Rose, "The Analysis of Angular Correlation and Angular Distribution Data," *Phys. Rev.* **91**, 610 (1953).

[2] R. E. Bell, R. L. Graham, and H. E. Petch, "Disintegration Scheme of I^{131}," *Can. J. Phys.* **30**, 35 (1952).

[3] J. R. Haskins and J. D. Kurbatov, "The Disintegration of I^{131}," *Phys. Rev.* **88**, 884 (1952).

[4] P. R. Bell, "The Scintillation Process," in *Beta and Gamma-Ray Spectroscopy* (ed. by Kai Siegbahn), North-Holland Publishing Co., Amsterdam, 1955.

[5] S. H. Vegors, L. L. Marsden, and R. L. Heath, *Calculated Efficiencies of Cylindrical Radiation Detectors*, IDO-16370 (Sept. 1, 1958).

[6] W. F. Miller, J. Reynolds, and W. J. Snow, *Efficiencies and Photofractions for Gamma Radiation on NaI(Tl) Activated Crystals*, ANL-5902 (August 1958).

[7] J. E. Francis, C. C. Harris, and J. I. Trombka, "Variation of NaI(Tl) Detection Efficiencies with Crystal Size and Geometry for Medical Research," ORNL-2204 (Feb. 12, 1957).

[8] W. R. Burrus, "Unscrambling Scintillation Spectrometer Data," *IRE Trans. on Nucl. Sci.* **INS-7**(2–3) (1960).

[9] R. G. Arns and M. L. Wiedenbeck, "Energy Levels of Re^{187}," University of Michigan Research Institute Report 2863-2-P (August 1960).

[10] Henry Scheffe, *The Analysis of Variance*, Wiley, New York, 1959.

[11] C. A. Bennett and N. L. Franklein, *Statistical Analyses in Chemistry and the Chemical Industry*, Wiley, New York, 1954.

[12] E. M. L. Beale, "On Quadratic Programming," *Naval Res. Logistics Quart.* **6** (Sept. 1959).

(4-4) NONLINEAR LEAST-SQUARES FITTING APPLIED TO GAMMA-RAY SCINTILLATION DETECTOR RESPONSE FUNCTIONS

R. O. Chester, R. W. Peelle, and F. C. Maienschein
Oak Ridge National Laboratory[1]
Oak Ridge, Tennessee

INTRODUCTION

All gamma-ray spectrum analysis techniques must have available the response of the data collection system for all gamma-ray energies covered by the experiment. In the following work, data were recorded as counts per pulse-height channel. Before analysis, data were converted to counts/kev vs pulse height in kev to make the data independent of

[1]Operated by Union Carbide Corporation for the U.S. Atomic Energy Commission.

analyzer gain (but not of channel width). Therefore, the response function for this data collection system is a function of the source gamma-ray energy, pulse height, and detector geometry. Source gamma-ray energy and pulse height are treated as independent variables, while detector geometry dictates the exact form of the analytic functions employed. A number of constants in the analytic functions were determined by best fits in the least-squares sense to actual data from calibrated sources.

The most widely used methods of response function generation first obtain counts per pulse-height channel for a number of monoenergetic source gamma rays. Interpolation between these fitted monoenergetic response functions has almost always been performed entirely by linear or higher order polynomial approximations. For a given pulse height, the relative number of counts per channel has been interpolated as a function of input gamma energy. All of these methods usually require storage and continual reference to the monoenergetic spectra. By contrast, the method described in this paper requires only the storage of 20 constants and a formula. Figure 1 shows a slab of the response function for a range of gamma-ray energies and one of the calibration spectra.

Each method, however, has unique advantages and disadvantages. The single formula approach was selected because the available monoenergetic spectra were relatively widely spaced in energy and several of the spectra involved two or more prominent gamma-ray energies. Physically unrealistic oscillations such as those that frequently arise in polynomial interpolations were unacceptable.

To illustrate the method, the response function for the single crystal will be discussed in detail. The method used for response function generation for the Compton and pair spectrometers will only be summarized.

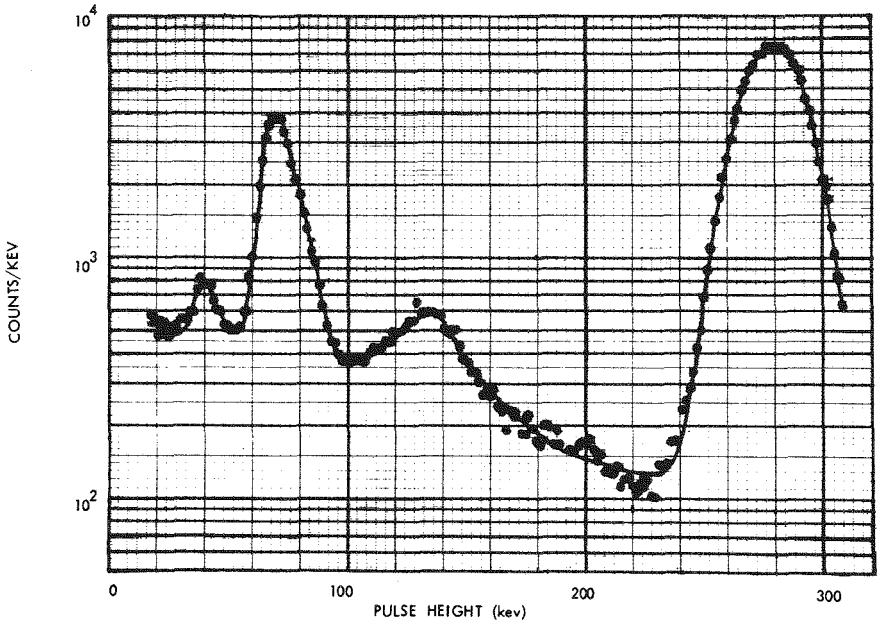

Fig. 1. A Slice of the Single-Crystal Response Function Showing the Calibration Spectrum for Cs^{137}.

PREPARATION OF THE DATA AND THE WEIGHT MATRIX

The data, obtained as counts/channel vs channel number, were converted to counts/kev vs energy corresponding to the pulse-height channel in kev by the following relations:

$$p_i = \frac{(C_i - Q - \Delta C_i)}{K},$$

$$y_i = \frac{(CC_i - B_i)K}{1 + (d\Delta C/dC)|_{C = C_i}},$$

where

p_i = absorbed electron energy corresponding to the ith pulse-height channel,

y_i = counts per kev in the ith pulse-height channel,

C_i = channel number,

CC_i = counts per channel in the ith pulse-height channel,

B_i = measured or estimated background in the ith pulse-height channel,

K = analyzer gain in channels/kev,

Q = analyzer zero, the channel number for which the pulse height is zero on a linearized scale,

ΔC_i = channel number difference to compensate analyzer nonlinearity for the ith pulse channel, based on sliding pulser measurements (typical values were between ±0.3 and ±0.002 channels).

The expression $(d\Delta C/dC)|_{C = C_i}$ is the derivative of a third order polynomial fit to ΔC vs C at $C = C_i$. Twenty channels were fitted at one time and each fit advanced ten channels. Therefore, except for the five channels at the low- and high-channel number ends of the analyzer, only the ten center channels of each fit were used to evaluate $d\Delta C/dC$. Typical values of $d\Delta C/dC$ ranged between ±0.03 and ±0.0001.

The observed counts per kev in each pulse-height channel, y_i, are assumed uncorrelated. As a result, the weight matrix for the data is diagonal.

The variance of y_i is in this case equal to $1/W_{ii}$,

where

variance of $y_i = [CC_i + (\Delta B_i)^2]\{K^2/[1 + (d\Delta C/dC)|_{C = C_i}]^2\}$,

W_{ii} = ith diagonal term of the weight matrix to be used in the least-squares fit,

$\Delta B_i = \sqrt{B_i}$ for a measured background of equivalent counting time, or ΔB_i = estimated error in an estimated background.

RESPONSE FUNCTION GENERATION

The first step in the interpolation procedure is the choice of an equation whose shape is believed to be adaptable to the experimental data by proper choice of the

free parameters. While the detail in the data as a function of pulse height in our case is quite fine, only relatively few points are available for the interpolation as a function of gamma energy. Therefore, special attention was given to the variation of the shape features of the response function with the source gamma-ray energy.

The observed counts per kev in the ith pulse-height channel of the observed spectrum for monoenergetic gamma rays of energy E, is approximated by the relation

$$y_i \tilde{=} \frac{Qt}{\Delta p_i} \int_{p_i - \Delta p_i/2}^{p_i + \Delta p_i/2} F(p, E, \mathbf{d}) dp = Qt\, f(p_i, E, \mathbf{d}) \tilde{=} Qt\, F(p_i, E, \mathbf{d}) \frac{\Delta p_i}{\Delta p_i}, \qquad (1)$$

where

Qt = source strength = total number of photons emitted with energy E,

Δp_i = width of ith pulse-height channel $\tilde{=} 1/K$,

$F(p, E, \mathbf{d})$ = number of counts per kev at energy, p, per photon of energy E, emitted by the source,

$f(p_i, E, \mathbf{d})$ = calculated counts per kev in the ith pulse-height channel per gamma ray of energy E.

If two or more gamma rays are given off by the isotope in question, the observed number of counts y_i is approximated by a sum of terms of the type in Eq. (1).

In practice, actually performing the integration was unnecessary except where $F(p, E, \mathbf{d})$ varied very nonlinearly within Δp_i. For example, it was considered unnecessary to integrate a Gaussian unless the peak was evident in fewer than five channels. In this case $Qt\, F(p_i, E, \mathbf{d})$ differs from $Qt\, f(p_i, E, \mathbf{d})$ by no more than 3%.

In generating response function formulas, an attempt was made to adhere to the following requirements:

1. Data from all the standard calibration sources should be used simultaneously in the nonlinear fitting procedure to obtain the fit parameters $\mathbf{d}$.
2. $F(p_i, E, \mathbf{d})$ should be the sum of terms, each of which represents an obvious shape feature of the observations when plotted as a function of pulse height for a fixed gamma energy E. (For example, for the single-crystal spectrometer, $F(p_i, E, \mathbf{d})$ = photopeak + Compton distribution + backscatter peak + escape peaks + x-ray peaks + iodine escape peaks.)
3. For convenience in combining source strength information, a single normalizing constant should appear before the entire expression $F(p_i, E, \mathbf{d})$, representing the photopeak efficiency.
4. The variation of the shape features with gamma-ray energy, E, should be physically plausible.

The function below is a simplification of the expression used for the single-crystal spectrometer data:

$f(p_i, E, \mathbf{d})$ = (photopeak area) [(unit area Gaussian for the photopeak)

+ (relative backscatter peak area) (unit area Gaussian for backscatter peak) + (Compton distribution) + (Gaussian for iodine escape peak)] .

Details of the single-crystal response function are discussed in Appendix II.

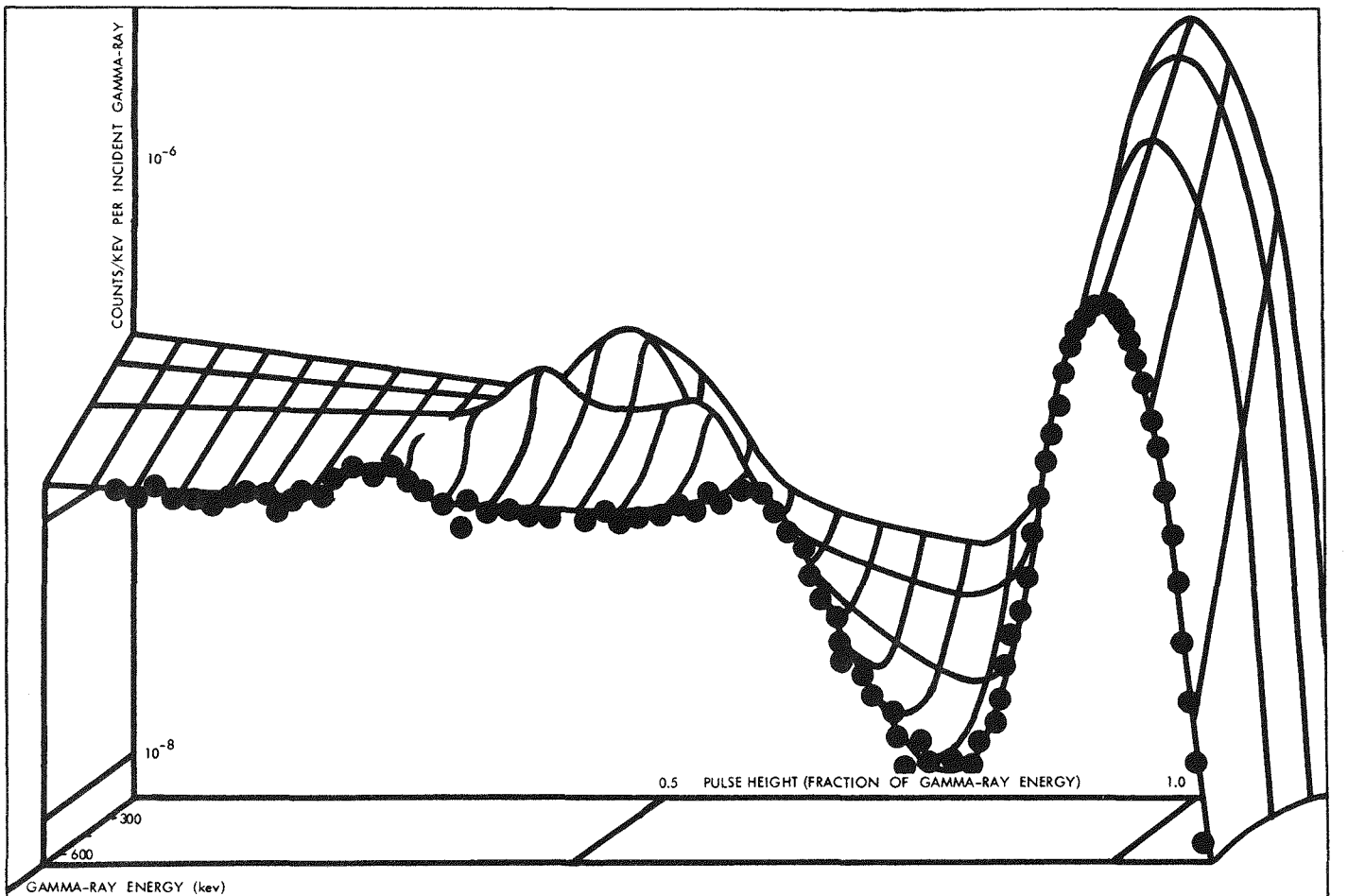

Fig. 2. Calibration Spectrum for Hg^{203}.

In addition, many of the calibration runs include x-ray peaks and iodine escape peaks, and some of the data contain two or more photopeaks and associated Compton and backscatter features. Figure 2 shows the calibration spectrum of Hg^{203} as an example.

CALCULATION OF FIT PARAMETERS

The above equation for the single-crystal response function is nonlinear in the fit parameters, d_k; therefore, it is necessary to use an iterative method for the solution of the least-squares problem [*1*, *9*, *11*]. A modified Gauss-Seidel method of analysis was employed [*4*, *5*, *14*] and is outlined below.

The function $f(p_i, E, \mathbf{d})$ is approximated by its value at some estimated $\mathbf{d}$, called $\mathbf{d}_0$, plus the first term in the Taylor's series expansion of $f(p_i, E, \mathbf{d})$ in the differences $\beta = \mathbf{d} - \mathbf{d}_0$:

$$f(p_i, E, \mathbf{d}) = f(p_i, E, \mathbf{d}_0) + \sum_k \left. \frac{\partial f(p_i, E, \mathbf{d})}{\partial d_k} \right|_{\mathbf{d} = \mathbf{d}_0} \beta_k ,$$

which can be written in matrix notation

$$\mathbf{f} = \mathbf{f}_0 + \mathbf{F}_0 \beta ,$$

where

$\mathbf{f}$ = vector whose ith component is $f(p_i, E, \mathbf{d})$,

$\mathbf{f}_0$ = vector whose ith component is $f(p_i, E, \mathbf{d}_0)$,

$\mathbf{F}_0$ = matrix whose ijth element is $(\partial f(p_i, E, \mathbf{d})/\partial d_j]|_{\mathbf{d} = \mathbf{d}_0}$.

Using this approximation, the weighted residual sum of squares, RSS, becomes

$$\mathrm{RSS} \cong \sum_{\substack{\text{sum over all} \\ \text{observed pulse-} \\ \text{height spectra} \\ \text{for one spectrometer}}} (\mathbf{y} - \mathbf{f}_0 - \mathbf{F}_0 \beta)^T \mathbf{W} (\mathbf{y} - \mathbf{f}_0 - \mathbf{F}_0 \beta) ,$$

where

$\mathbf{y}$ = vector whose ith component is y_i,

$\mathbf{W}$ = weight matrix for the input data.

The normal equations become

$$0 = \mathbf{S} = \sum_{\substack{\text{sum over all} \\ \text{observed pulse-} \\ \text{height spectra} \\ \text{for one spectrometer}}} \mathbf{F}_0^T \mathbf{W} (\mathbf{y} - \mathbf{f}_0 - \mathbf{F}_0 \beta) ,$$

where $\mathbf{S}$ = the vector whose kth component is $(1/2)(\partial \mathrm{RSS}/\partial \beta_k)$. The normal equations solved for β yield

$$\beta = \mathbf{A}^{-1} \sum \mathbf{F}_0^T \mathbf{W} (\mathbf{y} - \mathbf{f}_0) ,$$

where

$$\mathbf{A} = \Sigma\, \mathbf{F}_0^T\, \mathbf{W}\, \mathbf{F}_0 .$$

The above equation is just the analog of the usual expression of the linear least-squares solution for β, the corrections to the estimated values of the fit parameters, $\mathbf{d}_0$. Therefore, as long as the truncation of the Taylor expansion is adequate, the usual error analysis of linear least-squares fitting is applicable [*12*, *13*]. The only difference is that the final solution for $\mathbf{d}$ must be obtained by iteration.

The covariance matrix of $\mathbf{d}$ is given by [*6*, *5*, *8*, *10*, *11*]

$$\mathbf{V(d)} = \text{Expectation of } (\beta\beta^T) = \mathbf{A}^{-1} .$$

$\mathbf{A}$, $\mathbf{W}$, $\mathbf{F}_0$ are unaffected by the expectation operator and $\mathbf{V}(\mathbf{f}_0) = \mathbf{W}^{-1}$. This $\mathbf{V(d)}$ is thus based entirely on input errors and assumes an adequate fit.

Similarly, the variance of another function, $g(x_i, \mathbf{d}_0)$ of the parameters, $\mathbf{d}_0$, is given by [*2*, *3*, *8*, *11*]

$$\mathbf{V}(\mathbf{g}_0) = \mathbf{G}^T\, \mathbf{V(d)}\, \mathbf{G} = \mathbf{G}^T\, \mathbf{A}^{-1}\, \mathbf{G} ,$$

where

$\mathbf{G}$ = matrix whose ijth element is $[\partial g(x_i, \mathbf{d}_0)/\partial d_j]\big|_{\mathbf{d}=\mathbf{d}_0}$,

$\mathbf{g}_0$ = vector whose ith component is $g(x_i, \mathbf{d}_0)$,

x_i = ith value of an arbitrary variable, x.

In particular, if $x_i = E_i$ and $g(E_i, \mathbf{d}_0)$ is the width of the photopeak, that is,

$$g(E_i, \mathbf{d}_0) = (d_4 + d_5 \sqrt{E}) ,$$

then $G_{ij} = 0$ for i and $j \neq 4, 5$, $G_{i4} = 1$, and $G_{i5} = \sqrt{E_i}$. Then

$$\mathbf{V(g)}_{lk} = A_{44}^{-1} + A_{45}^{-1} (\sqrt{E_l} + \sqrt{E_k}) + A_{55}^{-1} \sqrt{E_l E_k} .$$

The standard error of $g(E_l, \mathbf{d}_0)$ is taken to be the root of the diagonal term:

$$\sqrt{\mathbf{V}(\mathbf{g}_{ll})} = \sqrt{\mathbf{A}_{44}^{-1} + 2\sqrt{E_l}\, A_{45}^{-1} + E_l A_{55}^{-1}} .$$

This example illustrates that the whole parameter variance matrix is needed to determine the uncertainty in any function of more than one of the fitting parameters.

The above is the usual result for a least-squares analysis, yielding experimental errors for the parameters which are determined by the weighting matrix of the input data. This result stems from the assumption that the correlations and variances of the difference $(\mathbf{y} - \mathbf{f}_0)$ are completely taken into account by the weight matrix, $\mathbf{W}$. This requires the assumption that the expectation value of $\mathbf{d}$ inserted into $\mathbf{f}$ will yield the expectation value of $\mathbf{y}$. In the present problem it is not expected that enough parameters have been properly incorporated into $f(p_i, E, \mathbf{d})$ to match perfectly the expectation value of any particular response curve; therefore lack of correlation among the input differences is not a sound assumption where relative counting statistics are small. The value of chi-square per degree of freedom for the single-crystal calibration sources was 2.1.

Lack of fit can be handled in several ways [3, 8]. No compensation for lack of fit was used in the problem under study since a systematic lack of fit was considered unimportant.

Three criteria are used to determine whether a least-squares solution has been obtained [11, 2, 3]. First, at the converged result, each β_i should be small compared to the error in the corresponding d_i; $\beta_i \leqq 0.03\sqrt{V_{ii}}$ was adequate in this problem, where $\sqrt{V_{ii}} = \sqrt{A^{-1}_{ii}}$. Second, the RSS was required to change less than 0.01% in three consecutive iterations. Third, $\beta^T \mathbf{S}$ was required to be $\leqq 0.01\sqrt{RSS}$, which is a check on the validity of the truncated Taylor expansion.

Use of the truncated Taylor expansion results in sizable errors when the estimated parameters, $\mathbf{d}_0$, are far from the final solution. A partial compensation is obtained by placing limits on how great a change may be made in any parameter in a single cycle [4, 5]. It is assumed that a unique minimum exists for the RSS, and very little evidence of nonuniqueness has arisen in this problem.

Constraints on the amount of parameter change can be applied in any manner which aids final convergence. Complications in selecting constraints arise from having nonlinear as well as linear dependence on the d_k's in the same function. Also the constraint criteria may become more complicated if a few of the parameters are known much more accurately than the rest of the parameters at the start of the iterations. Fairly satisfactory convergence is obtained in this problem by restricting each β_i/d_i to the range $-\frac{1}{4} \leqq \beta_i/d_i \leqq \frac{1}{2}$. This restricted β is multiplied by a scalar, h, so that $\mathbf{d} = \mathbf{d}_0 + h\beta$. With β fixed, the RSS is minimized with respect to h, and β set equal $h_{min}\beta$; h is restricted to the range $0 \leqq h \leqq 1$.

RESPONSE FUNCTION GENERATION FOR PAIR AND COMPTON SPECTROMETERS

With the pair spectrometer and Compton spectrometer, the methods of handling all the data simultaneously were not available and a simpler method of data handling was used [7].

These cases were handled in a manner which greatly complicated the generation of the variance matrix of the output parameters. The methods were just as those described above except that all observed pulse-height spectra were not simultaneously fitted. Each pulse-height spectrum was fitted with a set of parameters describing its pulse-height dependence. These parameters were averaged for all spectra representing the same radioactive source. Finally each of these pulse-height fitting parameters was in turn fitted as a function of gamma-ray energy. Since the input parameters for this latter fit were highly correlated, all the energy fits had to be performed simultaneously using a large nondiagonal weighting matrix. Considerable uncertainties were introduced by the need to handle in some manner the lack of fit in the fits as a function of pulse height. Furthermore, with the two-stage fitting process, one is never quite sure that the final result gives close to the best fit to the original calibration spectra.

SUMMARY

In summary, the greatest advantage of the system of response function determination described in this paper is that the response function uses both pulse-height

and input gamma-ray energy as independent variables. Therefore, the interpolation between monoenergetic spectra is handled at the same time the pulse-height spectrum fitting is being performed. The choice of response function is such that there is no oscillation outside the region fitted and furthermore the extrapolated response function is physically plausible. In addition, it is sometimes possible to select the response function such that the fit parameters may be related to physical constants and therefore reasonable first estimates of the parameters may be obtained from analysis of the detector. It may also be possible to pick the response function such that the number of fit parameters is less than would be required to describe the same region using polynomials. Plausible error estimates and correlations for the fit parameters can be calculated using regression theory as applied to nonlinear least-squares analysis.

Apparent disadvantages of the method described are primarily the manhours involved in programming and the expense associated with the computer time required to do the nonlinear fitting. A change in the detector geometry will involve a change in the numerical value of the parameters and in extreme cases might possibly involve a change in the description of the response function.

APPENDIX I

Notation List

$\mathbf{A}$ Least-squares matrix, $\mathbf{A} = \mathbf{F}_0^T \mathbf{W} \mathbf{F}_0$

B_i Background in the ith channel

ΔB_i Background error

C_i Channel number

CC_i Counts per channel in the ith pulse-height channel

ΔC_i Analyzer gain nonlinearity correction in the ith channel

$\mathbf{d}$ Vector whose components are the set of parameters required to completely describe the spectrometer response

d_k kth component of $\mathbf{d}$

$\mathbf{d}_0$ A fixed value of $\mathbf{d}$

E Gamma energy of the source

$f(p_i, E, \mathbf{d})$ Calculated counts per kev in the ith pulse-height channel per gamma ray of energy E:

$$Qt\, f(p_i, E, \mathbf{d}) = \frac{Qt}{\Delta p_i} \int_{p_i - (\Delta p_i/2)}^{p_i + (\Delta p_i/2)} F(p, E, \mathbf{d})\, dp \,,$$

$$\simeq Qt\, F(p_i, E, \mathbf{d})$$

$\mathbf{f}$ Vector whose ith component is $f(p_i, E, \mathbf{d})$

$\mathbf{f}_0$ Vector whose ith component is $f(p_i, E, \mathbf{d}_0)$

$\mathbf{F}_0$ Matrix whose ijth element is $\left.\dfrac{\partial f(p_i, E, \mathbf{d})}{\partial d_j}\right|_{\mathbf{d} = \mathbf{d}_0}$

$F(p, E, \mathbf{d})$ Number of counts per kev at energy, p, per photon of energy E emitted by the source

$\mathbf{g}_0$ Vector whose ith component is $g(x_i, \mathbf{d}_0)$

$g(x_i, \mathbf{d}_0)$ Arbitrary function of the fit parameters, $\mathbf{d}_0$, and an arbitrary independent variable x_i

$\mathbf{G}$ Matrix whose ijth element is $\left.\frac{\partial g(x_i, \mathbf{d}_0)}{\partial d_j}\right|_{\mathbf{d}=\mathbf{d}_0}$

h Number between zero and 1 used as a parameter to minimize the RSS

K Analyzer gain in channels/kev

p_i Energy corresponding to the ith channel

Δp_i Width of ith pulse-height channel $\tilde{=} 1/K$

Q Analyzer zero: channel number corresponding to zero pulse height

Qt Source strength = total number of photons emitted with energy E

RSS Residual sum of squares

$\mathbf{S}$ Vector whose kth component is $(1/2)(\partial \mathrm{RSS}/\partial \beta_k)$

$\mathbf{V}$ Variance matrix for the input data

$\mathbf{W}$ Weight matrix for the input data

x_i ith value of an arbitrary variable x

y_i Observed counts per kev in the ith pulse-height channel

$\mathbf{y}$ Vector whose ith component is y_i

β Vector defined by $\mathbf{d} - \mathbf{d}_0 = \beta$

APPENDIX II

Details of the Response Function $F(p_i, E, \mathbf{d})$ for a Single-Crystal Spectrometer

The photopeak unit area Gaussian is given by

$$\frac{\exp\{[-(p_i - E)/(d_4\sqrt{E} - d_5)]^2\}}{\sqrt{\pi}\,(d_4\sqrt{E} - d_5)},$$

where E = position of the photopeak, $(d_4\sqrt{E} - d_5) = \frac{1}{2}$ width of the photopeak at exp (-1) full amplitude, and the area of the photopeak is (Qt)(peak efficiency of the spectrometer for gamma rays of energy E).

The calculated resolution of the spectrometer as a function of gamma-ray energy is defined as (photopeak full width at half maximum)/(gamma-ray energy) and is given by

$$\frac{2\sqrt{\log_e 2}\,(d_5 + d_4\sqrt{E})}{E}.$$

The calculated peak efficiency for the spectrometer is computed as

$$\sum_{n=0}^{4} d_{n+16} E^n .$$

The quantity (relative backscatter peak area)(unit area Gaussian) is given by the expression

$$\frac{d_8 \left(1 + \dfrac{2E}{d_9}\right)^3 \exp\left\{ - \left[\dfrac{p_i - E/(1 + d_1 E)}{\sqrt{[d_4 \sqrt{E/(1 + d_1 E)} - d_5]^2 + 2500\, E^{3/2}}} \right]^2 \right\}}{\left(1 + \dfrac{2E}{d_9} + 2\dfrac{E^2}{d_9^2}\right) \sqrt{\pi} \sqrt{[d_4 \sqrt{E/(1 + d_1 E)} - d_5]^2 + 2500\, E^{3/2}}} ,$$

where

$E/(1 + d_1 E)$ = best fit backscatter peak position,

$\tilde{=}$ energy of 180° scattered gamma ray,

$d_1 \tilde{=}$ 2/rest energy of an electron,

$d_9 \tilde{=} 2/d_1$,

$d_4 \sqrt{E/(1 + d_1 E)} - d_5$ = width of a photopeak with energy $E/(1 + d_1 E)$.

The Compton distribution is given by the expression

$$\left\{ \frac{d_{10}}{1 + \exp[(d_2 - E)/d_3]} \right\} \left\{ \left[\frac{1 + B^2 Z}{Z + (1 - BZ)^2} \right]^{1/2} + d_{11} E^{-(d_{12} + d_{13} p_i)} \right\}$$

where

$$B = [1 + d_7 (E/d_{14} - 1)^2]$$

$$\times \frac{1 + d_7 (E/d_{14} - 1)^2 + \sqrt{d_7 (E/d_{14} - 1)^2 [2 + d_7 (E/d_{14} - 1)^2]}}{1 + \sqrt{2[1 + d_7 (E/d_{14} - 1)^2]\{1 + d_7 (E/d_{14} - 1)^2 + \sqrt{[2 + d_7 (E/d_{14} - 1)^2]\, d_7 (E/d_{14} - 1)^2}\}}} ,$$

$$Z = \exp\left[\frac{p_i - E^2/(E + d_6)}{d_4 \sqrt{E^2/(E + d_6)} - d_5} \right] ,$$

$E^2/(E + d_6)$ = position of the Compton distribution,

$\tilde{=}$ maximum energy of Compton-scattered electrons,

$d_6 \tilde{=}$ ½ rest energy of an electron $\tilde{=} 1/d_1$.

The approximate peak-to-total ratio for a fixed gamma energy is given by

$$\left\{ 1 + \frac{d_{10}}{\left[1 + \exp\left(\dfrac{d_2 - E}{d_3} \right) \right]} \frac{E_2}{(E + d_6)} \right\}^{-1} .$$

REFERENCES

[1] O. Kempthorne, *The Design and Analysis of Experiments*, p 55 ff., Wiley, New York, 1952.

[2] E. B. Wilson and R. R. Puffer, "Least Squares and Laws of Population Growth," *Proc. Amer. Acad. Arts and Sci.* (Boston) **68**, secs 23–35, 303–15; Appendix, secs 62–64, 343–47, and secs 70–71, 354–59; refs 366–69 and 377–78 (1933).

[3] P. B. Wood, *NLLS: A 704 Program for Fitting Nonlinear Curves by Least Squares*, K-1440 (Jan. 28, 1960).

[4] R. H. Moore and R. K. Zeigler, "The Use of High-Speed Computers in Determining the Parameters of Nonlinear Functions by Iterative Least Squares Methods," *Trans. Am. Nucl. Soc.* 1(2), 128–29 (1958).

[5] E. Whittaker and G. Robinson, *The Calculus of Observations*, pp 255–58, Blackie and Sons Ltd., London, 1949.

[6] W. E. Deming, *Statistical Adjustment of Data*, Wiley, New York, 1943.

[7] R. W. Peelle, R. O. Chester, and F. C. Maienschein, *Neutron Phys. Div. Ann. Progr. Rept. Sept. 1, 1961*, p 29–44, ORNL-3193.

[8] G. E. P. Box, "Fitting Empirical Data," *Ann. N. Y. Acad. Sci.* **86**, 792–816 (1960).

[9] H. O. Hartley, "The Modified Gauss-Newton Method for the Fitting of Nonlinear Regression Functions by Least Squares," *Technometrics* **3**, 269–80 (1961).

[10] S. L. Piotrowski, "Some Remarks on the Weights of Unknowns as Determined by the Method of Differential Corrections," *Proc. Natl. Acad. Sci. U.S.* **34**, 23–26 (1948).

[11] E. M. L. Beale, "Confidence Regions in Nonlinear Estimation," *J. R. Statis. Soc. Part B* **20**, 41–88 (1960).

[12] R. O. Chester, *Proceedings of the Total Absorption Gamma-Ray Spectrometry Symposium*, TID-7594, p 140 ff. (May 10–11, 1960).

[13] W. E. Kuykendall and R. E. Wainerdi, *Computer Techniques for Radioactivation Analysis*, TEES-2565-1 (May 1, 1960).

[14] W. R. Busing and H. A. Levy, *ORGLS, A General Fortran Least Squares Program*, ORNL-TM-271 (1962).

(4-5) ANALYSIS OF GAMMA-RAY SPECTRA[1]

J. E. Monahan, S. Raboy, and C. C. Trail
Argonne National Laboratory, Argonne, Illinois

A "fitting" technique which has been used in the analysis of discrete gamma-ray spectra is described in the first section of this report. An algorithm for the approximate solution of a class of problems in quadratic programming is given in the second section. This algorithm may be of value in the analytical unfolding of observed spectra.

THE SHAPE OF THE TOTAL-ABSORPTION PEAK

If simplifying assumptions are made concerning the mechanism by which an output pulse corresponding to an incident gamma ray is generated in a crystal spectrometer, it can be shown that the asymptotic form of the pulse-height distribution in the neighborhood of the total-absorption peak is Gaussian. However, because of the idealized nature of this derivation, it must be expected that a measured total-absorption peak will exhibit systematic deviations from this asymptotic form. One method of obtaining a measure of such deviations is to compare a measured pulse-height spectrum with the Edgeworth distribution,

$$\phi(q;\, q_0, \sigma, \gamma_1, \gamma_2, \ldots) = g(q;\, q_0, \sigma) - \frac{\gamma_1}{3!}\, g^{(3)}(q;\, q_0, \sigma) + \frac{\gamma_2}{4!}\, g^{(4)}(q;\, q_0, \sigma) + \ldots , \qquad (1)$$

where

$$g(q;\, q_0, \sigma) = \frac{1}{\sigma\sqrt{2\pi}} \exp\left[-\frac{1}{2}\left(\frac{q - q_0}{\sigma}\right)^2\right], \qquad (2)$$

and

$$g^{(\nu)}(q;\, q_0, \sigma) = (-1)^{\nu} H_{\nu}(q)\, g(q;\, q_0, \sigma) . \qquad (3)$$

Here $H_{\nu}(q)$ is the Hermite polynomial of order ν.

The data which have been analyzed in terms of this distribution were obtained with a scintillation spectrometer having an anticoincidence annulus [*1*]. A secondary peak due to Compton processes in which the incident gamma ray is backscattered through the entrance aperture of the spectrometer system (and thus escapes detection in the anticoincidence ring) is present in these measured pulse-height distributions. In order to take account of this in the hypothetical distribution, a term which approximates this contribution is added to the Edgeworth distribution assumed for the total-absorption peak. The final expression for the number of counts f_j expected

[1]Work performed under the auspices of the U.S. Atomic Energy Commission.

in channel j in the vicinity of the total-absorption peak is

$$f_j = a \int_{\Delta_j} dq\ \phi(q;\ q_0, \sigma, \gamma_1, \ldots) + bg(j;\ q_0 + \delta, \kappa\sigma) + c\ , \tag{4}$$

where Δ_j is the width of the pulse-height channel j, δ is the mean energy carried off by the backscattered photon in a Compton process as discussed above, and $\kappa\sigma$ is the "dispersion" of the backscattered peak. The coefficients a, b, and c are the respective intensities of the total-absorption peak, the backscattered peak, and the residual background. The values of these coefficients, as well as the moments $q_0, \sigma, \gamma_1, \ldots$, are to be determined by fitting Eq. (4) to the observed pulse-height distribution.

In the usual estimation procedures, such as the modified χ^2-minimum method, it is frequently necessary to combine neighboring channel readings in order that all observed frequencies $\bar{f}_j$ are roughly of equal statistical accuracy. This regrouping of data becomes increasingly important in the estimation of the higher-order moments of the distribution. The reason for this is that the high-order moments are sensitive to small variations in the frequencies observed in the tails of the distribution and this is just the region where the measured frequencies are small and consequently susceptible to relatively large statistical fluctuations. The necessity of regrouping the observational data can be circumvented by the use of the following estimation procedure which is suggested by the ω^2-minimum method [2] for testing goodness of fit.

Let $\bar{F}_j$ and F_j denote the observed and hypothetical cumulative distribution functions, namely,

$$\bar{F}_j = \sum_{l=j_0}^{j} \bar{f}_l \Big/ \sum_{l=j_0}^{j_1} \bar{f}_l\ , \qquad (j = j_0, j_0 + 1, \ldots, j_1)\ , \tag{5}$$

and

$$F_j(a, b, c, q, \sigma, \gamma_1, \ldots) = \sum_{l=j}^{j} f_l \Big/ \sum_{l=j_0}^{j_1} f_l\ , \qquad (j = j_0, j_0 + 1, \ldots, j_1)\ , \tag{6}$$

where $\bar{f}_l$ is the observed number of counts in pulse-height channel l, and f_l is the corresponding expected number as defined by Eq. (4). The channel numbers j_0 and j_1 denote the end points of that portion of the spectrum considered in the analysis. The accepted values of the parameters in the hypothetical distribution are defined to be those which minimize the quadratic ω^2, where

$$\omega^2 = \sum_{j=j_0}^{j_1} (F_j - \bar{F}_j)^2\ . \tag{7}$$

The estimates obtained by this method are independent of the grouping of the frequency data.

A number of response spectra observed for gamma rays in the energy interval from 100 to 3000 kev have been analyzed by the ω^2-minimum method. Only the first two terms of the Edgeworth distribution, Eq. (4), are retained in this analysis. The resulting values of $\gamma_1 \sigma^3/q_0^3 = \gamma_1 \nu^{3/2}$ are shown in Fig. 1 as a function of $1/E$, where E is the gamma-ray energy. This particular combination of parameters is considered

since it is expected [3] that $\gamma_1 \nu^{3/2}$ should increase quadratically with $1/E$. Obviously, no conclusion concerning such detailed dependence is possible on the basis of these results. However, there is an indication of a systematic positive skewness in the observed shape of the total-absorption peak, although this deviation from the simple Gaussian form is almost completely obscured by the fluctuations expected from ordinary counting statistics.

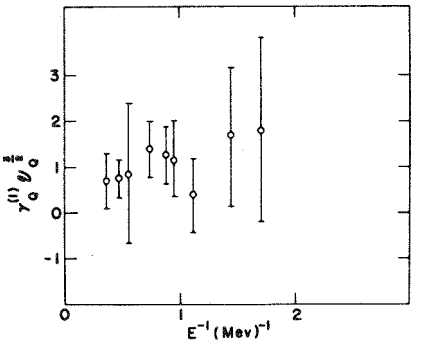

Fig. 1. The Observed Values of $\gamma_1 \sigma^3/q_0^3$ as a Function of $1/E$. The conversion factor between pulse height and energy is not included in the values of $\gamma_1 \sigma^3/q_0^3$ shown in this graph.

UNFOLDING OBSERVED SPECTRA

The problem of unfolding observed spectra is often approximately reduced to the problem of solving a set of simultaneous linear equations of the form

$$\sum_{j=1}^{n} R_{ij} g_j = f_i , \qquad (i = 1, \ldots, m; \quad m \geqq n) , \tag{8}$$

where R_{ij} is an element of the "response matrix" of the counting system, f_i is the observed number of counts in channel i, and g_j is a measure of the intensity of the jth component of the incident spectrum. Because of the sensitivity of large-scale linear systems to small errors in the observed values of f_i and R_{ij}, the direct solution of the system of Eqs. (8) seldom results in meaningful values of the components g_j.

It has been suggested by Burrus [4] that a practical solution of the unfolding problem might be the imposition of nonnegativity conditions

$$g_j \geqq 0 \qquad (j = 1, \ldots, n) \tag{9}$$

on the least-squares solution of the set of Eqs. (8).

The least-squares problem, neglecting the constraints in Eq. (9), is easily formulated. Let Λ^2 denote a diagonal $m \times m$ matrix where Λ_{jj}^2 is the relative weight assigned to the measured value f_j. Let $\tilde{R}$ denote the transpose of the response matrix R, and let B denote the inverse of the symmetric $n \times n$ matrix $\tilde{R}\Lambda^2 R$, that is,

$$B = (\tilde{R}\Lambda^2 R)^{-1} . \tag{10}$$

The least-squares solution of the set of Eqs. (8) is

$$g = B\tilde{R}\Lambda^2 f , \tag{11}$$

where g and f denote column vectors with components g_j, $(j = 1, \ldots, n)$, and f_i, $(i = 1, \ldots, m)$ respectively. For values of the components of g given by Eq. (11), the quadratic $\phi(g)$, defined by

$$\phi(g) = \sum_{i=1}^{m} \Lambda_i^2 (f_i - \sum_{j=1}^{n} R_{ij} g_j)^2 , \tag{12}$$

attains its minimum value.

A procedure which may give a physically meaningful approximation to the solution of the constrained least-squares problem is described below. The approximation depends on a sequence of transformations T_k, where $T_k g_l = g_l - g_k B_{kl}/B_{kk}$, $T_k B_{lm} = B_{lm} - B_{kl} B_{km}/B_{kk}$, and $T_k \phi(g) = \phi(g) + g_k^2/B_{kk}$. It can be shown [5] that the vector $T_k g$ is the least-squares solution of the set of equations obtained by setting the component g_k equal to zero in Eqs. (8). The matrix $T_k B$ is the corresponding "error matrix," and $T_k \phi(g)$ is the resulting value of the quadratic defined in Eq. (12).

The proposed "solution" of the unfolding problem is generated by the following sequence of operations.

1. Among the negative components of g, choose that component g_ρ for which $g_\rho^2/B_{\rho\rho}$ is a maximum; that is, from among those indices l for which $g_l < 0$, determine the index ρ for which $g_\rho^2/B_{\rho\rho} > g_l^2/B_{ll}$, $(g_\rho < 0,\ g_l < 0)$.

2. Carry out the transformation T_ρ for all components of g (both positive and negative) which have not previously been set equal to zero.

3. Replace all components g_l by $T_\rho g_l$ and all B_{lm} by $T_\rho B_{lm}$ and repeat the procedure indicated in (1). Note that the next transformation, say T_μ, is that for which $(T_\rho g_\mu)^2/T_\rho B_{\mu\mu} > (T_\rho g_l)^2/T_\rho B_{ll}$, $(T_\rho g_\mu < 0,\ T_\rho g_l < 0)$.

This iterative process should be terminated when the value of $q_\rho^2/B_{\rho\rho}$ in (1) is less than some constant α whose value is chosen such that $\alpha B_{\rho\rho}$ is a measure of the variance in q_ρ. The constraints in Eq. (9) are thus replaced by the slightly more realistic inequalities $q_l + \sqrt{\mathrm{var}(q_l)} \gtrsim 0$.

As yet this method has not been applied in any practical unfolding problem.

REFERENCES

[1] C. C. Trail and S. Raboy, *Rev. Sci. Instr.* **30**, 425 (1959).

[2] H. Wold, *A Study in the Analysis of Stationary Time Series*, p 191, Almquist and Weksells Boktrycheri, Uppsala, 1938.

[3] R. T. Julke, J. E. Monahan, S. Raboy, and C. C. Trail, ANL-6499 (April 1962).

[4] W. R. Burrus, private communication.

[5] J. E. Monahan, ANL-6061 (September 1959).

Session 5

Chairman: G. D. O'Kelley

Chemistry Division,
Oak Ridge National Laboratory,
Oak Ridge, Tennessee

(5-1) THE FUTURE OF DIGITAL COMPUTERS IN SCIENCE

John W. Carr III
Department of Mathematics, University of North Carolina
Chapel Hill, North Carolina

The general goal of this discussion is to point out marked deficiencies in the present relationship between men and semi-intelligent automata. I specifically use this term since the words *digital computer* – or even *general purpose digital computer* – are basically misleading. The information-transforming, electronic devices that we have are indeed very *special purpose* equipment patterned after one specific initial design, that due to Von Neumann and others in the mid-1940's. Even though these equipments were specifically designed for one or two very restricted classes of problems, peripheral research uses of these computers and some key productive uses have shown them to be what one might call "semi-intelligent automata."

A very large number of copies of this specific design for an electronic information-transforming device were built and put to use during the past 15 yr. The persons using these devices range from highly educated scientists to computer coders – I won't say programmers – trained in industrial education centers like the one in Burlington, N.C. A recent survey of an important cross section of computer users, the membership of the Association for Computing Machinery, showed that over 50% of the membership had undergraduate degrees or even less formal educational backgrounds. One might assume that those computer users not so professionally interested as to join this scientific society would probably have an even less adequate educational grounding.

My first hypothesis will be that the intellectual level of these machines dictates the intellectual level of the users. Although we have heard that Enrico Fermi actually coded for a computer and recommended that young physicists do likewise, this certainly did not start a trend. Von Neumann remains almost the only distinguished American mathematician who has directly contributed ideas concerning the nonnumerical use of computers. Leading mathematicians like Sobolev and Dorodnitsyn associated with computers in the Soviet Union are actually working more as scientific administrators than as scientists. The mathematicians in this country working with and around computers are, with some few exceptions, mainly numerical analysts.

The reasons for this lack of competent scientific talent associated with these somewhat revolutionary machines are based to some degree on educational failures within our universities, the economics of the present hardware, and the large number

of relatively important but scientifically unchallenging problems that must be solved using these new machines. However, the most obvious reason is the unintellectual nature of the machines themselves. They were first designed by scientists endeavoring to prove that some such machine could be built. This design, as might be expected, was "near-minimal" in the sense that only the required elements for operation were included and the model for the device was almost the simplest one conceivable.

Such a design worked, performed, and proved highly effective within a region of immediately pressing problems, mostly computational or simply combinatorial in nature. The major effort of the past 15 yr has been to extend the range of problems being solved to as many applications of this same basic kind of problem, repeated over and over again:

1. large computations, mainly from mathematical physics, relatively simple in formulation but requiring extremely large numbers of operations;
2. organized searching procedures to find the solution to problems where classical techniques offer no direct guides to a formal algorithm for solution;
3. "information-retrieval": file-maintenance and up-dating procedures on relatively small but complexly connected collections of data, or else on large but very simply structured collections of data; and
4. miscellaneous, in which most of the relatively few *different* and difficult problems occur.

The first three problem attacks made great use of the relatively large speed advantage in calculational speed, or speed of organized storage and retrieval over previous methods. In general they are not logically complex compared with the types of decisions and analyses made by intelligent human beings. These problems were in general formulated by persons of average competence among intellectual workers, and finally related to the machines by persons of a lower level of intellectual interest and training.

The machines themselves are nonintellectual and nonintelligent, and therefore generally unattractive to intelligent human beings for the following reasons:

1. The level of communication between man and machine is extremely low, and although the nature of this communication is more precise than that between an adult and the normal two-year-old child, the machine in linguistically far simpler. The language of communication with these machines contains almost always less than 100 command verbs, almost no methods of making declarative statements, and no method of giving definitions of any sort, evolving new syntax or semantical relations. The informational-organization methods available are so inferior to that of an ordinary library that no one would take a comparison seriously.

2. The information storage capacity of these machines is extremely small or else so hedged in by engineering restrictions and by the need for complex descriptions on the part of communicating humans that its actual use is narrowly limited for special purposes. It is far more difficult to initiate computer command searches than it is to tell a six-year-old child how to search an encyclopedia; and I find the results, after watching the growth of my own children as opposed to the computers I have known, again not worth comparing. Computers are not designed to "learn" in any sort of general purpose sense; even the special purpose learning that has been accomplished has been only after exceedingly detailed and complex human effort.

3. The actual physical input-output facilities of these semi-intelligent automata are very crude. While such a machine can input linguistic strings at a speed faster than a human being could read and comprehend, such strings are very limited and special purpose, narrowly restricted in vocabulary, and must be previously encoded into machine readable form by human beings. The output rate of the printing mechanisms attached to these automata markedly exceeds human performance, but is far less effective than other printing mechanisms used by humans. All of these input-output devices are tightly restricted as to symbology, thus precluding any really elaborate communicational notation. Even if such material being input were able to be scanned and interpreted, today none but a few experimental or highly specialized systems allow any sort of graphical or nonsymbolic input.

This rather hasty survey of the present-day characteristics of semi-intelligent automata shows why the level of their direct users, as far as scientific training and proven intellectual ability are concerned, is relatively low. These machines are not fit companions in any sort of intellectual activity. There is almost no intellectual challenge in their use, except in learning the solution of specialized problems. Because certain new problems are now solvable, they have stimulated mathematical and scientific activity in certain areas.

Their very simplicity has created as virtues in the class of machine users such otherwise questionable activities as over-emphasis on details, combinatorial manipulation of the simple languages involved to minimize certain only intuitively defined measures, and ability in detailed record-keeping as opposed to imagination. A premium has been placed on intuitive abilities of an ill-defined nature that do not include use of a formal inductive and deductive approach to problem solving.

PROBLEM SOLVING

It is just in the increased knowledge of what problem solving is, however, that these semi-intelligent automata have contributed to the picture of what their descendants could and might be. These machines have been recognized to be – in spite of, rather than because of, their present structure – artificial symbol manipulators. It has been recognized that, although they were originally designed to make decisions on numbers, encoding of symbols into numerical form allows a first approximation to machine decision making with symbols.

It has been recognized before the advent of these machines that many of the problems arising in scientific endeavor can be easily described in terms of formal languages, easily understandable to and usable by the human scientist (after a fairly rigorous apprenticeship in their use). Such languages are far more complex than the extremely simple computer languages that we have previously described. They are open-ended in that new semantical and syntactical configurations can be added. Special dialects for individual areas of study can be defined within more general structures. Because humans have conceived these languages and because of the flexibility of handwriting and movable type, limitations on symbology are generally nonexistent.

There exists a fair-sized scientific literature on the theoretical problems involved with manipulating such languages. Here, however, the usual pattern of mathematical investigation has been completely reversed. There exist a large

number of existence theorems as to solutions or lack of them – the literature of computability and undecidability – but a much smaller set of algorithms for solving particular problems. This is as if the abstract treatises on Hilbert space or functional analysis existed today with almost no work ever having been done on how to solve a system of linear equations.

It is within this framework that one possible new, and to me very important, concept of what a semi-intelligent automata should really be arises. It should be a highly talented aid in problem solving by a scientific investigator or by a group of scientific investigators. It should fulfill the functions of as many of such scientist's present problem-solving adjuncts as can be practicably mechanized:

(1) a notebook for keeping momentary data and informal ideas in a correlated file;
(2) a file for formal problem solution techniques, for proven statements obtained directly from experimental evidence, or deduced jointly from theory and experiment;
(3) a computer with a file of computational algorithms for performing numerical computations, either automatically as a part of more elaborate problems, or specifically on call;
(4) a mechanized library for performing all of these various retrieval techniques in an integrated fashion;
(5) a deductive inference machine for producing new results from experimental data, or for testing conjectures, proposed in this elaborate man-machine communication language;
(6) an inductive machine for producing hypotheses from masses of data and generalizations from specific linguistic statements already entered or deduced;
(7) a linguistically fluent machine, in symbols, grammar, and semantics, for handling the details of use, including testing of input strings, testing for inconsistencies, translating from nearby dialects, and maintaining control of the relations between this special-purpose locally oriented man-machine language and the more general more or less "universal" language(s) used as a "common-carrier" by other scientists and machines.

It is not apparent just what the physical and organizational structure of such a machine might be. It might be a mutually used facility, with a generalized structure used by many different workers and disciplines. Outwardly, to a user, it might look something like a book, a typewriter, a drafting board, a television set, and a telephone all connected together and available for his use. Or if the cost of duplication of such semi-intelligent automata in quantity can be brought down enough, there may be a local automaton for an individual worker, with similar input-output appearance, and the ability to be interconnected with centralized automata through automatic switching devices.

IMMEDIATE REQUIREMENTS

Whether this particular concept or another markedly different in nature is to be set up as one goal for progress to head towards, there are obvious requirements that must be taken with respect to equipment before progress anywhere in this direction can be made. Experimental equipments, reliable in performance, must be conceived,

designed, and used by scientists interested in such new and different devices. The basic pattern of language for such equipments must be a radically different one from that in the "Von Neumann" machines of today. The techniques of storage and recall of information must be markedly changed and built into the hardware itself. The automaton must have a variable, expandable syntax for its command language, so constituted that it is not the duty of the user to worry about the details of how this is to be mechanized. The machine must have a very large memory relative to those available today, with technical problems of access again no longer the user's responsibility.

Whether the mechanization of these procedures will be done with hardware, or with algorithms stored in accessible memory (what would be called "programs" today), is a question I leave open because of engineering considerations which still must dictate. The entire system should be planned as a whole and should be made so efficient in operational speed that the usual complaints against elaboracy of operation can be met – if possible. From the start, this new breed of automaton should be planned from the outside in, with the emphasis being placed on how it looks linguistically to the user. The linguistic command structure of this new machine should fit into the language of the user, not *vice versa*.

Techniques for the overall design of such equipment fortunately exist within the theory and practices of automatic programming and the hardware of certain isolated "paper computers" or local experiments. From the theoretical literature of logic, recursive function theory, and the foundations of mathematics have already come many linguistic structures that have been tried, some successfully and some unsuccessfully. The older algebraic languages give some crude approaches. Special purpose languages like IPL-V, COMIT, and many others contain examples of possible models as do the more recent proposals, ALGOL and COBOL, where formal studies by scientists and nonscientists were made of how a language should appear to a user.

Such "mutually conceived" languages all have marked restrictions in their structure, because they were defined by persons whose ultimate, if not immediate, concept of a language was limited by the requirements for implementation on today's restricted digital computers.

Research support, therefore, for studies in formal languages independent of machines, but oriented towards description of the solution of problems, may be very valuable. It will be from this work, from that of the logicians and workers in the fundamentals of mathematics, and from the more theoretical automatic programmers, that the linguistic and organizational structure must come. Professional production programmers, who conceive of computers as a continuing extension of their specialized techniques, cannot contribute; in fact, they would most often oppose the idea of a revolutionary quantum jump in the linguistic structure of computers. (The opposition to ALGOL is an example.)

It will probably be difficult, too, to find very many logical designers with conditioned experience in the design of Von Neumann–type machines, who would be open-minded or radical enough to abandon the traditional idea of the internal structure of a computer. A recent proposal by Professor Norman Scott of the University of Michgan shows an example of a willingness for experimentation. In this, Professor Scott proposed to rewire an easily reconnected, specially constructed commercial machine to include storage allocations and interconnection techniques used up until now only in programming systems.

The major step, of course, is the financing of a pilot project for building one of these entirely different computers as an experiment, just as the project headed by Von Neumann at Princeton was financed in the late 1940's by the Army.

It is my sincere belief that such a project should not be given to a computer manufacturer, except perhaps as the production partner for a design group that is completely independent. Such a group, designing such a machine, must not be hampered by commitments to a manufacturer's hardware resources, previous design procedures, tradition of equipment, etc. The results of the NORC, LARC, and Stretch projects would seem to me to be examples of the type of results not wanted.

A university group, a national laboratory, or a converted independent institute, like the Institute for Advanced Study was because of Von Neumann, would be the proper organization. It should be remembered that the Von Neumann-Princeton–designed digital computer "ran" only several years after other designs, later begun, had been carried through to completion. To an outsider, that project suffered at that time on the engineering side; yet the incomplete machine, with the reports that were produced, had far more influence than any other equipment on the machines that came afterward.

Again, I would urge that the design leadership of such a group be mathematical rather than engineering in training, since the prime goal is development of a mathematically oriented structure into which hardware presently available must be fitted. Logical designers with the proper background should be chosen to temper, not betray, this goal. The circuitry, storage, mechanisms, and input-output devices should be chosen from devices developmental at the time of design to meet the design requirements, not *vice versa*.

If such a project were set up, with a specific set of goals in mind, with adequate support, with leadership basically committed to the attainment of the idea, I can imagine 5 to 10 top scientific workers in formal languages, automatic programming, and logical design who would immediately join such a project. The graduate student resources of such computer-oriented schools as Carnegie Tech, Case, Harvard, M.I.T., and Illinois could produce a quantity of extremely good young men, if the project were done in the United States.

The cost of such a project would vary widely, from up to down, if done in the United States, or Britain or Western Europe. Presumably, the accrued advantages to United States science would more than make up the cost difference in doing the task here; the gain in the (often) higher technical capability of the network of United States computer component suppliers would also be an advantage.

The problem involved in the production of the first version of such a really semi-intelligent automaton is more difficult than that which faced the Von Neumann group in the 1945's. Its overall solution should cost more, perhaps markedly more. However, a well-planned and evaluated project in which the chances of overall success were rated more than even could justify expenditures of the tremendous sizes ranging from $5 to $100 million that might be involved, since the pay-off would come not only through a completed operating machine (a prototype from many production models), but as much so through the ideas that were tried, developed, and rejected along the way towards the final design.

I know that the following is an overworked argument, but nevertheless I believe it to be a true one: sooner or later, in a group such as this within the Soviet Union, some scientist with more technical or administrative authority than I have here in this country will propose a similar project within the Soviet Union, based perhaps as a culmination of the present work on mechanical translation, the work on information retrieval, or as an entirely different project. At some stage, one of the key mathematicians within the Soviet computer hierarchy, such as Academicians Sobolev or Dorodnitsyn, will become convinced that the odds on success of such an enterprise is favorable to the glory of himself, his institute, and the U.S.S.R., and such a project will begin then and there. Upon evaluation of equipment, widespread effectiveness of the use of computers, and developmental computer research, I would estimate this Soviet decision might occur in perhaps three to four years – all other things being equal – after a similar proposal is made in all seriousness, with a chance of success, in this country. However, from the point of view of the mathematical levels of competence of the comparable people that are involved, I do not believe that there is a gap of three to four years, and it may be that it will be some of the mathematicians who are convinced in the mathematical effectiveness of computers, who will be bold enough to make such a proposal.

Because such a semi-intelligent automaton as we have described here is not a *direct* contributor to any of the competitions between the U.S.A. and the U.S.S.R., it does not have the priority (nor the cost) of projects such as nuclear weaponry and space vehicles. However, the scientific leadership of the Soviet Union knows, on the basis of the Sputnik effort, the key effectiveness of digital computers. There exists a growing scientific discipline (centered professionally on the journal *Problems of Cybernetics,* for example) with a steady funneling of younger men from three or four key university computing centers (Kiev, Leningrad, Erevan, and of course, Moscow) into this research area. The seeds are planted, and if the course of imagination runs similar to that here in the United States, the Soviet Academy of Science or Department of Defense will hear a presentation far better documented than mine within 3 or 4 yr.

If the decision were made to do this, I think the resulting project would make a similar impact on Soviet science and technology as to what it might make here. At present, I would place my estimate of success of a United States project as somewhat higher – a conviction held mainly on the basis of quantity, not necessarily quality of effort in this area.

Not being privy to most of the government's secrets, I do not know whether or not such a project is in existence or plan today. I do feel strongly that, for example, the computer companies of today could no more do this job than the computer companies of 1945 could have produced Von Neumann's automaton. Perhaps behind the doors of some secret government laboratories there are enough brains working on this. I feel, at the moment, that there is not such a need for secrecy in such a project as there is in broadcasting it and getting it into the spirit of the computer users of today, whose morale, at least among the men I know with imagination, is at a low ebb. A goal like this is more like those of Project Apollo and NASA in its conception and results than like those of the Manhattan project.

(5-2) ROUND-TABLE DISCUSSION

The time remaining in Session 5, Thursday evening, October 18, was devoted to a round-table discussion of topics suggested by some of the Symposium participants and the Organizing Committee. The Panel was composed as follows:

G. D. O'Kelley, *Chemistry Division, Oak Ridge National Laboratory, Chairman*

D. A. Bromley, *Department of Physics, Yale University*

John W. Carr *III, Department of Mathematics, University of North Carolina*

A. J. Ferguson, *Nuclear Physics Division, Chalk River Laboratories*

Vincent P. Guinn, *General Atomic Division, General Dynamics Corp.*

M. H. Lietzke, *Chemistry Division, Oak Ridge National Laboratory*

L. Salmon, *Health Physics and Medical Divisions, Atomic Energy Research Establishment, Harwell*

O'KELLEY: First, I would like to pose a question which has come up several times in conversations at this conference: Who should do the programming of an experimental problem? That is, should an experimenter write his own program, or should he go to a mathematician to have his problem solved for him, always bearing in mind that there may be a semantic barrier between the experimenter and the mathematician?

LIETZKE: About six or seven years ago I had occasion to put my first problem on a computer; I went up to the Mathematics Panel at the Laboratory and asked them to program it for me. I checked in about every two weeks or so, and after three months – when I was just about ready to give the paper at a meeting – they finally gave me the result. I was driven into programming my own problems because of this; now, I would rather do it. For example, I may write a program and then want to change it immediately. It is just too difficult to get someone who is tied up with other problems to drop them for a little while to work on my problem so I can go back on the computer.

I don't think that I would be able to get as much work done if I had to rely on someone else to do my programming.

BROMLEY: I would like to make one comment. As a nuclear physicist, I fully subscribe to the idea that it would be a great idea to be able to do all of your own programming. But I really question whether any one of us will have enough time to actually do all the programming which will be required – rather, I think it's very important to understand what is involved and to be able to state very precisely what you want.

But I hope we can look forward to the day when you need to do relatively little of the programming yourself, since this would be a problem specialists could handle, given just the statement of what you want to put in and what you want to get out.

Regarding this question of the communications barrier between the people around the computer and the people in the laboratory, we have already seen some of this at the conference so far: The statisticians and mathematicians have looked rather askance at some of the things that have been going on.

SALMON: Back in England we don't have any choice about this. You either program it yourself or you just don't get it programmed. At Harwell now there is a tremendous number of people using the machines, all doing their own programming.

A slight danger sometimes arises in that people get "computer happy." They can't do a simple straightforward bit of work without a program to do it. They spend three weeks writing a program to perform a calculation which they could have done quite well back in the lab in an afternoon's work, and then they never use the thing again.

But that generally has passed. I really believe myself that people in this sort of field should learn how to program and in general should do their own programming. I just don't see how they can meet their own problems unless they do this, because it is only by doing their own programming and seeing what is happening that they are able to see just what they can and can't do.

FERGUSON: I might say that at Chalk River the situation is much the same. Chalk River is actually very well endowed by the Canadian Government. You can spend almost any amount of money on machinery, but not on people. Although we have a small professional computing group there, it is too small to be of very wide use to everybody.

GUINN: I would like to comment that in our activation analysis work at General Atomic, I chose what I thought was the cowardly way and decided to get one of the people in our computer group to take care of writing the program. This was to save me a great deal of time so that I could be doing other things.

It hasn't really worked out that way, though, because I have had to spend a great deal of time trying to teach the computer programmer what gamma-ray spectrometry is all about. So, I am not sure that I really saved any time in the long run.

O'KELLEY: Professor Carr, I wonder if you would care to comment on this from the mathematician's point of view?

CARR: Well, I would prefer to use the word "problem solver," because that is what we all are when we write a computer program. Now, if you are going to use a computer, it seems to be an impossible problem, unless you get further involved than just walking down to see what the color of the machine is and to get the coding sheets.

As has been pointed out at this meeting, somewhere in your mathematical training you should have learned something about statistics and about numerical analysis. I don't know enough about radiochemistry to say whether you can afford to spend any time at all on these subjects; but if you are going to be a really competent problem solver, you are going to need to know quite a lot about these things.

One trouble is that in school we teach you how to be a different sort of problem solver. In your freshman and sophomore and junior years you learn about the mathematics of continuity. You deal with functions which are continuous rather than discrete, and you get a great deal of training on such subjects.

Then all of a sudden, you come up against computing machines, which are discrete arithmetic and algebraic devices, and unfortunately most of us have not had any mathematics that tells us how to use them.

So probably one can argue that the background in numerical analysis is not completely adequate for any of us, and there is going to have to be an awful lot of self-teaching. May I say that many of the programmers, as well, don't know this sort of thing. I am not just talking about radiochemists in this connection.

O'KELLEY: The problem of programming leads rather naturally into another topic which Professor Carr touched on, and which also came up in discussions with Professor Wapstra this morning, and then again in his talk this afternoon. I refer to

the use of ALGOL. To most of us I'm certain that FORTRAN has been extremely valuable. It has made it possible for the experimenter to do even very complicated problems without a great deal of study. ALGOL seems to have other attractive features. I would like to ask for comments from those on the Panel who have had some experience with ALGOL.

LIETZKE: It just happens that my wife is the manager of the SHARE ALGOL project, so I have had quite an exposure to ALGOL.

During the last month or so I have written three or four programs in ALGOL just to get the feeling of the language. I found that I could learn it in about one day. I read the ALGOL-60 report and was ready to go to work.

The compiler for the IBM 7090 will be released very shortly, probably within the next month or six weeks. It is in the last stages of debugging right now. At present, it produces an assembly-level tape which can then be run through the FAP assembler.

A few features of the ALGOL language which have not been implemented in the present 7090 version are: (1) recursive procedures, (2) arrays called by value, (3) dynamic implementation of parameters called by name. In addition, there are restrictions on the use of dynamic own arrays.

The compile time is very fast – faster than FORTRAN – and is approximately the same as the assembly time.

I found from my own experience in programming in ALGOL that it is a more natural language to use than FORTRAN, and is fairly easy to learn. You don't have to do quite as much long-range planning for a longer program. I think it is probably more suited to scientific programming than FORTRAN is.

CARR: I can give you an example of the ease of learning ALGOL. We had a group of about 30 Ph.D.'s in a course at Chapel Hill this past summer. They were trained in chemistry, physics, mathematics, and statistics, and were going to be involved in the use of computers in universities. As part of our course, each person ran one or more – in most cases it was two or three – ALGOL programs by remote control at the Amsterdam computer center. Except for one or two "theological" arguments, which you get in these languages sometimes, these people were able to go ahead and learn ALGOL and to apply it to fairly elaborate programs.

I do not think that there is much argument between one language and the other, although I do feel that the presence of a large group of European users, including I think possibly a large group of Soviet users as well, may make ALGOL more valuable than it looks at the present time.

There are at present ALGOL compilers available for the IBM 7070, the Remington Rand 1103-A, and an approximation to it exists for the Burroughs 220. We are trying to finish one at Chapel Hill for the Remington Rand 1105. Soon there will be a number of these around.

We have a program that will take a FORTRAN program and translate it over into GET, our own present language. We see no reason why we shouldn't take FORTRAN decks and make them into ALGOL, and vice versa.

Such programs are not really very difficult to write if you know how to do it. The man who wrote our FORTRAN to GET program for us was a senior undergraduate who had never done one before. He only took three months.

Don't be frightened when people tell you that some of these problems are too complex; for example, an ALGOL compiler for a large computer was written in Denmark by a group of three or four people in a period of three months. They knew what they were

doing, because they had done a previous one. The "soft work" blockades that have been put up by some of the manufacturers are not really as necessary as they have been made out to be.

O'KELLEY: I am not familiar with the ALGOL language, and am curious about the input-output provisions. For example, does the ALGOL compiler for the IBM 7090 come complete with input-output provisions?

LIETZKE: Input-output was not defined in the ALGOL-60 report, but the format statements are FORTRAN format statements. So, instead of saying "write output tape" or "read input tape," you just say "input" or "output." Then there are arguments that go after it: Format statements, a data list, a Boolean operator, end of file, and so on.

O'KELLEY: I now would like to direct the discussion into another area which I know has concerned experimenters rather frequently. It is the choice of the medium which links the data-handling system to the computer. For example, in some automatic systems cards may be a very convenient medium, while in other cases it may be magnetic tape if high speed is required. This important choice depends on the design philosophy of the experiment, and on the experimental objectives. Perhaps members of the Panel might care to comment on certain specific examples showing why a particular medium was chosen to link the computer and the data-handling equipment together.

FERGUSON: Very shortly we are going to attempt the ultimate in connecting the source of data with the recipient, which will be the computer. In our tandem Van de Graaff accelerator control room at Chalk River, we are going to install a Digital Equipment Corporation PDP-1 computer which will be connected on-line to the counting equipment, so it can actually read the data on demand, and start processing it. We are looking forward to this very much.

At first we hope to apply this system to experiments involving the analysis of spectra. We don't expect to be able to use nearly as sophisticated programs for spectral analysis as we have been hearing about today. But, nonetheless, there are a great many things connected with an experiment which we experimenters have found very dull. A typical way to make measurements in our tandem control room is: We start and stop the counting equipment; then we read the data out on typewriters; and finally we sit down with a desk calculator and start adding up.

We propose to eliminate that immediately and, in fact, many other things as well. We will have the computer searching for peaks in the spectra and things like that.

There is one other application that I am promoting, and that is to program the computer to analyze pulses as they come in: This is becoming more and more important. I am very interested in a multiple counter array for use in angular correlation experiments. The method was described in a paper I presented at the Washington meeting of the American Physical Society this year. Two gamma-ray components out of a cascade will be detected, although it could actually detect three as well.

The array will have seven counters in it which will be connected to the computer. An event will consist of a time coincidence between two of the detectors, and it is going to be up to the computer to sort this all out. The computer will be told that a coincidence has occurred in two counters; it will then determine what counters they were, whether the peaks lie in certain acceptable regions, and, if they do, it will then record a count in one of forty-two different memory cells.

This is the sort of application of computers that I feel is becoming more and more important in nuclear analysis.

O'KELLEY: That is a very sophisticated approach indeed. I believe Professor Bromley has a comment to make.

BROMLEY: I would like to comment on two points: First of all, I would like to discuss the question of the more indirect connection between the source of data and the computer; this usually boils down, as Dr. O'Kelley has mentioned, to magnetic tape, paper tape, cards, or something of this sort.

Then I would like to present some of our plans which are similar to the approach just described by Dr. Ferguson.

To consider the first one, I think it is very difficult, if not impossible, to make any statement about an optimum means of connection, because it depends so critically on the experiment which is being done. I feel this is a problem that has plagued many of the discussions we have had here at this conference. In many cases it is possible to make such a statement; but there probably is no general, all-purpose solution.

For example, if you want maximum speed – as, for example, in the large, multi-parameter pulse-height analyzers which we and Oak Ridge are getting soon – then we are going to magnetic tape to get that maximum transfer speed. On the other hand, there are many applications where it is particularly advantageous to get nuclear data on cards, because in this way you can perform a sorting operation to the cards you want and get rid of the rest. Dr. Goodman at Oak Ridge has used cards to particular advantage in some of his work. If you use tape, then you must go either to cards or into a computer to obtain the sorting.

But to go on to the matter of a more direct link which Dr. Ferguson has mentioned, our interest in this stems from the fact that we hope in the very near future to get approval to start installing the first of the "Emperor" tandem Van de Graaff accelerators. Our hope there is to have this connected to a computer facility right from the beginning.

I won't say what kind of computer facility, because from what we have heard tonight, it is clear that it matters very little whether the computer is an IBM 7090, or whether it is a little black box which will sit under your desk, and which behaves like a 7090, but is really connected to a machine in Indiana. In any case, the accelerator itself is being designed so that all functional controls will be available in digital fashion. We can then proceed to remove a great fraction of the drudgery which is associated with experimental work in any field. In my own field, for example, I can think of a number of measurements in which this approach would be useful. One of the most deadly of all experiments is that of measuring an excitation function – that is, where you sit and look at what happens at a given energy; then, you set the machine to the next energy and look again, and keep on doing this until you drop dead or the machine does.

Obviously this is the sort of thing which can be and should be relegated to automatic control. The experimenter would specify a beginning energy and an energy increment and your computer would be connected, as Dr. Ferguson said, to the local analyzers. At each energy you would get a spectrum whose peaks are to be analyzed. If the peaks are due to gamma rays, a computer program would perform the analysis. If the spectra are due to particles from a reaction, the data are analyzed and corrected for the proper kinematic considerations.

The computer could also keep track of monitor counts or beam-current counts, so that the desired statistical accuracy is obtained. A gradient requirement is also advisable to ensure that if the data change very rapidly the increment will be reduced and the structure will not be lost.

For angular distributions, a similar approach is used. I will give an example of the sort of thing we are planning to do. Suppose you are interested in a binary reaction, for which you want to detect both the particle and the recoil nucleus. The particle detector is programmed to cover some angular span, and for each count the computer sets the particle detector at the required angle. The computer also determines the angle where the recoil should be and sends the recoil counter around to pick it out. An energy analysis is performed on both the particle and the recoil.

Again, the computer can keep account of the statistics, and can adjust the angular derivative to prevent loss of structure. All of the data then must be converted to the center-of-mass system, and this is normally done by carrying the data to the computer and stuffing some of it in when the computer laboratory will let you.

What you really want out of this whole business is a table which gives the angular distribution coefficients in the appropriate expansion. You don't care very much about the intermediate steps so long as you have the coefficients and an analysis of the errors.

If this sounds wonderful, it should, because we haven't done any of this yet! Nevertheless, these two examples are typical of our plans for future accelerator use. I think too much emphasis has been placed on the question of whether you want a small local computer or a large computer. The real question is that of access to the computer. Personally I am inclined to think there is an interim period in which we can probably use a small computer locally and also use it to augment a large one located at some special facility.

CARR: I can give you an example of an extreme case which I think is still being tested. At Ohio State University there is a large computer which does two things at once. It works real time on a military simulation problem which is in the back half of the building, within a locked room with guards on the outside. Out front there is a group of students and faculty members who also use this machine. Most of the time, I am told the people out front think they have control of the machine completely, and the people in the back think that they have control of the machine completely.

The point is that there is enough machine to satisfy the two groups most of the time. That is an extreme example, but there are other places where this sort of dual control is being done.

It took a fairly elaborate program to do this. It was done because the Air Force was willing to pay for almost all the machine by means of the back room, and the people out front were able to use it at a much lower cost.

O'KELLEY: I would like to ask what kind of machine this is.

CARR: This was an IBM 7090. There is a similar application of a Digital Equipment Corporation PDP-1, which is a much smaller machine.

O'KELLEY: When a proposal such as this comes up at a laboratory, the experimenters immediately raise howls of anguish, because we think that we won't all get a crack at the machine, and that we will run into the same old scheduling problem again. Apparently it can be made to work on a certain scale.

BROMLEY: There has been discussion at this conference, and there is discussion in general, about the question of economics. I think it is worth bearing in mind that, if you are concerned with a large accelerator, the running cost per hour on the accelerator far exceeds that of most computers.

So it is really not a question of conserving time of the computer, but of conserving effective time on your machine. If there is going to be any holdup, this is something you have to bear in mind.

CARR: I would like to suggest that it is very useful to consider, as Dr. Bromley has indicated, that expensive experiments make computer utilization possible.

There have been experimental real-time control, large-scale experiments, going on in this country as early as 1953 or 1954. One example here in the state of Tennessee is the flight research center at Tullahoma, which has a large wind tunnel. The cost of the wind tunnel experiments was such that a computer was connected to the equipment to give a rapid evaluation of the data and to help make decisions on what experiment should be done next.

Of course, computers are continuously monitoring the data from flights of missiles and spacecraft.

Another real time experiment we all should know about is the Air Defense System of the United States. This is a real-time experiment in which the machines are trying to make decisions on the presence or absence of unidentified aircraft over the continental United States and Canada.

This is one of the most complex information-processing networks that exists. Most of us do not appreciate the extent to which this system has been developed in its input-output, its man-machine relationships, and so on – mainly because it is a classified system.

These are some of the systems working now which are extremely complex experimental control systems with digital computers as the central device. Whether they are good for our own experiments in every case is another question.

All of these experiments, of course, are million-dollar experiments, and not all of us have that sort of money. But there is no question at all but what they can be done. The question over and over again is the economics of it.

O'KELLEY: I would like to ask Dr. Guinn to comment on activation analysis. I suppose here again the application of computers involves a matter of economics. I know that activation analysis is one field of radiochemistry in which there is enormous interest in the use of computers, and quite sophisticated automated systems are being used.

GUINN: The field of activation analysis is a fairly natural one for computers. It lends itself very nicely to it. If you are engaged in doing large numbers of analyses and processing droves of data, it is pretty obviously attractive if you can save a lot of time; and if the time you save amounts to more dollars than it costs to work the data up on the computer, it looks like an attractive approach.

I know I shouldn't say this among the people up here – probably many of you out there, too – but, frankly in this general field the computer problem itself is a trivial one. The problem is to get some data that are worth giving to the computer. That is the biggest problem, and I am really very serious about it. It is possible to get very rigorous reproducible data in very favorable cases that the computer can then do a very fine job on because the mathematics is quite straightforward – once the data are rigorous within counting statistics.

But if you are trying to do a lot of this work where you have all kinds of different materials to look at, many of them coming out rather unexpectedly with enormous counting rates and so on, the problem of getting good data is a serious one. To the best of my knowledge, nobody has completely licked the problem yet. There have been many approaches and many improvements. We are working on this a good bit ourselves.

Once we get to the point where we feel our data are really first class, and the volume of such work gets to the point where manual processing is really prohibitive, then the computer will be very useful. In the meantime we are developing a computer program, but the bigger problem is in getting the data.

SALMON: I would like to take up Dr. Ferguson's point about using the computer to do the pulse-height analysis. It always struck me as an extraordinary thing that one has had a pulse-height analyzer that collects binary information, carefully stores it in binary fashion, and then pumps the information out in decimal form. This decimal information goes into a computer, only to be reconverted back to binary form.

This is an awful waste of money and time. In fact, we have had a look at storing data directly onto magnetic tape; that is, the output of the analog-to-digital converter goes directly onto magnetic tape, not with a view to putting it onto a computer, but merely for storing data in a convenient form. But I really think that the suggestion of transferring information directly into a computer should receive some more serious consideration.

O'KELLEY: Did I understand that your magnetic tape system was not intended for use as a multiparameter system, but just as a single-parameter analyzer?

SALMON: Yes.

O'KELLEY: Of course, with magnetic tape it is not possible to count at very high rates.

SALMON: You also get into the difficulty that tape written on one machine may not be compatible with another. We have some experience with data storage on paper tape. At Harwell we have a small listing adding machine which is capable of accepting paper tape from one of our analyzers. Very simple operations have been performed, such as background subtraction and spectrum stripping.

O'KELLEY: I would now like to raise a question which has come up already in some of the discussions at this conference: How important to gamma-ray spectroscopists is the standardization of NaI scintillation spectrometers? That is, should we agree to use 3- by 3-in. NaI crystals at 10 cm, 7 cm, or some other distance, and should there be a standard counter shield whose environmental scattering properties are known?

For example, our group at Oak Ridge has for a number of years used a 3- by 3-in. NaI crystal, with a source-to-crystal distance of 9.3 cm. This source-to-crystal distance was one of several for which efficiency curves were readily available from the work of P. R. Bell and his associates. Our distance is rather arbitrary; in fact, I have been told that it was taken from the dimensions of a popular size of vacuum-tube carton which was used as a source holder in the early days!

SALMON: Our standard distance is 17.3 cm.

With regard to standardization, I think it is a good thing for everybody to be able to say about a spectrum, "This was done on a standard crystal, at a standard distance, in a standard geometry." The merit of this is obvious as far as radiochemists

are concerned. Heath has suggested the 3- by 3-in. NaI crystal, and we use these dimensions ourselves.

However, you can't always use a standard detector: different users may want slightly different conditions. A person with a whole-body counter probably wants to use a 9- by 6-in. crystal, or some other large size. But again, some form of standardization should be maintained for this type of measurement.

It is frustrating to try to use published spectra to aid in interpreting your own results, only to discover that the published curves were for a very different setup. With everyone going over to 3- by 3-in. crystals, I would put in a plea that workers in this field stick to that size and use Heath's shield dimensions.

I wouldn't be so fussy about the source-to-crystal distance, whether it is 17.3 or 9.3 cm, because allowances can always be made for this. But as far as general external conditions are concerned, then I really think some standardization is really required.

BROMLEY: Both Dr. Ferguson and I were brought up on 6.2 in. But I think this is another case where it is very important to keep in mind that the experiment may be such that it is not really necessary to go through with a very elegant standardization procedure.

It is quite clear that if you are going to do fallout monitoring or activation analyses where you have a fairly routine measurement which you are going to do, well and good. But I would certainly support what Professor Wapstra said earlier today, that in many specialized applications it is just not feasible, not even desirable, to worry about any sort of standardization. In such cases you can use whatever is conditioned by the experiment, and do the best you can about standardizing on site.

GUINN: I would like to comment, too, that for really accurate work in activation analysis it isn't possible to take anyone else's spectra. For example, while Heath's spectra are very precise, they are for his particular spectrometer.

It is virtually impossible to make another spectrometer just like it. Actual crystals differ in resolution, even though they are the same size. You might, if you surveyed enough crystal-photomultiplier combinations, get two that were virtually identical, but it would take a lot of work with this. So, in practice what you must do is calibrate your own particular crystal – that is, derive your reference spectra from it, not use somebody else's.

The curves that Heath has published are very useful. If you have a crystal which is approximately the same, you can use his tables and graphs very nicely to check identifications. But for the quantitative calculations that you would want to do with the computer, you would use your own set of reference spectra, not those.

One other comment I would like to make is that even if you do settle upon, for practical purposes, a 3- by 3-in. crystal, it doesn't make much sense in this particular kind of work to standardize on a distance because, if a sample is too hot to count at some particular distance, you would rather not throw it away or divide it up just to stick to that distance.

Instead, you would prefer to back it off to some other position. Then you must have reference spectra for different distances, which is what we do in our work. We have a monitoring counter which checks the samples first, and if they are too hot to be counted without gain shift at a particular setting, it tells us what particular distance we should use.

Finally, I would like to remark that, although a 3- by 3-in. crystal is a very good compromise and covers a lot of the sort of work you want to do, there are many special cases in which it is not the right crystal to use.

Just as an example, if you are trying to detect very low-energy gamma rays, say a few tenths of an Mev in the presence of a great deal of interference from something that is one, two, or three Mev, you certainly don't want to use a three-inch-thick crystal. You want to use a very, very thin crystal and you'll get much better results. So you don't want to standardize completely on any one size.

SALMON: I quite agree with the remarks there, but I believe that these reference spectra are very valuable, because the majority of workers only use the gamma spectrometer for a small fraction of their time. However, if they are confronted with reference spectra for different dimensions, they just can't understand how to use the information. This may sound trivial, but I think a very large number of users are barely able to understand how the spectrometer works.

O'KELLEY: I would like to comment also that, as a person who does quite a bit of gamma spectrometry, these reference curves are extremely useful to me. Certainly when you look at a piece of published research, you like to have at least a qualitative feeling for the quality of the data. If the spectrum is taken on a standard setup, it looks familiar, so you can understand and interpret it.

In spite of that advantage, there are special situations which we have all encountered. I suppose we have all been forced to use thin crystals for counting x rays. In Dr. Salmon's paper today, he commented on problems with soil samples that are quite thick and exhibit severe scattering. But these are all specialized applications and require specialized techniques.

At this point, I would like to invite the participation of the audience in a few remaining questions.

First, several people have mentioned to me during this conference that they feel there is a need for some kind of clearing house for computer programs of the sort that we have been discussing. In particular, I think people are interested in gamma-ray unfolding, the generation of response functions, and analysis of radioactive decay curves. I will say at the outset that although the Radiochemistry Subcommittee is a sponsor of this meeting, we are probably in no position to accept the responsibility for such a clearing house. However, I wonder if some of you might have opinions as to the usefulness of such an arrangement.

SHAFER: At IBM there is an arrangement known as SHARE, to which many programs from outside laboratories may be submitted in a standard format. These programs are cataloged and distributed to members of SHARE.

O'KELLEY: That is certainly one procedure. I think perhaps the question I should have asked is whether there was any need to do something in addition to this for programs which are in the formative stages and not ready for SHARE distribution — sort of a formal grapevine. As a result of this conference, I believe that we can consider that the informal grapevine is now well established.

There seems to be a lot of interest in getting a clearing house established to exchange programs. Maybe I should have asked whether there are volunteers.

NOSTRAND: It would be difficult for any one group to take on such a job unaided. However, if there is a group which has the capability and is willing to do so,

then I would suggest that financial support might be requested from some agency such as the Division of Isotopes Development of the AEC.

O'KELLEY: These remarks will appear in the *Proceedings* of this Symposium, and since the Atomic Energy Commission is one of the sponsors, perhaps someone there will take note of the need for a clearing house.

BROMLEY: I would like to enter a small plea in connection with any such collection of programs, and that is that any program be accompanied by an explicit statement of what peripheral equipment it was designed to run on. Otherwise there is some widget in left field which will take the program and chew it in little bits, even though your computer center has the same apparent specifications as the computer for which the program was originally written.

CARR: The Association of Computing Machinery collects a great deal of information in certain areas. For example, as Editor of *Computing Reviews*, I will be glad to accept for possible consideration any sort of bibliographies that anyone would like to have published and put on the record so they could go and find it three or four years from now.

Although I cannot speak for him, I am sure the Editor of the *Communications of ACM* would be interested in any possible proposals of program listings or a review article as to what is going on in this field. I think this is a possible outlet that perhaps might be useful to you in this situation.

SCOFIELD: It would be very useful to adhere to a standard notation, both in the *Proceedings* and in any programs exchanged through a clearing house.

O'KELLEY: I quite agree that this would be an extremely useful thing to do; however, I am not volunteering to do that in the *Proceedings*. It would require too much editing in that case, but as far as future action is concerned, standard notation is becoming highly desirable. The variety of notation used at this symposium points up this need.

NOSTRAND: There has been considerable interest in small computers at this conference. In the past, I feel that there may have been a reluctance for experimenters to publish programs, especially if done on a small computer.

SUNDERMAN: With regard to publication, there is not a wealth of information in the open literature concerning the programs that have been discussed in the last few days. The reports from various agencies under whose auspices they were produced – AEC reports and so on – are available to many of us; but they are not generally available to others.

I think we should consider when working with these programs how we might get them into a form which would be acceptable to various journals for actual publication of the techniques employed and the results of the application of these techniques to experimental data.

These are technique papers. As any radiochemist knows who has tried to get a technique published, this is not an easy thing to accomplish. It is not like getting the 394th method in the literature for the determination of iron. We should work toward a mechanism for getting this information published as soon as produced.

O'KELLEY: Now that so many people have had to prepare their work for the *Proceedings*, perhaps some of the papers will also be published in the open literature. Material can be published in our *Proceedings* under AEC sponsorship, and in journals

as well. If some of the authors should want to do this, we would consider such a course very desirable.

TROMBKA: Would it be possible to publish a companion volume to the *Proceedings*, which would contain only the computer programs discussed?

O'KELLEY: This can be considered later. It would be quite a chore to collect all the programs and publish them in a separate volume.

FERGUSON: I should like to remark that my program which was described this afternoon was written for the Burroughs 205 in machine language. It is not a FORTRAN program. I am very willing to supply the information to anybody who wants it. However, I think it would be very difficult to make this program generally useful, other than by describing the general techniques that were used in writing it.

GOLDIN: Does the Radiochemistry Subcommittee plan to publish a monograph in the *Radiochemical Techniques* series on the subject of gamma-ray spectrometry?

O'KELLEY: To date, we have published a monograph in that series on *Detection and Measurement of Nuclear Radiation*, which contains a rather long discussion of gamma-ray spectrometry. The report number is NAS-NS 3105.

Session 6

Chairman: D. N. Sunderman

Battelle Memorial Institute, Columbus, Ohio

(6-1) COMPUTER-COUPLED ACTIVATION ANALYSIS[1]

D. D. Drew, L. E. Fite, and R. E. Wainerdi
Activation Analysis Research Laboratory
Agricultural and Mechanical College of Texas
College Station, Texas

INTRODUCTION

The Texas A & M Activation Analysis Research Laboratory (AARL) has several systems which will automatically measure and record gamma-ray spectra [*1*]. One of these, the Mark I-Ia, has been used recently in a number of controlled, experimental runs made to establish the effectiveness of two computer programs. It is especially convenient to use since its final outputs are punched cards, suitable for direct computer input.

The two computer programs, AARL-10 and AA-4, were written to provide high-speed processing of large volumes of data at low computational cost. In using these programs, it is intended that several hundred samples be analyzed in a routine manner with the computer-coupled system. Several simplifying assumptions have been made to facilitate the computer programs. These include the assumption that samples having known qualitative composition of fewer than about ten elements will be processed in large groups having similar arrays of elements. The experiments described in this paper were made to establish the accuracy of automated analysis under these conditions, with each of the computer programs.

AARL-10 PROGRAM

The AARL-10 program, written by Breen [*2*], develops a system of n linear simultaneous equations and n unknowns. They are of the form

$$k_1\, g_1(n) + k_2\, g_2(n) + \ldots + k_m g_m(n) = D(n)\,, \qquad (1)$$

[1]This research was sponsored by the Division of Isotopes Development, United States Atomic Energy Commission, through the Texas Agricultural and Mechanical Research Foundation.

where $k_1, k_2, \ldots, k_m$ are the unknown coefficients, $g_1(n), g_2(n), \ldots, g_m(n)$ are the count values of the spectrum elements 1, 2, ..., m, in channel n. The term $D(n)$ is the count value of the data spectrum in channel n. The best statistical data are at peaks; the m values of n are chosen to be those channel numbers which correspond to a main peak in one of the element spectra.

The computer program scans the entire data spectrum and finds peaks using the "*students t*" test. Those elements having matching peaks are considered to be present. The values $k_1, k_2, \ldots, k_m$ are found, and weights of elements present are calculated using the usual decay and flux ratios. Some of the best results using AARL-10 were found by Breen [2] and are listed in Table 1.

There is one fundamental error in the concept of the AARL-10 program. When gamma rays from several different isotopes have similar energies, the spectra contain overlapping peaks. If they fall in the same spectrometer channels, there is no solution. If they fall in close proximity, the resulting simultaneous equations will be so similar that the system is ill-conditioned. This effect amplifies any errors in the data spectra. If, in correcting this, a channel which is not a peak location is used, the accuracy is reduced.

Table 1. Analysis of Single Element Standards by Mark I-Ia System and AARL-10 Program

Element	Actual Mass (mg)	Computed Mass (mg)
Antimony	5.76	6.55
Antimony	9.02	10.36
Antimony	12.78	12.64
Tin	34.8	35.58
Tin	16.86	16.86
Zinc	8.67	9.67
Zinc	15.2	16.36
Zinc	10.12	12.83

AA-4 PROGRAM

An extension of the AARL-10 program is the use of the entire spectrum for analysis. If the spectra of the various components add linearly, the total curve is a summation of all radioactivities present in the sample. The new program, AA-4, obtains a spectrum *best-fit* in the sense of least squares. This presupposes a reference library of the activated elements. In its operation it minimizes the expression

$$\sum_{n=i}^{n=j} [k_1\, w(n)\, g_1(n) + \ldots + k_m\, w(n)\, g_m(n) - w(n)\, D(n)]^2 , \qquad (2)$$

where $w(n)$ is a weighting function. The AA-4 program assumes $w(n) = (1/D)(n)$.

An artificial data spectrum, used to check out the AA-4 program, was generated by averaging the counts in each channel of ten different library spectra. The calculated coefficients should, of course, be 0.1. The ten library curves and the one data curve were each distorted by applying a 4% random error to the counts in each channel. This was done by multiplying 4% of the channel height by a random number between −1 and +1. The results are shown in Table 2.

Table 2. Analysis of an Aritificial Spectrum by Use of the AA-4 Program

Element	No Error[a]	Weighted[b]	Unweighted[b]
1	0.10000	0.1001	0.102
2	0.09991	0.0935	0.046
3	0.09991	0.0945	0.0898
4	0.10000	0.0995	0.997
5	0.10000	0.0963	0.1528
6	0.10000	0.0997	0.0984
7	0.10000	0.1012	0.1016
8	0.09999	0.1104	0.03525
9	0.10000	0.0975	0.9866
10	0.10000	0.1034	0.1058

[a]Computer solution with no error. The exact result should be 0.1.

[b]Computer solution with a maximum 4% error in libraries and data. The weighting function used was 1 per data.

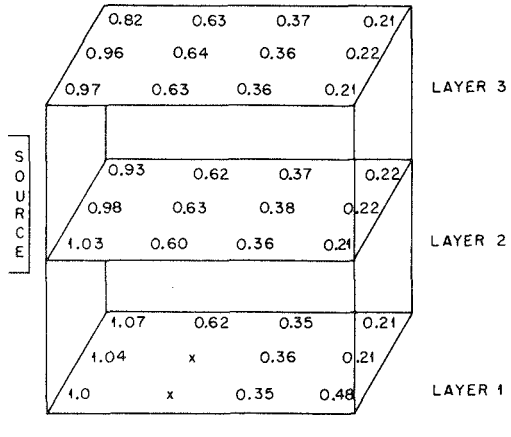

Fig. 1. Thermal Flux Variations in a 4 × 4 × 10 in. Aluminum Box.

Many of the data obtained from the Mark I-Ia system came from samples irradiated in a 4 × 4 × 10 in. aluminum box. The data and library samples were irradiated together, and, since the samples were in the same vicinity in the box, the assumption was made that the flux was uniform. This assumption was checked by placing a number

of known samples of copper in the box, 2 in. apart in the vertical and horizontal directions, and $2\frac{1}{2}$ in. apart down the length of the box. They were irradiated 6 hr and counted. The flux of the lower left sample, nearest the reactor, was assumed to be 1, and the rest of the fluxes were calculated by using the ratio of the main peak heights. The results are shown in Fig. 1.

RESULTS OF THE AA-4 PROGRAM

Table 3 lists the actual and computed weights of seven aluminum samples. These were irradiated and counted separately, using the pneumatic system of the Mark I-Ia system. The maximum error is 5%, and the average is 2.4%. The fourth sample was ignored.

Table 3. Analysis of Aluminum Standards by the Mark I-Ia System and the AA-4 Program

3d Al Run Sample No.		Sample Wt (mg)	Al (added)	Al (found)	Error (%)
001188	060118	1.37	0.725	0.742	+2.3
001190	080118	1.33	0.704	0.700	−0.6
001189	070118	1.31	0.694	0.685	−1.3
001016	010118[a]	1.32	0.699	0.438	
001187	050118	1.39	0.736	0.709	−3.7
001186	040118	1.35	0.715	0.751	+5.0
001192	100118	1.24	0.656	0.664	+1.2
				Average Error	+2.4%

[a]This sample contained visually less photopeak counts than any other.

Table 4 lists the results of a two-component system. Three mixtures and three libraries were irradiated about 6 hr in the aluminum box. After a waiting period of two days, each sample was counted four times, and the masses were calculated. Here, the accuracy was about 10%.

Table 5 lists the results of a four-component system. Three mixtures and three libraries were irradiated in the box, and each mixture was counted three times. Here it is interesting to note that deviation from the actual values is about twice the deviation from the average value. Zinc is low in all three samples, antimony is scattered around the actual, and sodium and potassium are always high.

The results of an analytical problem of general interest are given in Table 6. The analysis was for sodium, chlorine, and magnesium in blood sera.

Table 4. Computer Analysis of Gamma-Ray Spectra by the AA-4 Program Test: Data Reduction of a Two-Element Matrix for Activation Analysis

Sample (mg)	Determination[a]				
	1st	2d	3d	4th	Average
Mix-1					
Sb, 0.16	0.23	0.23	0.19	0.25	0.23
Zn, 16.07	13.02	13.71	15.66	14.75	14.29
Mix-2					
Sb, 0.16	0.21	0.22	0.24	0.24	0.23
Zn, 16.07	17.09	17.25	16.89	17.53	17.19
Mix-3					
Sb, 0.16	0.19	0.18	0.19	0.21	0.19
Zn, 16.07	15.47	18.88	16.30	17.09	16.94

[a]Precision: Sb, 0.22 ± 0.02 (9.1%); Zn, 16.14 ± 1.62 (10.0%).

Table 5. Computer Analysis of Gamma-Ray Spectra by the AA-4 Program Test: Data Reduction of a Two-Element Matrix for Activation Analysis[a]

Sample	Zn	Sb	Na	K
1–1	0.01759	0.00021	0.00269	0.02312
1–2	0.01431	0.00029	0.00238	0.02391
1–3	0.01343	0.00029	0.00250	0.02439
Average	0.01511	0.00026	0.00252	0.02380
Actual	0.02003	0.00022	0.00205	0.01995
2–1	0.01832	0.00016	0.00318	0.02935
2–2	0.01644	0.00023	0.00315	0.02936
2–3	0.01479	0.00020	0.00304	0.02960
Average	0.01651	0.00019	0.00312	0.02943
Actual	0.02009	0.00020	0.00200	0.02010
3–1	0.01572	0.00014	0.00308	0.02490
3–2	0.01451	0.00021	0.00287	0.02746
3–3	0.01933	0.00020	0.00309	0.02679
Average	0.01652	0.00018	0.00301	0.02638
Actual	0.02009	0.00020	0.00205	0.02010

[a]Mass in grams.

Table 6. Analysis of Blood Sera by Computer-Coupled Activation Analysis

Sample No.	Sodium (%)	Chlorine (%)	Magnesium (%)
1	2.67	4.08	0.38
1	2.91	4.36	0.78
2	2.63	4.34	0.51
2	2.16	3.80	0.24
3	2.62	4.32	0.48
3	2.88	4.40	0.43
4	2.06	3.86	0.20
4	2.94	4.39	0.48
6	2.21	4.19	0.24
6	2.91	4.25	0.33
6	3.04	4.20	0.26

CONCLUSIONS

Computer-coupled activation analysis will automatically process an analytical result from a weighed sample. The accuracy of this technique is comparable to other analytical procedures for a single radioactive isotope matrix. As the complexity of the samples increases, the accuracy of the technique decreases. This effect is the result of many variables. When the problems of flux mapping and standard library spectra have been resolved, better data are expected. Accuracy can also be improved with better weighting functions for the spectral curves. Factors such as spectral slope (total number of channels), channel number, and number of counts per channel are also being considered for weighting.

REFERENCES

[1] L. E. Fite, Derek Gibbons, R. E. Wainerdi, *et al., Computer Coupled Automatic Activation Analysis* [Annual Report, May 1, 1961, United States Atomic Energy Commission Contract No. At-(40-1)-2671 for the Division of Isotopes Development].

[2] W. M. Breen, "Digital Computer Coupling Techniques for Automatic Activation Analysis," M.S. thesis, Texas A & M, College Station, Texas, 1961.

(6-2) GAMMA-RAY SPECTROMETRY REQUIREMENTS FOR SPECTRUM STRIPPER AND COMPUTER CALCULATIONS IN ACTIVATION ANALYSIS STUDIES

V. P. Guinn and J. E. Lasch
General Atomic Division of General Dynamics Corporation
John Jay Hopkins Laboratory for Pure and Applied Science
San Diego, California

INTRODUCTION

Instrumental activation analysis [1] is based on gamma-ray spectrometry and involves the quantitative analysis of gamma-ray pulse-height spectra obtained after activation of samples. In simple cases at least one completely resolved photopeak of the radioisotope of interest (or one completely resolved photopeak of each radioisotope of interest) appears in the spectrum. In such cases quantitative estimation is readily accomplished by simple means such as measurement of the photopeak height or photopeak area, above the Compton continuum base, and comparison with the corresponding measurement on the spectrum of the activated pure-element standard sample. In these simple cases even an appreciable amount of gain shift can be tolerated without seriously affecting the accuracy of the final value.

However, for complicated cases, more involved pulse-height spectra are obtained, in which overlapping photopeaks occur. Two techniques have become quite prevalent recently for the partial or complete resolution of such complex spectra: spectrum stripping techniques and computer techniques. As will be shown, these techniques place rather severe requirements on the reproducibility of the gamma-ray spectrometry operations. The difficulties, and methods of circumventing these difficulties, are also discussed.

SPECTRUM STRIPPING

The spectrum stripping technique involves resolution of a complex pulse-height spectrum by subtracting, separately, the contribution from each radioisotope present in the sample in statistically detectable amounts. This may be done, in general, in either of two ways: (1) by counting a reference sample of the isotope to be removed, in subtract mode, in the same counter and under the same conditions as were employed in obtaining the complex sample spectrum, or (2) by subtracting a stored spectrum or tape (magnetic or punched paper) of the pure, single radioisotope pulse-height spectrum from the complex sample spectrum, using a variable multiplier. Both techniques are performed directly with the multichannel pulse-height analyzer, and complete subtraction must be determined by visual examination of the oscilloscope display. The technique is thus somewhat subjective. However, if the various spectra involved are obtained under almost exactly the same gain and if care is exercised by a skilled operator, quite satisfactory quantitative results can be obtained. If the reference samples or reference spectra represent also known weights of the elements in question, activated under known conditions and counted at known decay times,

the subtraction process also supplies the data from which the weight of each subtracted element in the unknown sample may be computed very simply.

COMPUTER SOLUTION OF PULSE-HEIGHT SPECTRUM DATA

An alternate approach to the quantitative resolution of a complex gamma-ray spectrum into its various statistically significant components is to utilize a purely mathematical technique. Typically, this may be accomplished by solving, by least-squares methods, a set of simultaneous equations, with at least as many independent equations as there are radioisotopes significantly contributing to the observed spectrum. There are a number of variations of this basic approach, many discussed in other papers of this Symposium [2] to [5]. However, all have one requirement in common: the coefficients derived from the pulse-height spectrum data of the reference samples (pure individual radioisotope species) are constants; that is, all the spectra utilized (unknown and reference) were obtained at almost exactly the same overall spectrometer gain. Computer solution of such a set of equations can then provide values for each species present in significant amounts, and its standard deviation, and also can supply firm upper limits for species not detectable. The method is not subjective.

PROBLEM OF GAIN SHIFT

The greatest difficulty in the path of successful utilization of either the spectrum stripper or the computer calculation methods of resolving complex pulse-height spectra into their components is, at present, not due to inadequacies of the spectrum stripping circuitry, of the electronic computers, or of the pulse-height analyzers, but rather to difficulties with the photomultiplier tubes employed in the NaI(Tl) scintillation detectors.

Under conditions of constant voltage applied to a given photomultiplier tube, the electronic gain (multiplication) of the tube is still found to vary somewhat with average tube counting rate (a function of counting rate and pulse-height distribution) and with time. Such effects have been observed and reported by a number of investigators, including Marshall, Coltman, and Hunter [6] and Caldwell and Turner [7].

A number of measurements of gain shifts have been made in this laboratory also, employing a particular 3- by 3-in. solid cylindrical crystal of NaI(Tl) coupled to a given Du Mont 6363 photomultiplier tube and an RIDL transistorized 400-channel pulse-height analyzer. These are discussed briefly below and are illustrated in Figs. 1 to 4.

The prompt effect of counting rate on overall gain is shown in Fig. 1 for three different photomultiplier tube voltages. The data were obtained with three different Au^{198} sources, which gave total counting rates (sum of all 200 analyzer channels used) of 47,000, 320,000, and 680,000 cpm respectively. The spectra were obtained promptly after placing a sample on the crystal. As expected, the gain shift at the higher voltages increases with increasing counting rate, amounting to a little more than 1% with the most active sample at the highest photomultiplier tube voltage (1040 v). As predicted, the gain shift is much less severe at a low phototube voltage (830 v) and in

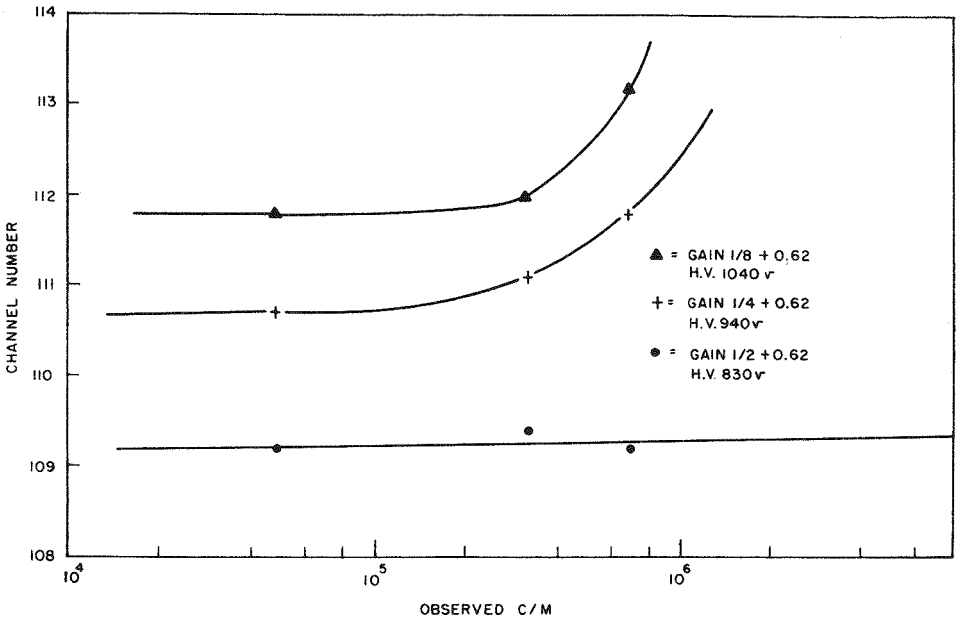

Fig. 1. Effect of Counting Rate on Gain at Various Photomultiplier Tube Voltages.

fact is negligible in this case even at a counting rate of 680,000 cpm. In these measurements the total gain was kept about the same (so that the 0.412-Mev Au^{198} photopeak was in the vicinity of channel 110) by increasing the amplifier gain as the phototube voltage was decreased. For easier graphical comparison the high voltages were adjusted slightly so that the low counting rate sample photopeak would fall approximately in channels 110, 111, and 112 respectively. Rather similar results on prompt gain shifts at high counting rates have been reported by Covell and Euler [8].

The long-term gain shift resulting from high counting rates is shown in Fig. 2. These measurements were carried out at a relatively high phototube voltage (1040 v). Three Au^{198} sources, producing total counting rates of 91,600, 142,000, and 167,000 cpm for sources *C*, *D*, and *E*, respectively, were used. From Fig. 2 it may be noted that the least active sample did not shift appreciably in gain even over a 2-hr counting. The intermediate-activity sample showed a gradual increase in gain (about 0.5%) during a counting period of about 1 hr. The most active sample also showed a gradual increase in gain (about 1%) during a counting period of about 1 hr. The approximate one-channel initial difference in the photopeak location of sources *C*, *D*, and *E* is not due to prompt gain shift but rather to slight increases in phototube high voltage so that the starting points would be in approximately channels 110, 111, and 112, respectively, for easier graphical comparison. The data of Fig. 2 were obtained from a 2-min count spectrum taken every 10 or 20 min, the sample remaining on the counter all the time. Long-term gain shift data for a number of different types of photomultiplier tubes have been reported by Covell and Euler [8].

The speed of recovery of gain, after a large gain shift has occurred, was studied also. Results of one set of measurements are shown in Fig. 3. With a phototube voltage of 1040 v, a very active Au^{198} sample (868,000 cpm) was placed on the crystal

and left there for 30 min, during which time four spectra were taken rapidly, at intervals, to determine the location of the photopeak. As can be seen from Fig. 2, the peak

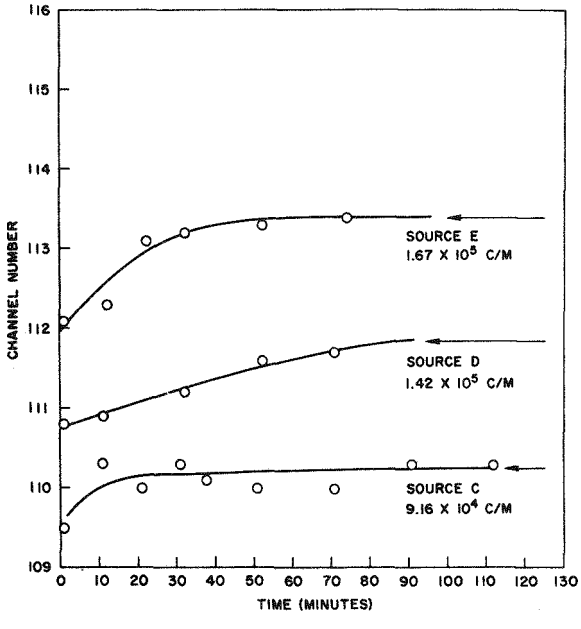

Fig. 2. Long-Term Counting Rate Gain Shifts.

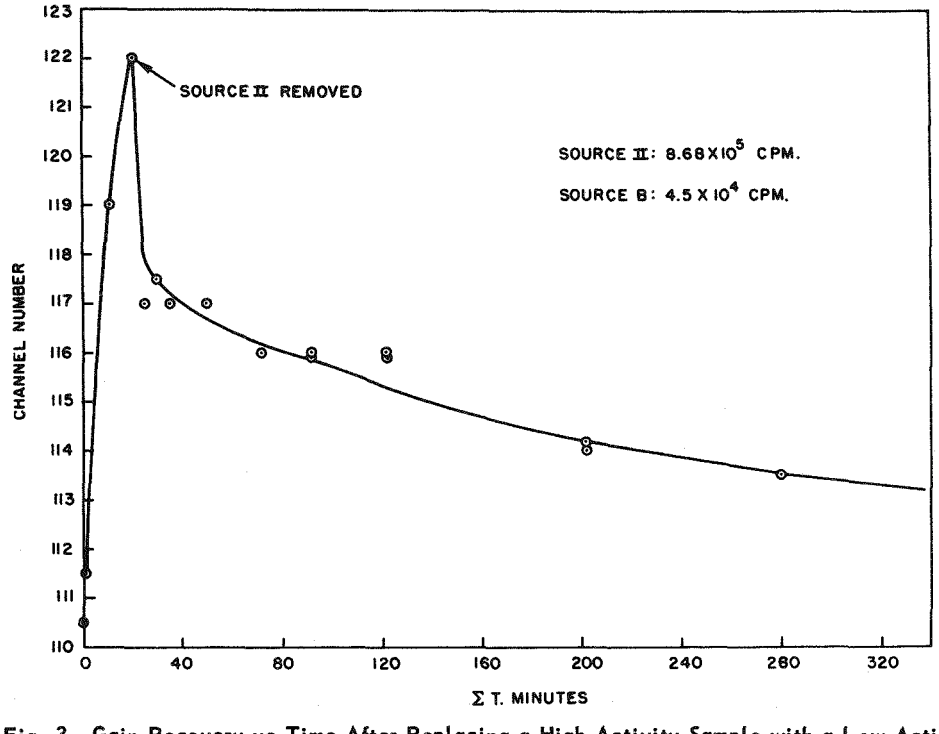

Fig. 3. Gain Recovery vs Time After Replacing a High Activity Sample with a Low Activity Sample.

moved from approximately channel 110 (at zero time) to 111 (1 min) to 119 (15 min) to 122 (30 min). At this point the very active sample was replaced by a low-activity Au^{198} sample (45,000 cpm). Spectra were then obtained at intervals for the next 6 hr, during which time the photopeak rapidly came back as far as channel 117 and then, more gradually, back as far as channel 114. Rather similar data, except that they involve an RCA 6342A phototube (with a large negative gain shift at high counting rates), have been presented by Covell and Euler [8], showing the same hysteresis behavior.

With regard to the possible effect of gain shift on counter resolution, resolution measurements in this laboratory (with Au^{198} samples of various strengths) have shown no measurable change in "instantaneous," or "true," resolution over a wide range of counting rates. However, there is, as expected, an apparent deterioration in resolution if one counts a very active sample for a relatively long period of time, a length of time during which gain shift is occurring to an appreciable extent. If the pulse-height data that have been accumulated over this entire period are then printed out as a single spectrum, a broader photopeak is observed. However, if counting is continued for a yet longer period of time, the gain approaches a new but constant value, and hence the apparent resolution begins to improve again. These effects are illustrated in the data of Fig. 4. In this case a fairly active Au^{198} sample (186,000 cpm) was

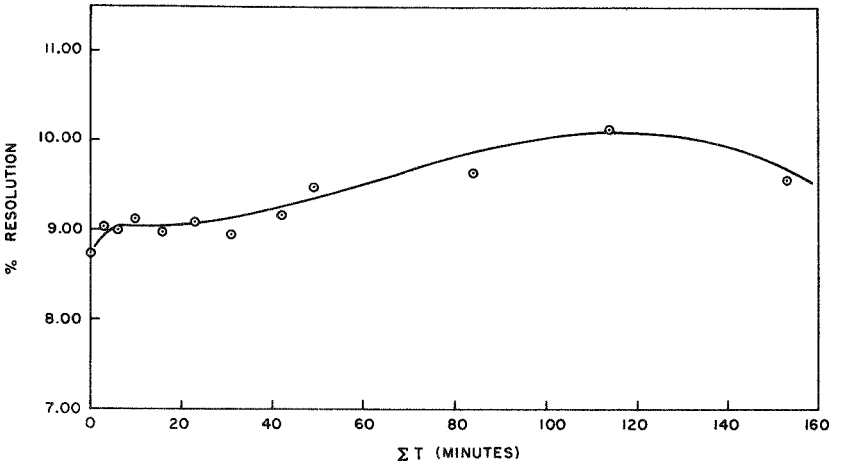

Fig. 4. Effect of Counting Time at High Counting Rates upon Apparent Counter Resolution.

placed on top of the crystal and left there for 153 min. At intervals the sample was counted for a brief period (0.2 min live time), and at each such time the total accumulated spectrum (accumulated in all the preceding 0.2-min counting periods) was printed out but not erased from the analyzer memory. The apparent resolution of the photopeak was then calculated for each readout, the results being those shown in Fig. 4. It is seen that the apparent resolution gradually changed from the initial ("true") resolution value of about 8.8–9.0% (at 0.412 Mev) up to a maximum of 10.2% (after 114 min) and then started to return, reaching a value of 9.6% at 153 min. These data are not quantitatively indicative of the effect of gain shift on apparent resolution, since the counting periods were not uniformly spaced, but they do indicate the general behavior. Because of the high counting rate and the limited storage capacity of the analyzer (10^5

counts/channel), it was not possible to accumulate counts during the total exposure time of 153 min but, instead, just for the sum of twelve 0.2-min counting periods shown.

METHODS OF MINIMIZING GAIN SHIFT

It is clear that very little gain shift can be tolerated if one wishes to employ spectrum stripping or computer solution techniques in the quantitative resolution of complex gamma-ray pulse-height spectra. From experience in this laboratory it is felt that the maximum allowable gain shift, when employing spectrum stripping techniques, is about one-fourth a channel out of 200 (or about 0.1%). For computer calculations it is felt that the maximum allowable shift may be a little larger, perhaps about one-half a channel out of 200 (or about 0.2%). With gain shifts greater than these tolerances, appreciable errors are introduced in the computed results, increasing with increasing gain shift. The possibility of normalizing spectra mathematically to correct for gain shift has been suggested, but the time-dependence (hysteresis) of the gain shift effect precludes the feasibility of doing this accurately.

A number of simple rules, by means of which gain shift problems can be at least greatly minimized, are apparent from a study of results in the literature and of data obtained in this laboratory, such as those presented in this paper. These rules are summarized as follows and are employed in this laboratory:

1. Operate the photomultiplier tube at minimum feasible high voltage and use maximum amplifier gain (since with present-day equipment the phototube is the most susceptible to gain shift at high counting rates, that is, more susceptible than the amplifier or pulse-height analyzer).

2. Do not count a rather active sample for a period of time any longer than is necessary to accumulate sufficient counting statistics (to avoid long-term gain shifts). Fortunately, highly active samples, which produce large gain shifts, need not be counted for more than a matter of seconds to provide good statistics for at least the major components.

3. Employ a screening counter to check the activity of samples before they are placed in the spectrometer. A few seconds of counting on a simple NaI(Tl) counter-ratemeter system is all that is required. If the activity level is low enough so that the equivalent counting rate on top of the main spectrometer crystal, at the desired gain (approximate conversion factors for converting screening counter rates to equivalent rates on the main spectrometer determined by simple calibrations), is less than a few hundred thousand counts per minute (the current gain shift tolerance rates of our spectrometer systems), the sample may be safely counted in the spectrometer, with negligible gain shift. If the screening counter rate indicates an excessive counting rate, the sample may be counted at one of five fixed poorer geometries (shelves at various distances above the spectrometer crystal). Again, previous rough calibrations indicate which shelf is best. Reference samples must then also be run on this shelf, since the detailed spectrum shapes do, of course, depend upon sample-to-crystal distance. If the sample is too active to be counted without gain shift on even the top spectrometer shelf, it should be (1) discarded, (2) allowed to decay until it can be counted suitably, or (3) an aliquot should be taken for counting. In general, samples too active to be counted without gain shift even on the top shelf will have been noted on milliroentgen per hour gamma-ray safety meters, even before any check on the screening counter.

4. Employ a plastic absorber (typically 1 cm thick) between sample and crystal to absorb most of the beta particles which would otherwise reach the crystal from the sample, with minimum production of bremsstrahlung. Contributions from beta particles and bremsstrahlung are undesirable in gamma-ray spectrometry, since they contribute to overall counting rate (and hence to gain shift) and to the general "Compton smear" of the spectrum, and they introduce greater dependence on sample density.

5. Avoid long-term counting-rate-independent gain shifts by frequent gain checks with a standard isotope source (such as Cs^{137}).

6. If necessary, employ a gain stabilization device, such as that described by Scherbatskoy [9], or the commercial device which has very recently become available.[1] A similar apparatus is also described by Fite, Gibbons, and Wainerdi [10].

7. Employ a photomultiplier tube of a type known to be least sensitive to counting rate gain shift and, if possible, selected from a group of such tubes on the basis of minimum gain shift. For example, Covell and Euler [8] have found that EMI photomultiplier tubes are outstanding in their relative freedom from gain shift at high counting rates. Their results also show a greater consistency, from one EMI tube to another, in their gain shift behavior than that shown by other photomultiplier tubes.

8. Since temperature affects the gain characteristics of photomultiplier tubes, preamplifiers, and amplifiers (especially if transistorized), and the electronics of multichannel analyzers (again, especially if transistorized), it is essential that the entire spectrometry unit, including detector, be located in a thermostatted, well-ventilated room.

OTHER PROBLEMS WHICH AFFECT THE ACCURACY OF SPECTRUM STRIPPER AND COMPUTER RESOLUTION OF COMPLEX GAMMA-RAY SPECTRA

In addition to gain shift, certain other problems can cause trouble with the spectrum stripper and computer methods of resolving complex pulse-height spectra into their components. Two of these are discussed below.

Beta Particle and Bremsstrahlung Contributions

Contributions from these sources can result in erroneous results in computer calculations but do not directly interfere with spectrum stripping (since the latter is based only on photopeak subtraction). For example, if a number of samples containing variable amounts of phosphorus are activated with thermal neutrons to detect certain other elements present which form gamma-emitting isotopes, computer results can be in error unless a P^{32} reference spectrum is included in the library of spectra employed in the computer calculation. With peak-searching routines the presence of pure beta emitters, such as P^{32}, is not detected and hence would not normally be included in the set of equations which the computer would set up and solve. Hence, the results for all the species detected and calculated would be in error. An example of this difficulty is shown in Fig. 5, which shows the pulse-height spectra obtained from an Au^{198} sample containing various amounts of P^{32}. The pulse-height distribution in the various channels is obviously greatly altered by the contributions of the P^{32} beta particle spectrum

[1] Spectrastat, Cosmic Radiation Laboratories, Inc.

(and bremsstrahlung arising from the P^{32} beta particles). A thicker plastic absorber than that used for these illustrative measurements could prevent even the most energetic of the P^{32} betas (1.71 Mev) from reaching the crystal, but some contribution from bremsstrahlung formed in the sample, its container, and the plastic absorber would still reach the crystal and be detected.

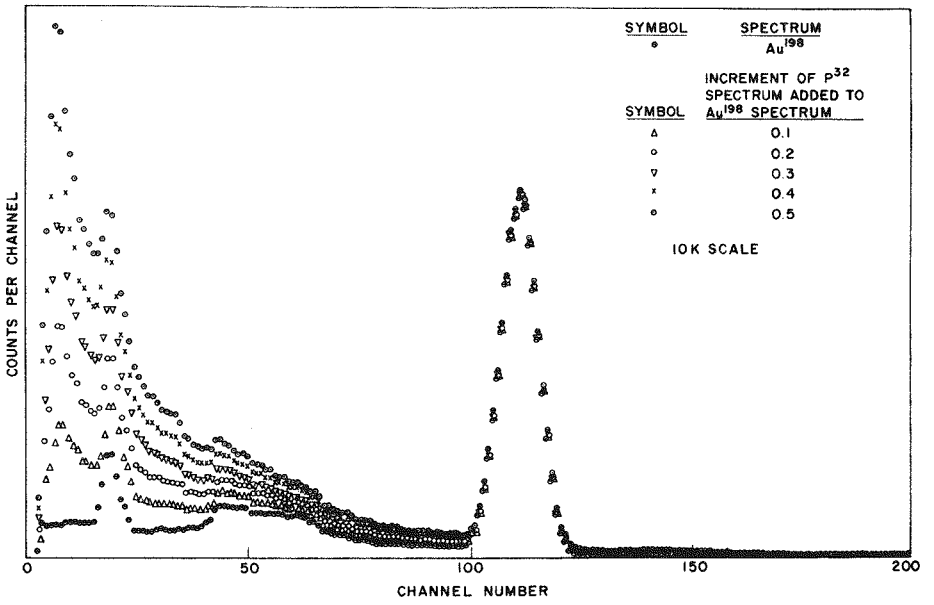

Fig. 5. Effect of P^{32} Beta Particles and Bremsstrahlung upon the Apparent Shape of the Au^{198} Gamma-Ray Spectrum.

Even if, in such a case, a P^{32} reference spectrum were introduced into the computer calculations, errors can arise if the samples vary appreciably in density and average atomic number, since the number and energy distribution of beta particles and bremsstrahlung photons getting out of the sample will depend on these factors. Thus, the "standard" P^{32} spectrum shape might be different for each sample.

This problem is not serious, in general, for low-energy beta particles (E_{max} <1 Mev), since they are readily absorbed with little bremsstrahlung formation but may become important with higher-energy beta particles. Even in those cases in which an induced activity emits a readily detectable gamma ray, as well as high-energy beta particles, difficulties can arise because of variations among the samples in density and atomic number, for example, if various samples are analyzed for aluminum via the $Al^{27}(n,\gamma)Al^{28}$ reaction – since Al^{28} emits 2.87-Mev E_{max} betas as well as 1.78-Mev gammas. Variations in sample density and Z can of course alter the number and energy distribution of gamma rays getting out of the sample, but small variations affect the beta particles much more than they affect the gamma rays.

Use of Inaccurate Reference Spectra

Unless very careful refinements are carried out, the use of certain types of reference spectra can lead to errors in computer results and, in some cases, to errors or complications in spectrum stripping results. The difficulty arises whenever a "pure" element is irradiated with thermal neutrons to provide a reference spectrum of, preferably, a single radioactive species. Difficulties can then arise because of (1) impurities in the "pure" element standard, (2) production of more than one (n,γ) radioactive product by the element, and (3) production of significant quantities of (n,p), (n,α), or $(n,2n)$ radioactive products by the element from the fast-neutron component of the predominantly thermal neutron flux. Presumably other activities, due to A^{41} production from air in the container and to impurities in the container itself, would have been already eliminated by obvious means (such as air flushing before counting, transfer to fresh containers before counting, or subtraction of A^{41} and activated container spectra) and background contributions similarly eliminated (by subtraction).

With regard to point (1), obviously very pure standards should be used. However, in many cases even the best available will show detectable activities, due to impurities, especially in spectra obtained at times very short, or very long, relative to that of the principal radioisotope. If standard spectra are to be employed over a wide range of irradiation and decay times, they should first be corrected by subtraction of each identified impurity contribution. If this is not done, the reference spectrum will differ somewhat in shape as a function of irradiation and decay times, since, in general, the impurity activities will have half-lives different from that of the principal radioisotope.

Point (2) is a difficulty that arises often but is more readily corrected. For example, if a very pure copper sample is activated in a highly thermal neutron flux, two copper radioisotopes are produced in significant amounts: 12.8-hr Cu^{64} (a positron emitter) and 5.1-min Cu^{66} (which emits 1.04-Mev gamma rays). At decay times of the order of an hour or less, both isotopes will contribute significantly to the observed spectrum, in amounts (for given counting conditions) depending on the irradiation and decay times involved. It is seldom feasible to count each unknown sample at exactly the same decay time as that at which the reference spectrum was obtained (in which case there would be no problem), and hence decay corrections are necessary. This is of course simple if only one half-life is involved but is more complicated if two or more half-lives are involved. In the example cited, one can obtain a rather pure Cu^{64} reference spectrum by simply waiting until the 5.1-min Cu^{66} activity has decayed out and then obtain a rather pure Cu^{66} reference spectrum by subtracting the Cu^{64} component out of the reference copper spectrum obtained at an earlier decay time. Then, separate Cu^{64} and Cu^{66} reference spectra can be utilized in either spectrum stripping or computer operations in a straightforward manner. Other cases, however, may be more involved, especially where more than two (n,γ) radioisotopes are produced by the element and/or where at least two of them have rather similar half-lives.

The production of radioisotopes in a single element by fast neutron reactions, as well as by thermal neutron reactions, can further complicate the situation [point (3)]. Even in the case of an element that is monoisotopic in nature, such as aluminum, the problem exists. For example, stable aluminum consists entirely of Al^{27}, which readily forms 2.3-min Al^{28} by thermal neutron (n,γ) reaction; but, it can also

form 9.5-min Mg^{27}, 15.0-hr Na^{24}, and 6.5-sec Al^{26m} by (n,p), (n,α), and $(n,2n)$ reactions, respectively, if fast neutrons are also present. The first two of these fast neutron products are also gamma emitters (as is Al^{28}), and the third one (Al^{26m}) is a positron emitter (and hence forms 0.511-Mev annihilation photons in the sample). Since all neutron sources used in neutron activation analysis generate neutrons initially as fast neutrons (e.g., as fission spectrum neutrons or as 14-Mev neutrons), one generates a thermal neutron flux by slowing these fast neutrons down in some sort of moderator. At the positions of high thermal neutron flux (usually required for high-sensitivity detection), there is normally still an appreciable fast neutron component, and hence the possibility of fast neutron reactions cannot be ignored. Since these products do not have the same half-life as the main product (in this case, Al^{28}), one must resolve the aluminum reference spectrum into pure spectra of Al^{28}, Mg^{27}, Na^{24}, and Al^{26m} in order to avoid the limitation of having to count unknown and reference at exactly the same decay time (following irradiation for identical periods of time).

In computing final results in a case such as that described above, one must of course allow for any formation of Al^{28} from fast neutron reactions on other elements possibly present in the sample: $Si^{28}(n,p)Al^{28}$ or $P^{31}(n,\alpha)Al^{28}$. Similarly, Mg^{27} can also be produced by $Mg^{26}(n,\gamma)Mg^{27}$ and $Si^{30}(n,\alpha)Mg^{27}$; Na^{24} also from $Na^{23}(n,\gamma)Na^{24}$ and $Mg^{24}(n,p)Na^{24}$; Al^{26m} is only formed from Al^{27}. These contributions, of course, not only complicate computer and spectrum stripping operations but also calculations by simple photopeak height or area measurement as well. One here often resorts to activations with and without cadmium wrapping of the sample to provide more accurate identification of the source of fast-neutron-produced components.

In hydrogen-containing samples, recoil protons generated by collisions between fast neutrons and sample protons can in certain cases also complicate matters by forming appreciable amounts of activities by (p,n) or (p,γ) reactions. Two well-known examples are the formation of 10.0-min N^{13} (a positron emitter) by the $C^{13}(p,n)N^{13}$ reaction (if the sample also contains carbon, as in all organic samples) [*11*] and the formation of 1.87-hr F^{18} (a positron emitter) by the $O^{18}(p,n)F^{18}$ reaction (if the sample also contains oxygen).[2]

In most neutron sources there is too low a flux of very high energy (> 5–10 Mev) gamma-ray photons to produce appreciable activities by (γ,n) or (γ,p) reactions, although this can be a problem if a potent source of photoneutrons, such as a high-energy electron linear accelerator, is employed.[3]

OTHER SOURCES OF ERROR

There are, of course, many other sources of error which can affect the accuracy of all methods of calculation, not just the results obtained from spectrum stripping and computer calculation. Such sources of error are thus extraneous to the present discussion, and most are quite obvious but may be simply mentioned here. They are errors due to (1) neutron flux variations from one sample (or reference) position to another, if not corrected for, (2) appreciable and variable amounts of neutron self-shielding, (3) appreciable and variable differences in the fast neutron moderating

[2]This reaction has been used in this laboratory to determine O^{18} in water samples obtained in O^{18} tracer studies.

[3]As in studies in this laboratory with a 45-Mev Linac.

powers of samples and standards, (4) appreciable and variable differences in sample size and hence counting geometry, (5) variations in sample and reference gamma-ray self-absorption and scattering (and the beta particle absorption and bremsstrahlung formation variations discussed previously).

It is assumed that timing errors in irradiation, decay, and counting (including spectrometer dead time) are both obviously possible and readily minimized so that they deserve only passing mention.

CONCLUSIONS AND SUMMARY

Instrumental neutron activation analysis is a potent analytical method but contains many possible sources of difficulty and error. These must be recognized and eliminated, minimized, or corrected for. Certain of these sources of error are peculiar to the spectrum stripping and/or computer solution methods of resolving complex gamma-ray spectrum data into their various components. Of these, the problem caused by spectrometer gain shift at high counting rates is perhaps the most serious. The gain shift problem is examined in some detail in the preceding discussion, exemplified by experiments carried out in this laboratory and shown in the figures. Also, practical means by which the gain shift problem can be greatly minimized, based on experience in this laboratory, are enumerated.

With suitable attention to problems such as gain shift, matrix matching, elimination of high-energy beta particles and their bremsstrahlung, and preparation of pure radioisotope reference spectra, instrumental neutron activation analysis, coupled with spectrum stripping or computer calculation methods, can be a powerful, wide-range, sensitive, accurate analytical method. At the present time the spectrum stripping technique is often used in this laboratory (in various phases of the Activation Analysis Program), and a peak-searching, weighted least-squares program is being developed for use with the laboratory's IBM 7090 computer.

REFERENCES

[1] V. P. Guinn and C. D. Wagner, *Anal. Chem.* **32**, 317 (1960).

[2] A. J. Ferguson, these Proceedings, paper 4-1.

[3] L. Salmon, these Proceedings, paper 4-2.

[4] J. I. Trombka, these Proceedings, paper 4-3.

[5] D. Drew, L. E. Fite, and R. E. Wainerdi, these Proceedings, paper 6-1.

[6] F. H. Marshall, J. W. Coltman, and L. P. Hunter, *Rev. Sci. Instr.* **18**, 504 (1947).

[7] R. L. Caldwell and S. E. Turner, *Nucleonics* **12**(12), 47 (1954).

[8] D. F. Covell and B. A. Euler, *Proceedings of the 1961 International Conference on Modern Trends in Activation Analysis, Held at Texas A. & M. College, December 15–16, 1961*, p 12, Texas A. & M. College, College Station.

[9] S. A. Scherbatskoy, *Rev. Sci. Instr.* **32**, 599 (1961).

[10] L. E. Fite, D. Gibbons, and R. E. Wainerdi, *Proceedings of the 1961 International Conference on Modern Trends in Activation Analysis, Held at Texas A. & M. College, December 15–16, 1961*, p 102, Texas A. & M. College, College Station.

[11] J. T. Gilmore and D. E. Hull, *Proceedings of the 1961 International Conference on Modern Trends in Activation Analysis, Held at Texas A. & M. College, December 15–16, 1961*, p 32, Texas A. & M. College, College Station.

(6-3) QUANTITATIVE ANALYSIS OF SETS OF MULTICOMPONENT TIME-DEPENDENT SPECTRA FROM THE DECAY OF RADIONUCLIDES[1]

W. L. Nicholson and J. E. Schlosser
Applied Mathematics

F. P. Brauer
Chemical Research and Development
Hanford Laboratories
Richland, Washington

INTRODUCTION

The identification and quantitative estimation of specific radionuclides contained in a sample requires information on the chemical and physical properties of the nuclide. Often the history of the sample together with a measurement of the radiation and/or decay characteristics of the sample can reduce or eliminate the need for chemical separations. The measurement of radiation type, energy, and/or half-life is sometimes necessary to assure "clean" chemical separations. Counting techniques can also frequently be used for isotopic ratio measurements. Gamma-ray scintillation spectrometry is the technique often used for energy and half-life measurements [1–4].

The availability of multichannel analyzers for recording gamma spectra has greatly increased the volume of data generated by the radiochemist. Processing and evaluation of such a volume of spectral data is not feasible without the aid of a digital computer. The use of digital computers for such analysis has been reported in the literature [5–9]. Complex mathematical and statistical techniques can be used in conjunction with a digital computer for quantitative analysis of gamma spectra.

---

[1]Work performed under Contract No. AT(45-1)-1350 between the U.S. Atomic Energy Commission and General Electric Company.

In our laboratory up to eight detectors are frequently used with a single multichannel analyzer equipped for selective storage and recycle operation. Electronic data processing techniques were used for the required data sorting operations (Fig. 1). Punched paper tape is used for transfer of the gamma-ray scintillation spectra from the multichannel analyzers to the electronic data processing center. The following additional information is automatically punched [*10*] on the paper tape prior to each read-out of the multichannel analyzer's memory:

1. start of data character;
2. analyzer live time;
3. analyzer number;
4. channel selector switch position;
5. time at end of count in 10^{-4} day up to 9999 days; and
6. detector number, calculation mode code, and sample number for each detector.

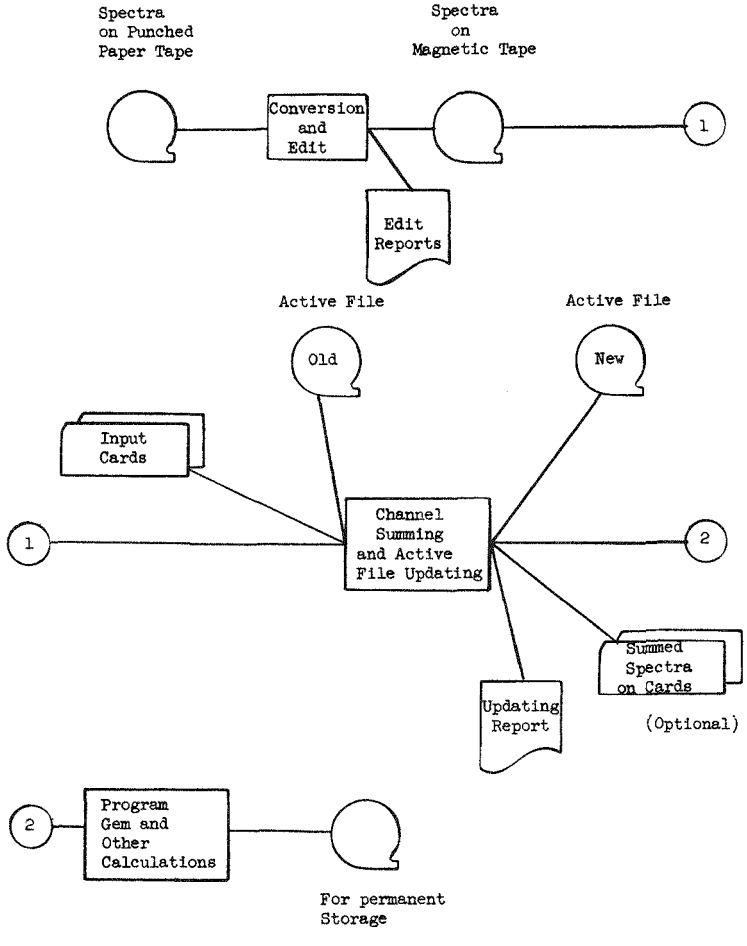

Fig. 1. Data Flow Chart.

Control parameters and other data are transferred by punched cards. The information on the punched paper tape is transferred to magnetic tape at the data processing center. It is then checked for parity, skipped channels, illegal characters, insufficient number of channels, and other errors associated with equipment malfunction. The data are then rewritten so that the first channel number for all spectra starts with zero. The identification information is duplicated and relocated immediately in front of each spectrum. The spectra with identification information are next sorted by detector number and calculation mode code. Each spectrum is next reduced to a set of channel groups, each composed of one or more channels. This operation is specified by the detector number and mode code. The proper selection of summing instructions reduces the errors introduced by gain changes or zero drifts normal with presently available instruments. The reduction in the number of channels also allows the storage of a series of spectra in fast memory during the computer calculation pass. The reduced spectra are then sorted and stored on magnetic tape until required by the computational program. Punched cards can also be prepared for input to other programs. Corrections or additions to the stored data can be made using punched card input.

The radiochemist can normally identify the nuclides which could possibly be in a given sample from the sample history. This information is used by our computational program. The program estimates the amount of each possible constituent and the precision of each estimate.

Other program characteristics include the ability to use spectra from several detectors for resolutions requiring decay information.

Counter backgrounds often vary more than is expected by counting statistics. Often in activation and other analyses an estimate of one or more short-lived nuclides is desired. Longer-lived nuclides of no interest may be contained in the sample. Two methods for estimating background (which can include long-lived activities present in the sample) were included in the program.

MATHEMATICS OF QUANTITATIVE ANALYSIS

Probability Model for Time Dependent Spectra

Let t_0 be an arbitrary, but fixed, moment of time called "time zero," which will function as a reference point in the ensuing discussion. A sample consisting of a mixture of k radionuclides is counted for r nonoverlapping time periods, and the pulse-height spectrum for each of these time periods is recorded independently with a multichannel analyzer. Let $(t_{1\gamma}, t_{2\gamma})(\gamma = 1, 2, \ldots, r)$ be the time interval over which the γth spectrum is recorded. Since the time periods are nonoverlapping, the end points of these intervals satisfy

$$t_0 \leqq t_{11} < t_{12} \leqq t_{21} < t_{22} \leqq t_{31} < \ldots < t_{r2} . \tag{1}$$

Initially, at time zero the mixture contains $N_\alpha(\alpha = 1, 2, \ldots, k)$ atoms of the αth nuclide. Each of these nuclides decays according to a pure death probability law (see ref [11], p 371). Let λ_α be the decay rate, or death rate, for the αth nuclide; that is, $\log_e 2/\lambda_\alpha$ is the half-life of the αth nuclide. Let $\tau_{\alpha\gamma}$ be the probability that a specified atom of the αth nuclide decays during the time interval $(t_{1\gamma}, t_{2\gamma})$. Then,

$$\tau_{\alpha\gamma} = \exp\left[-\lambda_\alpha(t_{1\gamma} - t_0)\right] - \exp\left[-\lambda_\alpha(t_{2\gamma} - t_0)\right] . \tag{2}$$

Let e be the total number of detection systems used to record the r spectra, and $r_j (j = 1, 2, \ldots, e)$ be the number of these spectra recorded with the jth detection system. The r_j spectra must be recorded consecutively. Thus, for example, the same detection system, used for spectra number 3,4,5 and 9,10,11,12, would be counted as two systems, first, with three spectra, and second, with four. Clearly,

$$\sum_{j=1}^{e} r_j = r . \tag{3}$$

The r_j pulse-height spectra recorded with the jth detection system all consist of total sample counts in m_j distinct channel groups. Let $G_{\alpha ij}$ be the efficiency factor in the ith channel group of spectra recorded with the jth system for detection of the αth nuclide; that is, $G_{\alpha ij}$ is the conditional probability that a count is registered in the ith channel group of the analyzer, given that the jth detection system is used and a single atom of the αth nuclide decays. Thus, the joint probability that a specified atom of the αth nuclide decays during the γth time period and is recorded in the ith channel group of the γth spectrum is

$$P_{\alpha i\gamma} = G_{\alpha ij} \tau_{\alpha\gamma} , \tag{4}$$

where

$$R_0 = 0 , \qquad R_j = \sum_{\beta=1}^{j} r_\beta \quad \text{and} \quad R_{j-1} < \gamma \leqq R_j \tag{5}$$

determines j from γ.

Let $X_{\alpha i\gamma}$ be the total number of counts recorded in the ith channel group of the γth spectrum due specifically to decay of the αth nuclide. For each α the set of chance variables

$$[X_{\alpha i\gamma} \,|\, i = 1, 2, \ldots, m_j ;\ R_{j-1} < \gamma \leqq R_j ;\ j = 1, 2, \ldots, e]$$

have a joint multinomial distribution (see ref [11], p 124), with size parameter N_α and probabilities given by (4). So, the average value of $X_{\alpha i\gamma}$ is

$$\text{ave}\,(X_{\alpha i\gamma}) = N_\alpha P_{\alpha i\gamma} , \tag{6}$$

and the covariance between $X_{\alpha i_1\gamma_1}$ and $X_{\alpha i_2\gamma_2}$ is

$$\text{cov}\,(X_{\alpha i_1\gamma_1}, X_{\alpha i_2\gamma_2}) = N_\alpha P_{\alpha i_1\gamma_1} (\delta_{i_1 i_2} \delta_{\gamma_1\gamma_2} - P_{\alpha i_2\gamma_2}) . \tag{7}$$

The symbol δ_{st} is the Kronecker delta function defined as

$$\begin{aligned} \delta_{st} &= 1 \text{ if } s = t ; \\ &= 0 \text{ if } s \neq t . \end{aligned} \tag{8}$$

Since the k nuclides decay independently, (7) can be generalized to give the covariance of any two $X_{\alpha ij}$ total counts as

$$\text{cov}\,(X_{\alpha_1 i_1\gamma_1}, X_{\alpha_2 i_2\gamma_2}) = N_{\alpha_1} P_{\alpha_1 i_1\gamma_1} (\delta_{i_1 i_2} \delta_{\gamma_1\gamma_2} - P_{\alpha_2 i_2\gamma_2}) \delta_{\alpha_1\alpha_2} . \tag{9}$$

Let $B_{i\gamma}$ be the total number of background counts recorded in the ith channel group of the γth spectrum. The set

$$[B_{i\gamma} \,|\, i = 1, 2, \ldots, m_j;\ R_{j-1} < \gamma \leq R_j\ ;\ j = 1, 2, \ldots, e]$$

of all background contributions to the spectra consists of mutually independent Poisson chance variables (see ref [11], p 115). As such,

$$\text{ave}\,(B_{i\gamma}) = q_{ij}\Delta_\gamma\ , \tag{10}$$

and

$$\text{cov}\,(B_{i_1\gamma_1}, B_{i_2\gamma_2}) = q_{i_1 j}\Delta_{\gamma_1}\delta_{i_1 i_2}\delta_{\gamma_1\gamma_2}\ . \tag{11}$$

Here, j is determined from γ in (10) and from γ_1 in (11) by (5). $\Delta_\gamma = t_{\gamma 1} - t_{\gamma 2}$ is the length of the γth counting period, and q_{ij} is the true average background count rate in the ith channel group of the jth detection system.

Let $Y_{i\gamma}$ be the observed total count in the ith channel group of the γth spectrum; that is,

$$Y_{i\gamma} = \sum_{\alpha=1}^{k} X_{\alpha i\gamma} + B_{i\gamma}\ . \tag{12}$$

As linear combinations of mutually independent chance variables, the average values and covariances of the $Y_{i\gamma}$'s are easily calculated from (6), (9), (10), and (11) to be

$$\text{ave}\,(Y_{i\gamma}) = \sum_{\alpha=1}^{k} N_\alpha P_{\alpha i\gamma} + q_{ij}\Delta_\gamma\ , \tag{13}$$

and

$$\text{cov}\,(Y_{i_1\gamma_1}, Y_{i_2\gamma_2}) = \sum_{\alpha=1}^{k} N_\alpha P_{\alpha i_1\gamma_1}(\delta_{i_1 i_2}\delta_{\gamma_1\gamma_2} - P_{\alpha i_2\gamma_2}) + q_{i_1 j}\Delta_{\gamma_1}\delta_{i_1 i_2}\delta_{\gamma_1\gamma_2}$$

$$= \delta_{i_1 i_2}\delta_{\gamma_1\gamma_2}\,\text{ave}\,(Y_{i_1\gamma_1}) - \sum_{\alpha=1}^{k} N_\alpha P_{\alpha i_1\gamma_1} P_{\alpha i_2\gamma_2}\ . \tag{14}$$

The model for the estimation problem discussed below consists of the set of observed total counts

$$[Y_{i\gamma} \,|\, i = 1, 2, \ldots, m_j;\ R_{j-1} < \gamma \leq R_j\ ;\ j = 1, 2, \ldots, e]$$

and the formulas for their averages and covariances, (13) and (14).

Estimation Problem

The precise form of the estimation problem depends upon how much is known about the parameters of the probability model discussed above. As a quantitative problem, by definition, the half-lives of the nuclides are known. Thus, in all cases

the λ_α's and, hence, the $\tau_{\alpha\gamma}$'s of formula (2), the individual nuclide decay probabilities are known.

The efficiency factors of the αth nuclide and the jth detection system can also be rewritten in a normalized form,

$$G_{\alpha ij} = G_{\alpha j} g_{\alpha ij} \qquad \text{with} \qquad \sum_{i=1}^{m_j} g_{\alpha ij} = 1 \, . \tag{15}$$

The physical interpretation of (15) is that the $g_{\alpha ij}$'s are the conditional probabilities governing allocation of counts given that the decay was recorded somewhere in the spectrum. Counting a pure nuclide in a detection system and normalizing the resulting background corrected spectrum provide estimates of the $g_{\alpha ij}$'s. Recent work of Heath [9] where mathematical functions are used to represent the fundamental parts of the spectrum gives a second method of obtaining the $g_{\alpha ij}$'s. In our solution of the estimation problem we tacitly assume that the $g_{\alpha ij}$'s are known without error. Of course, this assumption is a mathematical convenience which simplifies the theory. In reality, the assumption means that the errors in $g_{\alpha ij}$ estimates must on the average be much less than the counting statistic variation in the sample spectra.

If the geometry factors $G_{\alpha j}$ of (15), the ratios of decay rate to total spectrum count rate, are known, the quantitative analysis problem is to estimate the number of atoms of each nuclide at time zero, $N_1, N_2, \ldots, N_k$; or, equivalently, the time zero decay rates $\lambda_1 N_1, \lambda_2 N_2, \ldots, \lambda_k N_k$. If the $G_{\alpha j}$ are not known, the additional assumption that

$$G_{\alpha j} = f_{\alpha j} G_{\alpha 1} \qquad (j = 2, 3, \ldots, e) \tag{16}$$

and all $k(e-1)f_{\alpha j}$'s are known is needed. This means that the relative efficiencies of all detection systems with respect to the first one are known for each of the k nuclides. The quantitative analysis problem is now to estimate the expected number of decays from each nuclide that would be recorded as counts if the first detection system were used over an infinite time period starting at t_0, $G_{11} N_1, G_{21} N_2, \ldots, G_{k1} N_1$; or, equivalently, the time zero counting rates using the first detection system, $\lambda_1 G_{11} N_1, \lambda_2 G_{21} N_2, \ldots, \lambda_k G_{k1} N_k$.

In the sequel, the first situation is treated where geometry factors are known. The development is carried out in terms of $G_{\alpha ij}$'s. The second situation differs only in that $G_{\alpha ij}$ is replaced by $f_{\alpha j} g_{\alpha ij}$, N_α is replaced by $G_{\alpha 1} N_\alpha$, and "decay rate" is replaced by "counting rate."

Since the background counting rates $q_{i\gamma}$ are unknown, they must be treated as nuisance parameters in any method of quantitative analysis. In this paper, three different methods are described for handling background:

I. Replace the $q_{i\gamma}$ background parameters by estimates $\hat{q}_{i\gamma}$ calculated from background spectra recorded on each of the detection systems.

II. Include the $q_{i\gamma}$ as parameters to be estimated from the sample spectra at the same time the N_α are estimated.

III. Remove the $q_{i\gamma}$ from the model by *differencing* the successive spectra for every detection system.

Method I is classical. The first step in analyzing a simple spectrum is to correct it for background. The only problem which complicates the interpretation of the

estimates is that the background corrections are random. The additional uncertainty should be reflected in the standard deviations of the N_α estimates. Further, if several spectra are recorded with a single detection system and all are corrected with the same background spectrum, the resulting net sample spectra can be highly positively correlated. The situation is particularly difficult when the sample-to-background count ratio is low, say less than one.

Methods II and III are only applicable if several spectra are recorded with the same detection system. The assumption is made that the background counting rates remain constant over the total time period that a particular detection system is used. Method III is less affected than Method II by violation of the assumption in the form of a slow background shift.

Weighted Least-Squares Estimates

For all three methods of handling background nuisance parameters, a generalized least-squares technique is used to construct the estimates, say, $\hat{N}_\alpha$, of the true N_α values. With a set of uncorrelated, homoscedastic data, the least-squares principle of estimation selects the estimate so as to minimize the sum of squares of deviations between data and model prediction of data, say

$$\sum_i (\text{data}_i - \text{model}_i)^2 . \tag{17}$$

If the data are correlated and/or heteroscedastic, the familiar sum of squares (17) is replaced by a quadratic form

$$\sum_{i,j} \sigma^{ij} (\text{data}_i - \text{model}_i)(\text{data}_j - \text{model}_j) . \tag{18}$$

The weights σ^{ij}, in theory at least, are the elements in the inverse of the data covariance matrix. In matrix notation

$$\Sigma = (\sigma_{ij}) \qquad \text{and} \qquad \Sigma^{-1} = (\sigma^{ij}) , \tag{19}$$

where cov $(\text{data}_i, \text{data}_j) = \sigma_{ij}$. In our application of this generalized least-squares procedure, the covariance matrix Σ is unknown, since it is a function of the N_α. We substitute a rather crude estimate for Σ and proceed with the estimation as if our estimate were exactly equal to Σ. There is nothing wrong with this attack as long as we don't *ad hoc* claim for our estimates all the elegant properties of legitimate generalized least-squares estimates. To preserve the distinction between generalized least-squares estimates and those of this paper, we call our estimates Modified Generalized Least Squares (MGLS). Monte Carlo studies discussed below tend to indicate that with mild restrictions on the spectra total counts, the MGLS estimates actually do behave like generalized least-squares ones. Our crude estimate of Σ contains most of the information about the heteroscedasticity of the sample spectra and the correlation introduced by the different methods of handling background. It contains no information about the correlations among the sample spectra.

The three methods of analysis are described independently below in detail up to the point where the arguments are similar; the remaining steps are described just once.

Method I

For this method the only restriction on the data is that the number of sample spectra data points be greater than the number of nuclides; that is,

$$\sum_{j=1}^{e} (R_j - R_{j-1}) m_j > k \, . \tag{20}$$

Let $[b_{ij} | i = 1, 2, \ldots, m_j; j = 1, 2, \ldots, e]$ be a set of unbiased background spectra counting rate estimates based on a single sample background spectrum for each of the e detection systems. Specifically, b_{ij} is the estimate for the ith channel group of the jth detection system. Let L_j be the length of the time interval over which background was monitored for the jth detection system. Thus, each b_{ij} satisfies the relationship

$$b_{ij} = \frac{c_{ij}}{L_j} \, , \tag{21}$$

where c_{ij} is a total background count. The c_{ij}'s are assumed to be mutually independent Poisson chance variables. So, from (21)

$$\text{ave } (b_{ij}) = q_{ij} \, , \tag{22}$$

and

$$\text{cov } (b_{i_1 j_1}, b_{i_2 j_2}) = \delta_{i_1 i_2} \delta_{j_1 j_2} q_{i_1 j_1} / L_{j_1} \, .$$

Using the above background estimates the net sample count estimate for the ith channel of the γth spectrum is $Y_{i\gamma} - b_{ij} \Delta_\gamma$, where j is determined from γ by (5). The net sample spectra are unbiased estimates of the true background spectra, so

$$\text{ave } (Y_{i\gamma} - b_{ij} \Delta_\gamma) = \sum_{\alpha=1}^{k} N_\alpha P_{\alpha i \gamma} \, . \tag{23}$$

The covariance between the net counts is from (14) and (22):

$$\text{cov } (Y_{i_1 \gamma_1} - b_{i_1 j_1} \Delta_{\gamma_1}, Y_{i_2 \gamma_2} - b_{i_2 j_2} \Delta_{\gamma_2}) = \delta_{i_1 i_2} \delta_{\gamma_1 \gamma_2} \text{ ave } (Y_{i_1 \gamma_1})$$

$$+ \delta_{i_1 i_2} \delta_{j_1 j_2} \text{ ave } (b_{i_1 j_1}) \Delta_{\gamma_1} \Delta_{\gamma_2} / L_{j_1} - \sum_{\alpha=1}^{k} N_\alpha P_{\alpha i_1 \gamma_1} P_{\alpha i_2 \gamma_2} \, . \tag{24}$$

Since the N_α are not known, the exact covariances cannot be used as weights in the least-squares analysis. The form in which (24) is written illustrates directly what portion of the covariance can be estimated unbiasedly from the data at hand. The covariance estimate is

$$\text{cov } (Y_{i_1 \gamma_1} - b_{i_1 j_1} \Delta_{\gamma_1}, Y_{i_2 \gamma_2} - b_{i_2 j_2} \Delta_{\gamma_2})$$

$$= \delta_{i_1 i_2} (\delta_{\gamma_1 \gamma_2} Y_{i_1 \gamma_1} + \delta_{j_1 j_2} b_{i_1 j_1} \Delta_{\gamma_1} \Delta_{\gamma_2} / L_{j_1}) \, . \tag{25}$$

The third term of (24) is ignored in this estimate. For variances the effect is negligible since $Y_{i\gamma}$ is roughly linear in the $P_{\alpha ij}$'s while the third term is quadratic in them. The estimate (25) is admittedly poor for two net counts from different channels and/or different detection systems. For such a case, the estimate vanishes while in fact the two net counts are negatively correlated.

Use of the estimator (25) in place of the true covariance matrix elements means that the net sample count data can be processed in blocks, each block being a single channel group of a detection system. Specifically, the MGLS estimates are those N_α which minimize the quadratic form

$$\sum_{j=1}^{e} \sum_{i=1}^{m_j} \sum_{\gamma_1,\gamma_2=R_{j-1}+1}^{R_j} \sigma(i,j)^{\gamma_1\gamma_2} \left(Y_{i\gamma_1} - b_{ij}\Delta_{\gamma_1} - \sum_{\alpha=1}^{k} N_\alpha P_{\alpha i\gamma_1}\right) \times \left(Y_{i\gamma_2} - b_{ij}\Delta_{\gamma_2} - \sum_{\alpha=1}^{k} N_\alpha P_{\alpha i\gamma_2}\right). \tag{26}$$

Here, the $\sigma(i,j)^{\gamma_1\gamma_2}$ are the elements of the inverse of the estimated net sample count covariance matrix. Let

$$\Sigma(i,j) = [\sigma(i,j)_{\gamma_1\gamma_2}] \tag{27}$$

be this $(R_j - R_{j-1})$th order covariance matrix for the ith channel group of spectra collected on the jth detection system. From (25),

$$\sigma(i,j)_{\gamma_1\gamma_2} = \delta_{\gamma_1\gamma_2} Y_{i\gamma_1} + b_{ij}\Delta_{\gamma_1}\Delta_{\gamma_2}/L_j . \tag{28}$$

A pattern matrix with elements such as (28) can be inverted using general techniques discussed in [12]. The result is

$$\Sigma(i,j)^{-1} = [\sigma(i,j)^{\gamma_1\gamma_2}] , \tag{29}$$

where

$$\sigma(i,j)^{\gamma_1\gamma_2} = \frac{\delta_{\gamma_1\gamma_2}}{Y_{i\gamma_1}} - \frac{b_{ij}}{L_j + b_{ij}V_{ij}(\Delta,\Delta)} \frac{\Delta_{\gamma_1}}{Y_{i\gamma_1}} \frac{\Delta_{\gamma_2}}{Y_{i\gamma_2}} .$$

For any set of pairs (a_γ, b_γ), with $\gamma = R_{j-1} + 1, R_{j-1} + 2, \ldots, R_j$, the notation $V_{ij}(a,b)$ is defined by

$$V_{ij}(a,b) = \sum_{R_{j-1}+1}^{R_j} a_\gamma \frac{b_\gamma}{Y_{i\gamma}} . \tag{30}$$

From (26), (29), and standard generalized least-squares theory, the MGLS estimates $\hat{N}_\alpha$ are the solutions of the following system of k linear equations:

$$\sum_{\alpha=1}^{k} \left[\sum_{j=1}^{e} \sum_{i=1}^{m_j} A_{ij}^{\alpha\beta}\right] \hat{N}_\alpha = \sum_{j=1}^{e} \sum_{i=1}^{m_j} C_{ij}^{\beta} \quad (\beta = 1, 2, \ldots, k) . \tag{31}$$

The auxiliary quantities in (31) are defined as

$$A_{ij}^{\alpha\beta} = G_{\alpha ij} G_{\beta ij} \left[V_{ij}(\tau_\alpha, \tau_\beta) - \frac{b_{ij}}{L_j + b_{ij} V_{ij}(\Delta,\Delta)} V_{ij}(\tau_\alpha, \Delta) V_{ij}(\tau_\beta, \Delta) \right],$$

$$C_{ij}^{\beta} = G_{\beta ij} \left[\sum_{R_{j-1}+1}^{R_j} \tau_{\alpha\gamma} - \frac{b_{ij}\left(L_j + \sum_{R_{j-1}+1}^{R_j} \Delta_\gamma\right)}{L_j + b_{ij} V_{ij}(\Delta,\Delta)} V_{ij}(\tau_\beta, \Delta) \right]. \tag{32}$$

Method II

The same notation developed for Method I is used to describe Method II. Since background counting rates are estimated from the sample spectra, more data are needed than for Method I. At least two spectra must be recorded on each detection system, and the restriction (20) of Method I becomes

$$\sum_{j=1}^{e} (R_j - R_{j-1} - 1) m_j > k . \tag{33}$$

Since background estimates are not used, the total sample count model (13) is used for the MGLS estimation. The variance-covariance matrix estimate of (14) neglects the last term which contains the unknown N_α's. This matrix is diagonal and treats all sample total counts $Y_{i\gamma}$ as being independent. The MGLS estimates are those N_α and q_{ij} which minimize the quadratic form

$$\sum_{j=1}^{e} \sum_{i=1}^{m_j} \sum_{R_{j-1}+1}^{R_j} (1/Y_{i\gamma})(Y_{i\gamma} - \sum_{\alpha=1}^{k} N_\alpha P_{\alpha i\gamma} - q_{ij}\Delta_\gamma)^2 . \tag{34}$$

Using standard generalized least-squares theory the normal equations can be written down from (34). From these equations, the background counting rate estimates can be expressed directly in terms of the $\hat{N}_\alpha$ estimates as

$$\hat{q}_{ij} = \left[\sum_{R_{j-1}+1}^{R_j} \Delta_\gamma - \sum_{\alpha=1}^{k} \hat{N}_\alpha G_{\alpha ij} V_{ij}(\tau_\alpha, \Delta) \right] \Big/ V_{ij}(\Delta,\Delta) . \tag{35}$$

Substitution of (35) into the normal equations for the $\hat{q}_{ij}$ gives the $\hat{N}_\alpha$ as the solution to the system of k linear equations of the form (31) where the auxiliary quantities are defined as

$$A_{ij}^{\alpha\beta} = G_{\alpha ij} G_{\beta ij} \left[V_{ij}(\tau_\alpha, \tau_\beta) - \frac{V_{ij}(\tau_\alpha, \Delta) V_{ij}(\tau_\beta, \Delta)}{V_{ij}(\Delta,\Delta)} \right],$$

$$C_{ij}^{\beta} = G_{\beta ij} \left[\sum_{\gamma=R_{j-1}+1}^{R_j} \tau_{\alpha\gamma} - \sum_{\gamma=R_{j-1}+1}^{R_j} \Delta_\gamma \frac{V_{ij}(\tau_\beta, \Delta)}{V_{ij}(\Delta,\Delta)} \right]. \tag{36}$$

It is interesting to note that these formulas can be gotten directly from Method I by letting each $L_j = 0$. Thus, mathematically, a background estimate b_{ij} based on a counting interval of length zero is treated as no estimate and the sample spectra are used instead to estimate background.

Method III

The restrictions on the amount of data are the same as for Method II above, see (33). For the jth detection system, the $R_j - R_{j-1}$ sample spectra are replaced by $R_j - R_{j-1} - 1$ first differences, possibly adjusted to correct for variance in the length of the two counting periods. The ith channel group of the γth difference spectra is

$$Z_{i\gamma} = Y_{i\gamma} - (\Delta_\gamma/\Delta_{\gamma+1}) Y_{i\gamma+1} , \tag{37}$$

where $i = 1, 2, \ldots, m_j$ and $\gamma = R_{j-1} + 1, R_{j-1} + 2, \ldots, R_j - 1$. The model for the difference spectra is

$$\text{ave } (Z_{i\gamma}) = \sum_{\alpha=1}^{k} N_\alpha G_{\alpha ij} \phi_{\alpha\gamma} , \tag{38}$$

where $\phi_{\alpha\gamma} = \tau_{\alpha\gamma} - (\Delta_\gamma/\Delta_{\gamma+1})\tau_{\alpha\gamma+1}$. The covariances between the difference spectra adjusted counts are from (14):

$$\begin{aligned}\text{cov } (Z_{i_1\gamma_1}, Z_{i_2\gamma_2}) = \delta_{i_1 i_2} &\{[\delta_{\gamma_1\gamma_2} - \delta_{\gamma_1\gamma_2+1}(\Delta_{\gamma_2}/\Delta_{\gamma_2+1})] \text{ ave } (Y_{i_1\gamma_1}) \\ &- (\Delta_{\gamma_1}/\Delta_{\gamma_1+1})[\delta_{\gamma_1+1\gamma_2} - \delta_{\gamma_1+1\gamma_2+1}(\Delta_{\gamma_2}/\Delta_{\gamma_2+1})] \text{ ave } (Y_{i_1\gamma_1+1})\} \\ - \sum_{\alpha=1}^{k} N_\alpha &[P_{\alpha i_1\gamma_1} - (\Delta_{\gamma_1}/\Delta_{\gamma_1+1}) P_{\alpha i_1\gamma_1+1}][P_{\alpha i_2\gamma_2} - (\Delta_{\gamma_2}/\Delta_{\gamma_2+1}) P_{\alpha i_2\gamma_2+1}] .\end{aligned} \tag{39}$$

As for Method I, the estimate of the covariance matrix considers only that portion which can be estimated unbiasedly. So the estimate of (39) is

$$\begin{aligned}\text{cov } (Z_{i_1\gamma_1}, Z_{i_2\gamma_2}) = \delta_{i_1 i_2} &[\delta_{\gamma_1\gamma_2} - \delta_{\gamma_1\gamma_2+1}(\Delta_{\gamma_2}/\Delta_{\gamma_2+1})] Y_{i_1\gamma_1} \\ &- (\Delta_{\gamma_1}/\Delta_{\gamma_1+1})[\delta_{\gamma_1+1\gamma_2} - \delta_{\gamma_1+1\gamma_2+1}(\Delta_{\gamma_2}/\Delta_{\gamma_2+1})] Y_{i_1\gamma_1+1} .\end{aligned} \tag{40}$$

Again, as for Method I, the differenced spectra can be processed in blocks, each block being all the differences in a single channel group of a detection system. The MGLS estimates are those N_α which minimize the quadratic form

$$\sum_{j=1}^{e} \sum_{i=1}^{m_j} \sum_{\gamma_1,\gamma_2=R_{j-1}+1}^{R_j-1} \sigma(i,j)^{\gamma_1\gamma_2} \times \left(Z_{i\gamma_1} - \sum_{\alpha=1}^{k} N_\alpha G_{\alpha ij} \phi_{\alpha\gamma_1}\right)\left(Z_{i\gamma_2} - \sum_{\alpha=1}^{k} N_\alpha G_{\alpha ij} \phi_{\alpha\gamma_2}\right) . \tag{41}$$

The $\sigma(i,j)^{\gamma_1\gamma_2}$ are the elements of the inverse of the estimated differenced sample count covariance matrix. Let

$$\Sigma(i,j) = [\sigma(i,j)_{\gamma_1\gamma_2}] \tag{42}$$

be this $(R_j - R_{j-1} - 1)$th order covariance matrix for the ith channel group of the difference spectra collected on the jth detection system. From (40),

$$\sigma(i,j)_{\gamma_1\gamma_2} = [\delta_{\gamma_1\gamma_2} - \delta_{\gamma_1\gamma_2+1}(\Delta_{\gamma_2+1})]\, Y_{i\gamma_1} - (\Delta_{\gamma_1}/\Delta_{\gamma_1+1})[\delta_{\gamma_1+1\gamma_2} - \delta_{\gamma_1+1\gamma_2+1}(\Delta_{\gamma_2}/\Delta_{\gamma_2+1})]\, Y_{i\gamma_1+1} . \tag{43}$$

A succession of elementary row and column operations on the symmetric tridiagonal matrix $\Sigma(i,j)$ with elements (43) shows that $\Sigma(i,j)$ satisfies the matrix equation

$$E(i,j)^T \Sigma(i,j) E(i,j) = S(i,j) . \tag{44}$$

Here

$$\begin{aligned} E(i,j) &= [e(i,j)_{\gamma_1\gamma_2}] , \\ S(i,j) &= [s(i,j)_{\gamma_1\gamma_2}] \end{aligned} \tag{45}$$

are $(R_j - R_{j-1} - 1)$th order matrices. We now define the auxiliary quantity

$$\begin{aligned} a(i,j)_{R_{j-1}+1} &= 1 ; \\ a(i,j)_{\gamma} &= \sum_{m=R_{j-1}+1}^{\gamma} \left[\prod_{n=m+1}^{\gamma} (\Delta_{n-1}/\Delta_n)^2 \right] \left[\prod_{\substack{n=R_{j-1}+1 \\ n\neq m}}^{\gamma} Y_{in} \right] \end{aligned} \tag{46}$$

for $\gamma = R_{j-1} + 2, \ldots, R_j - 1$. The elements of the matrices (45) are

$$\begin{aligned} e(i,j)_{\gamma_1\gamma_2} &= 1 \text{ for } \gamma_1 = \gamma_2 , \\ &= \left[\prod_{n=\gamma_1+1}^{\gamma_2} Y_{in} \right] \left[\Delta_{\gamma_1} a(i,j)_{\gamma_1}/\Delta_{\gamma_2} a(i,j)_{\gamma_2} \right] \text{ for } \gamma_1 < \gamma_2 , \\ &= 0 \text{ for } \gamma_1 > \gamma_2 ; \\ s(i,j)_{\gamma_1\gamma_2} &= \delta_{\gamma_1\gamma_2} a(i,j)_{\gamma_1+1}/a(i,j)_{\gamma_1} . \end{aligned} \tag{47}$$

The elements of the inverse matrix $\Sigma^{-1}(i,j)$ can be calculated directly by using (47), since, from (44),

$$\Sigma(i,j)^{-1} = E(i,j) S(i,j)^{-1} E(i,j)^T . \tag{48}$$

Actually, the normal equations derived from (41) are easier to express and to solve if the structure of (48) is used and not the inverse elements *per se*. For any set of elements (b_n) with $n = R_{j-1} + 1, R_{j-1} + 2, \ldots, R_j - 1$, the notation, $L_{ij\gamma}(b)$ is

defined by

$$L_{ij\gamma}(b) = \sum_{n=R_{j-1}+1}^{\gamma} b_n \Delta_n a(i,j)_n \left(\prod_{m=n+1}^{\gamma} Y_{im} \right) \tag{49}$$

for $\gamma = R_{j-1} + 1, R_{j-1} + 2, \ldots, R_j - 1$. The normal equations for Method III $\hat{N}_\alpha$ estimates have the form of (31), with the auxiliary quantities defined as

$$\begin{aligned} A_{ij}^{\alpha\beta} &= G_{\alpha ij} G_{\beta ij} \sum_{\gamma=R_{j-1}+1}^{R_j-1} \frac{L_{ij\gamma}(\phi_\alpha) L_{ij\gamma}(\phi_\beta)}{\Delta_\gamma^2 a(i,j)_\gamma a(i,j)_{\gamma+1}} , \\ C_{ij}^{\beta} &= G_{\beta ij} \sum_{\gamma=R_{j-1}+1}^{R_j-1} \frac{L_{ij\gamma}(\Delta) L_{ij\gamma}(\phi_\beta)}{\Delta_\gamma^2 a(i,j)_\gamma a(i,j)_{\gamma+1}} . \end{aligned} \tag{50}$$

Methods I, II, and III

In accordance with generalized least-squares theory the covariance estimate $\hat{\sigma}_{\alpha\beta}$ for $\hat{N}_\alpha$ and $\hat{N}_\beta$ is obtained from the inverse of the kth order coefficient matrix A for the normal equations. Thus, with

$$A = \{A_{\alpha\beta}\}, \qquad A^{-1} = \{A^{\alpha\beta}\} , \tag{51}$$

and

$$A_{\alpha\beta} = \sum_{j=1}^{e} \sum_{i=1}^{m_j} A_{ij}^{\alpha\beta} ,$$

the covariance and resulting standard deviation estimates are

$$\hat{\sigma}_{\alpha\beta} = A^{\alpha\beta} \text{ and } \hat{\sigma}_\alpha = (A^{\alpha\alpha})^{1/2} . \tag{52}$$

Time zero disintegration rate estimates and their standard deviation estimates are $\lambda\hat{N}_\alpha$ and $\lambda\hat{\sigma}_\alpha$, respectively.

As a check on the fit of the model to the sample spectra, a number of indicators can be calculated. In the FORTRAN language program described in the next section, the normalized residuals,

$$(\text{data}_j - \text{model}_j)/\text{standard deviation data}_j , \tag{53}$$

are computed first. For the three methods these residuals are:

$$\text{I.} \quad \left(Y_{i\gamma} - b_{ij} \Delta_\gamma - \sum_{\alpha=1}^{k} \hat{N}_\alpha P_{\alpha i\gamma} \right) \left(Y_{i\gamma} + b_{ij} \Delta_\gamma^2 / L_j \right)^{-1/2} ,$$

$$\text{II.} \quad \left(Y_{i\gamma} - \hat{q}_{ij} \Delta_\gamma - \sum_{\alpha=1}^{k} \hat{N}_\alpha P_{\alpha i\gamma} \right) (Y_{i\gamma})^{-1/2} , \tag{54}$$

$$\text{III.} \quad \left(Z_{i\gamma} - \sum_{\alpha=1}^{k} \hat{N}_\alpha G_{\alpha ij} \phi_{\alpha\gamma} \right) \left[Y_{i\gamma} + (\Delta_\gamma / \Delta_{\gamma+1})^2 Y_{i\gamma+1} \right]^{-1/2} .$$

An average indicator for each channel group within a detection system can be calculated by forming the portion of the chi-square goodness of fit statistic which pertains to the residuals for the channel group and detection system in question. For the three methods, the indicators for the ith channel group and the jth detection system are:

$$\text{I. } \chi^2_{ij} = \sum_{\gamma=R_{j-1}+1}^{R_j} \left(Y_{i\gamma} - b_{ij}\Delta_\gamma - \sum_{\alpha=1}^{k} \hat{N}_\alpha P_{\alpha i\gamma} \right)^2 Y_{i\gamma}^{-1} - \frac{b_{ij} V_{ij}^2(\Delta,\Delta)}{L_j + b_{ij} V_{ij}(\Delta,\Delta)} (b_{ij} - \hat{q}_{ij})^2 ,$$

$$\text{II. } \chi^2_{ij} = \sum_{\gamma=R_{j-1}+1}^{R_j} \left(Y_{i\gamma} - \hat{q}_{ij}\Delta_\gamma - \sum_{\alpha=1}^{k} \hat{N}_\alpha P_{\alpha i\gamma} \right)^2 Y_{i\gamma}^{-1} , \tag{55}$$

$$\text{III. } \chi^2_{ij} = \sum_{\gamma=R_{j-1}+1}^{R_j - 1} \left[L_{ij\gamma} \left(Z_i - \sum_{\alpha=1}^{k} \hat{N}_\alpha G_{\alpha ij} \phi_\alpha \right) \right]^2 \left[\Delta_\gamma^2 \, a(i,j)_\gamma \, a(i,j)_{\gamma+1} \right]^{-1}$$

Summing over channel groups provides an indicator for the jth detection system. In all three methods this indicator is

$$\chi^2_j = \sum_{i=1}^{m_j} \chi^2_{ij} . \tag{56}$$

Finally, the chi-square goodness of fit test is

$$\chi^2 = \sum_{j=1}^{e} \chi^2_j . \tag{57}$$

If the model is correct, the chi-square statistic of (57) is approximately distributed as chi-square with

$$\sum_{j=1}^{e} (R_j - R_{j-1}) \, m_j - k$$

degrees of freedom for Method I and

$$\sum_{j=1}^{e} (R_j - R_{j-1} - 1) \, m_j - k$$

degrees of freedom for Methods II and III. If the chi-square statistic (57) indicates that the model does not agree with the data up to counting statistic variation, it may still be possible to estimate the standard deviations of the estimates by multiplying the elements $A^{\alpha\beta}$ of A^{-1} in formula (52) by χ^2/(degrees of freedom).

A slightly different form of the residual indicator is gotten by calculating a background counting rate estimate from every residual. An experimenter who is familiar with the background range for a detection system can often spot a detection system shift from such an array of background estimates. In all three methods these background count rate estimates calculated from residuals are:

$$\left(Y_{i\gamma} - \sum_{\alpha=1}^{k} \hat{N}_\alpha P_{\alpha ij} \right) (\Delta_\gamma)^{-1} . \tag{58}$$

PROGRAM GEM

A FORTRAN II language program for an IBM 7090 with a 32K memory was written to perform the MGLS calculations discussed above. A flow chart of this program is given in Fig. 2. The program, named GEM, exists in several forms differing principally in the input and output routines.

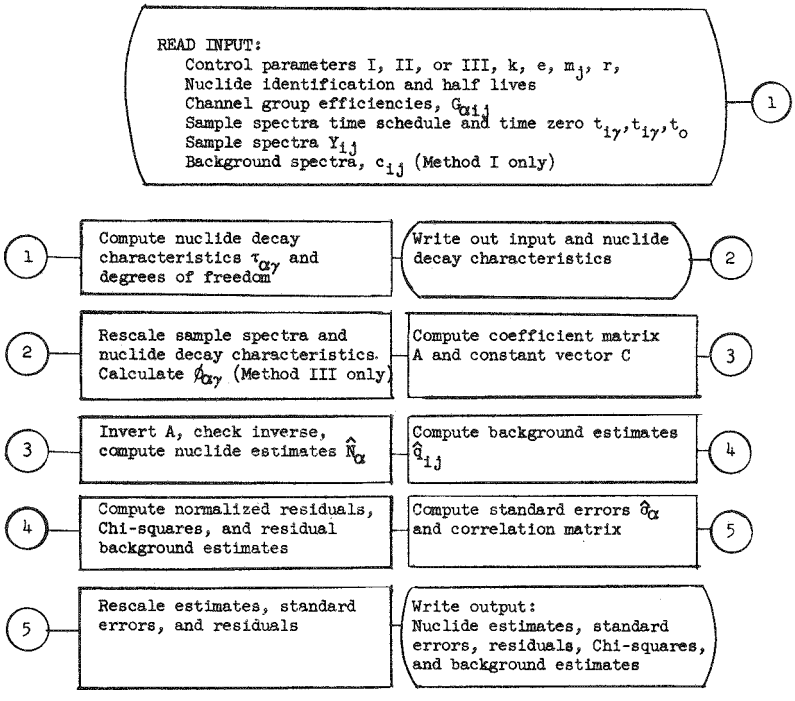

Fig. 2. GEM Flow Chart.

The present case restrictions in GEM were established to keep the memory requirements low because of the expected use of the program with other calculational programs. These present limitations are:

$$50 \text{ spectra, } 20 \text{ channel groups, } 10 \text{ nuclides, and } 3 \text{ detectors.} \tag{59}$$

The program with the limitations (59) requires less than 16,000 locations including the necessary FORTRAN library subroutines. The program could quite simply be modified to relax these restrictions. The following relationship,

$$\text{memory requirements} = 9500 + 4D + 7I + 7S + 4CD + 3SC + 3I^2 + 3SI + ID + CID\,, \tag{60}$$

where

S = number of spectra,

D = number of detectors,

C = number of channel groups,

I = number of nuclides,

can be used as a guide[2] in estimating the memory requirements of other maximum dimensions. Some other maximum configurations which are possible are:

Spectra	Channel Groups	Nuclides	Detectors	Estimated Memory Requirements
5	400	20	1	27,000
20	200	20	1	29,000
40	100	20	1	28,000

The program is a straightforward coding of the equations presented in the previous section with rescaling of the data where necessary to keep the numbers within bounds. Various calculational checks have been built into the program in an attempt to give more accurate results where possible or, at least, to flag where the calculation has failed. One such check is on the inversion of the coefficient matrix (51). The program normally uses a fast Jordan elimination routine which is checked for accuracy by multiplying the inverse by the matrix itself. If the product is not within the required accuracy (5×10^{-4}), the program uses a slower iterative (Crout method) routine. Experience has shown that the Crout method will be satisfactory in about half the cases where the Jordan elimination failed.

As a further check on the calculation, the program tests the status of the accumulator overflow and divide check indicators at nine points. When an indicator signals a miscalculation, a message is written in the output.

The GEM input consists of:

1. five control parameters defining
   (*a*) the calculation method to be used – I, II, or III,
   (*b*) the number of nuclides,
   (*c*) the number of detection systems,
   (*d*) the number of channel groups for each detection system,
   (*e*) the number of spectra;
2. identification for each nuclide and its half-life;
3. the channel group efficiencies;
4. the time schedule for counting the sample spectra, start time and stop time for each spectrum, and the time zero reference point;
5. the sample spectra as total counts in each channel group;
6. the background spectra as total counts in each channel group for each detection system and the time period over which each spectrum was taken (Method I only).

The GEM output consists of:

1. all input quantities;
2. the nuclide decay characteristic giving the fraction of each nuclide which would be expected to decay during each counting period;
3. the nuclide estimates in the form of time zero decay rates and number of atoms at time zero;

[2]Some changes in the maximum dimensions may require program changes not provided for in the relationship (60).

4. the standard errors of the time zero decay rates and number of atoms at time zero;
5. the estimated background spectra as counting rates for each detection system (Methods I and II only);
6. the correlation matrix of the nuclide estimates;
7. the normalized residuals (54) for each channel group of each spectrum;
8. the chi-square (55) for each channel group of each detection system;
9. the chi-square (56) for each detection system;
10. the chi-square (57) based on all data;
11. the background spectra as counting rates estimated from the residuals for each sample spectrum.

EXAMPLES

NaI(Tl) Gamma Pulse-Height Data

An 8- by 8-in. NaI(Tl) well crystal was used together with an RIDL transistorized 400-channel pulse-height analyzer to record several sets of gamma scintillation spectra. The instrument was operated with a channel width of 0.01 Mev. Separate radionuclide sources of $Ru\text{-}Rh^{103}$, $Ru\text{-}Rh^{106}$, I^{131}, $Cs\text{-}Ba^{137}$, carnotite, monazite, KCl, $Ce\text{-}Pr^{144}$, and $Zr\text{-}Nb^{95}$ were obtained. Each source and background was counted weekly for 11 weeks. All sources were counted for 1 min except for the KCl source which was counted for 10 min. The pulse-height data were stored separately on magnetic tape. Composite spectra were produced for each set of counts by nondestructive reading of the recorded spectra into the analyzer. The composite spectra were read out on punched paper tape. A single long count was also taken with each source and recorded on punched paper tape for calculation of the required channel group conditional probabilities $g_{\alpha ij}$ of Eq. (15). The 400-channel spectra were reduced by an IBM 7090 to 15 channel groups as follows:

Channel Group	Channels	Channel Group	Channels
1	12–16	9	105–129
2	17–21	10	130–168
3	22–29	11	169–200
4	30–43	12	201–240
5	44–56	13	241–290
6	57–71	14	291–340
7	72–83	15	341–399
8	84–104		

Various single and composite spectra were then analyzed using the GEM programs. In the case of a composite spectrum the total counting time of the components was used as the counting time of the composite spectrum so that the background contribution to the composite spectrum would be commensurate with background estimates. The results of several of these analyses are summarized in Tables 1 and 2.

Table 1. Decay Rate Estimates Using NaI(Tl) Gamma Pulse-Height Data

Conditions: 9 nuclides present, 15 channel groups, GEM Method I

Nuclide	Half-Life (days)	Time Zero Decay Rate	1 Spectrum		3 Spectra		6 Spectra		9 Spectra	
			Estimated Rate	Standard Error	Estimated Rate	Standard Error	Estimated Rate	Standard Error	Estimated Rate	Standard Error
$Ru\text{-}Rh^{103}$	40	150	161	19	141	34	143	19	148	17
$Ru\text{-}Rh^{106}$	365	378	361	41	438	69	407	45	395	42
I^{131}	8.05	189	195	86	240	35	245	27	165	15
$Cs\text{-}Ba^{137}$	1.09×10^4	419	428	7	437	11	428	7	431	7
Carnotite	1.65×10^{12}	507	547	14	536	21	527	14	539	12
Monazite	5.15×10^{12}	206	201	10	214	17	205	11	201	11
K^{40}	4.70×10^{11}	10,550	10,580	94	10,629	162	10,637	104	10,620	100
$Ce\text{-}Pr^{144}$	285	650	556	66	−88	114	475	78	473	79
$Zr\text{-}Nb^{95}$	65	126	120	6	114	9	117	6	117	6
Chi-square ratio			1.5		19		17		24	
Days between first and last spectrum					35		35		61	

Table 2. Decay Rate Estimates Using NaI(Tl) Gamma Pulse-Height Data

Case	Conditions	Nuclide	Half-Life (days)	Time Zero Decay Rate	Method I		Method II		Method III	
					Estimated Rate	Standard Error	Estimated Rate	Standard Error	Estimated Rate	Standard Error
A	9 nuclides present	I^{131}	8.05	189			184	247	184	247
	1 channel group (0.30 to 0.44 Mev)									
	9 spectra		Chi-square ratio				40		40	
B	Only I^{131} present	I^{131}	8.05	3410	3417	55	3470	50	3470	54
	15 channel groups									
	9 spectra		Chi-square ratio		3.5		2.8		2.8	
C	Only I^{131} present	$Ru\text{-}Rh^{103}$	40	0	−3.9	181				
	15 channel groups	$Ru\text{-}Rh^{106}$	365	0	41	493				
	1 spectrum	I^{131}	8.05	3410	3156	402				
		$Cs\text{-}Ba^{137}$	1.09×10^4	0	33	161				
		Carnotite	1.65×10^{12}	0	5.5	189				
		Monazite	5.15×10^{12}	0	41	179				
		K^{40}	4.70×10^{11}	0	−193	650				
		$Ce\text{-}Pr^{144}$	285	0	−1144	1781				
		$Zr\text{-}Nb^{95}$	65	0	12	78				
			Chi-square ratio		7					

The data in Table 1 give some indication of the positive and negative points of analyzing sets of time dependent spectra. Four sets of 15-channel group spectra containing 1, 3, 6, and 9 spectra, respectively, were analyzed with Method I of the GEM program. The total elapsed time over which the 9 spectra were recorded was 61 days, while for the 3- and 6-spectra sets it was 35 days. The same nine-component source was used for all spectra, and the counting was done in a single detector. These nuclides and their half-lives are listed in the first two columns of Table 1. Time zero was taken as the beginning of the recording of the first spectrum; that is, $t_0 = t_{11}$. The actual decay rates of the nuclides at time zero are listed in the third column of Table 1. The remainder of the table lists the decay-rate estimates $\lambda_\alpha N_\alpha$ based on analyzing the four sets of spectra and the standard errors of these estimates. Also the ratio of the chi-square statistic [see Eq. (57)] to the 95th percentile point of the appropriate chi-square distribution is listed at the foot of the standard error columns. A ratio of less than one indicates good agreement between model and data; that is, the model explains the data up to counting statistic variability. A large ratio indicates poor agreement; for example, the model may contain the wrong nuclides, and/or the detection system may have malfunctioned.

Inspection of the normalized residuals and background counting ratio estimated from residuals [see Eqs. (54) and (58)] of the GEM output for the nine-spectra case shows a depression of the low energy end of the spectrum during the course of recording the nine-sample spectra. The negative effect of this change in the shape of the pulse-height spectra is clearly seen in the chi-square ratios as they increase with the number of spectra in the set. The estimates appear to be insensitive to this degeneration in the fit of the model. Appearance is misleading. Addition of spectra to the analysis improves the precision of the estimation, and departure from the time-invariance assumption of the model decreases the precision. Table 1 is the result of these two diametrical factors operating simultaneously. The relative importance of the factors is a function of half-life. The precision with which the shortest lived nuclide, I^{131}, is estimated, as measured by the size of the standard error estimate, improves as spectra are added to the analysis. The precisions for the rest of the nuclides seem to be more dependent on the chi-square ratio than on the number of spectra.

Of the 36 estimates, 18 are within one standard deviation of the actual t_0 decay rate, 13 within 2, 4 within 3, and only 1 greater than 3. These figures are in close agreement with the usual interpretation of the standard error estimate based on the student's "t" distribution.

The data in Table 2 show the effect of putting either too many or too few components into the model. In all six cases I^{131} is present in the spectra. In case A the channel group of the I^{131} photopeak (0.30–0.44 Mev) was selected from the nine-spectra set discussed above in connection with Table 1. Methods II and III of the GEM program were used to estimate the t_0 decay rate of I^{131} with only the single I^{131} component in the model. In such a situation, Method I cannot be used since the background counting rate is not known. Methods II and III give the same estimate, 184, which is quite close to the actual decay rate of 189. The chi-square ratio clearly shows the model is inadequate. The systematic pattern of the normalized residuals (not shown) pinpoints the inadequacy to a multicomponent decay curve. With such a large standard error nothing really can be said concerning the presence of I^{131}.

Case *B* of Table 2 shows the estimation of I^{131} from a set of nine 15-channel group pure I^{131} spectra using the three methods of the GEM program. All three estimates agree with the correct decay rate. The chi-square ratios indicate that some perturbation over and above counting statistic variation is in the data. The normalized residuals (not shown) attribute most of this poorness of the fit to the two lowest energy channel groups.

Case *C* of Table 2 shows the analysis of just one of the 15-channel group spectra used in part *B*. The complete model with nine components was used for the analysis even though only I^{131} was present in the pulse-height spectrum. The standard errors for the eight components not present are all larger than the absolute value of the t_0 decay rates. Clearly, the analysis says that I^{131} is the only significant nuclide in the spectrum. A rerun of this data without the eight superfluous components in the model increases the precision with which the I^{131} t_0 decay rate is estimated. However, the precision is not as good as that in Case *B* since nine spectra were used as opposed to one in Case *C*.

Sources of $Ru\text{-}Rh^{103}$, $Ru\text{-}Rh^{106}$, I^{131}, and $Cs\text{-}Ba^{137}$ were placed together in the well of the NaI(Tl) crystal and counted weekly for eleven consecutive weeks. The eleven spectra were each reduced to 15 channel groups, and the resulting set was analyzed with the GEM program. Table 3 shows the estimates from fitting five different models with the appropriate GEM methods. Cases *A* and *B* of Table 3 clearly illustrate that Methods II or III can be used to estimate short-lived components I^{131} and $Ru\text{-}Rh^{103}$ without putting the long-lived ones in the model. Case *C* shows that when a medium-lived component $Ru\text{-}Rh^{106}$ is estimated with Methods II or III the estimation is not as precise. Case *D* is particularly interesting as three components are quite precisely estimated even though a relatively short-lived component $Ru\text{-}Rh^{103}$ has been omitted from the model. The large chi-square ratio is evidence of the poor fit of the model.

Finally, Case *E* shows the capabilities and failings of Methods II and III with the correct model. Method I with the aid of background information does a passable job of estimating the long-lived components. This case is the only one for which the standard error estimates are not realistic, being too small by about a factor of three. The large chi-square ratio gives reason to doubt the results of the estimation. The normalized residuals (not shown) are very wild, fluctuating from -10 to $+10$ for the lower energy half of the pulse-height spectrum. Surprisingly, Methods II and III still do a credible job of estimating the short-lived components. Essentially, what happens in the calculation is that the background and the longer-lived components are all treated as background. A fictitious average background is arrived at which in this instance was more realistic than the one supplied for the Method I calculation.

In all the above examples the chi-square ratios were greater than one. Clearly, the detection system (including background) used was unstable to the degree that counting statistic variation was no longer the major source of randomness in the data. Yet, statistically sound estimation of the individual nuclide t_0 decay rates was possible. By statistically sound, we mean that the standard error estimates were valid indicators of the precision of the decay rate estimates. Granting the fact that the estimation would have been more precise if the detection system (including background) had been time invariant, the authors feel that a fruitful alternative to absolute detection systems is reasonably stable systems coupled with high quality data evaluation.

Table 3. Decay Rate Estimates Using NaI(Tl) Gamma Pulse-Height Data

Conditions: 4 nuclides present, 15 channel groups, 11 spectra, 68 days between first and last spectrum

Case	Nuclide	Half-Life (days)	Time Zero Decay Rate	Method I		Method II		Method III	
				Estimated Rate	Standard Error	Estimated Rate	Standard Error	Estimated Rate	Standard Error
A	I^{131}	8.05	2910			3,052	139	3,052	139
		Chi-square ratio				16		16	
B	$Ru\text{-}Rh^{103}$	40	2710			2,663	193	2,663	193
	I^{131}	8.05	2910			2,879	93	2,879	93
		Chi-square ratio				7		7	
C	$Ru\text{-}Rh^{103}$	40	2710			2,472	214	2,472	214
	$Ru\text{-}Rh^{106}$	365	6800			3,398	1,763	3,386	1,750
	I^{131}	8.05	2910			2,860	92	2,860	92
		Chi-square ratio				6.9		6.8	
D	$Ru\text{-}Rh^{106}$	365	6800	7016	264				
	I^{131}	8.05	2910	3277	286				
	$Cs\text{-}Ba^{137}$	10900	6270	6087	119				
		Chi-square ratio		89					
E	$Ru\text{-}Rh^{103}$	40	2710	3268	128	2,472	247	2,473	244
	$Ru\text{-}Rh^{106}$	365	6800	5612	130	3,372	1,963	3,385	1,941
	I^{131}	8.05	2910	3081	128	2,808	123	2,809	122
	$Cs\text{-}Ba^{137}$	10900	6270	5949	54	−99,168	24,991	−100,085	24,835
		Chi-square ratio		18		5.9		5.8	

REFERENCES

[1] P. R. Bell, "The Scintillation Method," *Beta and Gamma-Ray Spectroscopy*, Interscience, New York, 1955.

[2] C. E. Crouthamel, *Applied Gamma-Ray Spectrometry*, Pergamon Press, New York, 1960.

[3] R. L. Heath, *Scintillation Spectrometry Gamma-Ray Spectrum Catalogue*, IDO-16408 (July 1957).

[4] R. W. Perkins, "High Sensitivity Gamma Ray Spectrometry," *Proceedings of the 1961 International Conference on Modern Trends in Activation Analysis, Held at Texas A. & M. College, December 15–16*, Texas A. & M. College, College Station, 1962.

[5] J. W. Nostrand and A. J. Farale, *704 Program Report, The Reduction of Gamma Spectral Data from a 100-Channel Pulse Height Analyzer,"* NP-9510 (April 1960).

[6] A. J. Ferguson, *A Program for the Analysis of Gamma-Ray Scintillation Spectra Using the Method of Least Squares,"* CRP-1055 (November 1961).

[7] H. M. Childers, "Analysis of Single Crystal Pulse-Height Distributions," *Rev. Sci. Instr.* **30**, 9 (1959).

[8] L. E. Fite, D. Gibbons, and R. E. Wainerdi, *Computer Coupled Automatic Activation Analysis*, TEES-2671-1 (May 1961).

[9] R. L. Heath, *Data Analysis Techniques for Gamma-Ray Scintillation Spectrometry*, IDO-16784 (May 1962).

[10] R. E. Connally, report in preparation.

[11] W. Feller, *An Introduction to Probability Theory and Its Applications*, Wiley, New York, 1950.

[12] S. N. Roy and A. E. Sarhan, "On Inverting a Class of Patterned Matrices," *Biometrika*, **43**, 227 (1956).

(6-4) COMPUTER APPLICATIONS IN NEUTRON ACTIVATION ANALYSIS

Alan J. Blotcky, Barney T. Watson, and Richard E. Ogborn
Radioisotope Service
Veterans Administration Hospital
Omaha, Nebraska

Neutron activation analysis is a very important tool in the fields of medicine and chemistry since it makes possible a simultaneous assay of the trace elements in blood, tissue, alloys, ceramics, and many other substances. It is the aim of this laboratory to devise a method of accomplishing this objective rapidly and with a minimum of recourse to pre- and postirradiation chemical procedures.

In developing a method of determining by neutron activation analysis the individual masses of a composite of trace elements such as blood serum, it is very desirable to use computer techniques since the stripping of multicomponent spectrums by hand is a tedious and time consuming process. Because the objective of the work in our laboratory is to analyze many serum samples daily, it is a necessity that a computer be used for data reduction.

A further objective of this laboratory is to show that activation analysis can be accomplished with a minimum outlay of capital. Consequently, in choosing a computer system, the IBM 1620 was selected.

The 1620 memory is 20,000 positions of six bits each or one-tenth the size of the 32K IBM 709-90 Series. The monthly rental for an IBM 1620 with paper tape input/output is $1,600, or one-fortieth (1/40) the cost of the IBM 7090 for basic computer rental [1].

The IBM 1620 system requires the equivalent of one full-time employee for processor maintenance, computer programming, and operation. Paper tape and printer paper expenses do not exceed $200 per year. Total room preparation is one 220-volt outlet and a floor space requirement of 150 ft^2. If normal room air conditioning is not available, a one-ton unit must be included. For an additional $865.00 per month, a 1622 card input/output unit and a 402 off-line parallel printer may be acquired. The above combination decreases the time for printing 400 channels of data from 35 to 9 min.

Now that a need for a computer has been established and a type selected, let us examine the problems associated with the method of analysis. The basic method of analysis in our laboratory is to compare, for mass determination, the photopeaks of a gamma spectrum of a composite of elements with the photopeaks of standards which have been irradiated with neutrons and allowed to decay for a comparable length of time. Since the standards are from a previously constructed library and are not irradiated at the same time as the unknown, the first step is to construct a valid set of standards. In order to accomplish this, a program was developed which accepts an unlimited number of 400-channel radiation analyzer punched paper tapes and then determines for each channel the average number of counts, the experimental standard deviation, and the relative percent error. Thus all standard curves are constructed by activating many different samples of the element and analyzing each sample on a 400-channel analyzer which punches the output onto 8-channel IBM-type paper tape. All of the standards have a relative percent error per channel of less than 5% in their significant portions.

Since the photopeaks of the standard curves are to be compared with those of the unknown composites, it is necessary that all standards and unknowns be normalized to the same flux. In order to accomplish this, a daily neutron flux value is computed from a gold wire irradiation and the value is then normalized to one and used as a factor to correct for any slight variation in flux.

The flow diagram of the standard generating tape is shown in Fig. 1.

With the standard tapes now generated and stored in what will be referred to as a library of standards, it is next necessary to develop a program for analyzing a composite gamma spectrum and determining the mass of each neutron-activated element present. In accomplishing this analysis, two basic methods have been used: (a) spectrum stripping and (b) simultaneous linear equations. The purpose of developing

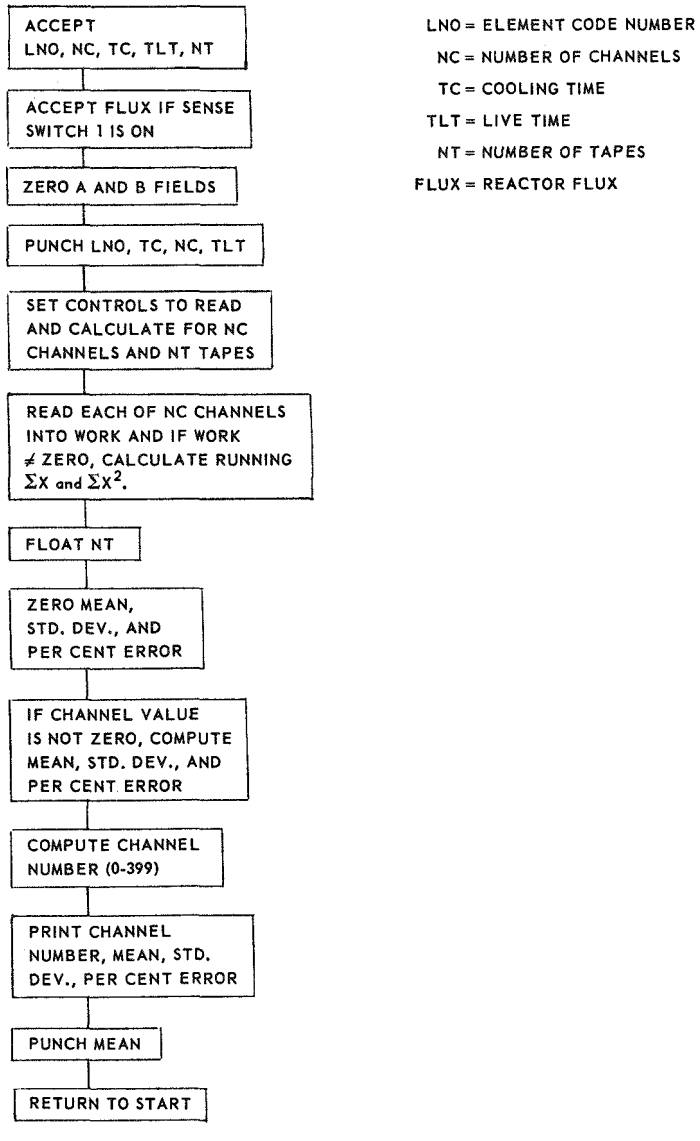

Fig. 1. Flow Diagram of the Program for Computing Standard Tapes.

both methods was to compare the accuracy and computer-use time of the two and to arrive at a decision as to when each should be used.

Before examining the two programs in detail, there are several physical corrections which are common to both methods. The counts per channel of each standard must be corrected for the decay time. The cooling or decay time is assumed to be the interval between the time when the sample is taken out of the reactor and the point half-way through the elapsed time of the analyzer. For example, if time out of

the reactor until count started = 4 min, time to count 10 min live time[1] = 10.10 min, then cooling time = 4 min + 10.10/2 = 9.05 min. Since this assumption is valid only as long as the elapsed time of counting is less than $\frac{1}{2}$ the half-life, a correction also must be made of the form [2]

$$\frac{a_c}{\bar{a}} = \frac{0.693\ \Delta t}{t_{1/2}} \cdot \frac{\exp\left[-0.347(\Delta t/t_{1/2})\right]}{1 - \exp\left[-0.693(\Delta t/t_{1/2})\right]}, \tag{1}$$

where $\bar{a}$ is the observed mean activity over the duration of the measurement; a_c is the corrected activity at one-half of the elapsed counting time; $t_{1/2}$ is the half-life of the nuclide; and Δt is the counting interval.

The stripping method starts by selecting the most energetic photopeak of the unknown spectrum and comparing the counts of the unknown sample in that photopeak to those of the standard curve of the element that has the characteristic photopeak. The ratio of (STD CTS)/(STD MASS) = (UNK CTS)/(UNK MASS) may then be used to compute the mass of the element in the unknown sample.

The proportionate amount of that standard element curve is then subtracted from the unknown sample spectrum. The residual curve may either by punched or printed out after each element has been stripped off the composite or after any number of elements have been stripped off. The procedure may then be repeated until the complete curve of the unknown sample is accounted for.

The block diagram of the mass determination by stripping program is shown in Fig. 2.

It may be noticed in Fig. 2 that NCHAN is the number of channels to be summed. This was done so that data could be smoothed by summing more than one channel. The program was originally written so that this could be variable, but we are now using 5 channels very satisfactorily. The 5-channel sum is also used for determining counts in the matrix method.

Because our transistorized RIDL 400-channel analyzer is kept in an air conditioned room and calibrated several times a day and analyzer dead time is less than 5%, no analyzer drift has been observed; consequently, no peak shift correction has been incorporated in the program. However, if this becomes a problem, provisions can be made to shift the unknown curve so that known peaks will coincide.

In the simultaneous linear equation solution, use is made of the fact that the proportionate parts of a composite spectrum may be assigned to the proper elements by solving a set of simultaneous linear equations of order k of the number of radioactive elements in the composite.

As an example of this method of solution, a three-element composite will be used. The three equations for the total counts in the selected photopeaks of elements 1, 2, and 3 are

$$a_{11}X_1 + a_{12}X_2 + a_{13}X_3 = b_1\ ,$$

$$a_{21}X_1 + a_{22}X_2 + a_{23}X_3 = b_2\ ,$$

$$a_{31}X_1 + a_{32}X_2 + a_{33}X_3 = b_3\ ,$$

[1]Live time — actual time that electronic circuitry of the radiation analyzer is accepting pulses.

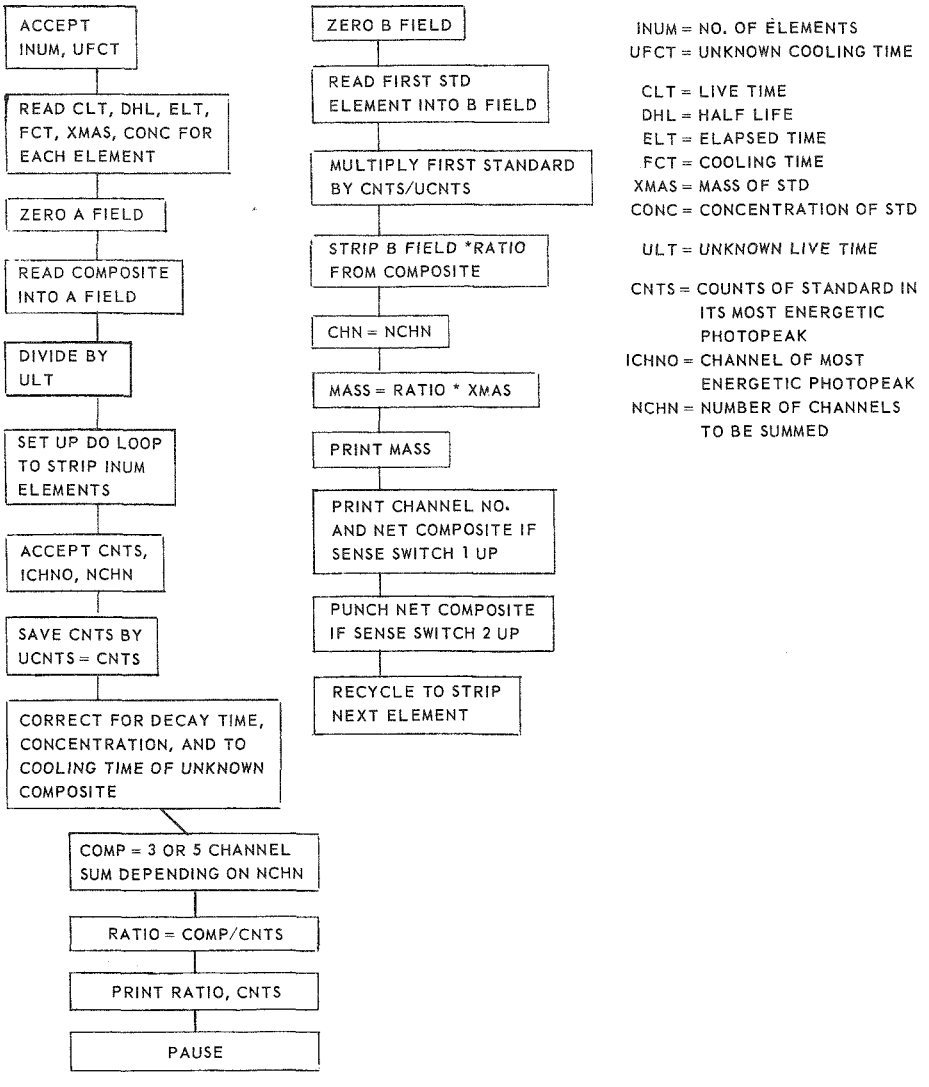

Fig. 2. Flow Diagram for the Stripping Program.

where the b_1, b_2, and b_3 are the counts of the selected photopeaks of elements 1, 2, and 3 in the composite spectrum.

The coefficients a_{ki} of the variables x_k are the ratios defined by $a_{ki} = N_{ik}/N_{ii}$, where N_{ik} is the number of counts of the ith element at the selected photopeak of the standard of element k, and N_{ii} is the counts of the ith element at its own selected photopeak. The values of a_{ki} are determined from the standard spectra in our library.

A matrix method is used to solve the simultaneous linear equations as follows:

$$A = \begin{bmatrix} a_{11} a_{12} a_{13} \\ a_{21} a_{22} a_{23} \\ a_{31} a_{32} a_{33} \end{bmatrix}. \qquad \text{Let } X = \begin{bmatrix} X_1 \\ X_2 \\ X_3 \end{bmatrix} \qquad \text{and } B = \begin{bmatrix} b_1 \\ b_2 \\ b_3 \end{bmatrix}.$$

The system of linear equations may be represented in matrix form by $AX = B$. Multiply by A^{-1} (the inverse of A):

$$A^{-1}(AX) = A^{-1}B \ ,$$

$$(A^{-1})(A)X = A^{-1}B \ , \qquad (2)$$

$$X = A^{-1}B \ .$$

Or, the values of X_1, X_2, X_3 that are

$$X = \begin{bmatrix} X_1 \\ X_2 \\ X_3 \end{bmatrix}$$

may be found by reinverting the matrix A and by multiplying by

$$B = \begin{bmatrix} b_1 \\ b_2 \\ b_3 \end{bmatrix} .$$

Figure 3 gives the flow chart for the matrix coefficient and mass ratio generator program. Figure 4 shows the flow chart for the eleven-element analysis program. The matrix coefficient and mass ratio generator program accepts raw counts from the standards and generates the necessary data for input to the eleven-element analysis program. This program outputs the matrix solution of the simultaneous linear equations (that is, the X_i counts of each element and the corresponding mass of each element in the composite spectrum). A sample of the eleven-element analysis program output is shown in Fig. 5.

RESULTS

To date, the two types of programs listed have been used to solve three-element composites containing calcium, manganese and magnesium in an aqueous solution, and four-element composites containing calcium, manganese, copper, and magnesium as polyvalent cations in an organic phase.

Figure 6 shows the individual and composite spectra of the aqueous solutions and Fig. 7 shows the curves for the four-element composites. The mass and percent error of the elements being assayed were as shown in Tables 1 and 2.

The matrix solution is generally more accurate, since the stripping method assumes that the contribution to the most energetic photopeak by elements with less energetic peaks is negligible. In contrast to this, the matrix method considers all contributions to each peak.

This may be illustrated by observing that in Fig. 7 there is a contribution by the copper to the 1.8-Mev manganese peak used in the analysis. This would not be considered in the stripping method but would be included in the matrix solution. The results of this omission in the stripping method are revealed by the generally smaller percent error of the matrix method as shown in the four-element comparison chart in Table 2.

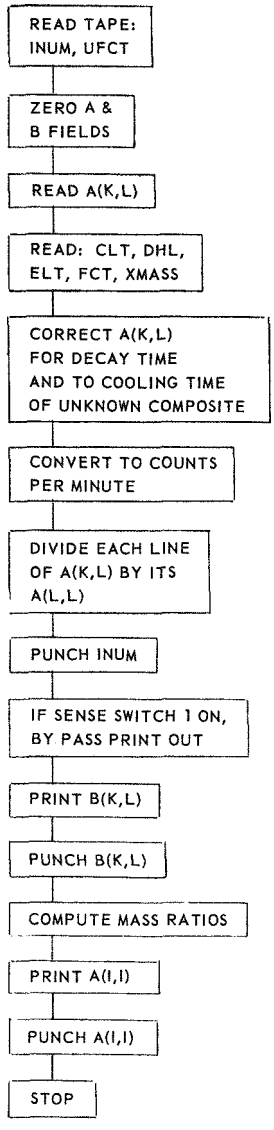

INUM = NUMBER OF ELEMENTS
UFCT = UNKNOWN COOLING TIME

A(K,L) = COUNTS OF INUM ELEMENTS IN EACH ELEMENT'S MOST ENERGETIC PHOTOPEAK

CLT = LIVE TIME
DHL = HALF LIFE
ELT = ELAPSED TIME
FCT = COOLING TIME
XMASS = MASS OF STD.

$$A_{corr} = \frac{0.693\Delta t}{t_{1/2}} \times \frac{e^{-0.347(\Delta t/t_{1/2})}}{1 - e^{-0.693(\Delta t/t_{1/2})}}$$

Δt = ELAPSED TIME

$$A_t^0 = A_t^{std}\, e^{+(.693t/t_{1/2})}$$

$$A_t^{unk} = A_t^0\, e^{-(.693t/t_{1/2})}$$

t = COOLING TIME

$t_{1/2}$ = HALF LIFE

A(I,I) = XMASS(I)/A(I,I)

Fig. 3. Flow Chart for the Program Which Generates the Matrix Coefficients and Mass Ratios.

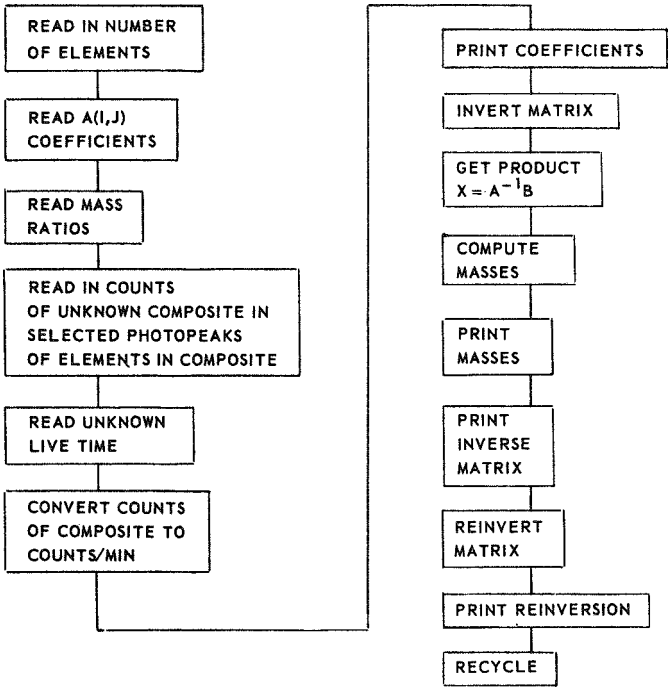

Fig. 4. The Eleven-Element Analysis Program.

MATRIX SOLUTION OF 3 × 3 COMPOSITE 6/15/62

LOAD DATA

1.0000000	1.6850766E-02	7.8755878E-04	ORIGINAL MATRIX
.80361597	1.0000000	3.6854930E-03	
1.0547533	10.841522	1.0000000	
101.64112	.32091769		COUNTS AND MASS FOR EACH ELEMENT
64.329282	9.4756743E-05		
729.96620	8.5620261E-02		
1.0078157	−8.7260590E-03	−7.6155412E-04	INVERSE MATRIX
−.83952332	1.0488880	−3.2044956E-03	
8.0387134	−11.362338	1.0355447	
1			
.99999994	1.6850766E-02	7.8755870E-04	REINVERTED MATRIX
.80361602	1.0000001	3.6854933E-03	
1.0547531	10.841523	1.0000001	

Fig. 5. Sample Output from the Eleven-Element Analysis Program.

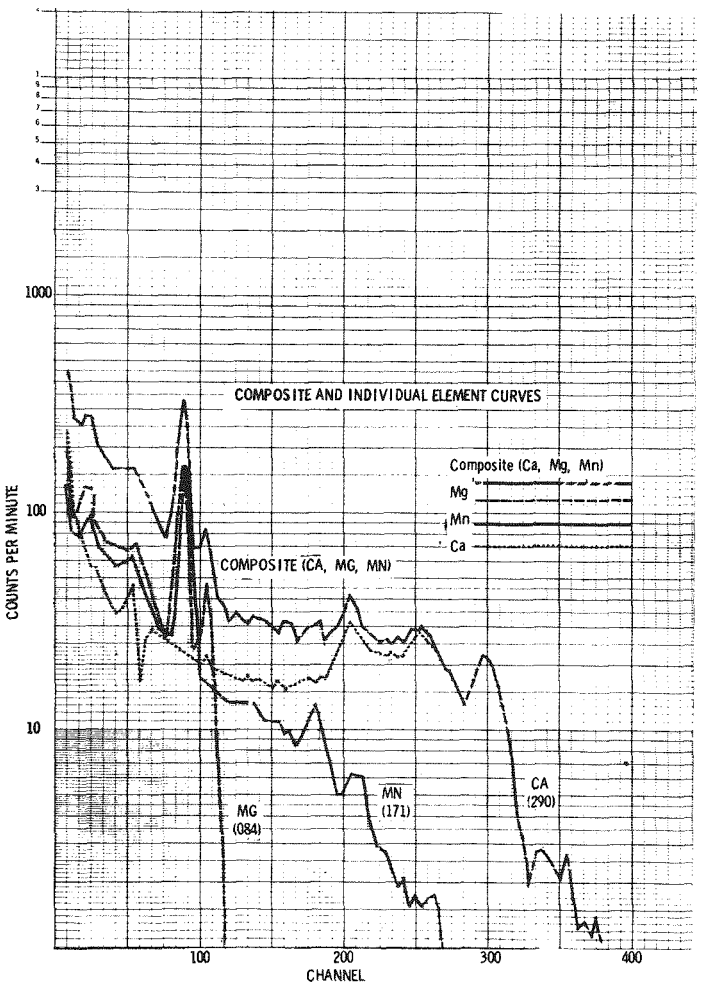

Fig. 6. Individual and Composite Gamma-Ray Spectra for the 3-Element Composite Samples.

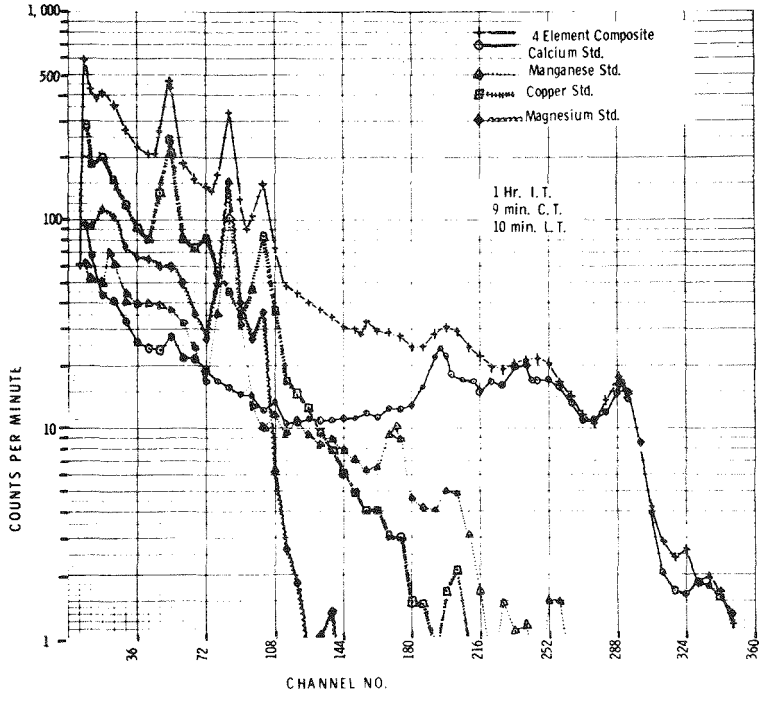

Fig. 7. Individual and Composite Spectra for the 4-Element Composite Samples.

Table 1. Analysis of 3-Element Composites. Results are given for averages of 5 samples

Element	Mass Taken (mg)	Error (%)	
		Stripping	Matrix
Ca	0.3298	−1.2	−1.7
Mn	0.000089	+6.3	+3.9
Mg	0.0909	+8.3	−3.5

There may be cases, however, where a combination of the stripping and matrix method would be indicated, since the matrix solution assumes one either knows all of the elements in the composite, or can guess the possible elements present. (If elements are included which are not in the unknown, the mass of these elements will either be zero or a very small positive or negative number.) If one cannot hazard a guess as to what all of the elements may be, and clear photopeaks exist, the unknown may be serially stripped and a residual printed out after each stripping. The resultant curves can then be analyzed and compared with those in a gamma spectrum catalog to find the unknown elements. If necessary, the unknown composite may be reirradiated and counted at different cooling times so that the half-lives of the unknowns can also be used for identification. When the above case does not have clear photopeaks, a

Table 2. Percentage Errors in the Analysis of 4-Element Composites

Run No.	Error (%)							
	Ca (0.3298 mg)[a]		Mn (0.0000898 mg)[a]		Cu (0.00910 mg)[a]		Mg (0.0909 mg)[a]	
	STRIP	MATRIX	STRIP	MATRIX	STRIP	MATRIX	STRIP	MATRIX
1	−1.0	−5.9	+16.0	−20.6	+42.0	+0.7	−38.0	−1.7
2	−0.3	−5.0	+24.0	−0.9	+42.0	+3.6	−39.0	−11.2
3	+4.0	−0.9	+14.0	−7.6	+43.0	−0.4	−28.0	+0.6
4	−3.0	−2.7	+50.0	+13.9	+44.0	+11.4	−52.0	−23.1
5	+2.0	−8.1	+59.0	+46.1	+42.0	+15.6	−62.0	−42.3
6		−6.5		+0.6		+6.6		−19.8
7		−2.5		+9.2		+9.9		−17.1
8		−4.4		+6.5		+7.3		−4.4
9		−8.0		+12.3		+8.6		−19.4
10		−0.1		+13.8		+1.7		−16.4
11		−7.1		+1.6		+6.3		−10.6
12		+2.4		+43.0		+12.2		−25.5
13		+1.9		+20.1		+20.0		−32.0
14		−4.9		+35.8		+18.8		−42.0

[a]Element and mass taken.

subsequent analysis system must be developed. This problem has not been considered for the present. If after the unknown elements are identified a more accurate determination is desired, the matrix solution may be used.

Running time for the solution of a four-element composite by the stripping method is approximately 45 min when only the final residual is printed. An additional 35 min is required for each additional printout. If, however, the previously mentioned card equipment is used, the 35 min is reduced to 9 min. The running time for the matrix solution does not exceed 4 min.

CONCLUSIONS

A comparison of the matrix method to the stripping method in the solution of a complex gamma spectrum must be in terms of (1) purpose of solution, (2) accuracy, and (3) the computer system available.

In solving a composite of known elements for quantitative analysis, the matrix solution is faster and more accurate than the stripping method.

In qualitative analysis to find out what elements are in the composite spectrum, the stripping method interspersed with hand spectrum analysis is necessary.

The matrix solution is much better adapted to use on a small unsophisticated computer system than the stripping technique, as any production methods of stripping would require a much more expensive computer system with several magnetic tape drives. Such a system would in turn require more complex programming to automate it than does our relatively inexpensive small computer.

ACKNOWLEDGMENTS

We wish to thank Mr. Arthur May for his help in irradiating the samples and Guy and Mary Clare Haven for their invaluable assistance in the chemical preparations of samples.

REFERENCES

[1] Adams Associates, *Computer Characteristics Chart.*

[2] G. B. Cook and J. F. Duncan, *Modern Radiochemical Practice*, p 57, Clarendon Press, Oxford, 1952.

(6-5) GAMMA-RAY SPECTRUM ANALYSIS APPLIED TO FISSION PRODUCT CONTAMINATION STUDIES

W. B. Seefeldt
Argonne National Laboratory[1]
Lemont, Illinois

Gamma-ray spectrum analysis was used as the sole means of obtaining analytical information in a recently completed program on fission product contamination relating to boiling water reactors in which rupture of fuel element cladding had occurred. Liquid, condensed steam, and metal samples from experimental equipment were counted with a 4- by 4-in. NaI(Tl) crystal using three fixed geometries in conjunction with a Nuclear Data 256 channel analyzer. A sustained effort was made to maintain a specified energy vs channel number calibration. Fission products taken into account include Ce^{141}, I^{131}, Ru^{103}, Nd^{147}, Cs^{137}, Zr^{95}-Nb^{95}, and Ba^{140}-La^{140}. Reference spectra of each fission product were obtained under each of the three counting geometries used. Gamma counts due to bremsstrahlung from beta emitters were also taken into account.

Throughout this paper the words "reference spectrum" will be used to describe the simple spectrum of 1 μc of a single fission product; in the case of Zr^{95}-Nb^{95} and Ba^{140}-La^{140}, the "reference spectrum" is that of 1 μc total of the fission products at equilibrium. The spectrum to be resolved will be called the "unknown spectrum."

Two basic techniques and a number of variations of each technique were employed to resolve the spectra: simple equations and least squares. Each technique ultimately

---

[1]Operated by the University of Chicago under Contract No. W-31-109-eng-38. Work performed under the auspices of the U.S. Atomic Energy Commission.

requires the solution of eight equations in eight unknowns. The principal difference is that in simple equations, eight pieces of information are used from each spectrum, whereas least squares is capable of utilizing all information in a spectrum. Principal equations are shown in Appendices A and B.

In theory the eight pieces of information used in preparing simple equations can be chosen at random. In practice the information is obtained in eight preselected energy regions corresponding to the energy of the principal peak of each of the eight reference fission products. (The preselected energy regions must be identical for all spectra used in the analysis.) A single piece of information might consist of the counting rate in one peak channel or of the combined counting rates of several channels. In this work two combinations of channel groupings were used: (1) the group of channels included those defining the principal peak and (2) the group of channels was taken as five, the peak channel plus two on either side. The groupings used are shown in Table 1.

Table 1. Channel Groups Used in Simple Equation Method

Fission Product	Channel Number Corresponding to Principal Peak	Energy of Principal Peak (Mev)	Channel Groups	
			Set 1	Set 2
Ce^{141}	17.7	0.145	14-22	16-20
Beta bremsstrahlung			23-39	22-26
I^{131}	45.8	0.364	40-52	44-48
Ru^{103}	62.2	0.498	55-68	60-64
Nd^{147}	66.3	0.533	59-74	64-68
Cs^{137}	82.4	0.661	74-91	80-84
Zb^{95}-Zr^{95}	95.0	0.75	84-103	93-97
Ba^{140}-La^{140}	197.4	1.60	182-212	195-199

The least-squares analysis was reasonably conventional; however, the equations were set up in a manner that has potential usefulness for error analysis (see Appendix B and later section of paper). Deviations squared were either unweighted (unit weight) or weighted by the reciprocal of the square of the estimated error. In this case the square of the estimated error is the counting rate itself. However, a maximum weight of 0.1 was specified in the computer program in recognition of the fact that counting rates less than 10 usually reflect the difference between gross counts and background counts of the order of 5 to 15, and the resulting error is associated with these rather than the difference count reflected by the counter.

All methods used require that the energy-channel relation of the counting equipment remain constant. Special efforts in this direction were made while obtaining both reference and unknown spectra. The position of a standard Na^{22} 1.79-Mev peak and a standard Ce^{144} 0.134-Mev peak was monitored to the nearest 0.1 channel, and corrections were made to ensure specifications. A partial record of the 1.79-Mev peak position is shown in Fig. 1 to illustrate the difficulty of maintaining precise control. The

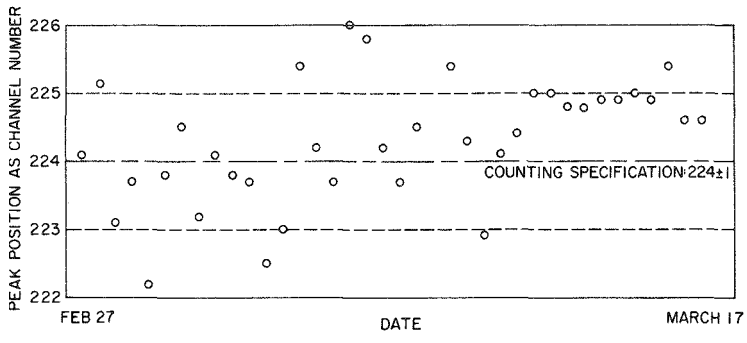

Fig. 1. Positions of Na^{22} Peak at 1.79 Mev, Monitored Three Times Daily for 13 Days.

0.134-Mev peak showed a similar pattern whose range in terms of channels was a factor of 4 less.

The least-squares method of solution lends itself to compensating rather easily for channel shifting due to bias. Compensation for gain is also possible but requires additional computer programming. In this work each unknown spectrum was analyzed three times: once in its original position, then shifted one channel up, then one channel down. The sums of the squares of the deviations (together with inspection of the difference spectra) indicate the best solutions, and further interpolation of these results reveals whether a fractional channel shift would further improve the fit.

SOLUTION OF SPECIFIC SPECTRA

An unknown spectrum of a metal deposition sample was used for comparing calculation methods and results. The spectrum was chosen for the following reasons: (1) the Ba^{140}-La^{140} peak is defined by points whose statistical variation was broad; (2) Cs^{137} is present as a minor constituent against a high background of Zr^{95}-Nb^{95}; and (3) Ce^{141} exists in sufficient quantity to reveal a moderate peak, although the peak is superimposed on a high Compton plateau. The variation of calculated results with calculation method and channel shifting will be shown.

The least-squares program (1) calculated the microcurie contribution of each fission product, (2) synthesized the original spectrum from the calculated results and reference spectra (this will be referred to as the "synthetic spectrum"), (3) computed the difference spectrum between the unknown and synthetic spectra, (4) algebraically summed the differences, and (5) summed the square of the differences. Table 2 shows the information by which the fit was judged relative to channel shifting. The flip-flop referred to is the order of the peaks in the difference spectrum that result from slight displacements of a Gaussian distribution on the synthetic spectrum compared to that on the unknown. The reversal of this order between the 0 and +1 channel position of the unknown indicates that the correct channel shift is within the range of 0 and +1. The summation of the square of differences indicates that shifting the unknown one channel up yields

Table 2. Curve Fitting of Synthetic Spectra to Unknown Spectrum

Calculation method: least squares

Channel Position of Unknown	Σd	Σd^2	Flip-Flop Order on Difference Spectrum
Unweighted least squares:			
−1	112	1.1×10^8	−,+
0	0.88	2.7×10^7	−,+
+1	0.84	1.2×10^7	+,−
Weighted least squares:			
−1	112	1.1×10^8	−,+
0	0.89	3.0×10^7	−,+
+1	0.81	1.3×10^7	+,−

a better fit than not shifting. Figure 2 shows the unknown spectrum and the best synthetic spectrum obtained by weighting. The good fit is evident visually. Figure 3 shows the difference spectra for the solutions in which the unknown spectrum was not shifted and also shifted one channel higher. The flip-flop of the difference peaks is evident, and the sizes of the peaks confirm that a channel shift up has improved the results. An expanded presentation of the Ce^{141} region (0.134 Mev) of the unknown and synthetic spectra (Fig. 4) reveals the effect of channel shift in this area. The computed microcurie contents of the Ce^{141} differ by 20%, and it is visually evident that the higher value more closely approximates the correct value. It is also observed

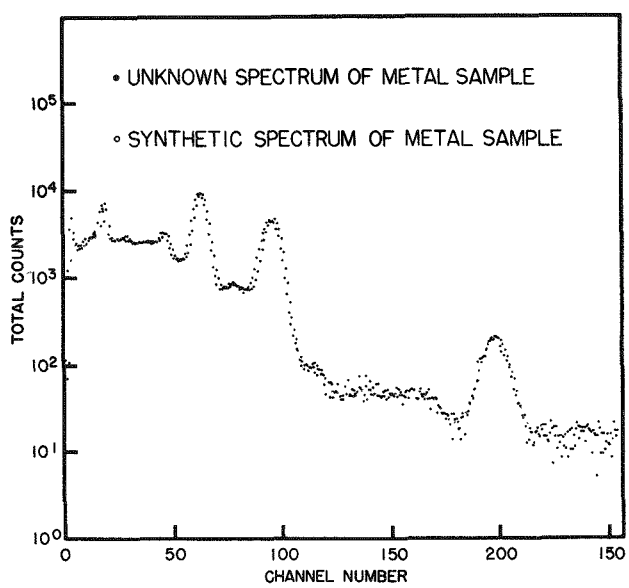

Fig. 2. Unknown Spectrum of a Metal Sample Compared with the Spectrum Synthesized from the Calculated Results and Reference Spectra.

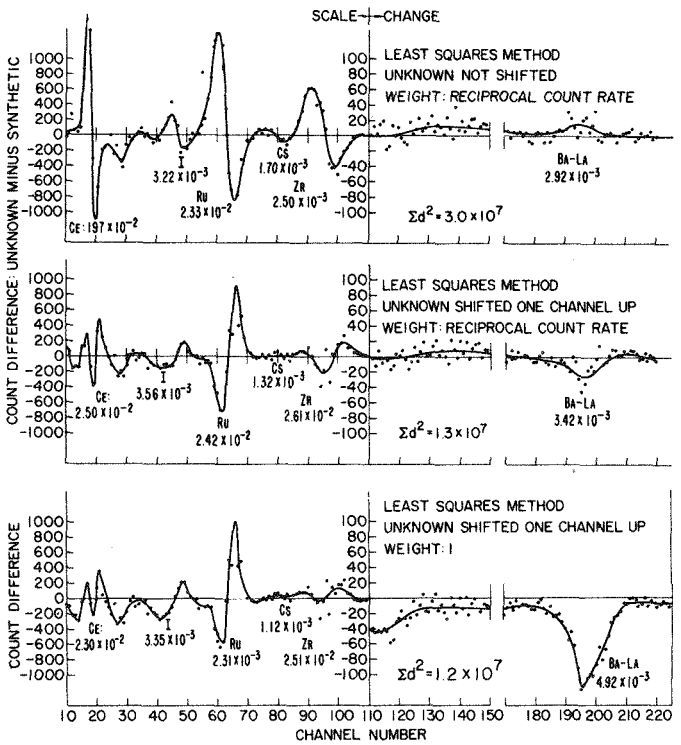

Fig. 3. Difference Plots of the Metal Sample Data for Solutions in Which the Unknown Sample Was Not Shifted and also Shifted One Channel Higher.

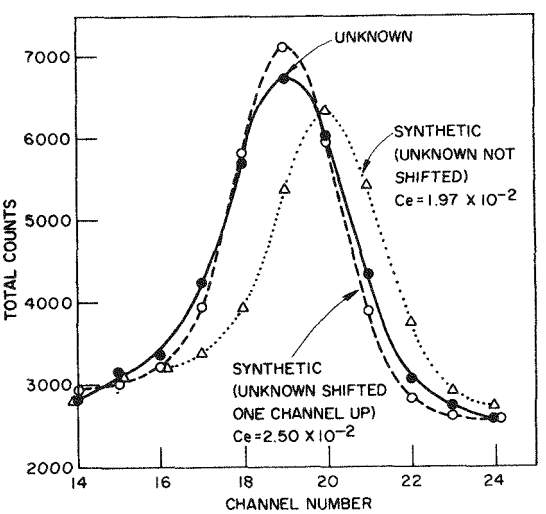

Fig. 4. Expanded Portion of Ce^{141} Region, Showing the Effect of Shifting the Unknown. (Least-squares method, weighted according to the reciprocal of the counting rate.)

that the resolution of the counting equipment at the time of counting the unknown had decreased from that obtained when the references were counted. The effect of channel shift in the Ba^{140}-La^{140} region (1.6 Mev) was small, since the peak width at half-height is about 11 channels. The Ce^{141} peak width at half-height is only about 3 channels.

A similar expanded presentation in the Ba^{140}-La^{140} area (Fig. 5) shows the effect of using weighted and unweighted methods of least-squares computation The calculated microcurie contents differ by about 35%, and again the result which most closely matches the unknown is evident. By not weighting, that is, by using a unit weighting factor, an undue influence is given to energy regions of high counting rate. It is clear that weighting is imperative when a spectrum includes a wide range of count rates.

A graphical compilation of most of the results was made; some comparisons are shown in Figs. 6 and 7. The cross-hatched bars are those associated with the most reliable results, i.e., those obtained when the unknown spectrum was shifted up one channel. As is to be expected, calculations for strong peaks such as Zr^{95}-Nb^{95} are relatively independent of computational method and channel shift. If the unweighted least-squares result for Ba^{140}-La^{140} is discarded, the statement is true for this fission product also. The surprising result is that Cs^{137} (Fig. 7), which has a microcurie content of about 1/20 that of Zr^{95}-Nb^{95}, shows as little variation as it does. However, the computed Cs^{137} content is sensitive to channel shifting but shows the smallest channel shift effect for the "five channel only" simple equation solution method. Cerium-141, the modest-sized peak on a high plateau, also is sensitive to channel shifting but less so for the simple equation solution methods than for the least squares.

Thorough statistical analyses are indicated to clarify the errors introduced by channel shifting and computational method. Without the benefit of such analyses, tentative conclusions would include: (1) weighted least squares used in conjunction with a criterion for best fit yield the most satisfactory set of computed results, and (2) the simple equation method using five peak channels only appears to yield nearly comparable results without having the channel shifting sensitivity of other methods.

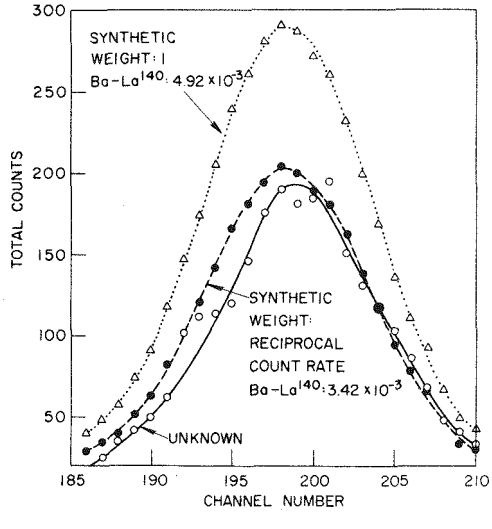

Fig. 5. Expanded Portion of the Ba^{140}-La^{140} Region, Showing the Effect of Weighting on the Least-Squares Method.

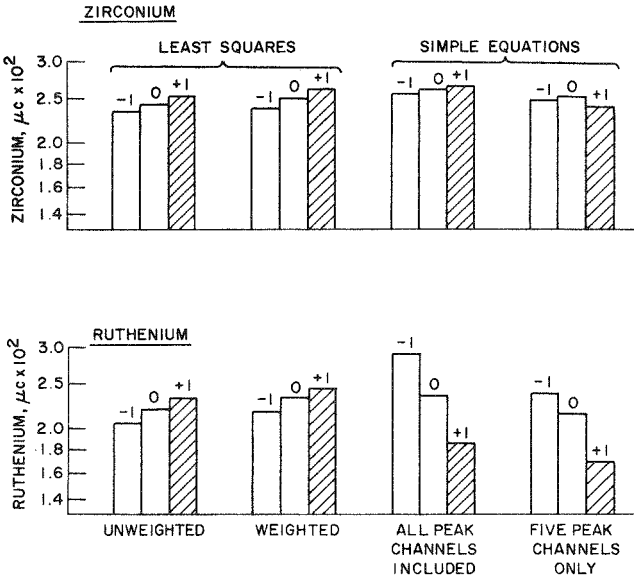

Fig. 6. Comparison Between the Results for Zr^{95} and Ru^{103}. The Channel shift for the unknown is indicated by −1, 0, +1.

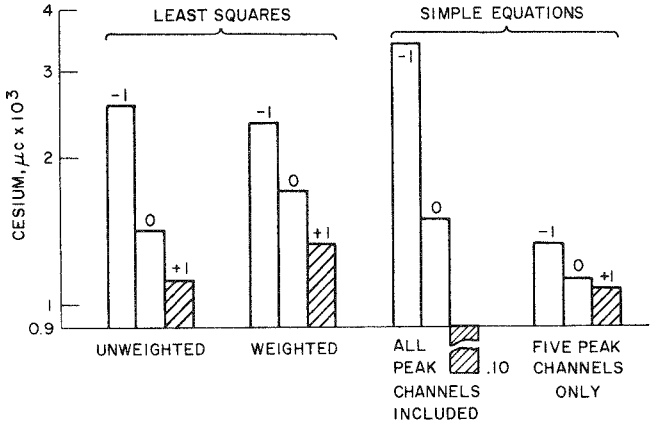

Fig. 7. Comparison of Cs^{137} Results Obtained by Different Methods. The channel shift for the unknown is indicated by −1, 0, +1.

A sample, which when counted showed the presence of an additional fission product not included in the library of reference spectra, was chosen for least-squares analyses to illustrate curve misfit. The unknown and synthetic spectra are shown in Fig. 8, and the difference plot is shown in Fig. 9. The fit is very good in the half of the spectrum up to channel 115 (about 0.90 Mev) but shows the aberrations at higher energies expected from the spectra of Fig. 8. Inspection of difference spectra

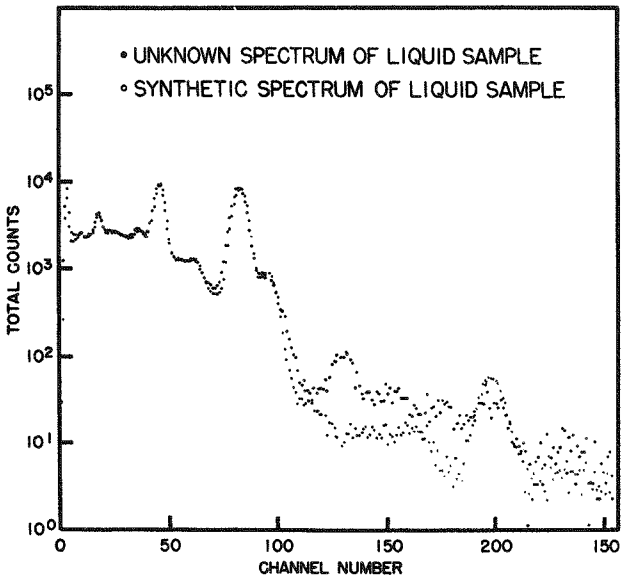

Fig. 8. Illustration of a Case in Which an Additional Fission Product Not Included in the Reference Library Was Present.

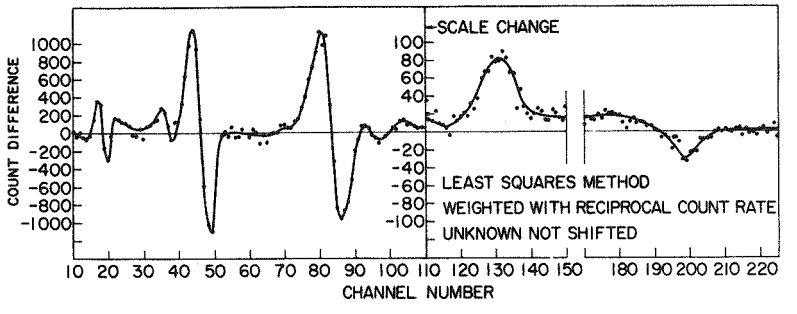

Fig. 9. Difference Plot for the Case of Figure 8.

must be made to ensure the validity of the assumption that 95% or more of the counts in the unknown result from fission products whose reference spectra are included in the reference library.

ERRORS DUE TO CHANGING RESOLUTION OF COUNTING EQUIPMENT

A mathematical analysis was made of single Gaussian peaks to determine the effect of changing counting resolution on calculated results based on least-squares methods. No experimental work was performed on this aspect of the problem nor was any effort made to take into account any effect due to the presence of a background

or Compton plateau. The reference spectrum was expressed as

$$F_r(x) = Be^{-a^2x^2},$$

where the integrated area under the peak is $(B/A)\sqrt{\pi}$. The unknown spectrum was expressed as

$$F_u(x) = KBe^{-K^2a^2x^2},$$

which has the same integrated area under the peak of $(B/A)\sqrt{\pi}$. The K is a factor that indicates the degree of change of resolution. The problem is to determine the value of the calculated coefficient (which will be called F) by which the reference must be multiplied to satisfy various least-squares criteria. Any deviation of F from 1 represents the error introduced as a result of resolution change. Five least-squares criteria were applied:

1. unweighted (unit weight factor),
2. weighting by the reciprocal of the unknown Gaussian,
3. weighting by the reciprocal of the reference Gaussian multiplied by the F,
4. weighting by the reciprocal of the geometric mean of the unknown Gaussian and the reference Gaussian multiplied by F, and
5. two successive solutions: the first is weighted by the reciprocal of the unknown Gaussian; the second is weighted by the reciprocal of the computed F from solution 1 multiplied by the reference Gaussian.

The results are shown as a function of resolution in Fig. 10. The unweighted criteria show the largest error sensitivity, ranging from negative computed values for poorer resolution of the unknown to positive values for improved resolution. By weighting the deviations squared by the reciprocal of the unknown, all calculated errors are

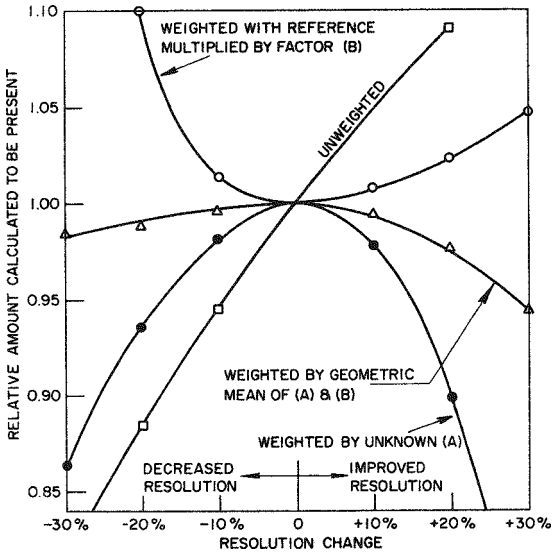

Fig. 10. Effect of Resolution Change on Calculated Results for Equal Gaussian Peaks.

negative but of a smaller magnitude than unweighted results. Weighting with the reciprocal of the reference spectrum multiplied by F introduces positive errors, whereas the weight of the geometric mean of the two results in small negative errors. However, it should be recognized that in practice it is not easily possible to weight with the reference multiplied by an F that is an integral part of the solution.

What is possible, however, is to solve for F using the weight of the unknown, then repeating the solution using the weight of the reference multiplied by the computed F. The new F from the second computation is now found to be independent of resolution change. The mathematics demonstrating this is shown in Appendix C. Whether this conclusion is valid for other than single Guassian peaks has yet to be demonstrated.

ANALYTICAL ANALYSIS OF ERRORS IN LEAST-SQUARES SOLUTIONS

From Appendix B the least-squares solution of an unknown spectrum is accomplished through the use of the following equation:

$$a_j = \sum_{i=1}^{254} \alpha_i(x) f(x) , \tag{1}$$

where a_j is the solution vector, $f(x)$ is the unknown spectrum, and

$$\alpha_i(x) = (M_{ij})^{-1} W(x) g_i(x) , \tag{2}$$

where $(M_{ij})^{-1}$ is the inverse of the matrix shown in Appendix B, $W(x)$ is the set of appropriately chosen weighting factors, and $g_i(x)$ is the vector of reference spectra. It can be shown that the error of the computed a_i's can also be expressed as a function of the $\alpha_i(x)$ in the following derived relation where δ is used to indicate estimated errors:

$$\delta a_j = \sum_{i=1}^{254} \alpha_i(x) \left[\delta f(x) - \sum_{j=1}^{8} a_j \delta g_j(x) \right] , \tag{3}$$

where $\delta f(x)$ is the set of estimated errors associated with the unknown spectrum, and $\delta g_j(x)$ are the sets of estimated errors of the reference spectra. If it can be assumed that the count rate in any given channel has a standard error equal to its square root, then

$$\delta f(x) = [f(x)]^{1/2} , \tag{4}$$

and

$$\delta g_j(x) = [g_j(x)]^{1/2} . \tag{5}$$

Substituting Eqs. (4) and (5) into Eq. (3) yields

$$\delta a_j = \sum_{i=1}^{254} \alpha_i(x) \left\{ [f(x)]^{1/2} - \sum_{j=1}^{8} a_j [g_j(x)]^{1/2} \right\} . \tag{6}$$

All terms are now known, and the δa_j vector can be evaluated.

To date, no experimental use has been made of this equation.

Appendix A

EQUATIONS FOR SIMPLE EQUATION METHOD

The basis used for both techniques of resolving gamma spectra is that the count rate in a particular channel position is the sum of the count rate contributions of each fission product to that channel.

Let us designate by $a_i (i = 1 \text{ to } 8)$ the number of microcuries of each of eight fission products present in the unknown. These are to be determined in our solution. Let us further designate $C_{i,k}$ as the counting rate contribution of 1 μc of the ith fission product in channel number k ($i = 1$ to 8; $k = 1$ to 254), and T_k as the counting rate in the unknown spectrum in channel k. All values of $C_{i,k}$ are taken directly from reference spectra. The following equation can then be written for a particular channel, k_1:

$$T_{k_1} = a_1 C_{1,k_1} + a_2 C_{2,k_1} + a_3 C_{3,k_1} + \ldots + a_8 C_{8,k_1} .$$

Similar equations can be written in seven other channel positions. A unique solution then exists for the eight equations in eight unknowns, and all a_i's ($i = 1$ to 8) can be determined directly.

It is clear that since there are 254 channels, 254 equations could be written where only eight are needed for a unique solution. The least-squares method shown in Appendix B permits the use of data in all channels.

Appendix B

EQUATIONS FOR LEAST-SQUARES METHOD OF SOLUTION[1]

The following definitions apply to this section:

$f(x)$ = unknown spectrum (x = channel number = 1 to 254)

$g_i(x)$, $g_j(x)$ = reference spectra ($i = j = 1$ to 8)

$W(x)$ = weighting factors

a_i, a_j = microcuries (unknown) of each fission product

$\left\{ \begin{matrix} \delta f(x), \delta g_i(x), \\ \delta g_j(x), \delta a_i \end{matrix} \right.$ = errors associated with quantities indicated

The assumption holds that the counting rate in a specific channel $f(x_1)$ is the sum of the counting rate contributions of each individual fission product

$$\sum_{j=1}^{8} a_j g_j(x_1) .$$

---

[1]The derivations following are principally the work of John Reynolds, Applied Mathematics Division of Argonne National Laboratory.

More generally,

$$f(x) = \sum_{j=1}^{8} a_j g_j(x) \,. \tag{1}$$

The weighted sums of deviations squared can then be expressed as

$$\epsilon = \sum_{x=1}^{254} W(x) \left[f(x) - \sum_{j=1}^{8} a_j g_j(x) \right]^2 . \tag{2}$$

Thus we may calculate the a's by minimizing ϵ, that is, by setting its partial derivatives with respect to each a_i equal to zero (eight normal equations in the eight unknowns, a_i, are thus generated).

$$-\frac{1}{2}\frac{\partial \epsilon}{\partial a_i} = 0 = \sum_{x=1}^{254} W(x) g_i(x) \left[f(x) - \sum_{j=1}^{8} a_j g_j(x) \right] , \tag{3}$$

$$\sum_{x=1}^{254} \left[W(x) g_i(x) \sum_{j=1}^{8} a_j g_j(x) \right] = \sum_{x=1}^{254} W(x) g_i(x) f(x) \,. \tag{4}$$

If we define the matrix (M_{ij}), such that its elements are

$$M_{ij} = \sum_{x=1}^{254} W(x) g_i(x) g_j(x) \,, \tag{5}$$

then Eq. (4) becomes (in matrix notation)

$$\left(M_{ij} \right) a_j = \sum_{x=1}^{254} W(x) g_i(x) f(x) \,, \tag{6}$$

or

$$a_j = \left(M_{ij} \right)^{-1} \sum_{x=1}^{254} W(x) g_i(x) f(x) \,. \tag{7}$$

If we define the vector $\alpha_i(x)$ as

$$\alpha_i(x) = \left(M_{ij} \right)^{-1} W(x) g_i(x) \,, \tag{8}$$

then Eq. (7) becomes

$$a_j(x) = \sum_{x=1}^{254} \alpha_i(x) f(x) \,. \tag{9}$$

This method of solution using the $\alpha_i(x)$'s has potential value for error analysis.

Error Analysis

In considering errors we let $f(x) + \delta f(x)$ be the measured f, $g_j(x) + \delta g_j(x)$ the measured g's, and $a_j + \delta a_j$ the calculated a's. Substituting these expressions into Eq. (4), we get

$$\sum_{x=1}^{254} \{W(x)[g_i(x) + \delta g_i(x)] \sum_{j=1}^{8} [a_j + \delta a_j] [g_j(x) + \delta g_j(x)]\}$$

$$= \sum_{x=1}^{254} W(x)[g_i(x) + \delta g_i(x)] [f(x) + \delta f(x)] . \qquad (10)$$

By expanding Eq. (10), dropping all second-order terms, and subtracting Eq. (4), we get

$$\sum_{x=1}^{254} \left[W(x) g_i(x) \sum_{j=1}^{8} \delta a_j g_i \right] = \sum_{x=1}^{254} W(x) g_i(x) \left[\delta f(x) - \sum_{j=1}^{8} a_j \delta g_j(x) \right] . \qquad (11)$$

Using the same matrix (M_{ij}) whose elements were defined in Eq. (5),

$$\left(M_{ij}\right) \delta a_j = \sum_{x=1}^{254} W(x) g_i(x) \left[\delta f(x) - \sum_{j=1}^{8} a_j \delta g_j(x) \right] , \qquad (12)$$

or

$$\delta a_j = \left(M_{ij}\right)^{-1} \sum_{x=1}^{254} W(x) g_i(x) \left[\delta f(x) - \sum_{j=1}^{8} a_j \delta g_j(x) \right] . \qquad (13)$$

Using the same vector $\alpha_i(x)$ as in Eq. (8),

$$\delta a_j = \sum_{x=1}^{254} \alpha_i(x) \left[\delta f(x) - \sum_{j=1}^{8} a_j \delta g_j(x) \right] , \qquad (14)$$

which is of the same form and uses the same $\alpha_i(x)$'s as does the solution for a_j's in Eq. (9) with $f(x)$ replaced by

$$\delta f(x) - \sum_{j=1}^{8} a_j \delta g_j(x) .$$

If the latter term can be evaluated (see main text), the δa_j's can be calculated.

Appendix C

ERRORS INTRODUCED BY RESOLUTION CHANGES ON A SINGLE GAUSSIAN

Equations are shown below for the calculation of errors due to resolution changes. The double solution technique in which calculated results are independent of resolution change is shown in detail.

The reference spectrum is given by

$$f_r(x) = Be^{-a^2 x^2} . \qquad (1)$$

The unknown spectrum is given by

$$f_u(x) = SKBe^{-K^2a^2x^2} . \tag{2}$$

The method requires the determination of a factor F by which Eq. (1) must be multiplied to satisfy the least-squares criteria applied. The correct result is that F should equal S. The integrated weighted square of the deviations is

$$\epsilon = \int_{-\infty}^{+\infty} d^2\, W(x)\, dx = \int_{-\infty}^{+\infty} W(x) \left(FBe^{-a^2x^2} - SKBe^{-K^2a^2x^2} \right)^2 dx . \tag{3}$$

The proper $W(x)$ is subtituted into Eq. (3), following which the integrals are evaluated. The factor F is calculated by minimizing ϵ, that is, by setting its partial derivative with respect to F equal to zero and then solving for F. The following $W(x)$'s were used:

1. $W(x) = 1$ (unweighted).
2. Weighted by the reciprocal of the unknown Gaussian:

$$W(x) = 1/SKBe^{-K^2a^2x^2} .$$

3. Weighted by the reciprocal of the reference Gaussian multiplied by F:

$$W(x) = 1/FBe^{-a^2x^2} .$$

4. Weighted by the geometric mean of Eqs. (2) and (3):

$$W(x) = \frac{1}{(FSK)^{1/2}\, B \exp\left[-\left(\frac{K^2 + 1}{2} \right) a^2x^2 \right]} .$$

5. Two successive solutions: the first weighted by Eq. (2) and the second by Eq. (3), using the value of F calculated in the first solution.

The mathematics is shown for the last method. When weighted, Eq. (3) becomes

$$\epsilon = \int_{-\infty}^{+\infty} \frac{\left(FBe^{-a^2x^2} - SKBe^{-K^2a^2x^2} \right)^2}{SKBe^{-K^2a^2x^2}} dx . \tag{4}$$

The expansion and simplification of terms results in

$$\epsilon = \int_{-\infty}^{+\infty} \frac{F^2B}{SK} e^{-(2-K^2)a^2x^2} dx - \int_{-\infty}^{+\infty} 2FBe^{-a^2x^2} dx + \int_{-\infty}^{+\infty} SKBe^{-K^2a^2x^2} dx . \tag{5}$$

After integration

$$\epsilon = \frac{F^2 B\pi^{1/2}}{aSK(2-K^2)^{1/2}} - \frac{2FB\pi^{1/2}}{a} + \frac{SB\pi^{1/2}}{a}. \tag{6}$$

Minimize ϵ, by taking its partial derivative with respect to F, equating to zero, and solving for F

$$\frac{\partial \epsilon}{\partial F} = \frac{2BF\pi^{1/2}}{aSK(2-K^2)^{1/2}} - \frac{2B\pi^{1/2}}{a} = 0\ , \tag{7}$$

$$F = KS(2-K^2)^{1/2}\ . \tag{8}$$

This expression shows the relation of the calculated F to resolution change. When $K = 1$, $F = S$. By designating this solution of F as F_1 and repeating the solution using a $W(x)$ of $1/F_1 B \exp(-a^2x^2)$, we will arrive at a second value of F, which we will designate as F_2. The expression for ϵ becomes

$$\epsilon = \int_{-\infty}^{+\infty} \frac{\left(F_2 Be^{-a^2x^2} - SKBe^{-K^2a^2x^2}\right)^2}{F_1 Be^{-a^2x^2}}\,dx\ . \tag{9}$$

Now, F_1 is known, F_2 is unknown. The known value of F_1 is substituted into Eq. (9).

After integration,

$$\epsilon = \frac{BF_2^2\pi^{1/2}}{aSK(2-K^2)^{1/2}} - \frac{2BF_2\pi^{1/2}}{aK(2-K^2)^{1/2}} + \frac{SKB\pi^{1/2}}{a(2-K^2)^{1/2}(2K^2-1)^{1/2}}. \tag{10}$$

If the minimum of ϵ is found by taking its partial derivative relative to F_2 which is then set equal to zero,

$$\frac{\partial \epsilon}{\partial F_2} = \frac{2BF_2\pi^{1/2}}{aSK(2-K^2)^{1/2}} - \frac{2B\pi^{1/2}}{aK(2-K^2)^{1/2}} = 0\ , \tag{11}$$

and

$$F_2 = S\ . \tag{12}$$

Thus, the calculated value of F_2 is found to be independent of resolution change.

The calculated functions of F resulting from the first four weighting methods are as follows:

(1) $$F = KS\left(\frac{2}{K^2+1}\right)^{1/2},$$

(2) $$F = KS(2-K^2)^{1/2},$$

(3) $$F = KS/(2K^2-1)^{1/4},$$

(4) $$F = \frac{KS}{3}\left\{\left(\frac{3-K^2}{K^2+1}\right)^{1/2} \pm \left[\frac{(3-K^2)}{(K^2+1)} + \frac{3(3-K^2)^{1/2}}{(3K^2-1)^{1/2}}\right]\right\}^{1/2}.$$

APPENDIX I

A BIBLIOGRAPHY OF PUBLICATIONS ON THE METHOD OF LEAST SQUARES

P. B. Wood
Central Data Processing Facility
Oak Ridge Gaseous Diffusion Plant
Oak Ridge, Tennessee

1. Theory of Least Squares

A. C. Aiken, "On Least Squares and Linear Combination of Observations," *Proc. Roy. Soc. Edinburgh* **A55**, 42–48 (1935).

A. C. Aiken, "Studies in Practical Mathematics. IV. On Linear Approximation by Least Squares," *Proc. Roy. Soc. Edinburgh* **A62**, 138–46 (1945).

F. N. David and J. Neyman, "Extension of Markoff's Theorem on Least Squares," *Biom. Res. Mem.* **2**, 238–49 (1933).

W. E. Deming, *Statistical Adjustment of Data*, Wiley, New York, 1943.

A. M. Mood, *Introduction to the Theory of Statistics*, pp 208–16, McGraw-Hill, New York, 1950.

C. R. Rao, *Advanced Statistical Methods in Biometric Research*, pp 75–80, Wiley, New York, 1952.

C. R. Rao, "Generalization of Markoff's Theorem and Tests of Linear Hypotheses," *Sankhya* **7**, part 1, 9–16 (1946).

C. R. Rao, "Markoff's Theorem with Linear Restrictions on Parameters," *Sankhya* **7**, part 3, 16–19 (1946).

C. R. Rao, "On Linear Combination of Observations and the General Theory of Least Squares," *Sankhya* **7**, part 3, 237–56 (1946).

J. B. Scarborough, *Numerical Mathematical Analysis*, pp 451–72, Johns Hopkins, New York, 1956.

2. Nonlinear Least Squares

Anonymous (n.d.), "Correlation and Optimization," *Preliminary Data 0003*, Computer Systems, Inc., Monmouth Junction, N.J.

G. E. P. Box, "Use of Statistical Methods in the Education of Basic Mechanisms," *Bull. Inst. Intenl. Stat.* **36**(3), 215–25 (1957).

G. E. P. Box, "Fitting Empirical Data," *Ann. N.Y. Acad. Sci.* **86**, 792–816 (1960).

H. O. Hartley, "The Modified Gauss-Newton Method for the Fitting of Nonlinear Regression Functions by Least Squares," *Technometrics* **3**, 269–80 (1961).

G. R. Keepin, T. F. Wimett, and R. K. Zeigler, "Delayed Neutrons from Fissionable Isotopes of Uranium, Plutonium, and Thorium," *J. Nucl. Energy* **6**(1, 2), secs 3 and 4A, 5–11 (1957).

K. Levenberg, "A Method for the Solution of Certain Nonlinear Problems in Least Squares," *Quart. Appl. Math.* **2**, 164–68 (1944).

R. H. Moore and C. G. Chezem, "Applications of the Iterative Least Squares Procedures," *Trans. Am. Nucl. Soc.* **1**(2), 129–30 (1958).

R. H. Moore and R. K. Zeigler, "The Use of High-Speed Computers in Determining the Parameters of Nonlinear Functions by Iterative Least Squares Methods," *Trans. Am. Nucl. Soc.* **1**(2), 128–29 (1958).

T. I. Peterson, "Kinetics and Mechanism of Naphthalene Oxidation by Nonlinear Estimation," *Chem. Eng. Sci.* **17**, 203–19 (1962).

E. B. Wilson and R. R. Puffer, "Least Squares and Laws of Population Growth," *Proc. Amer. Acad. Arts and Sci. (Boston)* **68**, secs 23–35, 303–15; Appendix, secs 62–64, 343–47, and secs 70–71, 354–59; refs, 366–69, and 377–78 (1933).

3. Variance Estimates in Nonlinear Least Squares

E. M. L. Beale, "Confidence Regions in Nonlinear Estimation," *J. R. Statis. Soc. Series B* **20**, 41–88 (1960).

S. L. Piotrowski, "Some Remarks on the Weights of Unknowns as Determined by the Method of Differential Corrections," *Proc. Natl. Acad. Sci. U.S.* **34**, 23–26 (1948).

E. J. Williams, "Exact Fiducial Limits in Nonlinear Estimation," *J. R. Statis. Soc. Series B* **24**, 125–39 (1962).

4. Other Problems and Techniques Related to Nonlinear Least Squares

H. B. Curry, "The Method of Steepest Descent for Nonlinear Minimization Problems," *Quart. Appl. Math.* **2**, 258–61 (1944).

F. Garwood, "The Application of Maximum Likelihood to Dosage-Mortality Curves," *Biometrics* **32**, 46–58 (1941).

A. E. Gleyzal, "Solution of Nonlinear Equations," *Quart. Appl. Math.* **17**, 95–96 (1959).

A. A. Goldstein, N. Levine, and J. B. Hereshoff, "On the 'Best' and 'Least qth' Approximations of an Overdetermined System of Linear Equations," *J. Assoc. Comp. Mach.* **4**, 341–47 (1957).

L. V. Kantrovitch, "On an Effective Method of Solving Extremal Problems for Quadratic Functionals," *C. R. (Dokl.) Acad. Sci. USSR* **48**, sec 1, 455–56 (1945).

A. Shenitzer, "Chebyshev Approximation of a Continuous Function by a Class of Functions," *J. Assoc. Comp. Mach.* **4**, 30–35 (1957).

APPENDIX II

ON THE MEANING AND USE OF "CHI-SQUARE" IN CURVE FITTING[1]

Roger H. Moore
Los Alamos Scientific Laboratory, University of California
Los Alamos, New Mexico

This note, prepared at the request of the editor of the Proceedings of the Gatlinburg Symposium on the Application of Computers to Nuclear and Radiochemistry is an effort to provide the casual user of statistical methods with a feel for the meaning and use of the quantity called "chi-square." It is *not* the author's intention that this presentation be a substitute for sound statistical advice. As a matter of fact, the section "Parting Shot" is, in the opinion of the author and his colleagues, the presentation's most important statistical concept. This oft-repeated plea by statisticians is no less valid for its venerability than it is for its basic rightousness.

SOME BASIC DEFINITIONS

It is useful at the outset to have some appreciation for the meanings of the terms "random variable," "distribution function," and "density function." Serving the present purpose are the following definitions which are based on those given in a basic statistical dictionary [*1*]. Common synonyms are parenthetically indicated immediately after the term being defined.

Definition 1. A random variable (chance variable, variate) is a quantity, say y, which may take any of the values of a specified set, say S, with a specified frequency or probability.

Definition 2. The distribution function (cumulative distribution function) $G(y)$ of a random variable y is the total frequency of members of the set S whose values are less than or equal to y. As a general rule the total frequency is taken to be unity.

Definition 3. The density function (frequency function, probability density) of a random variable y is an expression giving the frequency of a value attainable by the random variable y as a function of y. When y is a continuous random variable, the density function gives the frequency in an elemental range dy. The density function is sometimes conveniently regarded as the derivative of the distribution function.

It is not the author's intention that these definitions convey to the casual reader all the esoteric nuances contained in the terms. Rather, it is hoped only to provide a basis on which to build the following discussion.

NORMAL DISTRIBUTION

A probably familiar idea is the notion of a set of numbers being normally distributed.[2] What is usually meant by this notion is that the set of numbers is assumed to be a group of observations of a random variable whose density function has a

---

[1]Work performed under the auspices of the U.S. Atomic Energy Commission.

[2]Some writers, especially in physics, would use the term "Gaussian distributed."

particular form known as the normal density. For notation, let the random variable be called y. The set of observed values may be denoted $y_1, y_2, \ldots, y_n$, the subscript n indicating the number of values in the set. The normal density function can be written

$$g(y) = \frac{1}{\sqrt{2\pi\sigma}} e^{-[(y-\mu)^2/2\sigma^2]}, \qquad -\infty < y < \infty. \tag{1}$$

It may be recognized that the quantities μ and σ are the mean and standard deviation of the density function. These quantities are *parameters*; that is, they determine the position and shapes of the density. The estimation of these parameters follows the usual technique: μ is estimated by $\bar{y}$ where

$$\bar{y} = \left(\sum_{i=1}^{n} y_i \right) / n ,$$

and σ is estimated by the square root of s^2 where

$$s^2 = \left[\sum_{i=1}^{n} (y_i - \bar{y})^2 \right] / n - 1 .$$

In statistical parlance, $\bar{y}$ and s^2 are *statistics*, which is to say that they are computed from the sample values $y_1, y_2, \ldots, y_n$. Thus, since the sample values are random variables, the statistics $\bar{y}$ and s^2 are also random variables because they are functions of the observed values.

But, from definition 1, these statistics also have density functions which define the probabilities that $\bar{y}$ and s^2 will take on particular values. Finding densities for statistics is, in general, a major undertaking. Fortunately, most of these problems have already been faced, and the results are available if one knows about them and where to find them.

CHI-SQUARE DISTRIBUTION

Just as y could be said in the preceding section to be normally distributed because its density function was assumed to be of the form (1), a random variable z is said to have a chi-square distribution if its density is of the form

$$h(z) = \frac{1}{2^{k/2}\Gamma(k/2)} e^{-z/2} z^{(k-2)/2}, \qquad 0 \leqq z < \infty. \tag{2}$$

The only parameter in this distribution is k and is called the number of degrees of freedom; $\Gamma(k/2)$ is the usual gamma function.

Often the chi-square variable is written using its Greek symbol χ^2. When this is done the density (2) takes the form

$$h(\chi^2) = \frac{1}{2^{k/2}\Gamma(k/2)} e^{-\chi^2/2} (\chi^2)^{(k-2)/2}, \qquad 0 \leqq \chi^2 \leqq \infty. \tag{2'}$$

In particular, it must be remembered that the variable chi-square is just that – a variable that has a specific density function. It must also be remembered that the symbol χ^2 is nothing but a symbol, indicating a variable that has a chi-square density.

The chi-square distribution has several interesting properties. The most useful is the additive property; that is, the sum of two chi-square distributed variables is a chi-square variable. That is to say, if χ_1^2 has a chi-square distribution with k_1 degrees of freedom and χ_2^2 has a chi-square distribution with k_2 degrees of freedom, then their sum $\chi_3^2 = \chi_1^2 + \chi_2^2$ has a chi-square distribution with $k_3 = k_1 + k_2$ degrees of fredom.

The chi-square variable is closely related to the normal variable. Indeed, chi-square is often defined in terms of a normal variable in the following manner: Consider a random variable defined by $z = (y - \mu)^2/\sigma^2$, where y is a normally distributed variable whose mean and variance are μ and σ^2.[3] Then the density of z is the chi-square density (2). However, as shown earlier, it is not necessary to define chi-square in this way, since it is a perfectly respectable random variable in its own right.

An important use of the chi-square variable occurs when individuals are classified according to several characteristics, and a question to be answered concerns the independence of these characteristics. The term "contingency tables" is applied to data treated this way. Most basic statistics books contain discussion of this use of chi-square [2]. Care must be exercised, however, that contingency table concepts and notation are not carried over into the fitting of functions.

CHI-SQUARE AND CURVE FITTING

The question remains: How does a quantity called chi-square – often denoted by χ^2 – relate to the problem of curve fitting? The answer lies in the assumptions on which the curve fitting is accomplished.

Consider the case in which n pairs of numbers are observed. Denote the observations by $(y_1, x_1), (y_2, x_2), \ldots, (y_n, x_n)$. Assume that the pairs (y_i, x_i) are related by the following expression:

$$y_i = f(x_i; \alpha) + e_i, \quad i = 1, 2, \ldots, n. \tag{3}$$

The quantity α is a vector of p parameters which are to be estimated. If, a priori, it is agreed that α is to be estimated by minimizing the sum of the squares of the errors, the e_i in Eq. (3), it means that the following function of α is to be minimized:

$$Q(\alpha) = \sum_{i=1}^{n} e_i^2 = \sum_{i=1}^{n} [y_i - f(x_i; \alpha)]^2 . \tag{4}$$

The value of α, call it $\hat{\alpha}$, that minimizes the $Q(\alpha)$ in Eq. (4) is the least-squares estimate of the parameter α.

Now, suppose an additional assumption is made about the observations (y_i, x_i). This assumption is that the y_i's are observed values of a random variable that is normally distributed with mean $\mu_i = f(x_i; \alpha)$ and variance σ^2. The latter part of the assumption forces equal variability of the observations, no matter which pair of the (y_i, x_i) observations is under consideration. In the notation of Eq. (1), the normal

[3] The variable z defined in this way is often called "the square of a standardized normal."

density function, this assumption is written

$$g(y) = \frac{1}{\sqrt{2\pi}\sigma} e^{-\{[y - f(x;\alpha)]^2/2\sigma^2\}} . \tag{5}$$

From this assumption of normality, it can be developed that the required estimate of α (often called "the maximum likelihood estimate of α") is obtained by minimizing the expression

$$R(\alpha) = \left\{ \sum_{i=1}^{n} [y_i - f(x_i;\alpha)]^2 \right\} / \sigma^2 . \tag{6}$$

Examination of Eq. (4) shows that if $\hat{\alpha}$ minimizes $Q(\alpha)$, then the same $\hat{\alpha}$ also minimizes $R(\alpha)$ in Eq. (6). Hence the maximum likelihood estimate of α is identical with the least-squares estimate when it is assumed that the values of y are normally distributed with mean $f(x;\alpha)$ and common variance σ^2.

Consider now the case in which the function $f(x;\alpha)$ is linear in the elements of the parameter vector. Perhaps the simplest and most familiar linear model is that of a straight line: $f(x;\alpha) = \alpha_1 + \alpha_2 x$. When the maximum likelihood estimates of the intercept and slope, $\hat{\alpha}_1$ and $\hat{\alpha}_2$, are inserted into $R(\alpha)$, it can be shown that $R(\hat{\alpha})$ is a random variable which is distributed as chi-square with $(n - 2)$ degrees of freedom. It is extremely important to note that the quantity σ^2 must be in the denominater of $R(\hat{\alpha})$ in order that the expression be called chi-square. In particular, the unweighted sum of squares, $Q(\alpha)$ in Eq. (4), is *not* chi-square, even though it is evaluated at $\hat{\alpha}$.

When the function $f(x;\alpha)$ is not linear in at least one of the parameters, it generally is *not* true that $R(\hat{\alpha})$ has a chi-square distribution. However, it is common practice to treat $R(\hat{\alpha})$ as though it did have the same chi-square properties as those obtained in the linear model; that is, $R(\hat{\alpha})$ is said to be approximately chi-square distributed with $(n - p)$ degrees of freedom, where n is the number of observations and p is number of parameters in the vector α.

In many experimental situations it is not reasonable to assume that the variance of the variable y is the same for each experimental observation. Some sort of "weighting" to allow for this nonhomogeneity is dictated. As a result of this consideration, each experimental result is a triad of numbers (y_i, x_i, w_i). The various values of w_i are meant to indicate the relative worth ("weights") of the observations y_i. The estimates of the elements of the parameter vector α are obtained by minimizing the weighted sum of squares,

$$Q_w(\alpha) = \sum_{i=1}^{n} w_i [y_i - f(x_i;\alpha)]^2 . \tag{4'}$$

Substitution of the weighted least-squares estimate $\hat{\alpha}_w$ into Eq. (4′) does not guarantee that $Q_w(\hat{\alpha}_w)$ will have a chi-square distribution. However, if σ_i^2 is the variance of y_i and $w_i = 1/\sigma_i^2$ and y_i is assumed to be normally distributed, it is noted that

$$Q_w(\hat{\alpha}_w) = \sum_{i=1}^{n} \left[\frac{y_i - f(x_i;\hat{\alpha}_w)}{\sigma_i} \right]^2 \tag{4''}$$

has the same appearance as a sum of squares of standardized normals. In fact, if the function is linear in the elements of α and the variances are known constants, then $Q_w(\hat{\alpha}_w)$ has exactly a chi-square distribution with $(n - p)$ degrees of freedom – precisely the result obtained above for $R(\hat{\alpha})$ from Eq. (6).

When the function is not linear in at least one of the parameters, this exact result cannot be stated. However, once again, it is common practice to treat $Q_w(\hat{\alpha}_w)$ as though it were distributed as chi-square with $(n - p)$ degrees of freedom. Furthermore, it is seldom that the σ_i^2 can be assumed known. Approximate values must then be used, and this procedure also reinforces the statement that $Q_w(\hat{\alpha}_w)$ is only *approximately* chi-square distributed.

CHI-SQUARE AS A "FIGURE OF MERIT"

The term $Q_w(\hat{\alpha}_w)$ is often put forth as a figure of merit for the goodness of fit of a function to a set of experimental data. The basis for this usage comes from the following considerations. It has been shown earlier that chi-square with k degrees of freedom is a variable with a density function of the form (2). The variable z can take on values from zero to infinity according to the relative frequencies indicated by Eq. (2). Furthermore, the integral of $h(z)$ is equal to unity. Notationally, this remark takes the form

$$\int_0^\infty h(z)\, dz = 1. \tag{7}$$

If the upper limit of the integral (7) is finite, then the value of that integral is less than unity. Suppose that this upper limit is some fixed value z_0. Then the value of the integral is, say, p_0, which is the probability that the random variable z will take on a value less than or equal to the preset value z_0. This may be written

$$Pr(z \leq z_0) = \int_0^{z_0} h(z)\, dz = p_0 . \tag{8}$$

It should be clear that, as z_0 approaches infinity, p_0 approaches unity.

Suppose that $p_0 = 0.95$ is chosen. Then, by consulting tables of the chi-square cumulative distribution [3, pp 40–43], it is possible to determine the corresponding value z_0. This value depends on the number of degrees of freedom. Thus, for 10 degrees of freedom, $z_0 = 18.3$, while the result for 20 degrees of freedom is $z_0 = 31.4$.

Suppose further that a function has been fitted, that there are $(n - p) = 10$ degrees of freedom and that $Q_w(\hat{\alpha}_w) = 21.3$. Since $z_0 = 18.3$ for 10 degrees of freedom, it is seen that the probability of obtaining a value of $Q_w(\hat{\alpha}_w)$ as large as 21.3 is less than $0.05 = 1.00 - 0.95$. Hence, it might be concluded that 21.3 is too large to allow the assumption that a "good" fit has been obtained.

It is important at this juncture to recall the many assumptions that have led this far: (1) normality has been assumed to be the basic distribution for the y_i, (2) the "best" estimates of the parameters have been assumed, and (3) knowledge about the σ_i^2 has been assumed. Violation of any one of these assumptions usually leads to an inflated value for $Q_w(\hat{\alpha}_w)$. Thus, one should temper his flat rejection of $Q_w(\hat{\alpha}_w) = 21.3$ until he is certain that all the basic assumptions are satisfied.

Sometimes a related variable, $v = Q_w(\hat{a}_w)/(n - p)$, which has a "chi-square over degrees of freedom" density, is used to indicate a goodness of fit. Because the expected value of a chi-square variable with k degrees of freedom is the parameter k itself, the expectation of the variable v is unity. Tables for critical values of v are available [3, pp 44–46].

PARTING SHOT

Several instances of misuse and misinterpretation of quantities called chi-square have come to the author's attention in recent years. Most of these seem to have been the result of lack of proper statistical training on the part of the wrong-doer. Here, and in many other statistical matters, the potential harm resulting from such misuse is incalculable. Moreover, it is not excusable. If nothing else, this presentation will have served its purpose if it provides the experimenter with some of the language of statistics and induces him to consult a qualified statistician when a statistical problem arises.

ACKNOWLEDGMENT

The author wishes to express his gratitude to R. K. Zeigler and A. S. Goldman for their careful reading of this paper.

REFERENCES

The following books, of varying degrees of difficulty, are listed to provide the interested reader with some basic sources for statistical methodology. Most of the books, which certainly do not provide an exhaustive list, are standard among consulting statisticians. Thus, basic familiarity with a few of them will do much to provide a basis of understanding between the disciplines. This is not to say that the researcher should become a statistician, any more than the reverse situation should be true. However, just as the statistician must know about half-lives and reaction rates, so should the experimenter know about means and variances.

[1] M. G. Kendall and W. R. Buckland, *A Dictionary of Statistical Terms*, Hafner, New York, 1957.

[2] W. J. Dixon and F. J. Massey, Jr., *Introduction to Statistical Analysis*, 2d ed., pp 221–26, McGraw-Hill, New York, 1957.

[3] C. A. Bennett and N. L. Franklin, *Statistical Analysis in Chemistry and the Chemical Industry*, Wiley, New York, 1954.

[4] A. Hald, *Statistical Tables and Formulas*, Wiley, New York, 1952.

[5] A. Hald, *Statistical Theory with Engineering Applications*, Wiley, New York, 1952.

APPENDIX III

SYMPOSIUM PARTICIPANTS

Augustine, R. J.
U.S. Public Health Service
Montgomery, Ala.

Babb, David D.
Dikewood Corp.
Albuquerque, N.M.

Balagna, John P.
Los Alamos Scientific Lab.
Los Alamos, N.M.

Baratta, Edmond J.
U.S. Public Health Service
Winchester, Mass.

Barr, Donald W.
Los Alamos Scientific Lab.
Los Alamos, N.M.

Bate, L. C.
Oak Ridge National Lab.
Oak Ridge, Tenn.

Baurmash, Leonard
Atomics International
P.O. Box 309
Canoga Park, Calif.

Beiting, Robert J.
U.S. Public Health Service
Cincinnati, Ohio

Bingham, Carleton D.
Atomics International
Box 309
Canoga Park, Calif.

Bird, J. R.
AERE
Harwell, England

Blotcky, Alan
V.A. Hospital
Omaha, Neb.

Brauer, Fred P.
General Electric Co.
Richland, Wash.

Braun, Andrew G.
M.I.T. Radioactivity Center
Cambridge, Mass.

Bromley, D. A.
Yale University
New Haven, Conn.

Brooks, A. A.
Union Carbide Nuclear Corp.
ORGDP, P.O. Box P
Oak Ridge, Tenn.

Burns, Forest C.
Army Materials Res. Agency
Watertown, Mass.

Burrus, Walter Ross
Oak Ridge National Lab.
Oak Ridge, Tenn.

Burson, S. B.
Argonne National Lab.
Argonne, Ill.

Chapman, George T.
Oak Ridge National Lab.
Oak Ridge, Tenn.

Chester, R. O.
Oak Ridge National Lab.
Oak Ridge, Tenn.

Cook, Leroy
U.S. Public Health Service
1901 Chapman Avenue
Rockville, Md.

Cote, Robert E.
Argonne National Lab.
Argonne, Ill.

Covell, David F.
U.S. Naval Radiological
Defense Lab.
San Francisco 24, Calif.

Crouch, Donald F.
Phillips Petroleum Co.,
NRTS
Idaho Falls, Idaho

Cumming, James B.
Brookhaven National Lab.
Upton, L.I., N.Y.

Daves, Harold L.
Savannah River Plant
Aiken, S.C.

Dean, Phillip N.
Los Alamos Scientific Lab.
Los Alamos, N.M.

DeCarlo, Victor A.
Oak Ridge National Lab.
Oak Ridge, Tenn.

DeVoe, J. R.
National Bureau of Standards
Washington 25, D.C.

Drew, Dan
Texas A. & M.
College Station, Tex.

Dyer, Frank F.
Oak Ridge National Lab.
Oak Ridge, Tenn.

Eddlemon, J. D.
Charles Walsh Associates,
Inc.
Oak Ridge, Tenn.

Eldridge, J. S.
Oak Ridge National Lab.
Oak Ridge, Tenn.

Emery, Juel F.
Oak Ridge National Lab.
Oak Ridge, Tenn.

Ferguson, A. J.
Atomic Energy of Canada
Chalk River, Ont.

Ferguson, Robert L.
Oak Ridge National Lab.
Oak Ridge, Tenn.

Ford, George P.
Los Alamos Scientific Lab.
Los Alamos, N.M.

Funk, Emerson
University of Notre Dame
Notre Dame, Ind.

Gardiner, Donald A.
Oak Ridge National Lab.
Oak Ridge, Tenn.

Gardner, Donald G.
Illinois Inst. of Tech.
Chicago, Ill.

Garfinkel, Sam B.
National Bureau of Standards
Washington 25, D.C.

Gilat, Jacob
Oak Ridge National Lab.
Oak Ridge, Tenn.

Gold, Seymour
U.S. Public Health Service
Cincinnati 26, Ohio

Goldin, A. S.
U.S. Public Health Service
N.E.R.H.L.
Winchester, Mass.

Gordon, Clifford
Naval Research Lab.
Washington 25, D.C.

Gordon, Glen E.
M.I.T.
Cambridge, Mass.

Gosslee, D.
Oak Ridge National Lab.
Oak Ridge, Tenn.

Gove, N. B.
National Academy of Sciences
Washington, D.C.

Gray, Peter R.
Phillips Petroleum Co.
Bartlesville, Okla.

Gregory, James
Argonne National Lab.
Argonne, Ill.

Hahn, R. L.
Oak Ridge National Lab.
Oak Ridge, Tenn.

Heath, R. L.
Phillips Petroleum Co., AED
Idaho Falls, Idaho

Helmer, Richard G.
Phillips Petroleum Co.
Idaho Falls, Idaho

Hillman, Manny
Brookhaven National Lab.
Upton, L.I., N.Y.

Hoffman, Darleane C.
Los Alamos Scientific Lab.
Los Alamos, N.M.

Hogan, Mike
National Radiation Defense Lab.
San Francisco 2, Calif.

Iwami, Fred S.
Argonne National Lab.
Argonne, Ill.

Jarrard, John D.
Oak Ridge National Lab.
Oak Ridge, Tenn.

Johnson, Adrain E.
Union Carbide Corp.
270 Park Avenue
New York, N.Y.

Jurney, E. T.
Los Alamos Scientific Lab.
Los Alamos, N.M.

Kastenbaum, M. A.
Oak Ridge National Lab.
Oak Ridge, Tenn.

Keech, Gerald L.
McMaster University
Hamilton, Ont.

Kennett, T. J.
McMaster University
Hamilton, Ont.

Knight, F. D.
Savannah River Plant
Aiken, S.C.

Kolde, Harry E.
U.S. Public Health Service
Cincinnati, Ohio

Kramer, H. H.
Union Carbide Nuclear Co.
Tuxedo, N.Y.

Krebs, A.
Walter Reed Res. Inst.
Washington, D.C.

Lietzke, M. H.
Oak Ridge National Lab.
Oak Ridge, Tenn.

Liuzzi, Anthony
New York University
550 First Avenue
New York, N.Y.

Lund, John R.
Oak Ridge National Lab.
Oak Ridge, Tenn.

Lyon, W. S.
Oak Ridge National Lab.
Oak Ridge, Tenn.

Lytle, Jack R.
Harshaw Chemical Co.
Cleveland 31, Ohio

McQuilkin, Frank R.
Oak Ridge National Lab.
Oak Ridge, Tenn.

Mihelich, John W.
University of Notre Dame
Dept. of Physics
Notre Dame, Ind.

Monahan, James E.
Argonne National Lab.
Argonne, Ill.

Moore, Roger H.
Los Alamos Scientific Lab.
Los Alamos, N.M.

Morrison, David L.
Battelle Memorial Inst.
Columbus, Ohio

Nervik, W. E.
Lawrence Radiation Lab.
Livermore, Calif.

Nicholson, Wesley L.
General Electric Co.
Richland, Wash.

Nostrand, John
Grumman Aircraft
Bethpage, N.Y.

O'Brien, H. A.
Oak Ridge National Lab.
Oak Ridge, Tenn.

Oglesby, D. F.
Radiation Counter Lab.
5121 W. Grove Street
Skokie, Ill.

O'Kelley, G. D.
Oak Ridge National Lab.
Oak Ridge, Tenn.

Pasternack, Bernard S.
New York University
550 First Avenue
New York, N.Y.

Pate, Brian D.
Washington University
St. Louis, Mo.

Patterson, G. R.
Oak Ridge National Lab.
Oak Ridge, Tenn.

Patzelt, Paul
Institut fur Anorganische Chemie
Mainz, Germany

Peele, R. W.
Oak Ridge National Lab.
Oak Ridge, Tenn.

Poggenburg, J. K.
Lawrence Radiation Lab.
University of California
Berkeley 4, Calif.

Prestwich, W. V.
McMaster University
Hamilton, Ont.

Reed, Lyle Lee
General Electric Co.
Pleasanton, Calif.

Ricci, Enzo
Oak Ridge National Lab.
Oak Ridge, Tenn.

Robinson, Berol L.
Western Reserve University
Cleveland, Ohio

Rogers, Paul C.
Los Alamos Scientific Lab.
Los Alamos, N.M.

Salmon, Leonard
AERE
Harwell, England

Sax, N. I.
New York State Dept. of Health
Albany, N.Y.

Schlosser, Jim
General Electric Co.
Richland, Wash.

Schmidt, Charles T.
Harshaw Chemical Co.
Cleveland, Ohio

Schmittroth, L. A.
Phillips Petroleum Co.
Idaho Falls, Idaho

Schrack, Roald A.
National Bureau of Standards
Washington 25, D.C.

Scofield, Norman E.
U.S. Naval Radiation Defense Lab.
San Francisco, Calif.

Seefeldt, W. B.
Argonne National Lab.
Argonne, Ill.

Shafer, Robert E.
Lawrence Radiation Lab.
Livermore, Calif.

Slack, Lewis
NAS-NRL
2101 Constitution Avenue
Washington, D.C.

Starner, John W.
Los Alamos Scientific Lab.
Los Alamos, N.M.

Steinberg, Ellis P.
Argonne National Lab.
Argonne, Ill.

Summers, Donald L.
Dikewood Corporation
Albuquerque, N.M.

Sunderman, D. N.
Battelle Memorial Institute
Columbus, Ohio

Thompson, Jerry J.
Savannah River Plant
Aiken, S.C.

Treytl, William J.
Carnegie Tech.
Schenley Park
Pittsburgh, Pa.

Trombka, J.
Jet Propulsion Lab.
Pasadena, Calif.

Van Dilla, M. A.
Los Alamos Scientific Lab.
Los Alamos, N.M.

Wapstra, W. H.
Inst. Nuc. Physics Research
Amsterdam, The Netherlands

Wiggins, Marvin T.
Argonne National Lab.
Argonne, Ill.

Wilsky, Kai
Riso Roskilde
Denmark

Wood, Robert W.
325 Congressional Lane
Rockville, Md.

Wurster, Vija A.
Monsanto Research Corp.
Miamisburg, Ohio

Wylie, Kyral F.
Monsanto Research Corp.
Mound Laboratory
Miamisburg, Ohio

Yeager, Thomas B.
Public Health Service
Cincinnati, Ohio

Yearian, Mason R.
Stanford University
Stanford, Calif.

Zeigler, R. K.
Los Alamos Scientific Lab.
Los Alamos, N.M.

MONOGRAPHS IN THE RADIOCHEMISTRY AND THE RADIOCHEMICAL TECHNIQUES SERIES

The following lists the title issued in these related series. Copies of all titles shown are available from the U. S. Department of Commerce, Office of Technical Services, Washington 25, D. C.

Cadmium	NAS-NS-3001	Titanium	NAS-NS-3034
Arsenic	NAS-NS-3002	Cesium	NAS-NS-3035
Francium	NAS-NS-3003	Gold	NAS-NS-3036
Thorium	NAS-NS-3004	Polonium	NAS-NS-3037
Fluorine, Chlorine, Bromine, and Iodine	NAS-NS-3005	Tellurium	NAS-NS-3038
Americium and Curium	NAS-NS-3006	Niobium and Tantalum	NAS-NS-3039
Chromium	NAS-NS-3007	Lead	NAS-NS-3040
Rhodium	NAS-NS-3008	Cobalt	NAS-NS-3041
Molybdenum	NAS-NS-3009	Tungsten	NAS-NS-3042
Barium, Calcium, and Strontium	NAS-NS-3010	Germanium	NAS-NS-3043
Zirconium and Hafnium	NAS-NS-3011	Platinum	NAS-NS-3044
Astatine	NAS-NS-3012	Iridium	NAS-NS-3045
Beryllium	NAS-NS-3013	Osmium	NAS-NS-3046
Indium	NAS-NS-3014	Silver	NAS-NS-3047
Zinc	NAS-NS-3015	Potassium	NAS-NS-3048
Protactinium	NAS-NS-3016	Silicon	NAS-NS-3049
Iron	NAS-NS-3017	Uranium	NAS-NS-3050
Manganese	NAS-NS-3018	Nickel	NAS-NS-3051
Carbon, Nitrogen, and Oxygen	NAS-NS-3019	Palladium	NAS-NS-3052
Rare Earths — Scandium, Yttrium, and Actinium	NAS-NS-3020	Rubidium	NAS-NS-3053
Technetium	NAS-NS-3021	Sulfur	NAS-NS-3054
Vanadium	NAS-NS-3022	Sodium	NAS-NS-3055
Tin	NAS-NS-3023	Phosphorus	NAS-NS-3056
Magnesium	NAS-NS-3024	Liquid-liquid Extraction with High-molecular-weight A mines	NAS-NS-3101
Rare Gases	NAS-NS-3025	Separations by Solvent Extraction with Tri-n-octylphosphine Oxide	NAS-NS-3102
Mercury	NAS-NS-3026	Low-level Radiochemical Separations	NAS-NS-3103
Copper	NAS-NS-3027	Rapid Radiochemical Separations	NAS-NS-3104
Rhenium	NAS-NS-3028	Detection and Measurement of Nuclear Radiation	NAS-NS-3105
Ruthenium	NAS-NS-3029		
Selenium	NAS-NS-3030		
Transuranium Elements	NAS-NS-3031		
Aluminum and Gallium	NAS-NS-3032		
Antimony	NAS-NS-3033		